Report No. CDOT-2013-4
Final Report

IMPLEMENTATION OF THE AASHTO MECHANISTIC-EMPIRICAL PAVEMENT DESIGN GUIDE FOR COLORADO

Jagannath Mallela
Leslie Titus-Glover
Suri Sadasivam
Biplab Bhattacharya
Michael Darter
Harold Von Quintus

July 2013

COLORADO DEPARTMENT OF TRANSPORTATION
DTD APPLIED RESEARCH AND INNOVATION BRANCH

The contents of this report reflect the views of the author(s), who is(are) responsible for the facts and accuracy of the data presented herein. The contents do not necessarily reflect the official views of the Colorado Department of Transportation or the Federal Highway Administration. This report does not constitute a standard, specification, or regulation.

Technical Report Documentation Page

1. Report No. CDOT-2013-4	**2. Government Accession No.**	**3. Recipient's Catalog No.**
4. Title and Subtitle IMPLEMENTATION OF THE AASHTO MECHANISTIC-EMPIRICAL PAVEMENT DESIGN GUIDE FOR COLORADO		**5. Report Date** July 2013 **6. Performing Organization Code**
7. Author(s) Jagannath Mallela, Leslie Titus-Glover, Suri Sadasivam, Biplab Bhattacharya, Michael Darter, and Harold Von Quintus		**8. Performing Organization Report No.** CDOT-2013-4
9. Performing Organization Name and Address Applied Research Associates, Inc. 100 Trade Centre Dr., Suite 200 Champaign, IL 61820-7233		**10. Work Unit No. (TRAIS)** **11. Contract or Grant No.**
12. Sponsoring Agency Name and Address Colorado Department of Transportation - Research 4201 E. Arkansas Ave Denver, CO 80222		**13. Type of Report and Period Covered** Final Report **14. Sponsoring Agency Code**

15. Supplementary Notes
Contracting Officer's Technical Representative (COTR): Jay Goldbaum

16. Abstract
The objective of this project was to integrate the American Association of State Highway and Transportation Officials (AASHTO) Mechanistic-Empirical Pavement Design Guide, Interim Edition: A Manual of Practice and its accompanying software into the daily pavement design, evaluation, rehabilitation, management, and forensic analysis practices and operations of the Colorado Department of Transportation (CDOT).

The Pavement ME Design software (formerly DARWin-ME) is a state-of-the-practice analysis tool for evaluating new, reconstructed, and rehabilitated flexible, rigid, and semi-rigid pavement structures based on mechanistic-empirical principles. Using project specific traffic, climate, and materials data, Pavement ME Design estimates and accumulates pavement damage and other forms of deterioration over a specified design/analysis period and then applied transfer functions to transform damage/deterioration into distress and smoothness. The pavement designer then determines the adequacy of a desired pavement section by evaluating predicted distress and smoothness at a given reliability level at the end of the design period. As a forensic analysis tool, Pavement ME Design can be used to model a pavement structure, simulate the combined effect of application of traffic load and climate cycles, and determine the performance (or lack of) for a specified time period.

Implementation
The implementation of Pavement ME Design as a CDOT standard required modifications in some aspects of CDOT pavement design practices (materials testing, testing equipment, traffic data reporting, software/database integration, development of statewide defaults for key inputs, policy regarding design output interpretation, and others). Also, implementation required validation (and sometimes calibration) of the software's "global" pavement distress and smoothness prediction models for Colorado conditions. This was accomplished using data from Long Term Pavement Performance (LTPP) projects located in Colorado and CDOT pavement management system sections. Default key data inputs were also developed, as was guidance for using the Pavement ME Design procedure for pavement design in Colorado.

17. Key Words mechanistic-empirical design, MEPDG, hot-mix asphalt (HMA), portland cement concrete (PCC), rehabilitation, field testing, laboratory testing, local calibration	**18. Distribution Statement** This document is available on CDOT's Research Report website http://www.coloradodot.info/programs/research/pdfs

19. Security Classifi. (of this report) Unclassified	**20. Security Classif. (of this page)** Unclassified	**21. No. of Pages** 209	**22. Price**

IMPLEMENTATION OF THE AASHTO MECHANISTIC-EMPIRICAL PAVEMENT DESIGN GUIDE FOR COLORADO

by
Jagannath Mallela, Principal Civil Engineer
Leslie Titus-Glover, Principal Civil Engineer
Suri Sadasivam, Ph.D., Senior Civil Engineer
Biplab Bhattacharya, P.E., Senior Civil Engineer
Michael Darter, Ph.D., P.E., Principal Civil Engineer
Harold Von Quintus, P.E., Principal Civil Engineer

Report No. CDOT-2013-4

Prepared by
Applied Research Associates, Inc.
100 Trade Centre Dr., Suite 200
Champaign, IL 61820-7233
Phone: (217) 356-4500
Fax: (217) 356-3088

Sponsored by the
Colorado Department of Transportation
In Cooperation with the
U.S. Department of Transportation
Federal Highway Administration

July 2013

Colorado Department of Transportation
DTD Applied Research and Innovation Branch
4201 E. Arkansas Ave.
Denver, CO 80222
(303) 757-9506

ACKNOWLEDGEMENTS

The authors would like to thank CDOT's research and pavement management offices for their support on this research. Special thanks are due to Jay Goldbaum for his invaluable support and guidance throughout the study. The authors also wish to thank all project panel members for their availability and contributions at various stages of the research: Bill Schiebel, Robert Locander, John Kacisnki, Masoud Ghalie, Craig Wieden, Rex Goodrich, Gary DeWitt, and Mike Coggins.

EXECUTIVE SUMMARY

The objective of this project was to integrate the American Association of State Highway and Transportation Officials (AASHTO) Mechanistic-Empirical Pavement Design Guide (MEPDG), Interim Edition: A Manual of Practice and its accompanying software ME Pavement Design into the daily pavement design, evaluation, rehabilitation, management, and forensic analysis practices and operations of the Colorado Department of Transportation (CDOT).

Implementing the MEPDG in Colorado involved several major efforts to provide assurance to CDOT that the MEPDG pavement design procedure as a whole and key aspects/components of it (i.e., data inputs, prediction models, reliability, etc.) are compatible with Colorado experience. Implementation comprised of the following major tasks:

- **Verification, validation, and calibration of the MEPDG "global" models with Colorado pavement projects** to (if necessary) remove bias (consistent over- or under-prediction) and improve accuracy of prediction.
- **Design comparisons and sensitivity studies** to establish confidence in the pavement design results achieved when using the MEPDG.
- **Development of Colorado MEPDG Pavement Design Guide** that provides guidance to CDOT engineers and staff on (1) obtaining proper inputs, (2) running the MEPDG, and (3) interpretation of results for the design of new, reconstructed, and rehabilitated pavement structures.

Thus MEPDG implementation comprised of conducting research to (1) verify the MEPDG design procedure (sources of required traffic, climate, materials, design, construction input data, characterization of default inputs, performance criteria and reliability, distress/smoothness prediction, and so on), (2) calibrate the MEPDG procedure to local Colorado conditions if needed, and (3) develop CDOT MEPDG pavement design manual and engineers training materials.

Identification of MEPDG input data sources and characterization of default inputs comprised of (1) traffic, climate, and other pertinent data records assembly and review, (2) materials testing in the lab to determine strength, modulus, and other properties, and (3) field surveys, destructive testing, and non-destructive testing of in-service pavements to assess condition and strength among others. The outcome of this effort was the development of a project database with all key MEPDG input data required for the design and analysis of new and rehabilitated flexible and rigid pavements. One hundred twenty-six new HMA, new JPCP, HMA/JPCP, and unbonded JPCP over JPCP rehabilitated pavement projects located throughout Colorado were used to populate the project database. Collectively the 126 pavement projects represented the design, construction, and performance of Colorado pavements over many years.

The assembled data was used to develop statewide defaults of key MEPDG traffic, materials, design, and climate inputs and for distress/smoothness prediction models verification and calibration. The outcome of the prediction models verification and calibration effort was as follows:

- New and rehabilitated flexible pavements.
    - All four flexible pavement "global" performance models (alligator cracking, rutting, transverse cracking and smoothness (IRI)) were recalibrated for local Colorado conditions.
    - The recalibrated models showed significant improvement in goodness of fit and bias.
- New and rehabilitated jointed plain concrete pavement (JPCP).
    - All three JPCP "global" performance models (transverse cracking, transverse joint faulting, and smoothness (IRI)) were found to be adequate and required no further calibration for local Colorado conditions.
    - The MEPDG "global" models exhibited adequate levels of goodness of fit and bias.

Mathematical equations and algorithms used by the MEPDG to characterize variability in predicted distress and smoothness were also evaluated and revised as needed. Note that variability in predicted distress and smoothness is used as the basis for characterizing the reliability of pavement designs by the MEPDG

With the various MEPDG prediction models verified/calibrated, the next step was to integrate the local Colorado models into the MEPDG design procedure as assess designs produced for reasonableness. This was done by (1) conducting a comprehensive sensitivity analysis of the performance models and (2) performing design comparisons. The outcome of both of these indicated a reasonable set of distress and smoothness prediction models along with the design procedure that produced as expected trends in distress/smoothness predictions and reasonable pavement designs.

Using the outcome of the validation/calibration effort, the research team updated the current CDOT pavement design manual. The updated pavement design manual provides pavement designers and engineers with all the information required for pavement design and analysis using the MEPDG. It also provides guidance on how to develop MEPDG input files, run simulations and analysis, and interpret results. The research team also set up several databases with default CDOT materials, traffic, and climate data for use by CDOT staff in pavement design.

The use of the MEPDG pavement design procedure in Colorado will make it possible to design a pavement with the desired reliability at the optimum cost.

Implementation of the Research Findings

The work effort expended to complete this study has laid the groundwork for changing the pavement design paradigm within CDOT. The work products include this final report and the revised CDOT pavement design manual based on the MEPDG. The following next steps are recommended to advance the implementation of the MEPDG and the AASHTO ME Pavement Design software within CDOT:

- Establish an enterprise-level database of CDOT default inputs to cover performance criteria, reliability, traffic, climate, materials, and soils.
- Conduct 6 to 12 training sessions to train CDOT regions and consultants on the use of the AASHTO Pavement ME Design software in conjunction with the established CDOT inputs database and CDOT's revised pavement design manual.

Another significant activity that is recommended is to use the CDOT's locally calibrated MEPDG procedure to conduct real world pavement designs for approximately one year to (1) identify any issues with the design guidance provided and to complete the necessary revisions (2) advance the Departmental capability maturity with regard to the new procedure, e.g., in troubleshooting problems during the design phase and (3) develop a wider and acceptance of the procedure within the agency.

TABLE OF CONTENTS

LIST OF FIGURES

LIST OF TABLES

LIST OF ABBREVIATIONS

AADTT	Average annual daily truck traffic
AASHTO	American Association of State Highway and Transportation Officials
AC	Asphalt concrete
ALD	Axle load distribution
ATB	Asphalt treated base
ATLAS	Advanced Traffic Loading Analysis System
ATR	Automated traffic recorder
CAPA	Colorado Asphalt Pavement Association
CCC	Cubic clustering criterion
CDOT	Colorado Department of Transportation
CPR	Concrete pavement restoration
CRCP	Continuously reinforced concrete pavement
CTB	Cement treated base
CTE	Coefficient of thermal expansion
DGAB	Dense graded asphalt base
ESAL	Equivalent single axle load
FHWA	Federal Highway Administration
FWD	Falling Weight Deflectometer
HMA	Hot-mix asphalt
HWT	Hamburg Wheel Tracking
IDT	Indirect tensile
IRI	International Roughness Index
JPCP	Jointed plain concrete pavement
JTCP	Joint Technical Committee on Pavements
LCB	Lean concrete base
LTPP	Long Term Pavement Performance
MAF	Monthly adjustment factor
MEPDG	Mechanistic-Empirical Pavement Design Guide
NCDC	National Climatic Data Center
NCHRP	National Cooperative Highway Research Program
NRCS	National Resources Conservation Service
NWS	National Weather Service
OTIS	Online Transportation Information System
PATB	Permeable asphalt treated base
PCC	Portland cement concrete
PMA	Polymer modified asphalt
PSF	Pseudo F
PSI	Present serviceability index
PST2	Pseudo t2
QA	Quality assurance
QC	Quality control
R^2	Coefficient of determination
RLPD	Repeated load permanent deformation

SEE	Standard error of estimate
SMA	Stone matrix asphalt
SSURGO	Soil Survey Geographic (database)
USDA	United States Department of Agriculture
VAR	Variance
Vbeff	Volumetric moisture content
VFA	Voids filled with asphalt
VMA	Voids in mineral aggregate
WIM	Weigh-in-motion

CHAPTER 1. INTRODUCTION

Background

For many years, the Colorado Department of Transportation (CDOT) has used the 1993 American Association of State Highway and Transportation Officials (AASHTO) *Guide for Design of Pavement Structures* and the 1998 supplement to design new and rehabilitated flexible and rigid pavements (AASHTO 1993, AASHTO 1998). The 1993 AASHTO Pavement Design Guide originated from empirical pavement design equations developed in the late 1950s using pavement performance data collected under a national research program known as the AASHO Road Test (HRB 1962). Over the years, several editions of the AASHTO design guide have been published (AASHTO 1961, AASHTO 1972, AASHTO 1986, AASHTO 1993, AASHTO 1998).

The original empirical pavement design equations were improved over the years to address, as much as possible, identified weaknesses in the design procedure. Table 1 summarizes these identified weaknesses, such as (1) the absence of sophisticated materials and traffic loading characterizations algorithms and (2) the lack of algorithms that relate applied truck axle load with pavement mechanical responses that lead to the development and progression of damage, distresses, and smoothness loss.

Although these design guides have served as the primary tool for pavement design in the U.S. and beyond for many decades, and they have been used successfully to design many types of pavements, the inherent weaknesses of the design procedure have resulted in designs of many pavement structures that have under-performed or have failed prematurely. In 1996, the AASHTO Joint Technical Committee on Pavements (JTCP) proposed a shift from empirical-based to mechanistic-based pavement design. This was to be done through the development of a new pavement design guide based on mechanistic principles for the design of new and rehabilitated pavement structures.

Key aspects of mechanistic principles to be included in the new pavement design technology included (ARA 2004):

- Mechanistically characterizing paving materials properties (asphalt concrete, portland cement concrete, chemically stabilized unbound granular and soil materials) accurately and in real time.
- Simulating ambient temperature and moisture conditions and their interaction with pavement material properties.
- Simulating truck traffic loading and forecasting growth.Mechanistically calculating pavement response (i.e., stresses, strains, and deflections) due to traffic loadings for various environmental conditions.
- Relating pavement response to incremental damage and deterioration.
- Accumulating incremental pavement damage over time and relating accumulated pavement damage empirically to distress development and progression (cracking, rutting, faulting, punchouts, etc.).

Table 1. Summary of identified weaknesses in the 1961 through 1998 AASHTO pavement design procedures (ARA 2004, FHWA/NHI 2006).

Identified Weakness	Description & Remedial Action
Traffic characterization	(1) Description: a. Equivalent 18-kip single axle load (ESAL) was used to characterize the traffic loading. It is doubtful that the equivalency factors developed at the AASHO Road Test are applicable to today's traffic stream (combination of axle load levels and types of axles). b. Heavy truck traffic levels have increased tremendously since the 1960s. Interstate pavements were designed in the 1960s for 5 to 10 million ESALs, while the AASHO Road Test pavements carried approximately 1 million axle load applications. Today, interstate pavements are designed for 50 to 200 million axle loads or more. Thus, it is not realistic to expect the original empirical pavement design models to design for today's level of traffic without extrapolating the design methodology far beyond the original traffic inference space. Highly trafficked projects are thus likely to be under- or over-designed (see Figure 1) (2) Remedial action: None
Design	(1) Description: a. Shoulder type/edge support for rigid pavements: Gravel shoulders were used at the AASHO Road Test, so full-width paving effects are not adequately considered. b. Pavement subdrainage: Original flexible pavements were built in a "bathtub," resulting in a very poor subdrainage condition that was reflected in the pavement design models. c. Joint deterioration: For jointed rigid pavements, joint deterioration (characterized mostly in terms of load transfer efficiency (LTE)) and its impact on future pavement performance was not directly considered d. Rehabilitation: The AASHO Road Test included only new flexible and rigid pavements. Rehabilitated pavement was not considered. (2) Remedial action: a. The 1986 Pavement Design Guide introduced guidance for the design of subsurface drainage systems and modified the flexible and rigid pavement design equations to take advantage of improvements in performance due to good drainage. The benefits of drainage were incorporated into the structural number via the empirical drainage coefficients m and Cd. b. The 1986 Pavement Design Guide introduced a methodology for assessing the effects of environment on pavement performance. Specific emphasis is given to frost heave, thaw-weakening, and swelling of subgrade soils. c. The 1986 Pavement Design Guide introduced the J-factor representing joint load transfer. d. The 1993 Pavement Design Guide included a methodology for rehabilitation designs for flexible and rigid pavement systems using overlays. e. The 1998 supplement to the 1993 Pavement Design Guide provided an improved method for rigid pavement design.

Table 1. Summary of identified weaknesses in the 1961 through 1998 AASHTO pavement design procedures, continued (ARA 2004, FHWA/NHI 2006).

Identified Weakness	Description & Remedial Action
Materials characterization	(1) Description: a. Asphalt concrete: New, improved asphalt mixtures such as SuperPave, stone matrix asphalt, polymer-modified asphalt, etc., are not directly incorporated into the empirical design model. b. Base/subbase layers: A dense crushed unbound limestone aggregate base was used at the AASHO Road Test. The subbase layer was uncrushed and unbound gravel/sand. The unbound aggregate base/subbase produced a generally impervious granular "bathtub" that experienced significant loss of support during spring thaw, resulting in greater deterioration rates than typical. c. Durability: There were few material durability problems (such as asphalt stripping and corrosion of steel in concrete) over the 2-year AASHO Road Test period. Thus, the effect of long-term material durability on performance was not considered. (2) Remedial action: a. The 1972 Pavement Design Guide presented guidance for estimating structural layer coefficients a1, a2, and a3 for materials other than those at the AASHO Road Test. These guidelines were based primarily on a survey of state highway agencies regarding the values for the layer coefficients that they were currently using in design for various materials. The 1972 Pavement Design Guide recommends that, "because of widely varying environments, traffic, and construction practices, it is suggested that each design agency establish layer coefficients applicable to its own experience." b. The 1986 Pavement Design Guide introduced the resilient modulus for determining the structural layer coefficients for both stabilized and unstabilized unbound materials in flexible pavements.
Foundation characterization	(1) Description: Pavements at the AASHO Road Test site were constructed over a single silty-clay (AASHTO A-6) subgrade. The effect of this single subgrade was "built into" the empirical design models. (2) Remedial action: a. The 1972 Pavement Design Guide included an empirical soil support scale to reflect the influence of local foundation soil conditions for flexible pavements. This scale ranged from 1 to 10, with a soil support value Si of 3 corresponding to the silty clay foundation soils at the AASHO Road Test site and the upper value of 10 corresponding to crushed rock base materials. All other points on the scale were assumed from experience, with some limited checking through theoretical computations. b. For rigid pavements, the use of the Spangler/Westergaard theory for stress distributions in rigid slabs to incorporate the effects of local foundation soil conditions was added to the 1972 Pavement Design Guide to extend the rigid pavement design methodology to soil conditions other than those at the AASHO Road Test. Foundation soil conditions were characterized by the overall modulus of subgrade reaction, k, which is a measure of the stiffness of the foundation soil. c. The 1986 Pavement Design Guide introduced the use of the resilient modulus, Mr, as a stiffness parameter for characterizing the soil support provided by the subgrade. Mr is a measure of the resilient modulus of the soil recognizing certain nonlinear characteristics. d. The 1986 Pavement Design Guide introduced the use of nondestructive deflection testing for evaluating existing pavement and backcalculation of layer moduli.

Table 1. Summary of identified weaknesses in the 1961 through 1998 AASHTO pavement design procedures, continued (ARA 2004, FHWA/NHI 2006).

Identified Weakness	Description & Remedial Action
Empirical nature of pavement design equations	(1) Description: A combination of graphical techniques and least squares regression was used to develop the empirical pavement equations using approximately 2 years of pavement performance data. The original models have been "extended" over time based on empirical concepts, most of which have not been verified with field data. The procedure cannot solve for the required thickness of hot-mix asphalt (HMA), only structural number, which can lead to serious design deficiencies. (2) Remedial action: None
Functional form of empirical pavement models	(1) Description: The form of the mathematical models used to fit the performance data collected at the AASHO Road Test (i.e., 2 years of gradually sloping downward serviceability trends) does not appear to fit the shape of the long-term performance trends of many in-service pavements that have demonstrated the opposite shape (i.e., they show more rapid loss of serviceability in the initial years, before leveling off)—see Figure 2. (2) Remedial action: None
Climate	(1) Description: The pavement design models were developed over a 2-year period at the AASHO Road Test site in northern Illinois; thus, they have been calibrated for just one climatic condition and 2 years of climatic cycles, both of which are serious limitations of the procedure. (2) Remedial action: a. In 1972, an empirical regional factor, R, was introduced to provide an adjustment to the flexible pavement structural number for local environmental and other considerations. Values for the regional factor were estimated from serviceability reduction rates in the AASHO Road Test. These estimates varied between 0.1 and 4.8, with an annual average value of about 1.0. The regional factor was not recommended for special conditions, such as serious frost conditions, or other local problems. b. The ability to adjust for other climates was included in the original models through the addition of a drainage coefficient in 1986. The drainage coefficient, however, includes only a portion of the effect of climate (i.e., moisture, not temperature or freeze-thaw cycles). Highways loaded in other climates would have different rates of deterioration.

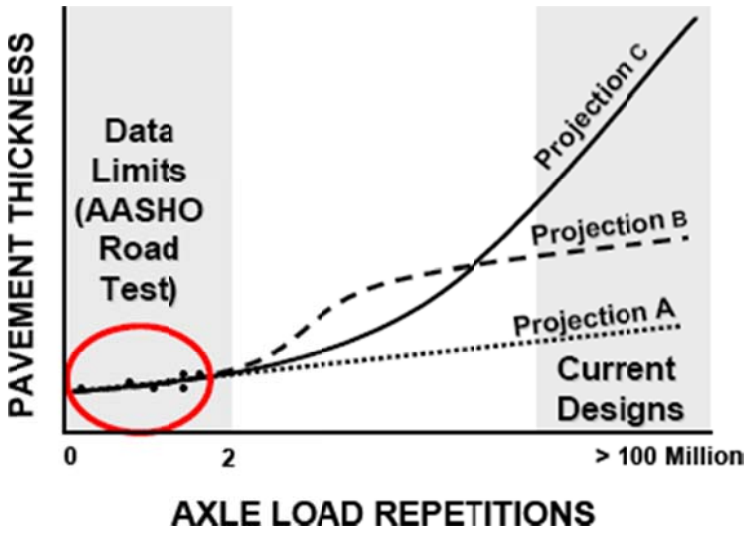

Figure 1. Extrapolation of traffic levels in current AASHTO pavement design procedures (FHWA/NHI 2006).

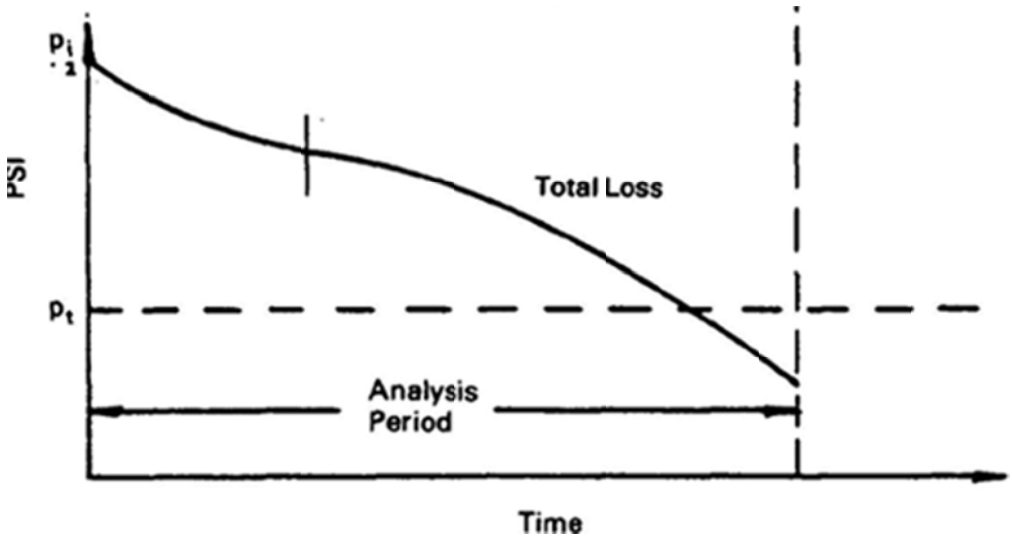

Figure 2. Plot showing change in pavement serviceability versus time (FHWA/NHI 2006).

- Relating distress development and progression to smoothness loss.
- Calibrating the theoretical models to field-observed distresses and smoothness.
- Providing realistic design reliability prediction for selected key performance criteria.
- Developing realistic and uniform guidelines for designing new and rehabilitated flexible, rigid, and composite pavements.

Work on the new pavement design guide, called the Mechanistic-Empirical Pavement Design Guide (MEPDG), was concluded under National Cooperative Highway Research Program (NCHRP) Project 1-37A—Development of the 2002 Guide for Design of New and Rehabilitated Pavement Structures—in 2004. The new pavement design methodology consisted of several NCHRP Research Reports and pavement design manuals and accompanying research-grade pavement design software (ARA 2004).

The 2004 version of the MEPDG has undergone several independent reviews and refinements since initial completion. AASHTO adopted the revised MEPDG in 2007 as an interim standard for pavement design in the U.S. The following professional versions of the research products have since been developed (AASHTO 2008, AASHTO 2013):

- *Mechanistic-Empirical Pavement Design Guide, Interim Edition: A Manual of Practice*.
- AASHTOWare Pavement ME Design.

Pavement ME Design uses state-of-the-practice mechanistic-based pavement analysis and distress prediction algorithms. The distress prediction models were calibrated using field-observed distress and International Roughness Index (IRI) data from several hundred experimental flexible, rigid, and composite in-service pavements located throughout the U.S. as part of the Federal Highway Administration (FHWA) Long Term Pavement Performance (LTPP) database and other national databases (e.g., MnROAD). These models are hence termed "global" calibrated models.

Overview of the AASHTO's Pavement ME Design

Pavement ME Design can be used to design or perform forensic analysis of 17 new and rehabilitated pavement types, namely (AASHTO 2008):

- New or reconstructed HMA pavement.
- New or reconstructed jointed plain concrete pavement (JPCP) and continuously reinforced concrete pavement (CRCP).
- Rehabilitation with HMA—HMA overlay on existing HMA, JPCP, or CRCP.
- Rehabilitation with portland cement concrete (PCC)—Bonded or unbonded JPCP overlay of existing JPCP, CRCP, and flexible pavement.
- Rehabilitation with PCC—Bonded or unbonded CRCP overlay of existing JPCP or CRCP.
- Rehabilitation with PCC—JPCP or CRCP overlay of existing HMA.
- JPCP rehabilitation—Concrete pavement restoration (CPR) and diamond grinding.

The Pavement ME Design approach is presented in Figure 3.

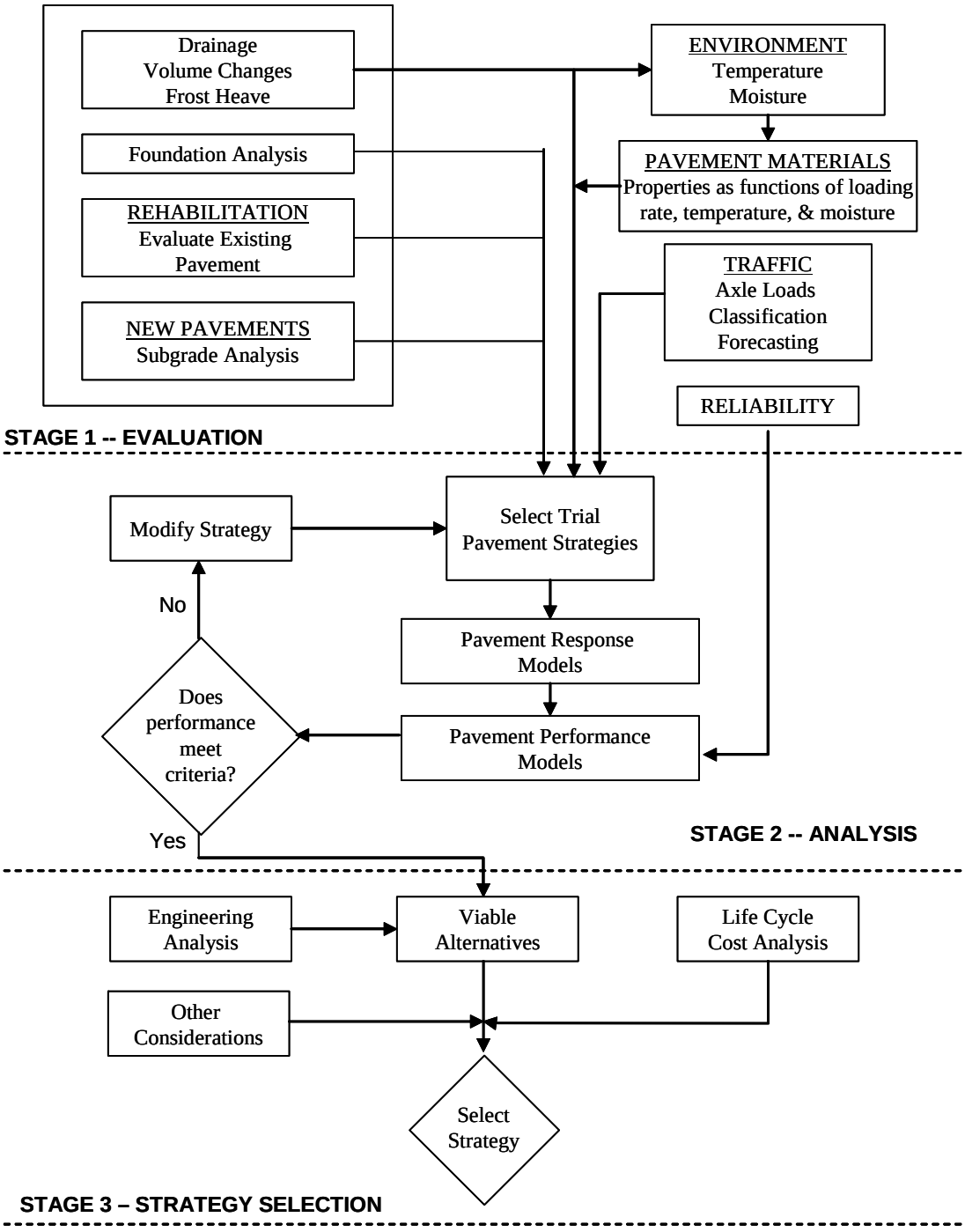

Figure 3. Pavement ME Design pavement design methodology.

The Pavement ME Design approach involves the following (AASHTO 2008):

- Development of input values. For the analysis, establishment of performance criteria (not-to-exceed distress thresholds) and associated design reliability levels for each criterion.
- Structural/performance analysis. The analysis approach is an iterative one that begins with the selection of an initial trial design. The trial section is analyzed incrementally over time using the pavement response and distress models, and the outputs of the analysis are accumulated damage (the expected amount of distress and smoothness over time). If the trial design does not meet the performance criteria, modifications are made and the analysis re-run until a satisfactory result is obtained. An optimization routine is available to solve for adequate thickness of the HMA and PCC layers and other factors.
- Activities required for evaluating structurally viable design alternatives. These activities include an engineering analysis and life cycle cost analysis of the alternatives.

Pavement ME Design provides a uniform and comprehensive set of procedures for the design of new and rehabilitated flexible and rigid pavements. It employs common design parameters for traffic, subgrade, climate, and reliability for all pavement types. Recommendations are provided for the structure (layer materials and thickness) of new and rehabilitated pavements, including procedures to select pavement layer thickness, rehabilitation treatments, subsurface drainage, foundation improvement strategies, and other design features. The procedures can be used to develop alternate designs using a variety of materials and construction procedures.

The benefits of Pavement ME Design are many, and they will impact all levels of pavement operation, from planning through design and construction, to ongoing maintenance and rehabilitation, to eventual reconstruction. The major benefits are summarized as follows (AASHTO 2008):

- Ability to assess the impact of new and innovative pavement materials (asphalt binders, recycled aggregates, etc.) on pavement performance.
- Ability to assess the impact of aging and long-term durability of materials on performance.
- Distress/IRI prediction models far superior to current empirical serviceability prediction models.
- Design reliability approach is sound at low and high traffic levels.
- More cost-effective designs (through better handling of reliability and better handling of the interactions between materials and site factors).
- Fewer premature pavement failures caused by deficient design and materials (the MEPDG allows the user to analyze “what if” scenarios to quantify the impact of design assumptions of pavement life).
- Less likelihood of very thick over-design for heavy traffic (currently caused by deficient empirical equations based on a few million trucks at the AASHO Road Test).
- Improved tool for innovative contracting, assessing effects of substandard quality of construction, etc.

- Improved tool for highway cost allocation studies, pavement management, etc.
- Improved tool for specialized designs (impacts of special truck loadings, cold temperatures, high groundwater table, etc.).

MEPDG Implementation in Colorado

CDOT has been preparing for the implementation of the MEPDG since 2001, when CDOT and the Colorado Asphalt Pavement Association (CAPA) initiated a project to develop a road map for implementing the MEPDG flexible pavement design and analysis procedure in Colorado. The road map was developed from a series of facilitated meetings between CDOT, CAPA, and industry representatives. An analogous rigid pavement design road map also was also developed in 2001. These road maps were updated and refined in 2007 and served as a guide for implementing version 1.0 of the MEPDG.

Objective of Study

The objective of this study is to provide all information and documents necessary for CDOT and industry to use the latest MEPDG software (Pavement ME Design) on a day-to-day basis for the design and analysis of new and rehabilitated pavement structures in Colorado.

Scope of Study

The following activities and products were developed during the course of the project to achieve the study objective:

1. Identify resources needed to implement the MEPDG.
2. Validate and calibrate version 1.0 of the MEPDG specific to Colorado site conditions, materials, and typical design features used to construct new pavements and rehabilitate existing pavements.
    a. Confirm or adjust input default values for Colorado conditions.
    b. Confirm or adjust the calibration coefficients to avoid biased designs.
    c. Recommend any changes in policy and procedure that will be needed.
3. Prepare a design manual and other documents to establish consistent use of the MEPDG and resulting designs.
4. Recommend design reliability levels and performance criteria levels for design of various highway classes.
5. Establish traffic and materials libraries that are representative of the truck traffic and paving materials found in Colorado. These libraries will facilitate the use of consistent inputs and provide ease of use by importing specific inputs into the MEPDG that are representative of Colorado roadways.
6. Provide training on the use of the verified and calibrated MEDPG, along with training materials that CDOT can continue to use and update for future reference.

Organization of Report

This report documents work done under this project, specifically the tasks listed below, that resulted in implementation of the MEPDG in Colorado:

- Task 0 – Project kick-off meeting and coordination task.
- Task 1 – Database development.
- Task 2 – Field investigations and laboratory materials testing.
- Task 3 – Verification of current MEPDG.
- Task 4 – Local calibration and validation of performance models.
- Task 5 – Development of CDOT MEPDG design manual.
- Task 6 – Deployment of concurrent designs during transition to MEPDG method.
- Task 7 – Development of default input libraries.
- Task 8 – Training program delivery.
- Task 9 – Preparation and submittal of the draft final and final reports.

Chapter 2 describes the framework utilized for MEPDG global models validation and local calibration (if needed) for Colorado conditions. The framework was adapted after the guidelines presented in the AASHTO *Guide for the Local Calibration of the Mechanistic-Empirical Pavement Design Guide* (AASHTO 2010).

Chapter 3 describes the development of experimental and sampling plan for Colorado MEPDG models validation/calibration, while chapter 4 describes project selection and development of the validation/calibration database. Chapter 4 also provides a full and detailed description of CDOT traffic, climate, and materials test data used to develop default libraries, along with records review, data assembly and cleansing, and laboratory/field testing done as part of the database development effort.

Chapter 5 presents a detailed description of the statistical analysis performed to validate and calibrate the MEPDG models and design procedure for Colorado conditions. Chapter 6 presents work done to validate the new local MEPDG models and design procedure for Colorado (sensitivity analysis and design comparisons).

Chapter 7 summarizes the work done under this project and the outcomes. Recommendations for future work are also presented in this chapter. Appendix A presents details of the MEPDG distress and IRI models for the pavement types of relevance to this project.

CHAPTER 2. FRAMEWORK FOR LOCAL CALIBRATION OF THE MEPDG IN COLORADO

This chapter presents a framework for local calibration of the MEPDG. It is adapted after the AASHTO *Guide for the Local Calibration of the Mechanistic-Empirical Pavement Design Guide* (AASHTO 2010). In all, model validation and local calibration consists of the 11 steps described in this chapter.

Step 1: Selection of Hierarchical Input Level for Each Input Parameter

The AASHTO MEPDG Manual of Practice describes hierarchical input levels as follows (AASHTO 2008):

- Level 1 inputs provide for the highest level of accuracy and, thus, would have the lowest level of uncertainty or error. Level 1 material inputs require laboratory or field testing, such as the dynamic modulus testing of HMA, site-specific axle load spectra data collections, or nondestructive deflection testing.
- Level 2 inputs provide an intermediate level of accuracy and would be closest to the typical procedures used with earlier editions of the AASHTO Pavement Design Guide. Level 2 inputs typically would be user-selected, possibly from an agency database, could be derived from a limited testing program, or could be estimated through correlations such as using R-value to estimate resilient modulus.
- Level 3 inputs provide the lowest level of accuracy. Inputs typically would be user-selected values based on national averages, engineering experience, or typical averages of an input for the region or state.

For MEPDG model validation and local calibration, the AASHTO local calibration guide recommends selecting an appropriate mix of MEPDG hierarchical input levels (1 through 3) consistent with the agency's day-to-day practices for characterizing pavement inputs for design. If good Level 3 and Level 2 procedures and recommendations are developed during local calibration, these inputs should provide reasonable designs. Of course, the more Level 1 inputs, the better.

In addition, inputs found to have a major impact on MEPDG distress/IRI predictions must be characterized as accurately as possible using the highest possible hierarchical input level. This is because the mix of hierarchical input levels used for models calibration ultimately has a major impact on predicted distress/IRI standard error or deviation. Predicted distress/IRI standard error is a key component of the variability terms used in calculating design reliability. The models' standard error was derived using inputs derived from all three levels; however, there was a considerable proportion of Level 1 and 2 inputs for all of the projects used in calibration.

Step 2: Develop Local Experimental Plan and Sampling Template

A detailed, statistically sound experimental plan/sampling template is required for use in identifying and selecting Colorado pavement projects for use in MEPDG model validation and local calibration. The experimental plan was designed to ensure the following:

- Determine bias in MEPDG distress/IRI predictions (using national coefficients).
- Establish cause of bias, if present.
- Determine local calibration coefficients for each distress/IRI model with identified bias. The new model local calibration coefficients must be established to reduce bias and maximize accuracy.

A key aspect of the experimental/sampling template was to ensure that it could be used to obtain a mix of pavement projects that reflect current and future CDOT pavement types, design features, material types, and site conditions. Key factors used in defining the sampling template are:

- Pavement type.
- Surface layer thickness.
- Climate zone.
- Base and subgrade type.
- Asphalt concrete (AC) mix binder type.
- Rigid pavement design features (load transfer mechanism, edge support, etc.).
- Truck traffic applications level.

Once the sampling template was defined, attempts were made to obtain an adequate number of pavement projects to populate each cell within the sampling template (i.e., a full factorial balanced factorial with replicate pavement projects within each populated cell). Where this was not possible, a fractional balanced factorial was adopted and used, as it was too costly to fully populate all cells with projects.

Step 3: Estimate Sample Size for Specific Distress/IRI Prediction Models

Under this step the minimum number of projects required to validate/calibrate the MEPDG global models was determined. The minimum sample size in theory was to be determined separately for each distress/IRI prediction model. However, in practice the maximum number of projects required for each pavement type is adopted. The AASHTO Guide for the Local Calibration of the MEPDG provides recommendations for determining sample size and this was adopted for this project.

Step 4: Select Pavement Projects

Once the required minimum number of projects for local calibration/validation is determined the next step is to identify local projects to populate the sampling template. Potential of sources of pavement projects are presented as follows:

- National and local research/experimental test pavements.
- Pavement management sections in general.

The candidate projects must be reviewed for selection based on criteria described in steps 1 through 3, including:

- Historical distress/IRI of selected projects should cover the reasonable range of values typical for Colorado (including the threshold values).
- As much as possible, they must be representative of current and future CDOT pavement design and construction practices.
- They must be representative of Colorado site (traffic, climate, and subgrade) conditions.

In general, the selected projects must have the fewest number of structural layers. For rehabilitated pavements, projects with detailed historical distress/IRI data before and after rehabilitation must be given a higher priority. Projects with unconventional designs and material types must be selected only if they represent anticipated future designs.

Step 5: Extract and Evaluate Distress and Project Data

This step involves the following four activities:

1. Extract, review, and convert historical measured distress/IRI data for each identified project into the units predicted by the MEPDG. This involves assembling relevant historical measured distress and smoothness data for the selected projects from agency pavement management system data tables, research reports, research-type experimental projects databases, and so on. The assembled data are then reviewed for accuracy, reasonableness, and consistency. As needed, the raw distress/IRI data as measured and reported are converted into the MEPDG reporting units for each performance indicator. Note that the MEPDG distress and smoothness predictions are defined according the *LTPP Distress Identification Manual* (Miller & Bellinger 2003).
2. Compare performance indicator magnitudes to the design threshold values (see Table 2).
    a. This involves a comparison of the magnitudes of the design threshold values and historical distress/IRI measurements from the selected projects. The goal is to determine whether measured distress/IRI to be used in calibration/validation cover the agency's design threshold values. Using projects with historical measured distress/IRI values close to the design threshold values ensures that the models are calibrated/validated to predict distress/IRI accurately within the range of distress/IRI of greatest importance to the agency.
    b. Each project was assigned the same weight during statistical analysis (calibration/validation). Assigning the same weight implies that repeated distress/IRI measures of each project will be approximately the same. A key step is to determine the number of distress/IRI records available for each selected project. Once this is done, possible significant differences in the number of records available must be noted for corrective action to be taken as part of statistical analysis.

3. Evaluate the distress data to identify anomalies and outliers. Bivariate plots of distress and IRI versus pavement age must be developed for each project and distress/IRI performance indicator. Each plot is then reviewed and evaluated. The review is limited to visual inspection of time series plots showing the progression of distress and IRI to (1) determine if observed trends in distress/IRI progression are reasonable, (2) identify potential anomalies (e.g., significant decrease in distress/IRI magnitude indicating an occurrence of significant rehabilitation or maintenance event), and (3) identify potential outliers. The results of this exercise serve to:
    a. Identify projects exhibiting unreasonable trends in distress/IRI progression and correct the anomalies identified, if possible. Otherwise, the project is removed from the project database for the given anomalous performance indicator. It must be noted that each distress type and IRI were treated separately; thus, removal of a project from, say, the rutting database does not imply that it was also removed from the transverse cracking database.
    b. Individual distress/IRI observations identified as outliers or erroneous are removed. Examples include zero measurements that could represent non-entry values and significantly high or low distress/IRI values deemed unreasonable.
    c. Individual distress/IRI observations measured after the performance of a significant maintenance or rehabilitation event that altered the design of the pavement or condition of the pavement significantly were removed.
4. Extract, review, and assemble all MEPDG inputs required for project distress/IRI predictions. The MEPDG requires several categories of input data. For this project, data were obtained primarily from two sources: the LTPP database and CDOT databases (e.g., traffic, materials, performance). Additional data to complement these data sources were obtained from the MEPDG, National Climatic Data Center (NCDC), and the United States Department of Agriculture (USDA) Natural Resources Conservation Service (NRCS) Soil Survey Geographic (SSURGO) database. Following the data assembly, review, and cleanup effort, the final selection of projects with adequate detailed information for validation and local calibration is completed.

Table 2. Summary of distress/IRI thresholds (AASHTO 2008).

Pavement Type	Performance Indicator	Performance Indicator Threshold (@ 90 Percent Reliability) (σ)
New HMA and HMA-overlaid HMA	Alligator cracking	=< 20 percent lane area
	Transverse "thermal" cracking	Crack spacing =< 100 ft of 630 ft/mi
	Rutting	=< 0.4 in
	IRI	=< 169 in/mi
New JPCP and CPR	Faulting	=< 0.15 in
	Transverse cracking	=< 10 percent slabs
	IRI	=< 169 in/mi

Step 6: Conduct Field and Forensic Investigations

Field and forensic investigations are done to obtain additional information on the selected pavement projects as needed to complete the project database. Key information typically acquired from field and forensic investigations includes (1) subgrade/foundation strength and modulus, (2) visual distresses present at the pavement surface and nature of these distresses (top-down vs. bottom-up cracking and distribution of rutting with the pavement layers), (3) layer thicknesses, and (4) AC/PCC material properties.

Field investigation mostly includes pavement visual condition survey, nondestructive pavement deflection testing, laboratory analyses of cored/bulk material, and review of a pertinent geotechnical exploration report conducted independently by others. These data typically are augmented with laboratory evaluation of material samples obtained from cores and bulk specimens to document and characterize surface and subsurface materials and load-bearing conditions beneath and within the pavements and trenches. Note that if data inputs obtained from the various databases along with default MEPDG and CDOT inputs are deemed reasonable and adequate, field or forensic investigation will not be required.

Field and forensic investigations typically comprise the following:

- Development of materials sampling and testing plan to obtain missing data or validate/confirm existing data. This plan typically is developed after a thorough review to determine what types of data are available and of good quality, data available of dubious quality, and data not available. Once this is established, the material plan is developed to obtain all missing data and performing limited amounts of testing to determine the accuracy and reasonableness of data of dubious origins.
- Determination of whether forensic investigations are required. Forensic investigations typically are conducted to determine problems with the pavement substructure (cracking type present, rutting in subgrade, materials failure, and so on). Pavements with suspected substructure issues are candidates for forensic investigations; otherwise, this step is not required. Regardless of individual project issues, there generally is a need to perform a few such investigations to test MEPDG assumptions, such as the percentage of rutting that occurs in each pavement layer (surface AC, base, and subgrade) or whether AC transverse cracking are thermal cracks or otherwise (e.g., shrinkage or reflected cracks).

Step 7: Assess Local Bias—Validation of Global Calibration Values to Local Conditions, Policies, and Materials

This step involves:

1. Developing MEPDG input files for each of the selected projects.
2. Developing measured distress, IRI, and corresponding pavement age for each of the selected projects.
3. Executing the MEPDG for each selected project and predicting pavement distresses and IRI (at 50 percent reliability) over the life of the project.

4. Extracting predicted distress and IRI data from the MEPDG outputs that match measured distress and IRI (step 2).
5. Performing statistical analysis to validate the model.

Bias is defined as the consistent under- or over-prediction of distress/IRI. The presence or absence of bias between measured and predicted distress/IRI was determined by performing linear regression, hypothesis tests, and a paired t-test using a significance level of 0.05 or 5 percent, as described below:

- Develop a linear regression model to define the relationship between the dependent variable, MEPDG-predicted distress/IRI (Y variable), and the explanatory variable, measured distress/IRI (X variable), as shown in Figure 4.

$$Y_i = b_0 + m(X_i) \quad (1)$$

- Hypothesis 1: Determine whether the linear regression model developed using measured and MEPDG predicted distress/IRI has an intercept (b_0) of zero:
    a. Using the results of the linear regression analysis, test the following null and alternative hypotheses to determine if the fitted linear regression model has an intercept (b_0) of zero:
        i. H_0: $b_0 = 0$.
        ii. H_A: $b_0 \neq 0$.

    A rejection of the null hypothesis (p-value < 0.05) would imply the linear model had an intercept significantly different from zero at the 5 percent significant level. This indicates that using the distress/IRI model within the range of very low measured distress/IRI values will produce biased predictions.

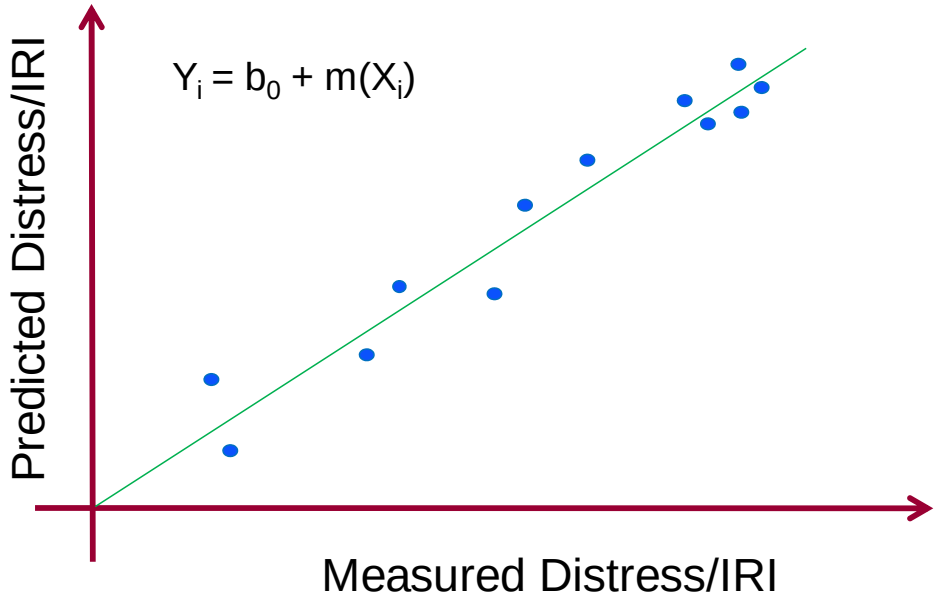

Figure 4. Example of relationship between measured and predicted distress/IRI.

- Hypothesis 2: Determine whether the linear regression model developed using measured and MEPDG predicted distress/IRI has a slope (m) of 1.0:
    a. Using the results of the linear regression analysis, test the following null and alternative hypothesis to determine if the fitted linear regression model has an slope (m) of 1.0:
        i. H_0: m = 1.0.
        ii. H_A: m ≠ 1.0.

        A rejection of the null hypothesis (p-value < 0.05) would imply that the linear model has a slope significantly different from 1.0 at the 5 percent significant level. This indicates that using the distress/IRI model outside the range of measured distress/IRI used for analysis will produce biased predictions.
- A third hypothesis test (Hypothesis 3: Paired t-test) was done to determine whether the measured and MEPDG predicted distress/IRI represented the same population of distress/IRI. The paired t-test was performed as follows:
    a. Perform a paired t-test to test the following null and alternative hypothesis:
        i. H_0: Mean measured distress/IRI - mean predicted distress/IRI = 0.
        ii. H_A: Mean measured distress/IRI - mean predicted distress/IRI ≠ 0.

        A rejection of the null hypothesis (p-value < 0.05) would imply the measured and MEPDG distress/IRI are from different populations. This indicates that, for the range of distress/IRI used in analysis, the MEPDG model will produce biased predictions.

A rejection of any of the three null hypotheses indicates some form of bias in predicted distress/IRI. Models that successfully passed all three tests were deemed to be unbiased. The presence of bias does not necessarily imply that the prediction model is inadequate and cannot be deployed for use in analysis. It only means that there is some bias present along the range of possible distress/IRI predictions. For example, the IRI models may produce unbiased predictions for the typical IRI range of 30 to 250 in/mi. The same model may, however, produce biased predictions for measured IRI values close to zero. Such a model can be used without modifications through local calibration.

Step 8: Eliminate Local Bias of Distress and IRI Prediction Models

The process to eliminate significant bias resulting from the use of the MEPDG global models begins with attempting to find the cause of bias. In general, this is done by performing the steps presented in Table 3. The MEPDG model global/local calibration coefficients that can be modified to reduce bias are presented in Tables 4 and 5.

Table 3. Process for minimizing bias in MEPDG predicted distress/IRI.

Step	Identification of Cause of Bias	Remedial Action
1	Examine predicted versus measured distress/IRI plot for each individual project and identify projects for which predicted and measured distress/IRI varies significantly.	If these projects are less than, say, 10 percent of the total, examine them thoroughly for erroneous inputs and assumptions. Erroneous inputs and assumptions may be the cause of erroneous predictions of distress/IRI leading to significant bias. Once these are identified and corrected, repeat the process and check if significant bias is still present. If bias is eliminated, adopt the global coefficients for use. Otherwise, modify global/local coefficients as needed to eliminate significant bias.
2	Identify key input variables that impact each distress type and IRI and develop a plot of residuals (i.e., predicted – measured distress or IRI) versus the given key input variable. Check the plots for trends. The presence of trends (e.g., increase in residuals corresponds to increase in PCC thickness) is an indicator of over or under prediction of distress or IRI with change in PCC thickness.	Identify the global/local coefficients that most impact the key inputs that relate to bias. Modify the global/local coefficients as needed to eliminate significant bias.
3	Determine if bias is just random and cause cannot be assigned.	Modify global/local coefficients as needed to eliminate significant bias.

Table 4. Recommendations for modifying MEPDG flexible pavement distress/IRI models global/local coefficients to eliminate bias.

Distress	Eliminate Bias	Reduce Standard Error
Alligator cracking	C_2, k_{f1}	C_1 and k_{f2}, k_{f3}
Rutting (all layers)	k_{r1}, β_{s1}, β_{r1}	k_{r2}, k_{r3} and β_{r2}, β_{r3}
Transverse cracking	β_{f3}	β_{f3}
IRI	C_4	C_1, C_2, C_3

Table 5. Recommendations for modifying MEPDG JPCP distress/IRI models global/local coefficients to eliminate bias.

Distress	Eliminate Bias	Reduce Standard Error
Faulting	C_1 through C_7	C_1 through C_7
Transverse cracking	C_1, C_2	C_1, C_2
IRI	C_1 through C_4	C_1 through C_4

Step 9: Assess the Standard Error of the Estimate

After significant bias is eliminated, models coefficient of determination (R^2) and standard error of the estimate (SEE) is computed using the local calibration coefficients to evaluate new calibrated models goodness of fit. The new model's R^2 and SEE is then compared to the MEPDG global calibration R^2 and SEE (see Table 6). Engineering judgment is then used to determine the reasonableness of both diagnostic statistics. Models exhibiting a poor R^2 (i.e., R^2 less than 50 percent) or excessive SEE (significantly higher than the values presented in Table 5) are deemed as having a poor goodness of fit.

Table 6. Summary of MEPDG global models statistics.

Pavement Type	Performance Model	Model Statistics		
		Coefficient of Determination, R^2	Standard Error of Estimate, SEE	Number of Data Points, N
New HMA	Alligator cracking	0.275	5.01 percent	405
	Transverse "thermal" cracking	Level 1*: 0.344 Level 2*: 0.218 Level 3*: 0.057	—	—
	Rutting	0.58	0.107 in	334
	IRI	0.56	18.9 in/mi	1926
New JPCP	Transverse "slab" cracking**	0.91	4.93 percent	1676
	Transverse joint faulting**	0.54	0.031 in	1198
	IRI	0.60	17.1 in/mi	163

*Level of inputs used for calibration.
**Obtained from NCHRP 20-07(288) calibration of JPCP and CRCP distress models.

Step 10: Reduce Standard Error of the Estimate

Models deemed as having a poor goodness of fit will require further adjustments to the global/local coefficients. Improvements can be made by removing errors in inputs for individual projects, which is often the cause of poor prediction. In addition, improvements must be made using statistical tools to optimize coefficients to maximize R^2, minimize SEE, and eliminate significant bias. Statistical optimization tools and software will most likely be needed to complete this step.

Step 11: Interpretation of Results, Deciding Adequacy of Calibration Parameters

A limited sensitivity analysis of the locally calibrated models must be conducted to determine the reasonableness of predictions and how predictions differ with the MEPDG nationally calibrated models. Based on this sensitivity analysis, adjustments can be made to the locally calibrated models as needed.

CHAPTER 3. DEVELOPMENT OF EXPERIMENTAL AND SAMPLING PLAN FOR COLORADO MEPDG MODELS VALIDATION/CALIBRATION

Select Hierarchical Input Level for Each Input Parameter

The hierarchical input levels of key inputs are determined from sensitivity analysis and agency practices (i.e., the greater the sensitivity of an input, the higher the hierarchical input level required). Table 7 presents a summary of recommended hierarchical input levels determined through national sensitivity analysis of the MEPDG models as part of NCHRP Projects 1-37A and 1-40D. The hierarchical input levels presented in Table 7 are recommended for Colorado.

Develop Local Experimental Plan and Sampling Template

The main goal for selecting roadway segments was to identify pavement sections with design and site features most representative of Colorado conditions (design, materials, and site) for use in validating/calibrating MEPDG models. Some of the criteria considered, adapted from the AASHTO Guide for the Local Calibration of the MEPDG, are listed below (AASHTO 2010):

- Amount of distress/IRI data: Distress/IRI data from at least three condition surveys must be available for each roadway segment to estimate the incremental increase in distress over time. It is also suggested that at least one of the distress measurements be made when the pavement is more than 10 years old, to ensure the following:
    - Pavement condition reflects the effect of traffic load applications, climate/seasonal cyclic changes in materials condition, and changes in time-dependent material properties (increased strength, degradation, fatigue, etc.).
    - Proper characterization of occurrence of distress (early construction or materials failure versus fatigue) for use in the determination of any bias and SEE.
    - Repeat condition surveys to reduce the inherent variability of distress measurements and estimate the measurement error for a particular distress.
- Consistency of distress measurements: It is imperative that a consistent definition and measurement of the surface distresses be used throughout the calibration and validation process. The distresses should be measured in accordance with the LTPP Distress Identification Guide, or information provided to convert those distress measurements into values equivalent to the *LTPP Distress Identification Manual* (Miller & Bellinger 2003). All data used to establish the inputs for the models (including, material test results, climatic data, and traffic data) and performance monitoring should be collected or measured in accordance with standard procedures (e.g., AASHTO, ASTM, CDOT). Roadway segments must be selected with the fewest number of structural layers and materials (e.g., one PCC layer, one or two HMA layers, one unbound base layer, and one subbase layer) to reduce the amount of testing and input required for material characterization. These roadway segments need to include the types of new construction and rehabilitation strategies typically used or specified by the agency. In other words, the roadway segments used to define SEE should include the range of materials and soils that are common to an area or region and the physical condition of those materials and soils.

Table 7. Recommended hierarchical input levels for MEPDG models validation/calibration in Colorado.

Input Group		Input Parameter	Validation Input Level Used
Truck Traffic		Axle load distributions (single, tandem, tridem, and quad)	Level 1 (field measured from WIM stations)
		Truck volume distribution	Level 1 (field measured from WIM stations)
		Lane & directional truck distributions	Level 3 (MEPDG defaults) unless urban with complicated lane and exit situation then Level 1
		Truck wheel base percentages	Level 1 (average determined for CDOT)
		Tire pressure	Level 3 (MEPDG defaults)
		Axle configuration, tire spacing	Level 3 (MEPDG defaults)
		Truck wander	Level 3 (MEPDG defaults)
Climate		Temperature, wind speed, cloud cover, precipitation, relative humidity	Level 2 (Virtual weather stations created using NCDC climate data embedded in the MEPDG)
Material Properties	Unbound Layers & Subgrade	Resilient modulus – subgrade	Level 2; FWD deflection measurements & backcalculation of subgrade moduli and modulus of subgrade reaction
		Resilient modulus – unbound granular and chemically treated base/subbase layers	Level 3 (MEPDG defaults)
		Unbound base/ subgrade soil classification	Level 1 (lab test data)
		Moisture-density relationships & other volumetric properties	Level 2 (Computed from gradation and Atterberg limits data)
		Soil-water characteristic relationships	Level 3 (MEPDG defaults)
		Saturated hydraulic conductivity	Level 2 (Computed from gradation and Atterberg limits data)
	HMA	HMA dynamic modulus	Level 2 (Computed using material gradation, air void, binder type, etc. data)
		HMA creep compliance & indirect tensile strength	Level 2 (Computed using material gradation, air void, binder type, etc. data)
		Volumetric properties	Level 3 (CDOT defaults)
		HMA coefficient of thermal contraction	Level 3 (MEPDG defaults)
	PCC	PCC elastic modulus	Level 1 (lab test data) Level 2 (computed from PCC compressive strength)
		PCC flexural strength	Level 1 (lab test data) Level 2 (computed from PCC compressive strength)
		PCC coefficient of thermal expansion	Level 1 (lab test data) Level 2 (determined based on coarse aggregate geological type)
All Materials		Unit weight	Level 3 (MEPDG defaults)
		Poisson's ratio	Level 3 (MEPDG defaults)
		Other thermal properties; conductivity, heat capacity, surface absorptivity	Level 3 (MEPDG defaults)

FWD = Falling Weight Deflectometer

- Roadway segments with and without overlays are needed for the validation/calibration sampling template. Those segments that have detailed time-history distress data before and after rehabilitation should be given a higher priority for use in the experiment because these segments can serve in dual roles as both new construction and rehabilitated pavements, and the condition of a given section prior to overlay is key to post-overlay distress development and progression. Roadway segments with HMA overlays should be limited to one HMA overlay during the monitoring period.
- Roadway segments that include non-conventional mixtures or layers should be included in the experimental sampling matrix to ensure that the model forms and calibration factors are representative of these mixtures. Non-conventional mixtures can include stone matrix asphalt (SMA), polymer modified asphalt (PMA), open-graded drainage layers, cement-aggregate mixtures, and high-strength PCC mixtures. Many of the LTPP test sections used to develop the global models were built with conventional HMA and PCC mixtures. The flexible sections excluded open-graded drainage, SMA, and PMA layers. There were numerous sections with open-graded mixtures in the JPCP sections.
- Traffic data or the number of trucks using the roadway for each truck classification need to be well defined. In other words, Level 1 traffic inputs, normalized truck volume values, are required.
- HMA volumetric properties, gradation, and asphalt content need to be available from construction or project records. The initial air voids, if not available, can be determined by backcasting from current/available air void levels.
- Level 1 or 2 PCC thickness, strength, moduli, and coefficient of thermal expansion (CTE) are required inputs.

Tables 8 and 9 present simplified sampling templates that were used as the basis for identifying roadway segments for local calibration for new HMA and HMA overlays and new JPCP and unbonded JPCP overlays, respectively. For the new and rehabilitated pavement types of interest, the following factors were considered in developing the sampling template:

- New HMA pavement and HMA overlay of existing HMA and rigid pavements:
    - Soil type (coarse-grained, fine-grained soil, non-expansive [PI <20], and fine-grained, expansive [PI>20]).
    - New HMA or overlay thickness (< 4-in, 4- to 8-in, and > 8-in).
    - Binder type (neat, modified)
    - Climate zone (hot, moderate, cool, and very cool).
    - Surface type (conventional, deep-strength, and full-depth HMA).
    - Base type (aggregate base [class 6 or other classes], asphalt treated materials).
    - Existing pavement type
        i. HMA overlay of flexible pavement including Superpave, SMA, or PMA mix types.
        ii. JPCP.
- New JPCP, JPCP overlay over existing HMA pavement, and unbonded JPCP overlay over existing JPCP.
    - New PCC or unbonded PCC slab thickness (< 10-in, 10- to 11-in, and > 11-in).
    - Base type (no base layer, aggregate material, cement treated base [CTB]/lean concrete base [LCB], permeable asphalt treated base [PATB]).

- Doweled/nondoweled PCC.
- Edge support (standard slab width or widened slab) or (HMA/untied PCC shoulder or tied PCC shoulder).
- Existing pavement condition (good, fair, poor), for unbonded overlay only.

Colorado defines four environmental/climate zones based on the highest 7-day average maximum air temperature or pavement location elevation. These climate zones are described in Table 10.

Table 8. Sampling template for new HMA and HMA overlaid existing HMA pavements.

HMA Thickness	Binder Type	Climate Zone[1]	Subgrade Type			
			Fine-Grained Soil		Coarse-Grained Soil	
			Conv. HMA[2]	Full-Depth HMA[3]	Conv. HMA[1]	Full-Depth HMA[3]
< 4-in	Neat	Hot/Moderate				
		Cool				
		Very Cool				
	Modified	Hot/Moderate				
		Cool				
		Very Cool				
4- to 8-in	Neat	Hot/Moderate				
		Cool				
		Very Cool				
	Modified	Hot/Moderate				
		Cool				
		Very Cool				
> 8-in	Neat	Hot/Moderate				
		Cool				
		Very Cool				
	Modified	Hot/Moderate				
		Cool				
		Very Cool				

1. See Table 10.
2. Conventional HMA is typically and HMA layer placed over thick dense graded aggregate base (DGAB) over the prepared subgrade. Conventional HMA could also include surface treatments (chip seal, fog seal, slurry seal or crack seal) on conventional HMA.
3. Full-depth HMA is typically HMA over asphalt treated base (dense or drainable) over a prepared subgrade.

Table 9. Sampling template for new JPCP, JPCP overlays of existing flexible pavements, and unbonded JPCP of existing JPCP.

PCC Thickness	Base Type[1]	Nondoweled Transverse Joint			Doweled Transverse Joint		
		12-ft Slab Width		Widened Slab (13- or 14-ft)	12-ft Slab Width		Widened Slab (13- or 14-ft)
		HMA Shoulder	Tied PCC Shoulder		HMA Shoulder	Tied PCC Shoulder	
< 10-in	DGAB						
	CTB/LCB						
	ATB						
10- to 12-in	DGAB						
	CTB/LCB						
	ATB						
> 12-in	DGAB						
	CTB/LCB						
	ATB						

CTB = cement treated base, LCB = lean concrete base, ATB = asphalt treated base

Table 10. Description of Colorado environmental zone.

CDOT Environmental Zone	Highest 7-Day Average Maximum Air Temperature, ^{o}F
Hot (Southeast and West)	> 97
Moderate (Denver, Plains, and West)	90 to 97
Cool (Mountains)	81 to 88
Very Cool (High Mountains)	< 81

Identify Pavement Projects for Filling Sampling/Experimental Template

Pavement projects for local calibration/validation were identified from two sources: (1) LTPP research-grade roadway segments in Colorado and (2) CDOT pavement management system roadway segments. As all of the projects used in the global calibration of the MEPDG models were LTPP test sections (research-grade sites), it is expected that the LTPP sites in Colorado should have all required data for use in fully validating and calibrating the MEPDG distress/IRI prediction models under various environmental, aging, and traffic application scenarios. The Guide for the Local Calibration of the MEPDG highlights the importance of replication of roadway segments or test sections within the sampling matrices (AASHTO 2010). Thus, an effort was made to identify replicates within the sampling matrix, if at all possible.

Estimate Sample Size for Specific Distress/IRI Prediction Models

The AASHTO Guide for the Local Calibration of the MEPDG applies the following equation below for determining minimum number of projects required for model validation and calibration (AASHTO 2010):

$$n = \left(\frac{Z_{\alpha/2}\sigma}{E} \right)^2 \quad (2)$$

where

$Z_{\alpha/2}$ = the score for having α percent of the data in the tails, i.e., P(|Z| > z) = α for a 90 percent confidence interval $Z_{\alpha/2}$ = 1.601

σ = performance indicator threshold (i.e., design threshold limit, see Table 11)

E = tolerable bias at 90 percent reliability = $Z_{\alpha/2}$ *SEE

SEE = distress/IRI models standard error of the estimate (see Table 11)

For this project, design reliability and confidence interval were both assumed to be 90 percent. Table 11 presents a summary of distress/IRI thresholds and MEPDG nationally calibrated model SEE. Regardless of the minimum number of projects determined, the AASHTO Guide for the Local Calibration of the MEPDG recommends the minimum number of projects presented in Table 12 (AASHTO 2010).

Table 11. Summary of distress/IRI thresholds and MEPDG nationally calibrated model SEE (obtained from AASHTO 2008).

Pavement Type	Performance Indicator	Performance Indicator Threshold (at 90% Reliability) (σ)	SEE	Minimum No. of Projects Required for Validation & Local Calibration
New HMA and HMA-overlaid HMA	Alligator cracking	20 percent lane area	5.01 percent	16
	Transverse "thermal" cracking	Crack spacing > 100 ft. of 630 ft/mi	150 ft/mi	18
	Rutting	0.4 in	0.107 in	14
	IRI	169 in / mi	18.9 in/mi	80
New JPCP and JPCP subjected to CPR[1]	Faulting	< 0.15 in	0.033 in	21
	Transverse cracking	< 10 percent slabs	4.52 percent	5
	IRI	169 in/mi	17.1 in/mi	98

1. CPR = concrete pavement repair or restoration.

Table 12. Minimum number of pavement projects required for the validation and local calibration (AASHTO 2010).

Pavement Type	Performance Indicator	Distress Classification	Minimum Number of Projects
Flexible	Alligator cracking	Load-related cracking	30
	Transverse "thermal" cracking	Non-load-related cracking	30
	Rutting	Distortion	20
	IRI	Not applicable	Not provided
Rigid	Faulting	Distortion	20
	Transverse cracking	Load-related cracking	30
	Punchouts	Load-related cracking	30
	IRI	Not applicable	Not provided
Composite HMA-overlaid PCC	Reflection "transverse" cracking	Not classified	26
	IRI	Not applicable	Not provided

CHAPTER 4. PROJECTS SELECTION AND DEVELOPMENT OF CLIMATE AND TRAFFIC DATABASE TO VALIDATE/CALIBRATE MEPDG MODELS

The MEPDG implementation process involved developing a sampling template for project identification and calibration/validation database population. The two sources of data were the CDOT pavement management system and the LTPP database. This chapter describes work done to identify and select candidate projects for inclusion into the project calibration/validation database, as well as the development of the database.

Identification and Selection of Pavement Projects

Project Identification

The LTPP database contained 72 research-type new HMA, HMA-overlaid existing HMA and JPCP, new JPCP, and unbonded JPCP overlay of JPCP projects in Colorado. A breakdown of the project types is presented in Figure 5. Note that some projects were double or triple counted, as they belonged to different pavement type categories at different time periods due to rehabilitation done over the course of their service life.

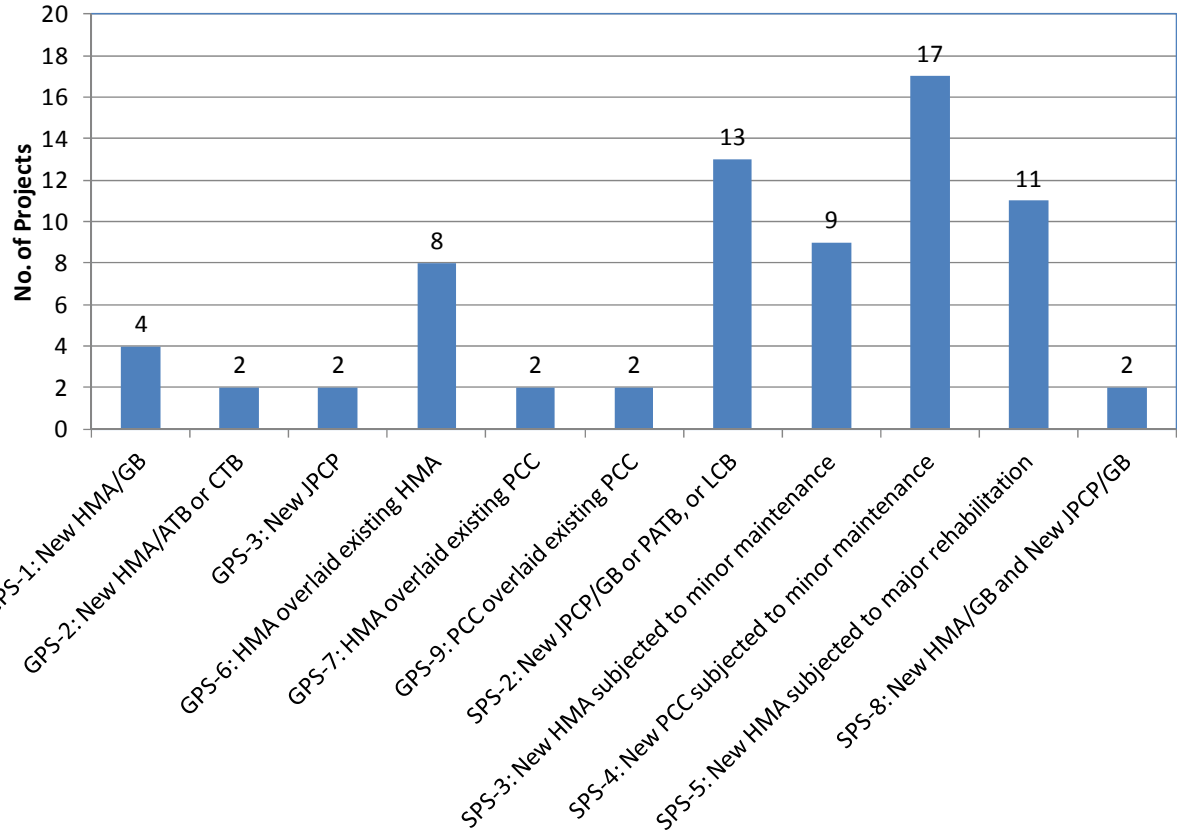

Figure 5. Breakdown of the LTPP project types in Colorado.

The CDOT state highway system consists of 11,192 lane miles of pavement. Approximately 9,954 miles are HMA pavements, and 1,225 miles are PCC pavements. The entire state highway system was divided into 112,009 individual pavement management sections with an average length of 0.1 miles (approximately 500 ft). A map showing the CDOT state highway system is presented in Figure 6.

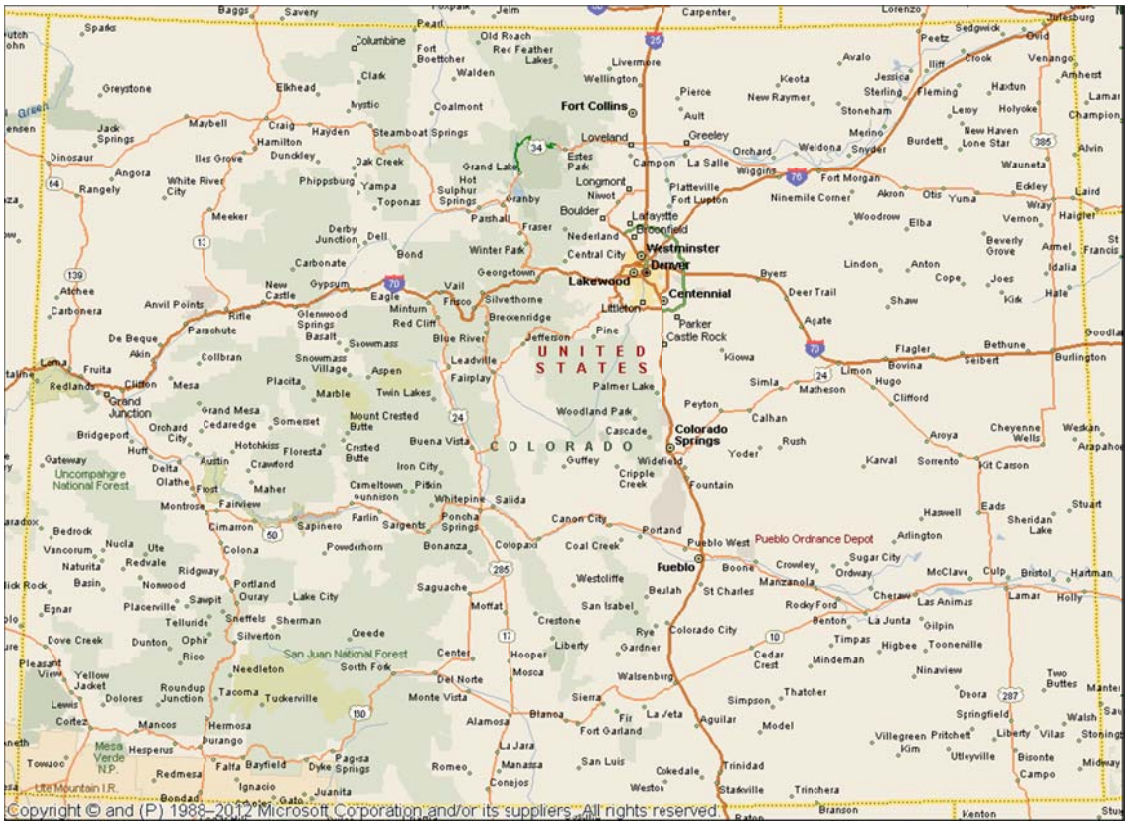

Figure 6. CDOT state highway system.

Criteria for Pavement Projects Selection

Pavement projects were selected for the development of the project database as follows:

- Research-grade pavement projects.
  - Research-grade LTPP projects were used to develop and calibrate the MEPDG global models.
  - Thus, they contain at least at Level 3 all input data required for local calibration analysis.
  - The sole criterion for inclusion into the CDOT local calibration/validation database is whether they represent a pavement type of interest.
  - The pavement type information presented in Figure 5 shows that all 72 LTPP projects in Colorado may be included in the project database.

- Pavement management system projects.
    - Must have available distress/IRI data from at least three condition surveys collected within the past 7 to 10 years. This will ensure that all time-dependent inputs (i.e., material properties, traffic growth and accumulation, cyclic change in climate, cyclic change in groundwater and foundation properties) are properly taken into account in validation/calibration of the models.
    - Consistency of distress/IRI measurements with MEPDG: Available distress/IRI data must be consistent in terms of both definition and precision with the MEPDG and, thus, LTPP protocols. This means that distress/IRI must be measured in accordance with the *LTPP Distress Identification Manual* (Miller & Bellinger 2003) or it should be possible to convert the reported distress/IRI into values equivalent to LTPP measurements.
    - Consistency of materials, traffic, climate, and other measurements with MEPDG: All data used to establish the inputs for the models (including, material test results, climatic data, and traffic data) should be collected or measured in accordance with MEPDG standard procedures. Otherwise, it should be possible to convert as needed to be compatible with the MEPDG/LTPP.
    - Roadway segments should be selected with the fewest number of structural layers and materials (e.g., one PCC layer, one or two HMA layers, one unbound base layer, and one subbase layer) to reduce the amount of testing and input required for material characterization.
    - Roadway segments selected should as much as possible reflect CDOT construction and rehabilitation strategies. In other words, the roadway segments used to define SEE should include the range of construction practices (PCC curing, joint sawing, tack coat placement, bonding at layer interface, initial IRI, etc.) and rehabilitation practices (grinding equipment and specifications, joint repairs and dowel retrofit, joint sealant types applied for resealing, etc.).
    - Roadway segments with and without HMA and PCC overlays are needed for the validation/calibration sampling template. Those segments that have detailed time-history distress data before and after rehabilitation should be given a higher priority for inclusion into the project database, as the proper characterization of the existing pavement prior to rehabilitation is key to developing accurate prediction models.
    - Roadway segments or projects with HMA overlays should be limited to one HMA overlay during the monitoring period.
    - Roadway segments that include non-conventional mixtures or layers should be included in the experimental sampling matrix to ensure that the model forms and calibration factors are representative of these mixtures. Non-conventional mixtures can include SMA, PMA, open-graded drainage layers, cement-aggregate mixtures, and high-strength PCC mixtures.
    - Traffic data need to be well defined. Level 1 traffic inputs, normalized truck volume values, are required.
    - HMA as-placed volumetric properties, gradation, and asphalt content need to be available from construction or project records. If not available, there should be information available to backcast initial air voids.

Description of Selected Projects

Based on the selection criteria presented, a total of 127 new and rehabilitated pavement projects were selected from the LTPP and CDOT pavement management system databases. It must be noted that not all of the CDOT pavement management system projects had all the required data. However, such projects were selected for inclusion in the project database on the assumption that the required information can be assembled through field and laboratory testing.

Figures 7 through 9 show maps of Colorado, along with the locations of the selected pavement projects. Tables 13 through 15 present basic descriptive information for the selected pavement projects. Figures 10 through 18 present histograms showing the distribution of key descriptive features of the selected projects.

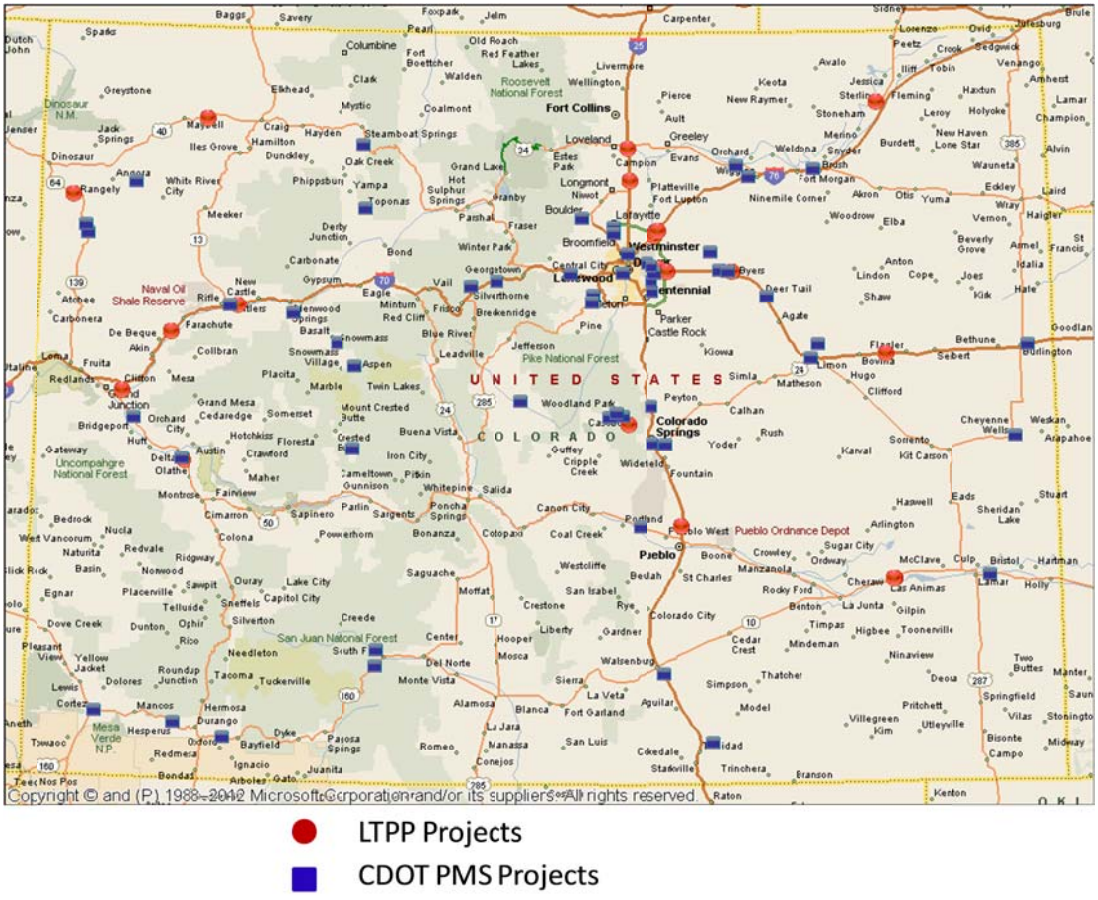

Figure 7. Map of selected pavement projects along the Colorado highway system.

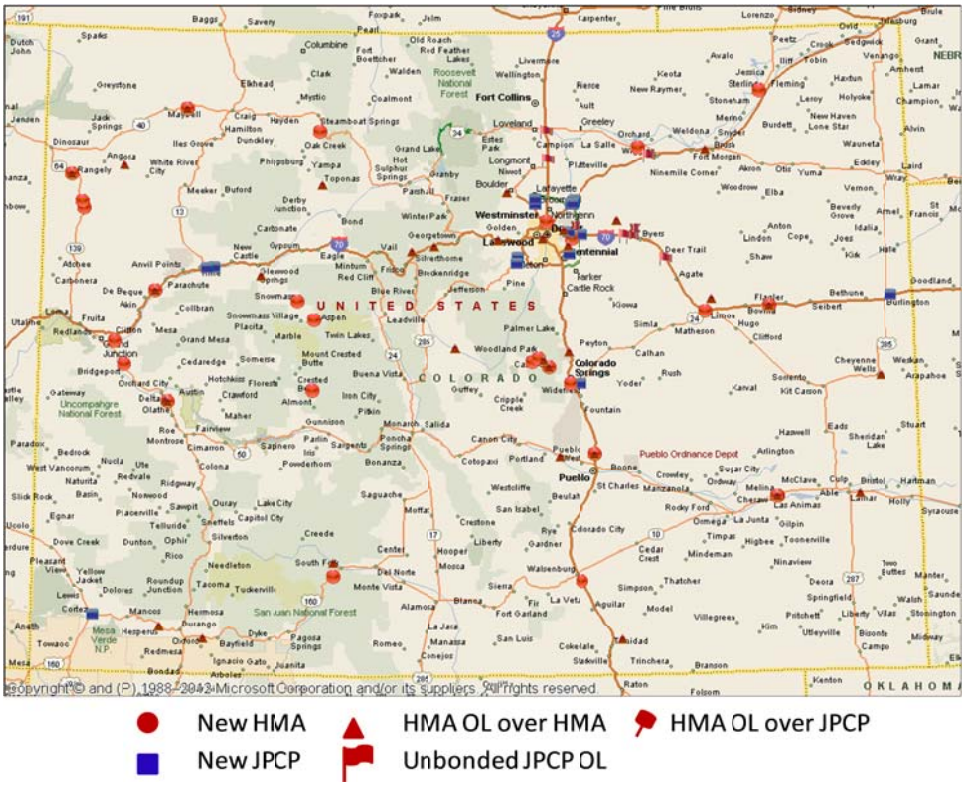

Figure 8. Map showing selected pavement types along the Colorado highway system.

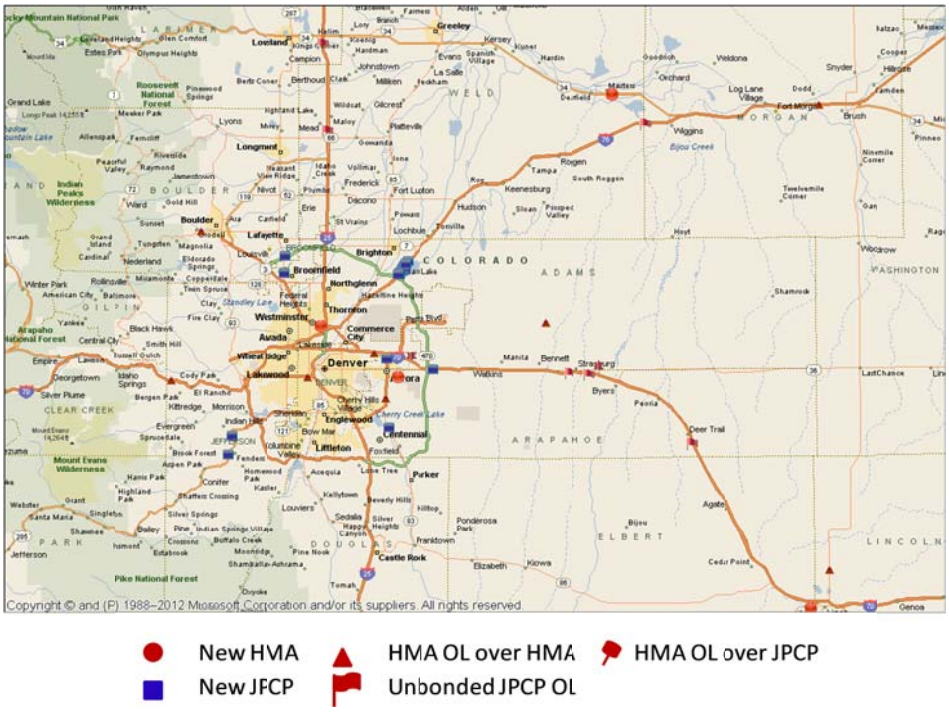

Figure 9. Map showing rehabilitated pavement projects in the Denver area.

Table 13. Inventory information (highway type, route, & direction) for selected projects.

Project Type	ARA ID	CDOT/LTPP ID	Project Name	Highway Type	Route No.	Route ID	Direction
CDOT	1	11328	IM 0704-178	Interstate	70	070A	WB
CDOT	2	11327	IM 0704-177	Interstate	70	070A	WB
CDOT	3	88452	IR(CX) 70-4(153)	Interstate	70	070A	EB
CDOT	4	91044	FC-NH(CX) 024-3(036)	U. S.	24	024G	EB
CDOT	5	12441	STA 0711-013	State	71	071D	NB
CDOT	6	91022	ACIM 070-5(53)	Interstate	70	070A	WB
CDOT	7	13817	NH 0405-029	U. S.	40	040H	EB
CDOT	8	12685	NH 0505-033	U. S.	50	050B	EB
CDOT	9	13936	STA 1604-007	U. S.	160	160C	EB
CDOT	10	12393	BR 0251-150	Interstate	25	025A	SB
CDOT	11	12529	NH 0503-056	U. S.	50	050A	EB
CDOT	12	13390	IM 0252-342	Interstate	25	025A	SB
CDOT	13	10175	C 0243-042	U. S.	24	024G	EB
CDOT	14	13131	NH 0242-031	U. S.	24	024A	EB
CDOT	15	11959	STA 0242-026	U. S.	24	024A	EB
CDOT	16	13440	NH 0242-033	U. S.	24	024A	EB
CDOT	17	13932	IM 0252-358	Interstate	25	025A	SB
CDOT	18	12187	NHS 0831-076	State	83	083A	NB
CDOT	19	92021	NH(CX) 225-4(39)	Interstate	225	225A	NB
CDOT	20	13353	STA 2254-063	Interstate	255	225A	NB
CDOT	21	91094	MU-STU 0030(006)	State	30	030A	EB
CDOT	22	12297	NH 0061-066	U. S.	6	006G	EB
CDOT	23	11918	SP 0253-150	U. S.	36	036B	WB
CDOT	24	13356	STA 0704-199	Interstate	70	070A	EB
CDOT	25	10326	NH 2873-071	U. S.	287	287C	NB
CDOT	26	93216	NH(CX) 160-1(029)	U. S.	160	160A	EB
CDOT	27	13959	STA 1191-017	State	119	119A	WB
CDOT	28	11865	NH 0341-046	U. S.	34	034A	WB
CDOT	29	89168	IR(CX) 076-1(150)	Interstate	76	076A	EB
CDOT	30	11979	C 0761-170	Interstate	76	076A	EB
CDOT	31	13258	C 0403-043	U. S.	40	040B	EB
CDOT	32	12448	STA 006A-030	U. S.	6	006F	WB
CDOT	33	13435	STA 0061-069	State	9	009D	SB
CDOT	34	13513	NH 0242-034	U. S.	24	024A	EB
CDOT	35	13087	STR 135A-019	State	135	135A	SB
CDOT	36	13880	PLH 149A-020	State	149	149A	SB
CDOT	37	92976	NH(CX) 160-2(049)	U. S.	160	160A	EB
CDOT	38	13505	STA 1602-084	U. S.	160	160A	WB
CDOT	39	11970	NH 1601-046	U. S.	160	160A	WB
CDOT	41	13325	NH 0501-045	U. S.	50	050A	EB
CDOT	42	12153	NH 0501-038	U. S.	50	050A	EB
CDOT	43	13085	PLH 139A-026	State	139	139A	SB
CDOT	44	11213	PLH 139A-023	State	139	139A	NB
CDOT	45	13106	STA 0641-011	State	64	064A	WB
CDOT	46	00000	I70-1(44) 89	Interstate	70	070A	WB
CDOT	47	12018	STR 131A-024	State	131	131B	SB

Table 13. Inventory information (highway type, route, & direction) for selected projects.

Project Type	ARA ID	CDOT/LTPP ID	Project Name	Highway Type	Route No.	Route ID	Direction
CDOT	48	13866	STA 131A-028	State	131	131B	NB
CDOT	49	13864	STA 0821-063	State	82	082A	WB
CDOT	50	11780	HB 0821-047	State	82	082A	EB
CDOT	51	12271	SP 0821-053	State	82	082A	WB
CDOT	52	12321	STA 079A-009	State	79	079B	NB
CDOT	53	84076	FCUNH(CX)CY287-3(37)	U. S.	287	287C	NB
CDOT	54	11546	NH 2854-063	U. S.	285	285D	NB
CDOT	55	93015	NH(CX) 285-4(48)	U. S.	285	285D	NB
LTPP	56	8_0213_1	LTPP	Interstate	76	N/A	EB
LTPP	57	8_0214_1	LTPP	Interstate	76	N/A	EB
LTPP	58	8_0215_1	LTPP	Interstate	76	N/A	EB
LTPP	59	8_0216_1	LTPP	Interstate	76	N/A	EB
LTPP	60	8_0217_1	LTPP	Interstate	76	N/A	EB
LTPP	61	8_0218_1	LTPP	Interstate	76	N/A	EB
LTPP	62	8_0219_1	LTPP	Interstate	76	N/A	EB
LTPP	63	8_0220_1	LTPP	Interstate	76	N/A	EB
LTPP	64	8_0221_1	LTPP	Interstate	76	N/A	EB
LTPP	65	8_0222_1	LTPP	Interstate	76	N/A	EB
LTPP	66	8_0223_1	LTPP	Interstate	76	N/A	EB
LTPP	67	8_0224_1	LTPP	Interstate	76	N/A	EB
LTPP	68	8_0259_1	LTPP	Interstate	76	N/A	EB
LTPP	69	8_0501_1	LTPP	Interstate	70	N/A	EB
LTPP	70	8_0501_2	LTPP	Interstate	70	N/A	EB
LTPP	71	8_0502_1	LTPP	Interstate	70	N/A	EB
LTPP	72	8_0502_2	LTPP	Interstate	70	N/A	EB
LTPP	73	8_0503_1	LTPP	Interstate	70	N/A	EB
LTPP	74	8_0503_2	LTPP	Interstate	70	N/A	EB
LTPP	75	8_0504_1	LTPP	Interstate	70	N/A	EB
LTPP	76	8_0504_2	LTPP	Interstate	70	N/A	EB
LTPP	77	8_0505_1	LTPP	Interstate	70	N/A	EB
LTPP	78	8_0505_2	LTPP	Interstate	70	N/A	EB
LTPP	79	8_0506_1	LTPP	Interstate	70	N/A	EB
LTPP	80	8_0506_2	LTPP	Interstate	70	N/A	EB
LTPP	81	8_0507_1	LTPP	Interstate	70	N/A	EB
LTPP	82	8_0507_2	LTPP	Interstate	70	N/A	EB
LTPP	83	8_0508_1	LTPP	Interstate	70	N/A	EB
LTPP	84	8_0508_2	LTPP	Interstate	70	N/A	EB
LTPP	85	8_0509_1	LTPP	Interstate	70	N/A	EB
LTPP	86	8_0509_2	LTPP	Interstate	70	N/A	EB
LTPP	87	8_0559_1	LTPP	Interstate	70	N/A	EB
LTPP	88	8_0559_2	LTPP	Interstate	70	N/A	EB
LTPP	89	8_0560_1	LTPP	Interstate	70	N/A	EB
LTPP	90	8_0560_2	LTPP	Interstate	70	N/A	EB
LTPP	91	8_0811_1	LTPP	Ramp		N/A	EB
LTPP	92	8_0812_1	LTPP	Ramp		N/A	EB

Table 13. Inventory information (highway type, route, & direction) for selected projects.

Project Type	ARA ID	CDOT/LTPP ID	Project Name	Highway Type	Route No.	Route ID	Direction
LTPP	93	8_1029_1	LTPP	U. S.	40	N/A	WB
LTPP	94	8_1029_5	LTPP	U. S.	40	N/A	WB
LTPP	95	8_1047_1	LTPP	State	64	N/A	WB
LTPP	96	8_1047_2	LTPP	State	64	N/A	WB
LTPP	97	8_1053_1	LTPP	U. S.	50	N/A	NB
LTPP	98	8_1053_2	LTPP	U. S.	50	N/A	NB
LTPP	99	8_1057_1	LTPP	State	141B	N/A	SB
LTPP	100	8_2008_1	LTPP	U. S.	50	N/A	WB
LTPP	101	8_3032_1	LTPP	Interstate	70	N/A	EB
LTPP	102	8_6002_1	LTPP	Interstate	25	N/A	NB
LTPP	103	8_6002_2	LTPP	Interstate	25	N/A	NB
LTPP	104	8_6013_1	LTPP	U. S.	14	N/A	EB
LTPP	105	8_7035_1	LTPP	Interstate	70	N/A	EB
LTPP	106	8_7035_2	LTPP	Interstate	70	N/A	EB
LTPP	107	8_7036_1	LTPP	Interstate	70	N/A	EB
LTPP	108	8_7776_1	LTPP	Interstate	70	N/A	EB
LTPP	109	8_7780_1	LTPP	U. S.	24	N/A	WB
LTPP	110	8_7780_2	LTPP	U. S.	24	N/A	WB
LTPP	111	8_7781_1	LTPP	U. S.	50	N/A	WB
LTPP	112	8_7781_2	LTPP	U. S.	50	N/A	WB
LTPP	113	8_7783_1	LTPP	Interstate	70	N/A	EB
LTPP	114	8_7783_3	LTPP	Interstate	70	N/A	EB
LTPP	115	8_9019_1	LTPP	Interstate	25	N/A	NB
LTPP	116	8_9020_1	LTPP	Interstate	25	N/A	SB
LTPP	117	8_A310_1	LTPP	U. S.	50	N/A	NB
LTPP	118	8_A310_2	LTPP	U. S.	50	N/A	NB
LTPP	119	8_A320_1	LTPP	U. S.	50	N/A	NB
LTPP	120	8_A330_1	LTPP	U. S.	50	N/A	NB
LTPP	121	8_A340_1	LTPP	U. S.	50	N/A	NB
LTPP	122	8_A350_1	LTPP	U. S.	50	N/A	NB
LTPP	123	8_B310_1	LTPP	U. S.	50	N/A	WB
LTPP	124	8_B310_2	LTPP	U. S.	50	N/A	WB
LTPP	125	8_B320_1	LTPP	U. S.	50	N/A	WB
LTPP	126	8_B330_1	LTPP	U. S.	50	N/A	WB
LTPP	127	8_B350_1	LTPP	U. S.	50	N/A	WB

Table 14. Inventory information (CDOT region, county, highway functional class, & no. of lanes) for selected projects.

Project Type	ARA ID	CDOT/LTPP ID	Begin MP	CDOT Region	County	Highway Functional Class
CDOT	1	11328	309.00	1	Adams	Rural principal arterial-Interstate
CDOT	2	11327	312.00	1	Arapahoe	Rural principal arterial-Interstate
CDOT	3	88452	330.00	1	Arapahoe	Rural principal arterial-Interstate
CDOT	4	91044	375.80	1	Elbert	Rural major collector
CDOT	5	12441	107.00	1	Lincoln	Rural minor collector
CDOT	6	91022	440.00	1	Kit Carson	Rural principal arterial-Interstate
CDOT	7	13817	471.00	1	Cheyenne	Rural major collector
CDOT	8	12685	442.00	2	Prowers	Rural major collector
CDOT	9	13936	350.00	2	Las Animas	Rural minor collector
CDOT	10	12393	47.10	2	Huerfano	Rural principal arterial-Interstate
CDOT	11	12529	299.00	2	Pueblo	Rural Major Collector
CDOT	12	13390	139.50	2	El Paso	Urban principal arterial-Interstate
CDOT	13	10175	309.10	2	El Paso	Urban principal arterial-other
CDOT	14	13131	280.00	2	Teller	Rural major collector
CDOT	15	11959	283.30	2	Teller	Rural major collector
CDOT	16	13440	288.00	2	Teller	Rural major collector
CDOT	17	13932	155.00	2	El Paso	Rural principal arterial-Interstate
CDOT	18	12187	67.30	6	Arapahoe	Urban principal arterial-other
CDOT	19	92021	11.10	6	Adams	Urban principal arterial-Interstate
CDOT	20	13353	6.00	6	Arapahoe	Urban principal arterial-Interstate
CDOT	21	91094	11.40	6	Arapahoe	Urban major collector
CDOT	22	12297	284.30	6	Denver	Urban major collector
CDOT	23	11918	56.70	6	Adams	Urban principal arterial-other
CDOT	24	13356	281.00	6	Denver	Urban principal arterial-Interstate
CDOT	25	10326	301.40	4	Boulder	Urban principal arterial-other
CDOT	26	93216	38.95	5	Montezuma	Urban principal arterial-other
CDOT	27	13959	40.00	4	Boulder	Rural principal arterial-other
CDOT	28	11865	139.00	4	Weld	Rural major collector
CDOT	29	89168	61.00	4	Morgan	Rural principal arterial-Interstate
CDOT	30	11979	86.00	4	Morgan	Rural principal arterial-Interstate
CDOT	31	13258	272.20	1	Jefferson	Rural major collector
CDOT	32	12448	229.00	1	Clear Creek	Rural minor collector
CDOT	33	13435	103.20	1	Summit	Urban major collector
CDOT	34	13513	245.00	1	Park	Rural major collector
CDOT	35	13087	16.70	3	Gunnison	Rural minor collector
CDOT	36	13880	4.00	5	Rio Grande	Rural minor collector
CDOT	37	92976	182.80	5	Rio Grande	Rural major collector
CDOT	38	13505	96.00	5	La Plata	Rural major collector
CDOT	39	11970	72.00	5	La Plata	Rural major collector
CDOT	41	13325	73.00	3	Delta	Urban major collector
CDOT	42	12153	47.00	3	Mesa	Rural major collector
CDOT	43	13085	57.00	3	Rio Blanco	Rural minor collector
CDOT	44	11213	60.00	3	Rio Blanco	Rural minor collector
CDOT	45	13106	43.50	3	Rio Blanco	Rural minor collector
CDOT	46	00000	93.00	3	Garfield	Rural principal arterial-Interstate

Table 14. Inventory information (CDOT region, county, highway functional class, & no. of lanes) for selected projects.

Project Type	ARA ID	CDOT/LTPP ID	Begin MP	CDOT Region	County	Highway Functional Class
CDOT	47	12018	66.00	3	Routt	Rural Minor Collector
CDOT	48	13866	33.00	3	Routt	Rural Minor Collector
CDOT	49	13864	4.50	3	Garfield	Rural principal arterial-other
CDOT	50	11780	26.10	3	Pitkin	Rural principal arterial-other
CDOT	51	12271	38.00	3	Pitkin	Rural principal arterial-other
CDOT	52	12321	7.50	1	Adams	Rural major collector
CDOT	53	84076	298.50	6	Broomfield	Urban principal arterial-other
CDOT	54	11546	242.00	1	Jefferson	Rural principal arterial-other
CDOT	55	93015	245.00	1	Jefferson	Rural principal arterial-other
LTPP	56	8_0213_1	18.46	6	Adams	Rural principal arterial-Interstate
LTPP	57	8_0214_1	18.46	6	Adams	Rural principal arterial-Interstate
LTPP	58	8_0215_1	18.46	6	Adams	Rural principal arterial-Interstate
LTPP	59	8_0216_1	18.46	6	Adams	Rural principal arterial-Interstate
LTPP	60	8_0217_1	18.46	6	Adams	Rural principal arterial-Interstate
LTPP	61	8_0218_1	18.46	6	Adams	Rural principal arterial-Interstate
LTPP	62	8_0219_1	18.46	6	Adams	Rural principal arterial-Interstate
LTPP	63	8_0220_1	18.46	6	Adams	Rural principal arterial-Interstate
LTPP	64	8_0221_1	18.46	6	Adams	Rural principal arterial-Interstate
LTPP	65	8_0222_1	18.46	6	Adams	Rural principal arterial-Interstate
LTPP	66	8_0223_1	18.46	6	Adams	Rural principal arterial-Interstate
LTPP	67	8_0224_1	18.46	6	Adams	Rural principal arterial-Interstate
LTPP	68	8_0259_1	18.46	6	Adams	Rural principal arterial-Interstate
LTPP	69	8_0501_1	386.45	1	Lincoln	Rural principal arterial-Interstate
LTPP	70	8_0501_2	386.45	1	Lincoln	Rural principal arterial-Interstate
LTPP	71	8_0502_1	386.45	1	Lincoln	Rural principal arterial-Interstate
LTPP	72	8_0502_2	386.45	1	Lincoln	Rural principal arterial-Interstate
LTPP	73	8_0503_1	386.45	1	Lincoln	Rural principal arterial-Interstate
LTPP	74	8_0503_2	386.45	1	Lincoln	Rural principal arterial-Interstate
LTPP	75	8_0504_1	386.45	1	Lincoln	Rural principal arterial-Interstate
LTPP	76	8_0504_2	386.45	1	Lincoln	Rural principal arterial-Interstate
LTPP	77	8_0505_1	386.45	1	Lincoln	Rural principal arterial-Interstate
LTPP	78	8_0505_2	386.45	1	Lincoln	Rural principal arterial-Interstate
LTPP	79	8_0506_1	386.45	1	Lincoln	Rural principal arterial-Interstate
LTPP	80	8_0506_2	386.45	1	Lincoln	Rural principal arterial-Interstate
LTPP	81	8_0507_1	386.45	1	Lincoln	Rural principal arterial-Interstate
LTPP	82	8_0507_2	386.45	1	Lincoln	Rural principal arterial-Interstate
LTPP	83	8_0508_1	386.45	1	Lincoln	Rural principal arterial-Interstate
LTPP	84	8_0508_2	386.45	1	Lincoln	Rural principal arterial-Interstate
LTPP	85	8_0509_1	386.45	1	Lincoln	Rural principal arterial-Interstate
LTPP	86	8_0509_2	386.45	1	Lincoln	Rural principal arterial-Interstate
LTPP	87	8_0559_1	386.45	1	Lincoln	Rural principal arterial-Interstate
LTPP	88	8_0559_2	386.45	1	Lincoln	Rural principal arterial-Interstate
LTPP	89	8_0560_1	386.45	1	Lincoln	Rural principal arterial-Interstate
LTPP	90	8_0560_2	386.45	1	Lincoln	Rural principal arterial-Interstate
LTPP	91	8_0811_1		6	Adams	Rural local collector

Table 14. Inventory information (CDOT region, county, highway functional class, & no. of lanes) for selected projects.

Project Type	ARA ID	CDOT/LTPP ID	Begin MP	CDOT Region	County	Highway Functional Class
LTPP	92	8_0812_1		6	Adams	Rural local collector
LTPP	93	8_1029_1	69.75	3	Moffat	Rural principal arterial-other
LTPP	94	8_1029_5	69.75	3	Moffat	Rural principal arterial-other
LTPP	95	8_1047_1	16.6	3	Rio Blanco	Rural major collector
LTPP	96	8_1047_2	16.6	3	Rio Blanco	Rural major collector
LTPP	97	8_1053_1	75.3	3	Delta	Rural principal arterial-other
LTPP	98	8_1053_2	75.3	3	Delta	Rural principal arterial-other
LTPP	99	8_1057_1	160.65	3	Mesa	Urban principal arterial - other
LTPP	100	8_2008_1	401.93	2	Bent	Rural principal arterial-other
LTPP	101	8_3032_1	95.75	3	Garfield	Rural principal arterial-Interstate
LTPP	102	8_6002_1	106.35	2	Pueblo	Rural principal arterial-Interstate
LTPP	103	8_6002_2	106.35	2	Pueblo	Rural principal arterial-Interstate
LTPP	104	8_6013_1	235.4	4	Logan	Urban principal arterial-other
LTPP	105	8_7035_1	286.25	1	Adams	Rural principal arterial-Interstate
LTPP	106	8_7035_2	286.25	1	Adams	Rural principal arterial-Interstate
LTPP	107	8_7036_1	308.55	1	Arapahoe	Rural principal arterial-Interstate
LTPP	108	8_7776_1	290.3	1	Adams	Rural principal arterial-Interstate
LTPP	109	8_7780_1	291.26	2	El Paso	Rural principal arterial-other
LTPP	110	8_7780_2	291.26	2	El Paso	Rural principal arterial-other
LTPP	111	8_7781_1	402.18	2	Bent	Rural principal arterial-other
LTPP	112	8_7781_2	402.18	2	Bent	Rural principal arterial-other
LTPP	113	8_7783_1	67.66	3	Garfield	Rural principal arterial-Interstate
LTPP	114	8_7783_3	67.66	3	Garfield	Rural principal arterial-Interstate
LTPP	115	8_9019_1	246.5	4	Weld	Rural principal arterial-Interstate
LTPP	116	8_9020_1	256.4	4	Larimer	Rural principal arterial-Interstate
LTPP	117	8_A310_1	75.3	3	Delta	Rural principal arterial-other
LTPP	118	8_A310_2	75.3	3	Delta	Rural principal arterial-other
LTPP	119	8_A320_1	75.3	3	Delta	Rural principal arterial-other
LTPP	120	8_A330_1	75.3	3	Delta	Rural principal arterial-other
LTPP	121	8_A340_1	75.3	3	Delta	Rural principal arterial-other
LTPP	122	8_A350_1	75.3	3	Delta	Rural principal arterial-other
LTPP	123	8_B310_1	401.93	2	Bent	Rural principal arterial-other
LTPP	124	8_B310_2	401.93	2	Bent	Rural principal arterial-other
LTPP	125	8_B320_1	401.93	2	Bent	Rural principal arterial-other
LTPP	126	8_B330_1	401.93	2	Bent	Rural principal arterial-other
LTPP	127	8_B350_1	401.93	2	Bent	Rural principal arterial-other

Table 15. Inventory information (construction/rehab date, long/lat & elevation) for selected projects.

Project Type	ARA ID	CDOT/LTPP ID	Pavement Type	Const. Year	Rehab Year	Latitude, deg	Longitude, deg.	Elev., ft
CDOT	1	11328	Unbonded JPCP overlay over existing JPCP	1963	1998	39.7	-104.4	5406
CDOT	2	11327	Unbonded JPCP overlay over existing JPCP	1963	1997	39.7	-104.3	5397
CDOT	3	88452	Unbonded JPCP overlay over existing JPCP	1967	1993	39.6	-104.0	5266
CDOT	4	91044	New HMA	1998		39.3	-103.7	5421
CDOT	5	12441	HMA overlay (cold in place recycle) over existing HMA	1977	2000	39.3	-103.7	5517
CDOT	6	91022	JPCP overlay over existing HMA	1969	1995	39.3	-102.2	4091
CDOT	7	13817	HMA overlay (cold in place recycle) over existing HMA	1966	2002	38.8	-102.3	4223
CDOT	8	12685	Superpave HMA overlay over existing HMA	1973	2001	38.1	-102.5	3577
CDOT	9	13936	Superpave HMA overlay over existing HMA	1963	2003	37.2	-104.4	5939
CDOT	10	12393	New HMA	2001		37.6	-104.7	6245
CDOT	11	12529	HMA overlay (hot in place recycle) over existing HMA	1973	1999	38.4	-104.9	5191
CDOT	12	13390	New HMA	2001		38.8	-104.8	5930
CDOT	13	10175	New JPCP	1996		38.8	-104.7	6084
CDOT	14	13131	New HMA	2002		39.0	-105.1	9082
CDOT	15	11959	New HMA	2002		39.0	-105.1	8710
CDOT	16	13440	Superpave HMA overlay over existing HMA	1975	2001	39.0	-105.0	8060
CDOT	17	13932	HMA overlay (hot in place recycle) over existing HMA	1953	2002	39.0	-104.8	6618
CDOT	18	12187	HMA overlay of existing JPCP	1984	1999	39.6	-104.8	5689
CDOT	19	92021	New JPCP	1994		39.8	-104.8	5355
CDOT	20	13353	AC overlay over existing JPCP	1971	2002	39.7	-104.8	5600
CDOT	21	91094	New HMA	1999		39.7	-104.8	5475
CDOT	22	12297	SMA overlay over existing HMA	1980	2000	39.7	-105.0	5273
CDOT	23	11918	New HMA	2001		39.8	-105.0	5272
CDOT	24	13356	HMA overlay of existing JPCP	1963	2002	39.8	-104.9	5325
CDOT	25	10326	New JPCP	1996		40.0	-105.1	5218
CDOT	26	93216	New JPCP	1994		37.3	-108.6	6180
CDOT	27	13959	Superpave HMA overlay over existing HMA	1969	2002	40.0	-105.3	5627
CDOT	28	11865	New HMA	2001		40.3	-104.2	4486
CDOT	29	89168	Unbonded JPCP overlay of	1959	1992	40.2	-104.1	4570

Table 15. Inventory information (construction/rehab date, long/lat & elevation) for selected projects.

Project Type	ARA ID	CDOT/LTPP ID	Pavement Type	Const. Year	Rehab Year	Latitude, deg	Longitude, deg.	Elev., ft
			existing JPCP					
CDOT	30	11979	HMA overlay of existing JPCP	1962	1998	40.3	-103.7	4262
CDOT	31	13258	Superpave HMA overlay over existing HMA	1968	2000	39.7	-105.4	7463
CDOT	32	12448	HMA overlay (hot in place recycle) over existing HMA	1986	1999	39.7	-105.9	10869
CDOT	33	13435	Superpave HMA overlay over existing HMA	1978	2004	39.7	-106.1	8711
CDOT	34	13513	HMA overlay (hot in place recycle) over existing HMA	1969	2003	39.0	-105.7	8911
CDOT	35	13087	New HMA	2001		38.8	-106.9	8448
CDOT	36	13880	HMA overlay (hot in place recycle) over existing HMA	1953	2002	37.7	-106.7	8264
CDOT	37	92976	New HMA	1999		37.6	-106.7	8468
CDOT	38	13505	HMA overlay (hot in place recycle) over existing HMA	1975	2001	37.2	-107.7	6874
CDOT	39	11970	HMA overlay (cold in place recycle) over existing HMA	1971	2001	37.3	-108.1	8232
CDOT	41	13325	HMA overlay (hot in place recycle) over existing HMA	1936	2001	38.7	-108.0	5091
CDOT	42	12153	New HMA	2002		38.9	-108.4	4967
CDOT	43	13085	New HMA	2002		39.9	-108.7	5858
CDOT	44	11213	New HMA	2000		39.9	-108.7	5750
CDOT	45	13106	Superpave HMA overlay over existing HMA	1962	2001	40.2	-108.4	5545
CDOT	46	00000	New JPCP	1976		39.5	-107.7	5350
CDOT	47	12018	New HMA	2002		40.4	-106.8	6866
CDOT	48	13866	Superpave HMA overlay over existing HMA	1962	2002	40.1	-106.8	8338
CDOT	49	13864	HMA overlay (hot in place recycle) over existing HMA	1955	2002	39.5	-107.3	5988
CDOT	50	11780	New HMA	2000		39.3	-107.0	6852
CDOT	51	12271	New HMA	2002		39.2	-106.9	7825
CDOT	52	12321	Superpave HMA overlay over existing HMA	1983	1999	39.8	-104.4	5310
CDOT	53	84076	New JPCP	1995		39.9	-105.1	5460
CDOT	54	11546	New JPCP	1999		39.6	-105.2	7436
CDOT	55	93015	New JPCP	1997		39.6	-105.2	6966
LTPP	56	8_0213_1	New JPCP	1993		39.9	-104.8	5077
LTPP	57	8_0214_1	New JPCP	1993		39.9	-104.8	5077
LTPP	58	8_0215_1	New JPCP	1993		39.9	-104.8	5077
LTPP	59	8_0216_1	New JPCP	1993		39.9	-104.8	5077

Table 15. Inventory information (construction/rehab date, long/lat & elevation) for selected projects.

Project Type	ARA ID	CDOT/LTPP ID	Pavement Type	Const. Year	Rehab Year	Latitude, deg	Longitude, deg.	Elev., ft
LTPP	60	8_0217_1	New JPCP	1993		39.9	-104.8	5077
LTPP	61	8_0218_1	New JPCP	1993		39.9	-104.8	5077
LTPP	62	8_0219_1	New JPCP	1993		39.9	-104.8	5077
LTPP	63	8_0220_1	New JPCP	1993		39.9	-104.8	5077
LTPP	64	8_0221_1	New JPCP	1993		39.9	-104.8	5077
LTPP	65	8_0222_1	New JPCP	1993		39.9	-104.8	5077
LTPP	66	8_0223_1	New JPCP	1993		40.0	-104.8	5077
LTPP	67	8_0224_1	New JPCP	1993		39.9	-104.8	5077
LTPP	68	8_0259_1	New JPCP	1993		40.0	-104.8	5077
LTPP	69	8_0501_1	New HMA	1974		39.3	-103.2	5128
LTPP	70	8_0501_2	HMA overlay of existing HMA	1974	1991	39.3	-103.2	5128
LTPP	71	8_0502_1	New HMA	1974		39.3	-103.2	5128
LTPP	72	8_0502_2	HMA overlay of existing HMA	1974	1991	39.3	-103.2	5128
LTPP	73	8_0503_1	New HMA	1974		39.3	-103.2	5128
LTPP	74	8_0503_2	HMA overlay of existing HMA	1974	1991	39.3	-103.2	5128
LTPP	75	8_0504_1	New HMA	1974		39.3	-103.2	5128
LTPP	76	8_0504_2	HMA overlay of existing HMA	1974	1991	39.3	-103.2	5128
LTPP	77	8_0505_1	New HMA	1974		39.3	-103.2	5128
LTPP	78	8_0505_2	HMA overlay of existing HMA	1974	1991	39.3	-103.2	5128
LTPP	79	8_0506_1	New HMA	1974		39.3	-103.2	5128
LTPP	80	8_0506_2	HMA overlay of existing HMA	1974	1991	39.3	-103.2	5128
LTPP	81	8_0507_1	New HMA	1974		39.3	-103.2	5128
LTPP	82	8_0507_2	HMA overlay of existing HMA	1974	1991	39.3	-103.2	5128
LTPP	83	8_0508_1	New HMA	1974		39.3	-103.2	5128
LTPP	84	8_0508_2	HMA overlay of existing HMA	1974	1991	39.3	-103.2	5128
LTPP	85	8_0509_1	New HMA	1974		39.3	-103.2	5128
LTPP	86	8_0509_2	HMA overlay of existing HMA	1974	1991	39.3	-103.2	5128
LTPP	87	8_0559_1	New HMA	1974		39.3	-103.2	5128
LTPP	88	8_0559_2	HMA overlay of existing HMA	1974	1991	39.3	-103.2	5128
LTPP	89	8_0560_1	New HMA	1974		39.3	-103.2	5128
LTPP	90	8_0560_2	HMA overlay of existing HMA	1974	1991	39.3	-103.2	5128

Table 15. Inventory information (construction/rehab date, long/lat & elevation) for selected projects.

Project Type	ARA ID	CDOT/LTPP ID	Pavement Type	Const. Year	Rehab Year	Latitude, deg	Longitude, deg.	Elev., ft
LTPP	91	8_0811_1	New JPCP	1993		39.9	-104.8	5095
LTPP	92	8_0812_1	New JPCP	1993		39.9	-104.8	5095
LTPP	93	8_1029_1	New HMA	1972		40.5	-107.9	5920
LTPP	94	8_1029_5	HMA overlay of existing HMA	1972	2003	40.5	-107.9	5920
LTPP	95	8_1047_1	New HMA	1983		40.1	-108.8	5260
LTPP	96	8_1047_2	HMA overlay of existing HMA	1983	1992	40.1	-108.8	5260
LTPP	97	8_1053_1	New HMA	1984		38.7	-108.0	5140
LTPP	98	8_1053_2	HMA overlay of existing HMA	1984	2001	38.7	-108.0	5140
LTPP	99	8_1057_1	New HMA	1985		39.1	-108.5	4586
LTPP	100	8_2008_1	New HMA	1972		38.1	-103.2	3894
LTPP	101	8_3032_1	New JPCP	1977		39.5	-107.7	5345
LTPP	102	8_6002_1	New HMA	1958		38.4	-104.6	4904
LTPP	103	8_6002_2	HMA overlay of existing HMA	1958	1996	38.4	-104.6	4904
LTPP	104	8_6013_1	New HMA	1965		40.6	-103.2	3935
LTPP	105	8_7035_1	HMA overlay of JPCP (New)	1965		39.8	-104.8	5500
LTPP	106	8_7035_2	HMA overlay of existing JPCP	1965	1994	39.8	-104.8	5500
LTPP	107	8_7036_1	HMA overlay of JPCP (New)	1961		39.7	-104.3	5380
LTPP	108	8_7776_1	New JPCP	1988		39.7	-104.7	5280
LTPP	109	8_7780_1	New HMA	1973		38.9	-105.0	7400
LTPP	110	8_7780_2	HMA overlay of existing HMA	1973	2001	38.9	-105.0	7400
LTPP	111	8_7781_1	New HMA	1972		38.1	-103.2	3894
LTPP	112	8_7781_2	HMA overlay of existing HMA	1972	1991	38.1	-103.2	3894
LTPP	113	8_7783_1	New HMA	1984		39.4	-108.1	5000
LTPP	114	8_7783_3	HMA overlay of existing HMA	1984	2003	39.4	-108.1	5000
LTPP	115	8_9019_1	Unbonded JPCP overlay of existing JPCP	1966		40.2	-105.0	4970
LTPP	116	8_9020_1	Unbonded JPCP overlay of existing JPCP	1962		40.4	-105.0	4550
LTPP	117	8_A310_1	New HMA	1984		38.7	-108.0	
LTPP	118	8_A310_2	HMA overlay of existing HMA	1984	1990	38.7	-108.0	
LTPP	119	8_A320_1	New HMA	1984		38.7	-108.0	
LTPP	120	8_A330_1	New HMA	1984		38.7	-108.0	

Table 15. Inventory information (construction/rehab date, long/lat & elevation) for selected projects.

Project Type	ARA ID	CDOT/LTPP ID	Pavement Type	Const. Year	Rehab Year	Latitude, deg	Longitude, deg.	Elev., ft
LTPP	121	8_A340_1	New HMA	1984		38.7	-108.0	
LTPP	122	8_A350_1	New HMA	1984		38.7	-108.0	
LTPP	123	8_B310_1	New HMA	1972		38.1	-103.2	
LTPP	124	8_B310_2	HMA overlay of existing HMA	1972	1990	38.1	-103.2	
LTPP	125	8_B320_1	New HMA	1972		38.1	-103.2	
LTPP	126	8_B330_1	New HMA	1972		38.1	-103.2	
LTPP	127	8_B350_1	New HMA	1972		38.1	-103.2	

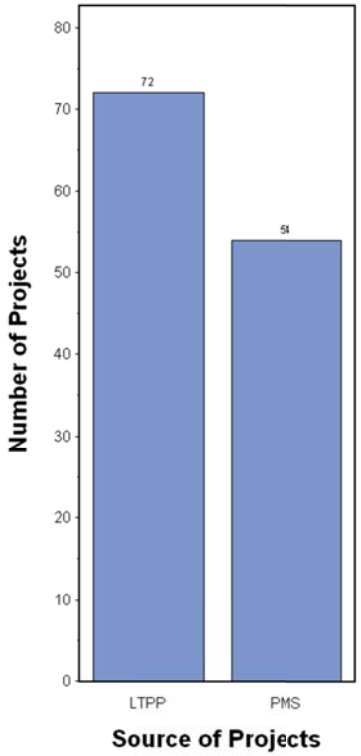

Figure 10. Histogram showing distribution of source of selected projects.

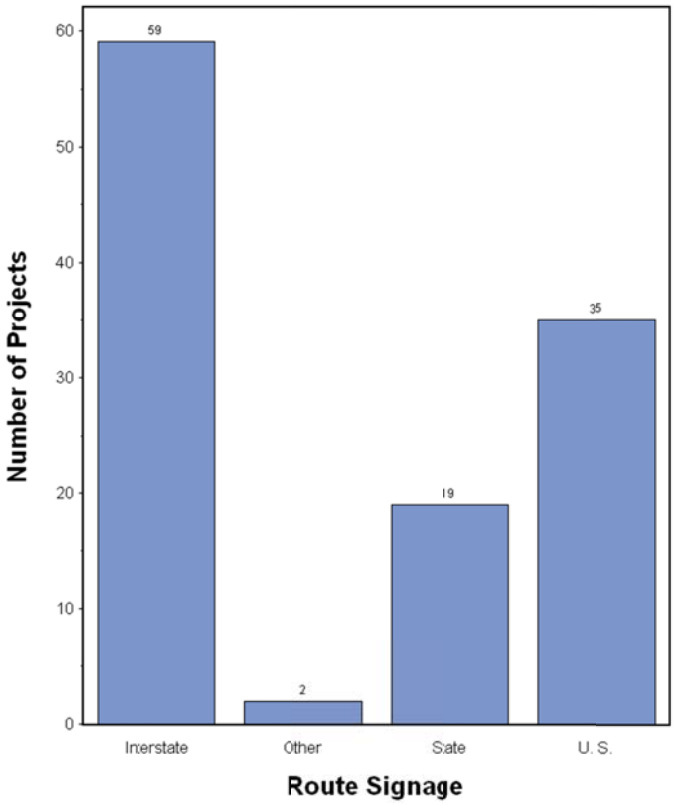

Figure 11. Histogram showing distribution of route signage.

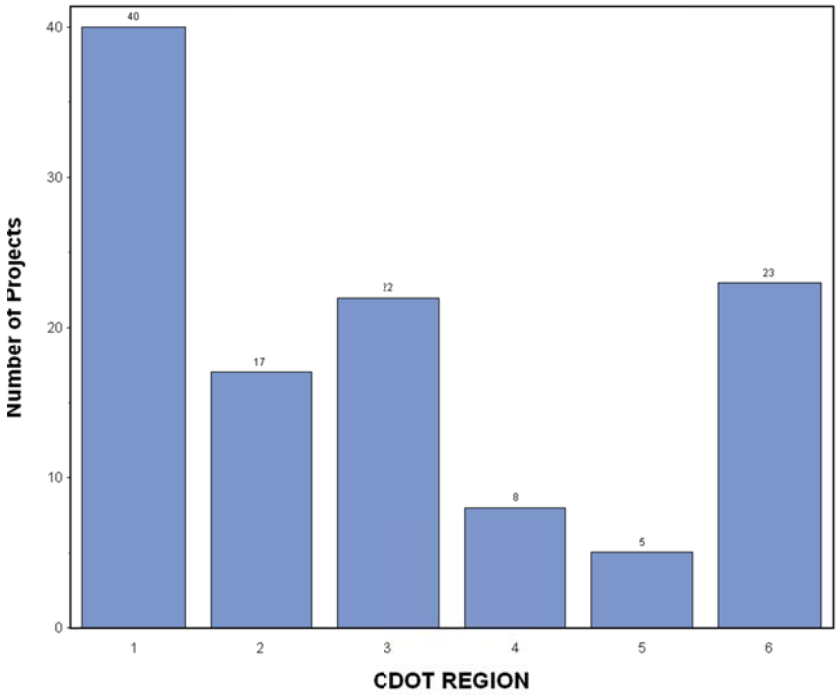

Figure 12. Histogram showing distribution of CDOT regions in which selected projects are located.

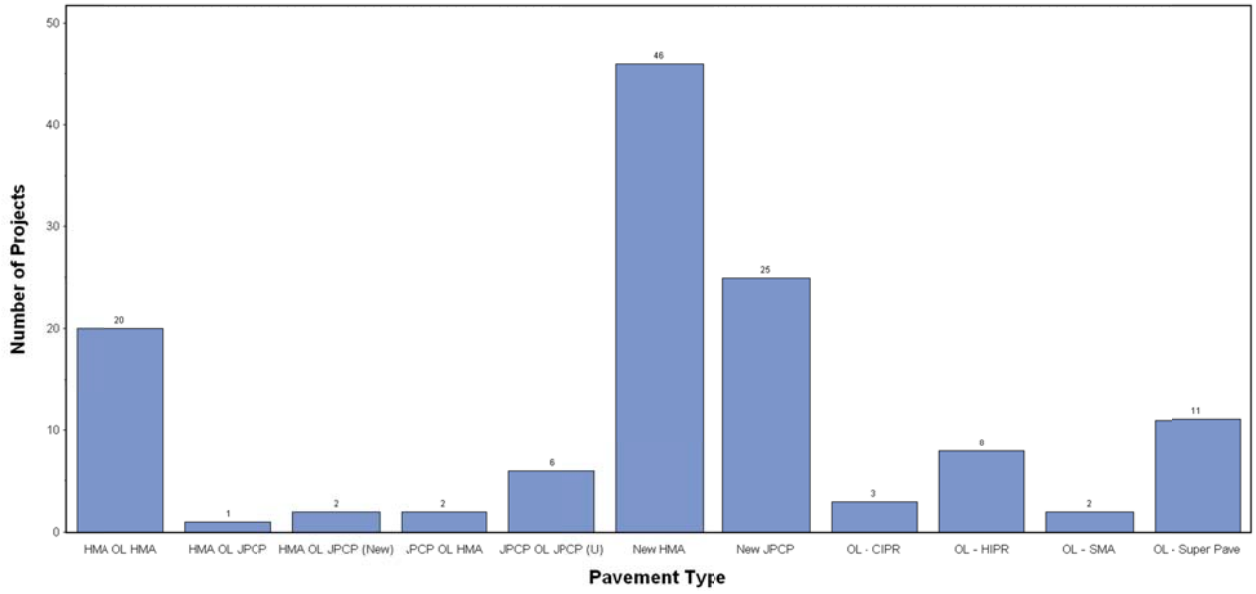

Figure 13. Histogram showing distribution of pavement type.

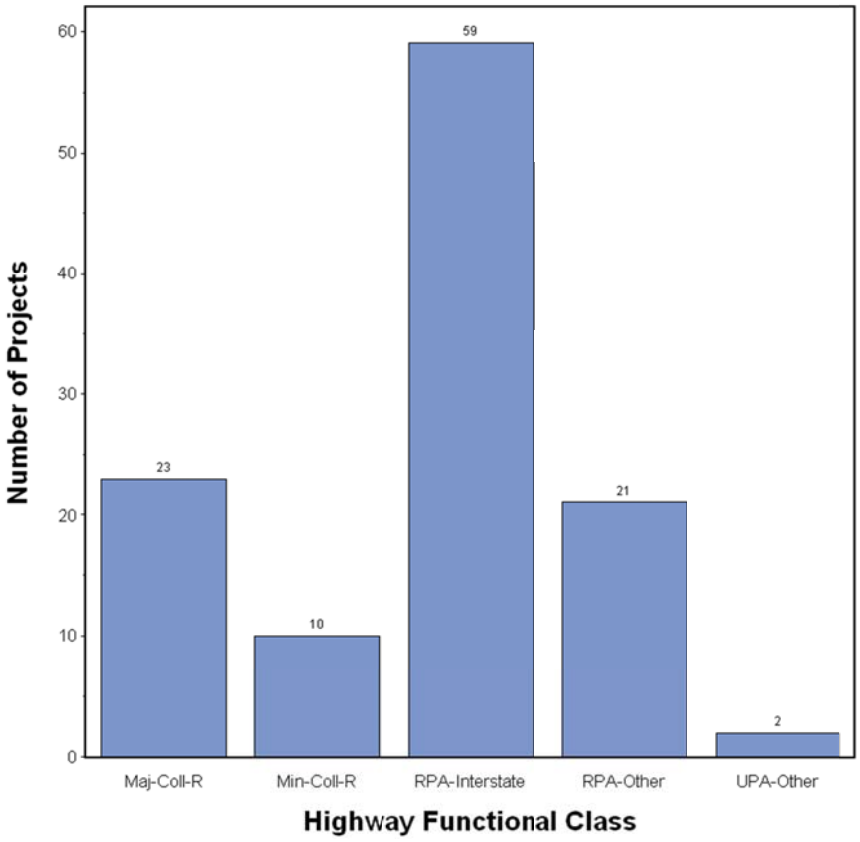

Figure 14. Histogram showing distribution of highway functional class.

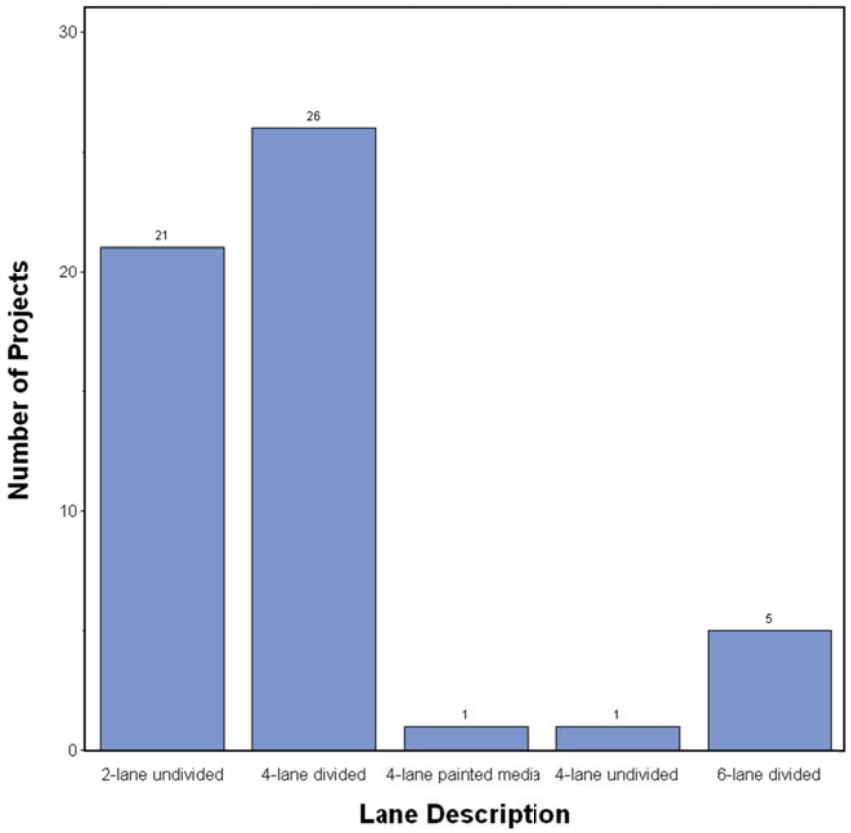

Figure 15. Histogram showing distribution of facility number of lanes.

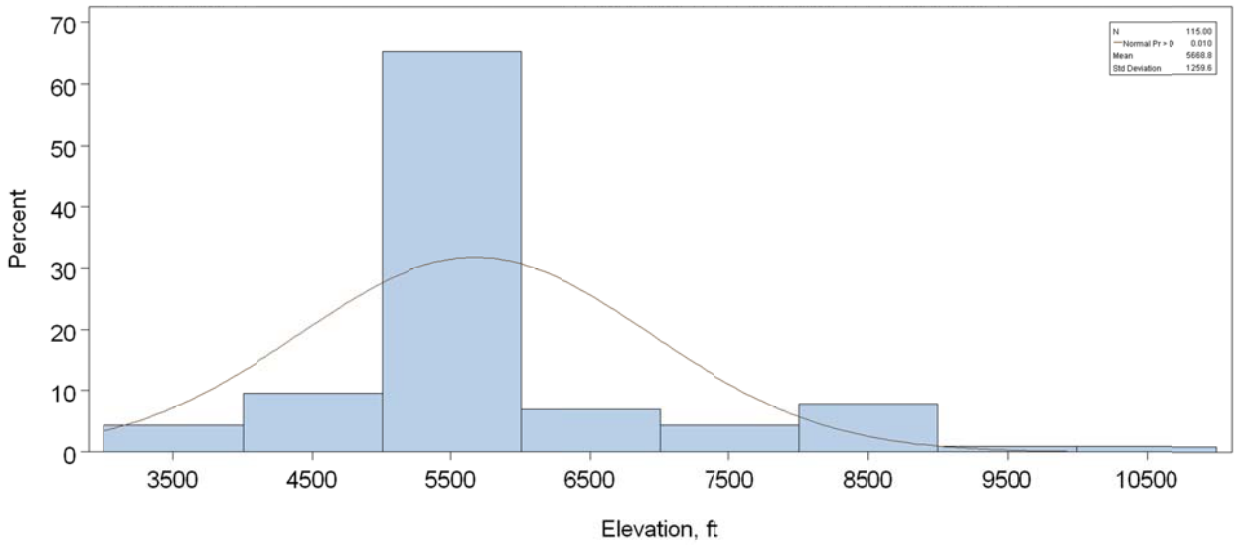

Figure 16. Histogram showing distribution of pavement location elevation.

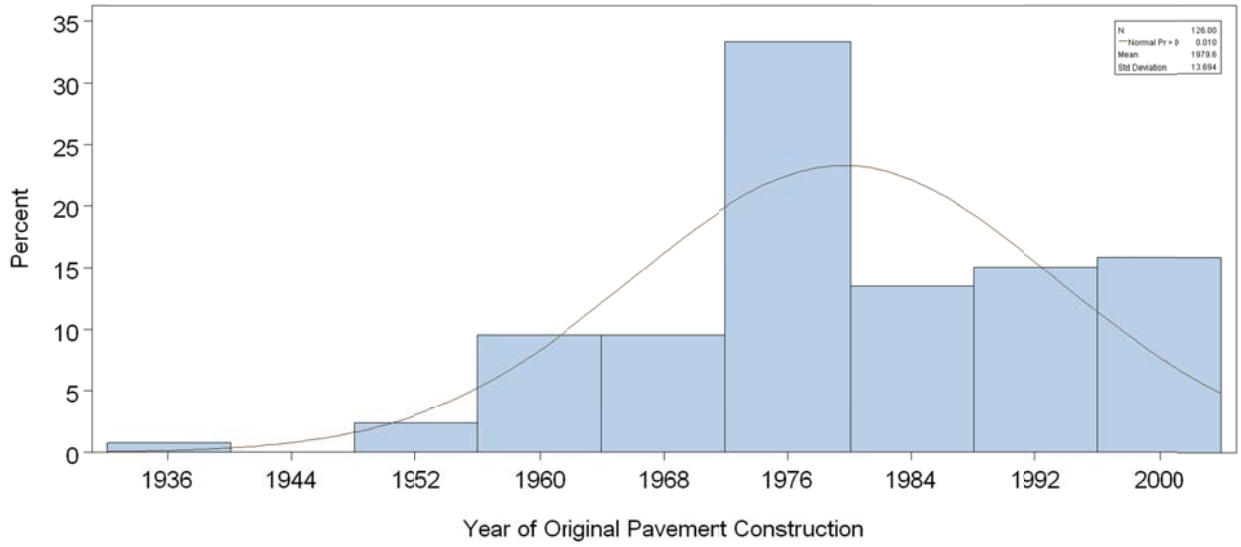

Figure 17. Histogram showing distribution of original construction year.

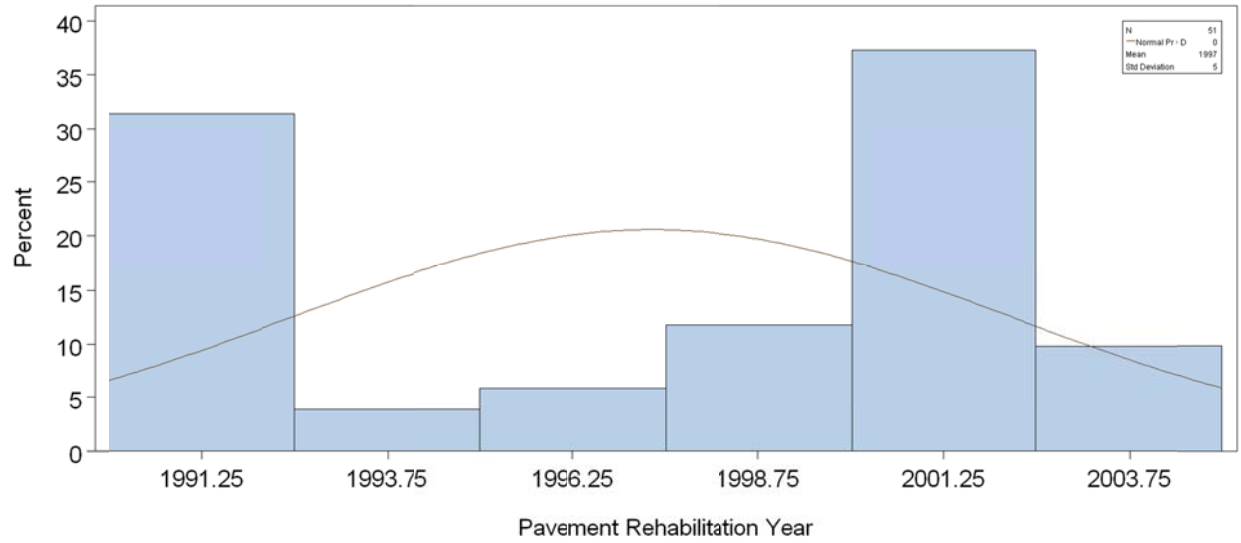

Figure 18. Histogram showing distribution of pavement rehabilitation (overlay placement) year.

Pavement design and inventory data were obtained from LTPP data tables and CDOT records to define in detail the project type, structure, layer types and materials, location, etc. The assembled information was used to populate the sampling templates developed to identify and select project types of interest for use in MEPDG model validation/calibration. The populated sampling templates are presented in Tables 16 and 17. There were not enough projects selected to achieve all possible high, average, low combinations of all the sampling templates input factors (i.e., full factorial experimental design). However, the partial experimental design obtained was deemed adequate to meet the goals for model validation/calibration, and the projects selected collectively represented Colorado pavement design practices, materials properties, site conditions, and construction practices.

Table 16. Experimental template populated with new HMA and HMA-overlaid HMA pavement projects for use in MEPDG flexible pavement model calibration/validation in Colorado.

HMA Thickness	Binder Type	Climate Zone[3]	Subgrade Type			
			Fine-Grained Soil		Coarse-Grained Soil	
			Conv. HMA[1]	Full-Depth HMA[2]	Conv. HMA[1]	Full-Depth HMA[2]
< 4-in	Neat	Hot/Moderate	1047_1, 1057_1, 2008_1, 7781_1, B310_1, B320_1 B350_1, 0501_2, 0505_2, 0506_2, A310_2, 1047_2 6002_1, 7781_2, 7783_3, 9-13936, 22-12297		0502_2, 0509_2 7780_1, 7-13817	
		Cool	38-13505		31-13258, 34-13513	
		Very Cool			33-13435	
	Modified	Hot/Moderate	41-13325, 45-13106 48-13866		49-13864	
		Cool	44-11213			
		Very Cool	36-13880		32-12448	
4- to 8-in	Neat	Hot/Moderate	0501_1, 0504_1, 0505_1, 0506_1, 0507_1, 0559_1 1053_1, 7783_1, A310_1, A320_1, A330_1, A340-1 A350_1, B330_1, 0504_2, 0507_2, 0559_2, B310_2 1053_2, 5-12441, 8-12685, 11-12529		0502_1, 0503_1 0508_1, 0509_1 0560_1, 1029_1 1029_5, 0503_2 0508_2, 0560_2	
		Cool			50-11780	
		Very Cool	15-11959, 39-11970		16-13440	14-13131
	Modified	Hot/Moderate	47-12018 6002_2, 52-12321	4-91044	43-13085, 27-13959	
		Cool			51-12271, 17-13932	
		Very Cool			37-92976, 35-13087	
> 8-in	Neat	Hot/Moderate			12-13390	21-91094
		Cool				
		Very Cool				
	Modified	Hot/Moderate	10-12393		42-12153, 28-11865	23-11918
		Cool				
		Very Cool				

1. Conventional HMA is typically and HMA layer placed over thick dense graded aggregate base (DGAB) over the prepared subgrade. Conventional HMA could also include surface treatments (chip seal, fog seal, slurry seal or crack seal) on conventional HMA.
2. Full-depth HMA is typically HMA over asphalt treated base (dense or drainable) over a prepared subgrade.
3. See Table 10.

Table 17. Experimental template populated with new JPCP, JPCP overlays of flexible pavements, and unbonded JPCP of JPCP projects for use in MEPDG JPCP model calibration/validation in Colorado.

PCC Thickness	Base Type[1]	Nondoweled Transverse Joint			Dowelled Transverse Joint		
		12-ft Slab Width		Widened Slab (13- or 14-ft)	12-ft Slab Width		Widened Slab (13- or 14-ft)
		HMA Shoulder	Tied PCC Shoulder		HMA Shoulder	Tied PCC Shoulder	
< 10-in	DGAB					13-10175	
	CTB/LCB		26-93216		0213, 0214 0811	55-93015 54-11546 25-10326	
	ATB	9019[2] 9020[2]	3032 29-89168[2]		0217, 0218 0219	53-84076	
10 to 12-in	DGAB		18-12187[3]		0221, 0222		
	CTB/LCB				0259		
	ATB				7776, 0215 0216, 0812	19-92021	
> 12-in	DGAB				0220	3-88452[2]	
	CTB/LCB				0223, 0224	6-91022[3]	
	ATB						

1. CTB = cement treated base, LCB = lean concrete base, ATB = asphalt treated base
2. Unbonded JPCP
3. JPCP over existing HMA

Extracting, Assembling, and Evaluating Project Data (Project Database Development)

The MEPDG requires input data in several categories. For this implementation project, pavement data were obtained primarily from the following sources:

- LTPP inventory, traffic, climate, materials, maintenance/rehabilitation databases.
- LTPP construction guidelines and reports.
- CDOT Online Transportation Information System (OTIS) (data from over 120 permanent automated traffic recorder [ATR] and 13 continuous weigh-in-motion [WIM] sites).
- CDOT pavement management system data tables.
- CDOT design/construction reports.
- CDOT construction quality assurance (QA) testing databases.
- CDOT pavement research and forensic examination reports.
- Field testing/surveys and laboratory testing of extracted materials.
- Colorado Climate Center.
- NCDC database and the USDA NRCS SSURGO database.

Details of data sources are presented in Tables 18 and 19.

Table 18. LTPP sources of MEPDG input data for development of CDOT MEPDG calibration/validation database.

Data Category		Source of Information (LTPP Data Tables)
Inventory		INV_GENERAL, INV_AGE, INV_ID, SPS_GENERAL, SPS _ID, SPS2_PCC_PLACEMENT_DATA SPS8_PCC_PLACEMENT_DATA SPS5_OVERLAY, SECTION_COORDINATES
Structure definition		TST_L05B
Traffic		TRF_HIST_EST_ESAL, TRF_MON_EST_ESAL TRF_MEPDG_AADTT_LTPP_LN, TRF_MEPDG_AX_DIST_ANL TRF_MEPDG_AX_PER_TRUCK, TRF_MEPDG_HOURLY_DIST TRF_MEPDG_MONTH_ADJ_FACTR, TRF_MEPDG_VEH_CLASS_DIST TRF_MONITOR_AXLE_DISTRIB, TRF_MONITOR_LTPP_LN
Materials	Layer type and materials description	TST_L05B
	In situ FWD deflection testing	MON_DEFL_DEV_CONFIG, MON_DEFL_LOC_INFO MON_DEFL_TEMP_VALUES, FWD_Drop_Data_States_AL_ID
	Asphalt	INV_PMA_ASPHALT, TST_AG04, RHB_ACO_PROP, RHB_HMRAP_NEW_AC_PROP
	PCC	INV_PCC_MIXTURE, TST_PC01, TST_PC02, TST_PC03, TST_PC04, TST_PC09, SPS Experiment Guidelines
	Chemically stabilized	TST_TB02
	Unbound aggregate & subgrade soils	TST_SS01_UG01_UG02, TST_UG04_SS03
Climate		NCDC & Colorado Climate Center
Design		INV_PCC_JOINT, SPS Experiment Guidelines, SPS-1, -2, -5, -6 construction reports, INV_GENERAL, SPS_GENERAL
Construction		SPS-1, -2, -3, -5, -6, -9 Construction reports
Performance	HMA alligator cracking	MON_DIS_AC_REV
	HMA transverse “thermal” cracking	MON_DIS_AC_REV
	Total rutting	MON_T_PROF_INDEX_SECTION
	JPCP transverse “slab” cracking	MON_DIS_JPCC_REV
	JPCP transverse joint faulting	MON_DIS_JPCC_FAULT_SECT
	IRI	MON_PROFILE_MASTER

Table 19. CDOT sources of MEPDG input data for development of CDOT MEPDG calibration/validation database.

Data Category			Source of Information (CDOT Data Tables)
Inventory			CDOT data libraries
Structure definition			CDOT data libraries, construction QA records/database, Resident Materials Engineer files
Traffic			CDOT OTIS, WIM/ATR data
Materials		Layer type and materials description	CDOT data libraries, construction QA records/database, Resident Materials Engineer files
		Asphalt	Laboratory testing
		PCC	Laboratory testing
		Chemically stabilized	Insitu FWD deflection testing and characterization of materials properties, MEPDG defaults
		Unbound aggregate & subgrade soils	Insitu FWD deflection testing and characterization of materials properties
Climate			NCDC & CDOT weather stations climate data files
Design			CDOT data libraries, construction QA records/database, Resident Materials Engineer files
Construction			CDOT data libraries, construction QA records/database, Resident Materials Engineer files
Performance	HMA alligator cracking		Manual visual distress surveys, coring and examination of cores, CDOT pavement management system
	HMA transverse "thermal" cracking		Manual visual distress surveys, coring and examination of cores, CDOT pavement management system
	Total rutting		Manual visual distress surveys & trenching, CDOT pavement management system
	JPCP transverse "slab" cracking		Manual visual distress surveys, coring and examination of cores, CDOT pavement management system
	JPCP transverse joint faulting		Manual visual distress surveys, CDOT pavement management system
	IRI		Profile measurements and computation of smoothness (IRI), CDOT pavement management system

Extraction and Assembly of Pertinent Data

The first step in developing the project database for model validation/calibration was to extract relevant information from the various data sources identified in Tables 18 and 19. As the identified data/information came in various formats and standards (electronic and hard copies), a wide variety of software tools and methods was applied to extract pertinent data in an orderly and efficient manner. Data extraction basically consisted of the following steps:

1. For each selected project, define location references that many be used to extract data from the many sources identified in Tables 18 and 19. Examples of project location references used data extraction and assembly are as follows:
    a. LTPP: SHRPID, STATE_CODE, CONSTRUCTION_NO (see Table 20).
    b. CDOT OTIS: ROUTE_NO, BEGIN MILEPOST, END MILEPOST (see Figure 19).
    c. NCDC & Colorado Climate Center: LATITUDE, LONGITUDE.

d. CDOT pavement management system: CDOT PMS ID, CDOT REGION, ROUTE_SIGN, ROUTE_NO, DIRECTION, BEGIN MILEPOST, END MILEPOST.

Note that multiple location references are required to extract data from different sources.

2. Develop basic database with as many location references as needed for each selected project (see example in Table 20).
3. For each data source (in electronic or hard copy format) identify pertinent data (e.g., LTPP table TST_L05B contains information on pavement structure, layer thicknesses, and material description) and applicable location reference system.
4. Develop appropriate algorithms and routines as needed using database software tools (e.g., MS Access, MS Excel, SAS) for extracting pertinent data. Note that data in paper format (hard copy) was manually converted into electronic form before extraction and assembly in the project database. An example of the routines developed in MS Access and used for data extraction and assembly is presented in Figure 20.

Table 20. Example of multiple project location references used for data extraction and assembly.

CDOT ID	SHRP ID	CONST. No.	ROUTE SIGN	ROUTE No.	HWY	DIRECTION	BEGIN MP	END MP	CDOT REGION
11328	N/A	N/A	Interstate	70	70A	WB	309	308.8	1
11327	N/A	N/A	Interstate	70	70A	WB	312	311.8	1
88452	N/A	N/A	Interstate	70	70A	EB	330	330.2	1
91022	N/A	N/A	Interstate	70	70A	WB	440	439.8	1
12393	N/A	N/A	Interstate	25	25A	SB	47.1	46.9	2
13390	N/A	N/A	Interstate	25	25A	SB	139.5	139.3	2
13932	N/A	N/A	Interstate	25	25A	SB	155	154.8	2
92021	N/A	N/A	Interstate	255	255A	NB	11.1	11.3	6
N/A	3032	1	Interstate	70	70	EB	95.75		3
N/A	6002	1	Interstate	25	25	NB	106.35		2
N/A	6002	2	Interstate	25	25	NB	106.35		2
N/A	1029	1	U.S.	40	40	WB	69.75		3
N/A	1029	5	U.S.	40	40	WB	69.75		3
N/A	1053	1	U.S.	50	50	NB	75.3		3
N/A	1053	2	U.S.	50	50	NB	75.3		3
N/A	2008	1	U.S.	50	50	WB	401.93		2
N/A	1057	1	State Route	141B	141B	SB	160.65		3
N/A	6013	1	U.S.	14	14	EB	235.4		4

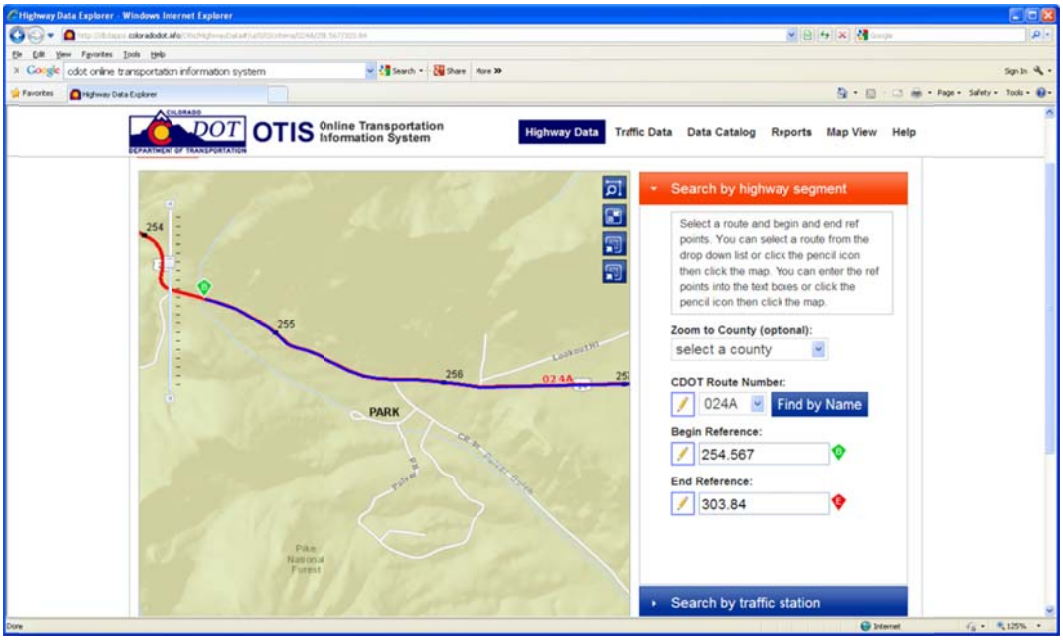

Figure 19. CDOT OTIS graphic showing location referencing used for traffic data extraction.

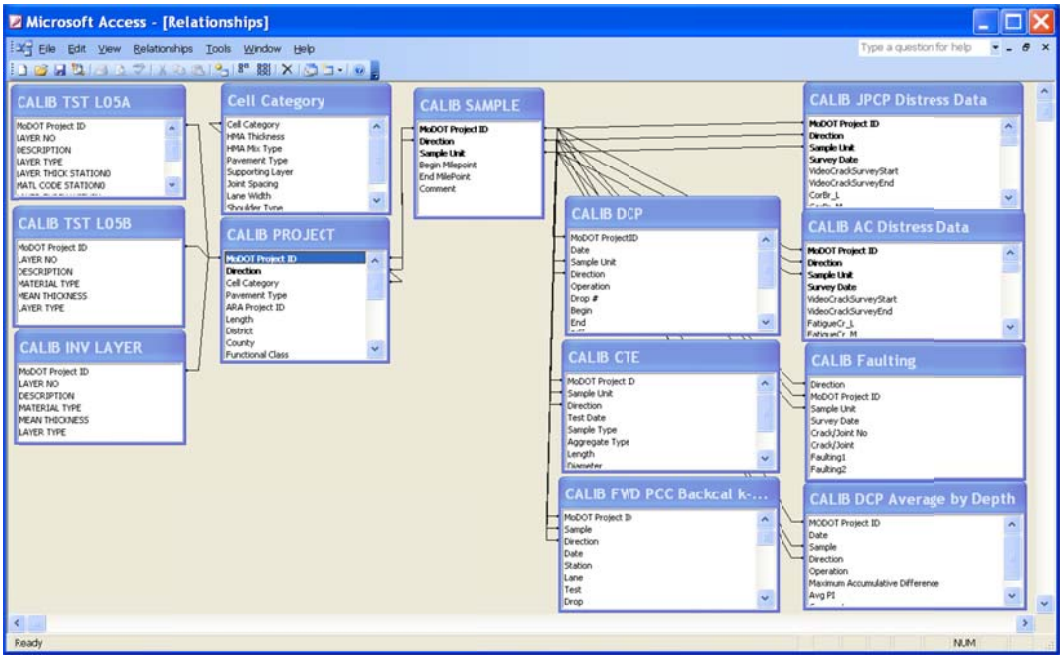

Figure 20. Example of the routines developed in MS Access and used for data extraction and assembly.

Evaluation of Assembled Project Data and Final Project Database Development

The assembled project database was reviewed and evaluated to determine the following:

- Data deemed to be reasonable and accurate.
- Data deemed to be potentially anomalous, erroneous, or outliers.
- Missing data.

This was done using a variety of techniques, including:

- Computing basic statistics (mean, max., min, standard deviation) for use in identifying outliers and erroneous data elements. In general, inputs that fell outside the range of mean + 3σ were deemed outliers.
- Comparison of input data with engineering expectations (i.e., layer thickness must be greater than zero).
- Developing time based plots of key variables to determine reasonableness of magnitudes and change in magnitude over time (see Figures 21 through 24).

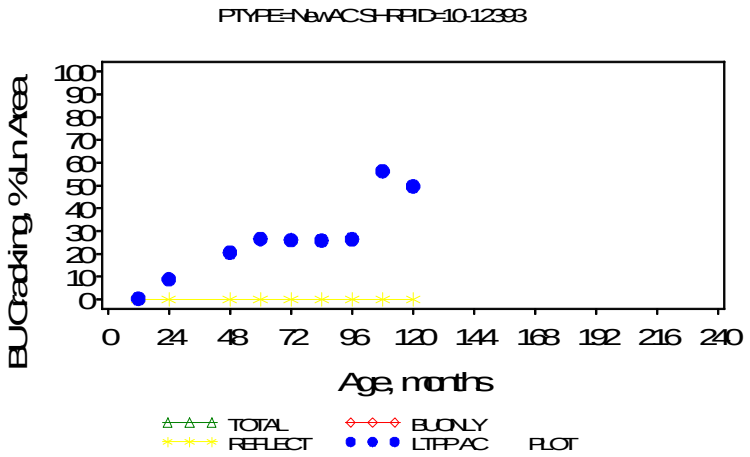

Figure 21. Plot showing change in alligator (bottom-up fatigue) cracking over time for CDOT project 12393.

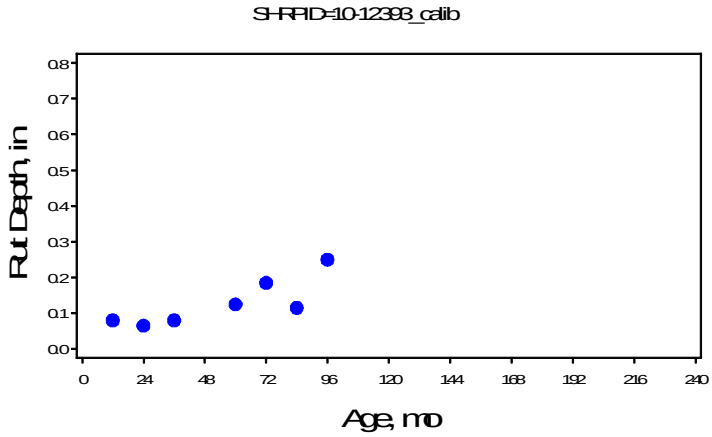

Figure 22. Plot showing change in total rutting over time for CDOT project 12393.

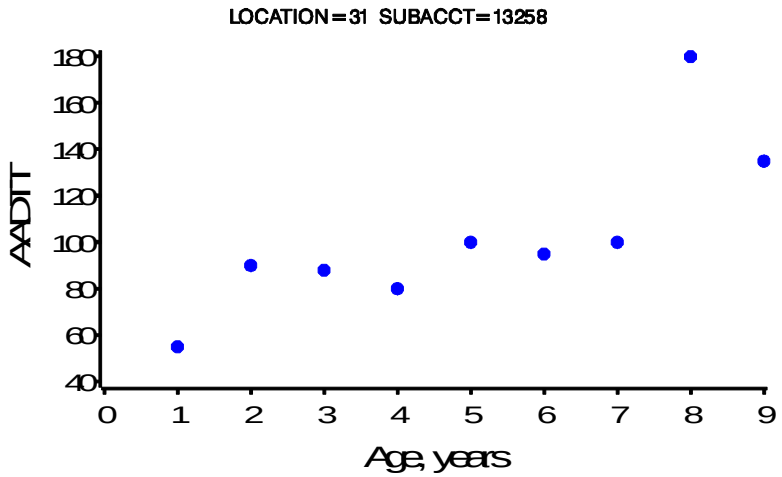

Figure 23. Plot showing change in average annual daily truck traffic (AADTT) over time for CDOT project 13258.

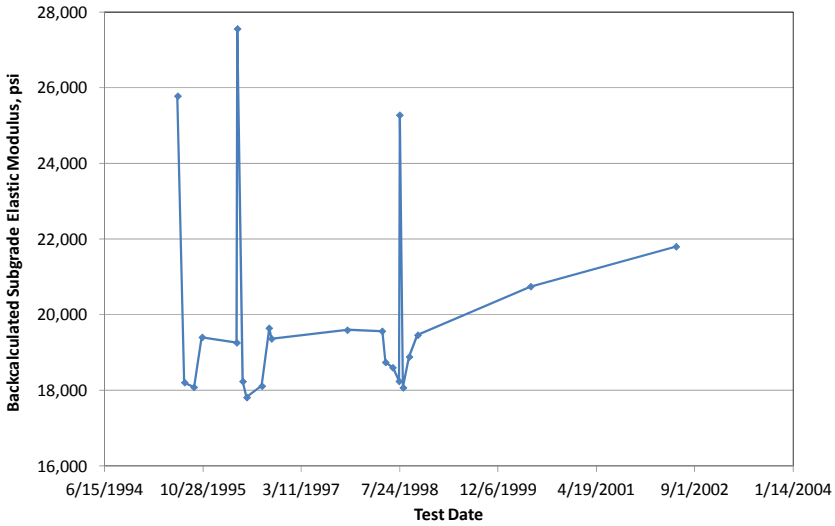

Figure 24. Plot showing change in backcalculated subgrade elastic modulus over time for LTPP project 0501.

Data inputs deemed as outliers or erroneous were flagged and remedial action was taken, in the form of (1) replacing with more reasonable information from other sources or (2) removal from the project database without replacement, leaving only accurate and reasonable data in the project database. Thus, for each project, data elements not available in the project database were deemed missing and not available.

Although agencies invest significant resources to compile and maintain vast amounts of data for use in pavement management, research, etc., for most situations it is virtually impossible to maintain a database that is complete with all records populated with reasonable, accurate data. Also, because of the complexity of the MEPDG, most agencies do not regularly maintain all the types of information required as inputs.

Estimating Missing Data

Evaluation of the assembled project database revealed considerable gaps in data required for MEPDG model validation/calibration. A summary of data availability is presented in Table 21. There are several methods of resolving gaps/missing data in a database. Below is a summary of some of the commonly applied strategies to resolve such situations:

- Discarding Projects with Missing Data: Discarding projects with incomplete records/missing data is practical only when (1) the number of projects is very small compared to the total number of projects (say, less than 5 percent of projects), (2) the missing data for a given project are very expensive (e.g., 80 percent of all required data), or (3) the missing data are fundamental for successfully conducting analysis (e.g., definition of pavement structure is missing or traffic volume data). For this project, discarding projects with missing data was not a feasible option since none of the projects selected met any of the criteria described.
- Estimation of Missing Data Element: Estimating missing data elements using correlations with other data elements (e.g., relating PCC flexural strength with compressive strength) is a very common practice for replacing missing data. The MEPDG provides several relationships for making such estimates and provides "national" defaults where the use of such relationships is not feasible.
- Forensic Examination: Missing data elements for a given project can be obtained through forensic examination of the project (e.g., coring, extraction, of cores, and examination and testing to determine pavement structure, layer thicknesses, material types, etc.). Estimates of the missing data can also be obtained through constitution of similar materials in the laboratory and testing for the required properties/inputs.

The estimation of missing data and forensic examinations options were utilized as needed to acquire missing data. Work done to acquire missing data is presented in the following sections.

Estimating Missing Traffic Data

A full list of missing traffic data elements is provided in Table 21. Default Colorado estimates of the missing data were developed using traffic data from LTPP and CDOT WIM sites (see Figure 25) and CDOT ATR sites. WIM and ATR data for each site were analyzed using the MS-ATLAS (Advanced Traffic Loading Analysis System) software as follows (see Figure 26):

- Assemble raw WIM/ATR traffic data (CDOT WIM and processed LTPP WIM data).
- Perform quality assessment of the raw and processed traffic data to verify data accuracy and reasonableness. Data cleansing was done based on data availability by site and year as follows (see Table 22 and Figure 27 for examples):
    - Data availability:
        - More than 200 days of WIM/ATR data available: Included in analysis to determine defaults.
        - Between 100 & 200 days of WIM/ATR data available: Eliminated if nonconforming to national distributions and expected trends.
        - Less than 100 days of WIM/ATR data available: Not included.

Table 21. Summary of data availability for MEPDG models validation/calibration.

Input Group		Input Parameter	Recommended Input Level	Data Availability	
				LTPP	Pavement Management System
Truck Traffic		Axle load distributions	Level 1 (field measured from WIM)	Available*	Not available
		Vehicle class distribution	Level 1 (field measured from WIM)	Available	Not available
		Number of axles per truck	Level 1 (field measured from WIM)	Available	Not available
		Monthly adjustment factors	Level 1 (field measured from WIM)	Available	Not available
		Hourly adjustment factors	Level 1 (field measured from WIM)	Available	Not available
		Lane & directional truck dist.	Level 3 (MEPDG defaults)	Available	Available
		Tire pressure	Level 3 (MEPDG defaults)	Available	Available
		Axle config. & tire spacing	Level 3 (MEPDG defaults)	Available	Available
		Truck wander	Level 3 (MEPDG defaults)	Available	Available
		Initial AADTT and growth rate	Level 1 (field measured from ATR/WIM)	Available	Available
Climate		Temperature, wind speed, cloud cover, precipitation, relative humidity	Level 2 (virtual weather stations created using NCDC climate data embedded in the MEPDG)	Insufficient	Insufficient
Material Properties	Unbound aggregate & Subgrade	Resilient modulus – subgrade	Level 2; FWD deflection measurements & backcalculation	Available	Not available
		Resilient modulus – unbound granular and chemically treated base/subbase layers	Level 3 (MEPDG defaults)	Available	Available
		Unbound base/ subgrade soil classification	Level 1 (lab test data)	Available	Not available
		Moisture-density relationships & other volumetric properties	Level 2 (Computed from gradation and Atterberg limits data)	Available	Not available
		Soil-water characteristic relationships	Level 3 (MEPDG defaults)	Available	Available
		Saturated hydraulic conductivity	Level 2 (computed from gradation and Atterberg limits data)	Available	Not available
	HMA	HMA dynamic modulus	Level 2 cComputed using material gradation, air void, binder type data)	Available	Not available
		HMA creep compliance & indirect tensile strength	Level 1 (lab testing)	Not available	Not available
		Volumetric properties	Level 3 (CDOT defaults)	Not available	Not available
		HMA coefficient of thermal contraction	Level 1 (lab testing)	Available	Not available
	PCC	PCC elastic modulus	Level 1 (lab test data) Level 2 (computed from PCC compressive strength)	Available	Not available
		PCC flexural strength	Level 1 (lab test data) Level 2 (computed from PCC compressive strength)	Available	Not available
		PCC coefficient of thermal expansion	Level 1 (lab test data) Level 2 (based on coarse aggregate)	Available	Not available
All Materials		Unit weight	Level 3 (MEPDG defaults)	Available	Available
		Poisson's ratio	Level 3 (MEPDG defaults)	Available	Available
		Thermal conductivity, heat capacity, surface absorptivity	Level 3 (MEPDG defaults)	Available	Available

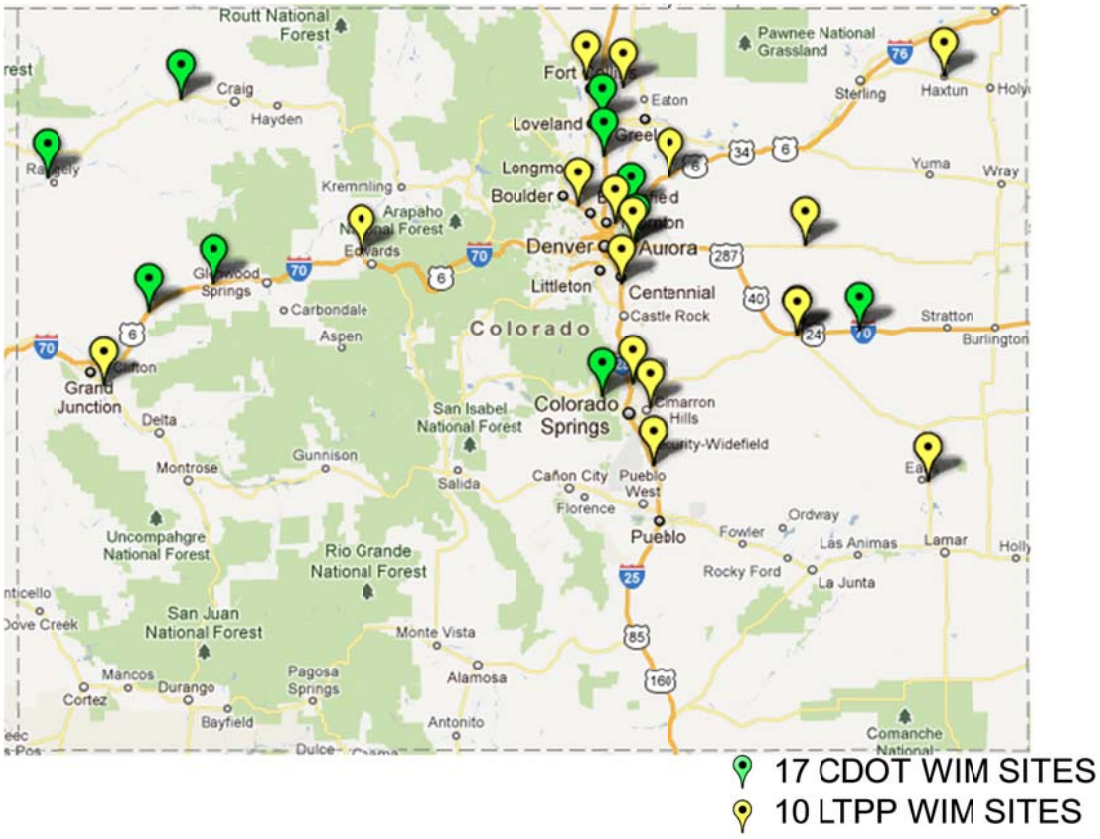

Figure 25. Location of LTPP and CDOT WIM sites in Colorado used for developing default MEPDG traffic inputs.

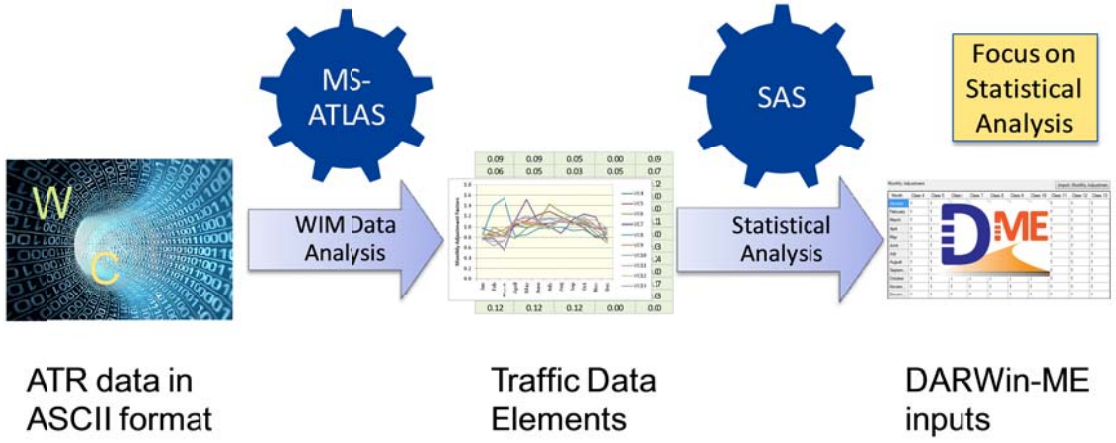

Figure 26. WIM traffic data analysis procedure.

Table 22. Examples of records availability for WIM/ATR sites in Colorado.

Station ID	Record Year						
	2000	2001	2002	2003	2004	2005	2006
000001	366	350	365	347	31*	349	332
000002		226	357	224		319	10*
000004	366	270	362	298	251		
000005	365	342	323	319		314	357
000007	151**	350	365	248		322	333
000008	48*	297	354	290		308	329
000009	24*	259	277	336		323	286
000010		289	290	66*	209	322	

*Eliminated
**Included based on distribution shape and pattern.

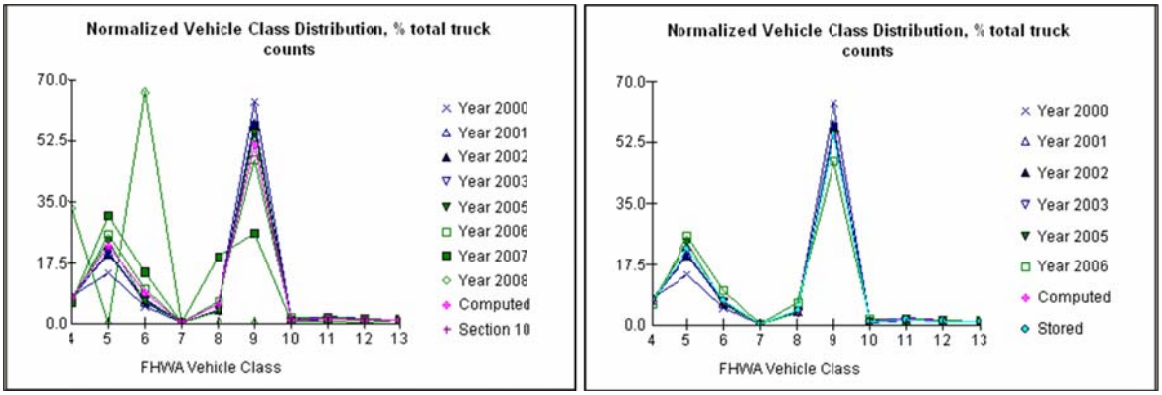

Figure 27. Example plot showing distribution of vehicle class (several years) for a WIM site in Colorado.

- Developing plots for use in accessing reasonableness of data and trends in data over the years):
  - Plot of percent truck versus hour of the day (midnight through 11:00 PM) for all years with data available for a given site.
  - Plot of monthly adjustment factor versus month of the year (January through December) for all years with data available for a given site.
  - Plot of percent trucks versus vehicle class (classes 4 through 13) for all years with data available for a given site.
  - Plot of number of single, tandem, tridem, and quad axles per truck versus vehicle class (classes 4 through 13) for all years with data available for a given site.
  - Plot of percent single, tandem, tridem, and quad trucks versus axle load (e.g., for single axles 3000 to 41000 lb in 1000-lb increments) for all years with data available for a given site.
- Review the plots for consistency, accuracy, and completeness (this did not involve basic quality assurance/quality control checks of the raw traffic data, but

rather a check of MEPDG computed traffic inputs). Examples of the checks that were done are as follows:

  - Whether hourly truck distribution factors add up to 100 percent or if monthly adjustment factors add up to 12.
  - Occurrences of long zero or "flat" periods in the monthly adjustment or hourly distribution data (several months or hours with no data).
  - Whether plots of axle loads versus percentage of all axles display distinct peaks as expected, and whether the percentage of all axles of a given axle type adds up to 100.
  - Was there consistency in trends over the years with data?

- Process the raw data using MS-ATLAS to obtain normalized vehicle class distribution, normalized axle load spectra by class, axle per class coefficients, base year truck volume and annual growth, monthly truck volume adjustment coefficients, and hourly truck volume distribution.
- Develop default MEPDG traffic inputs for Colorado sites by identifying natural groupings or clusters for various traffic data elements through statistical cluster analysis—across highway functional class (interstates or U.S. routes), highway location (urban or rural), geographic regions, and so on. Compare Colorado traffic with the MEPDG national defaults and finalize default inputs.

The main objective of traffic data analysis was to (1) determine how representative available traffic data are for pavement design in Colorado using the MEPDG, (2) detect natural groupings or clusters within the available traffic data, and (3) develop defaults for Level 2/3 MEPDG traffic inputs for pavement design. Satisfying the project objectives required performing statistical analysis to determine natural clusters within the traffic and the optimum number of clusters.

Natural clusters within the large Colorado traffic data assembled were determined using statistical multivariate hierarchical cluster analysis. Multivariate hierarchical cluster analysis is a statistical procedure used to group "like" observations together when the underlying structure of the data is unknown. Hierarchical cluster analysis consists of either a series of successive divisions of the assembled traffic data set, which is for analysis considered a single cluster, or a merger of data from individual sites to form a single cluster. The divisions or mergers are done according to their similarities in the individual data sets. The similarities are based on distances between individual data sets of clusters within the larger database. Thus, cluster analysis begins with grouping individual sites with the smallest distances between them to form the first set of clusters. Next, the individual sites with the next smallest distances between them and the clusters are added to the original set of clusters. This continues until all individual observations and clusters end up together in one large group. Although clusters can be developed using a variety of different methods, all the methods available apply some measure of distance between observations as a basis for creating clusters.

Since the cluster analysis methodology does not require prior knowledge of the number of clusters with a given set of data, it is critical that a procedure be applied to determine the optimum number of clusters within the database being analyzed. There is no clear-cut method for determining the optimum number of clusters within a data set. Thus, analysts must depend on a combination of diagnostic statistics to determine the optimum number of clusters. Although

several such statistics are available, for this study, five diagnostic statistics were selected for use in determining optimum number of clusters: cubic clustering criterion (CCC), cumulative and partial squared multiple correlation (R^2), eigenvalue and associated variance (VAR), pseudo F (PSF), and pseudo t^2 (PST2).

Vehicle Class Distribution

Figure 28 presents an example of the outputs obtained from statistical cluster analysis. The CDOT vehicle class distributions belong to three groupings that can be described as follows:

- Cluster 1: Primary peak for class 5. Smaller peaks for class 8 & class 9. Primarily for four-lane rural principal arterial-other.
- Cluster 2: Primary peak for class 9. Smaller peaks for class 5. Primarily for four-lane rural principal arterial-Interstate.
- Cluster 3: Two distinct peaks for classes 5 and 9. Smaller peaks for class 8. Primarily for two-lane rural major collectors, two-lane rural principal arterial-other, and four-lane urban principal arterial.

Vehicle class distributions of the three CDOT clusters are presented in Figure 29.

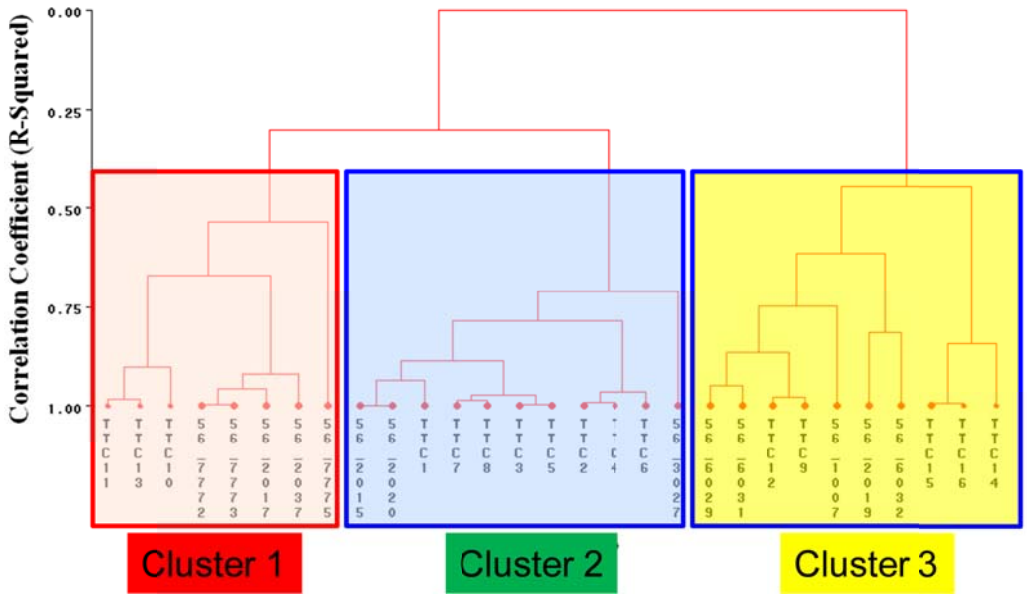

Figure 28. Example of the outputs obtained from statistical cluster analysis.

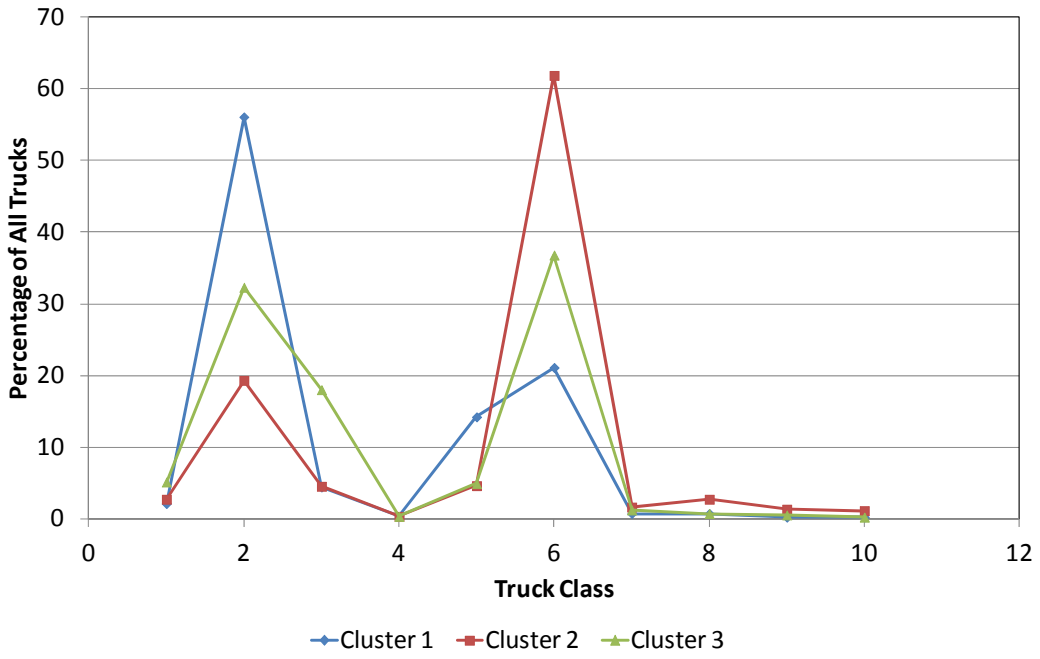

Figure 29. Distribution of vehicle class for the three clusters/groupings identified for Colorado.

Axle Load Distribution

Axle load distribution (ALD) was computed for all sites with WIM data. A cluster analysis similar to that conducted for other vehicle class distribution data was conducted. Cluster analysis focused on truck classes 5 and 9, which represented over 80 percent of all trucks. The overall results from the cluster analysis showed that the following:

- Colorado WIM distribution comprised of two clusters/groups, namely:
  - Typical highways regardless of location and functional class.
  - Haulage roads (see Figure 30).
    - Site No. 107900 (US 24) near Colorado Springs.
    - Site No. 11 (I-70) near Eagle and Edwards.
    - Site No. 8 (SH 287) near Fort Collins/LaPorte.
- Statewide averages of axle loads generally heavier than MEPDG averages.

Thus, the use of statewide averages was recommended for typical loading conditions for all highway types and functional classes, and site-specific (Level 1) axle load spectra are recommended for special haul routes. Figures 31 through 33 present plots of CDOT statewide ALD and MEPDG national defaults. Figure 34 presents cumulative tandem axles ALD distribution for CDOT statewide average, MEPDG, and Site 8-00008 (SH 287, near Fort Collins). The information in Figure 34 shows that 30 percent of the Site 8 trucks had tandem axles heavier than 32 kips, while both MEPDG and CDOT statewide defaults indicated only 20 percent of tandem axles heavier than 32 kips. The 10 percent increase in weight will have a significant impact on damage imparted to flexible and rigid pavements.

Figure 30. Examples of location of special haulage roads showing significant differences in ALD when compared to other locations within the state highway system.

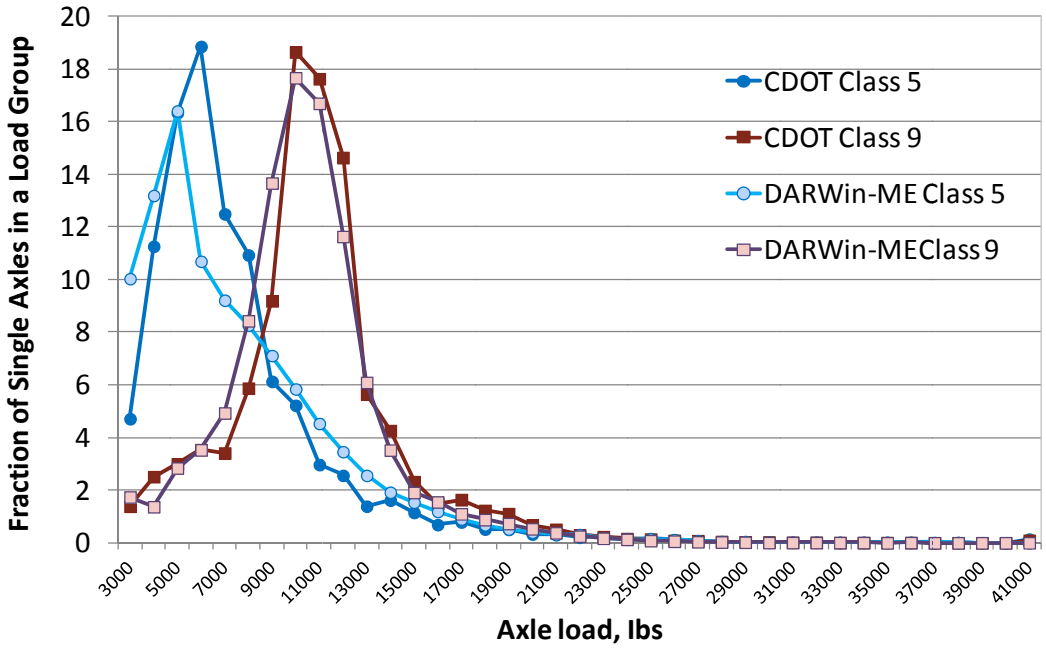

Figure 31. Statewide and national ALD for single axles of class 5 and 9 trucks.

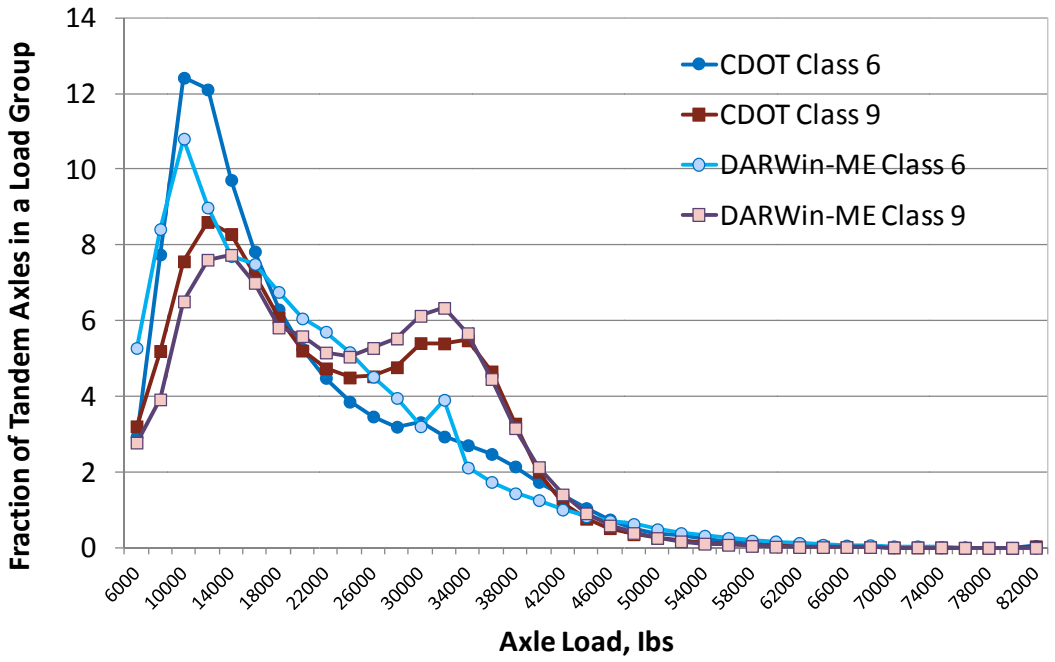

Figure 32. Statewide and national ALD for tandem axles of class 6 and 9.

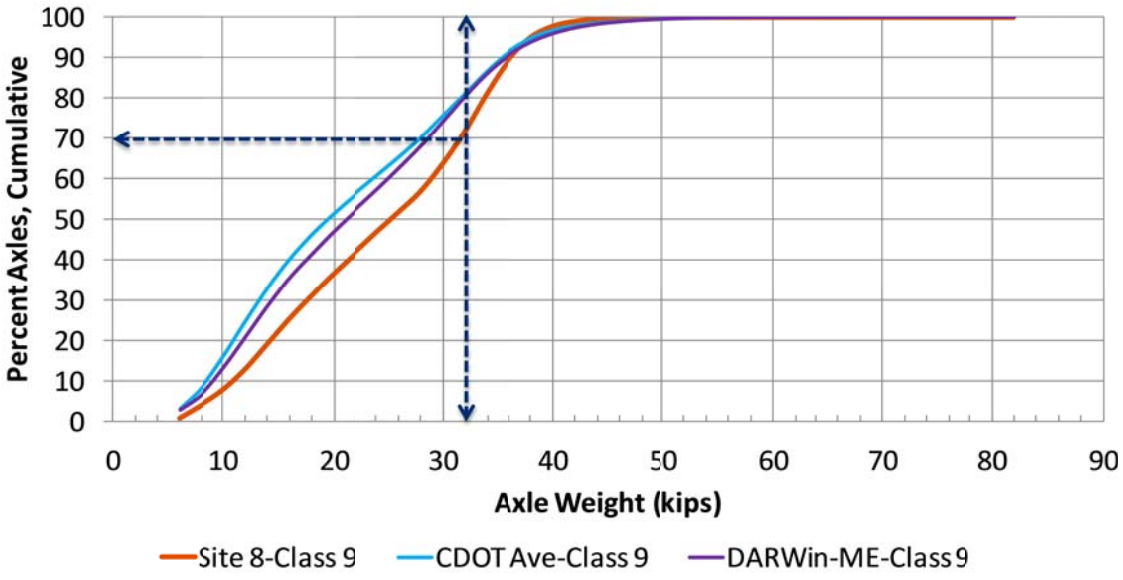

Figure 33. CDOT statewide average, MEPDG, and Site 8-00008 ALD for tandem axles.

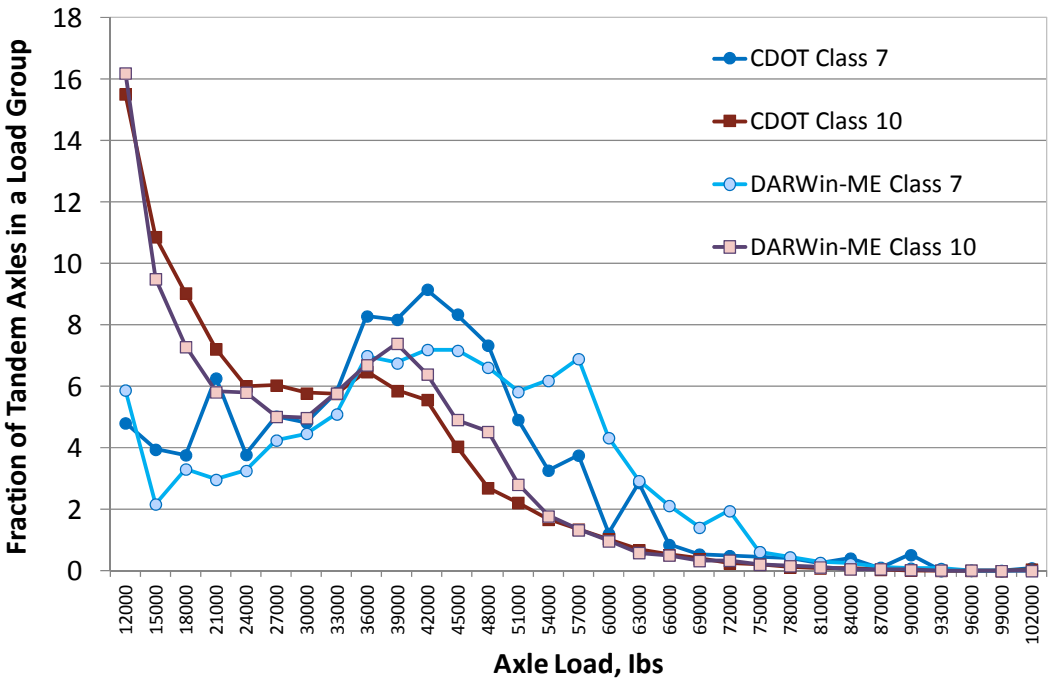

Figure 34. Statewide and national ALD for tridem axles.

Axle per Truck Class Factors

The number of single, tandem, tridem, and quad axles per truck is used to determine the total number of axles of each type to pass over the design traffic lane over the analysis period. For some trucks, such as class 5, the number of single axles is set by the classification criteria at 2.00. For others, this value varies somewhat depending on the definition of the classification. Cluster analysis was conducted using all sites with WIM data for class 9 trucks to determine if there were any significant differences in axles per truck across the state. The cluster analysis results basically indicated a single cluster for class 9 trucks. This result indicates that the various sites did not show significantly different axles per truck values. Thus, statewide averages of axles per truck for each truck class were estimated and recommended for use as defaults for pavement design using the MEPDG in Colorado. Figure 35 shows axle per truck factors for truck classes 4 through 13 for single, tandem, tridem, and quad axles in Colorado. The Colorado and national MEPDG axle per truck factors for single and tandem axles are similar, but for tridems and quad axles there are considerable differences.

Monthly Adjustment Factors

The monthly truck adjustment factor (MAF) input in the MEPDG gives the opportunity to fine-tune a design considering month-to-month truck volumes. The national defaults were 1.00 for each month, which provides for the same truck volume each month of a given year. For this project, the MAF was computed for all sites with WIM and ATR data. A cluster analysis similar to that conducted for other vehicle class distribution data was conducted. The overall results from the cluster analysis showed that the monthly truck adjustment factors break down into basically a single cluster. By far, most Colorado sites had MAFs that do not vary significantly from each other in terms of class 5 and class 9 trucks. The analysis included only sections with

all 12 months MAF. Thus, MAFs from all sites were used to develop statewide averages and defaults. The default MAFs for class 5 and 9 trucks are presented in Figure 36.

Hourly Truck Volume Distribution

Hourly truck distribution data over 24 hours are available for most of the ATR and WIM sites. Cluster analysis was performed to determine whether the hourly truck distributions from the sites located throughout the state belonged to a single or multiple grouping. Potential groupings were investigated by geographical location, functional class, and so on. The results of the analysis showed a single grouping for the entire state, as location, functional class, etc., had no significant impact on the distributions.

Thus, a single statewide default hourly truck volume distribution was developed; see Figure 37. The CDOT default hourly truck volume distribution was similar to the MEPDG national default.

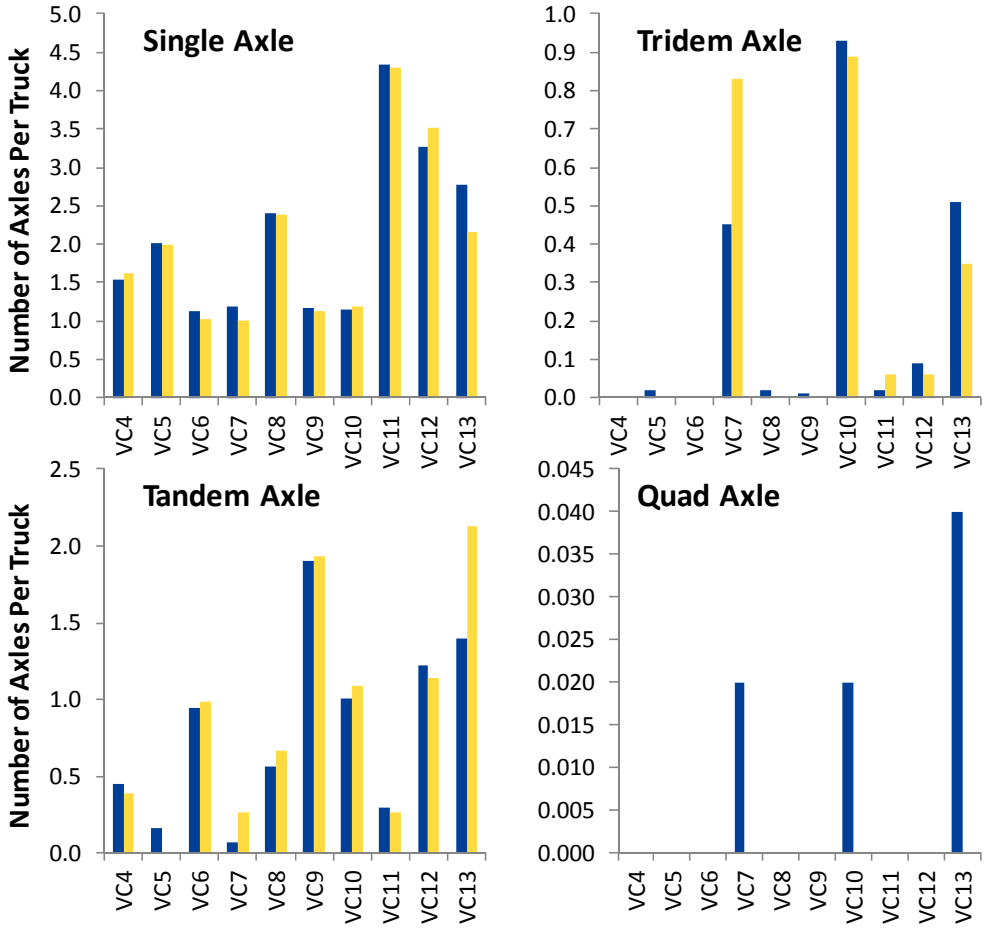

Figure 35. Statewide and national MEPDG averages for axle per trucks.

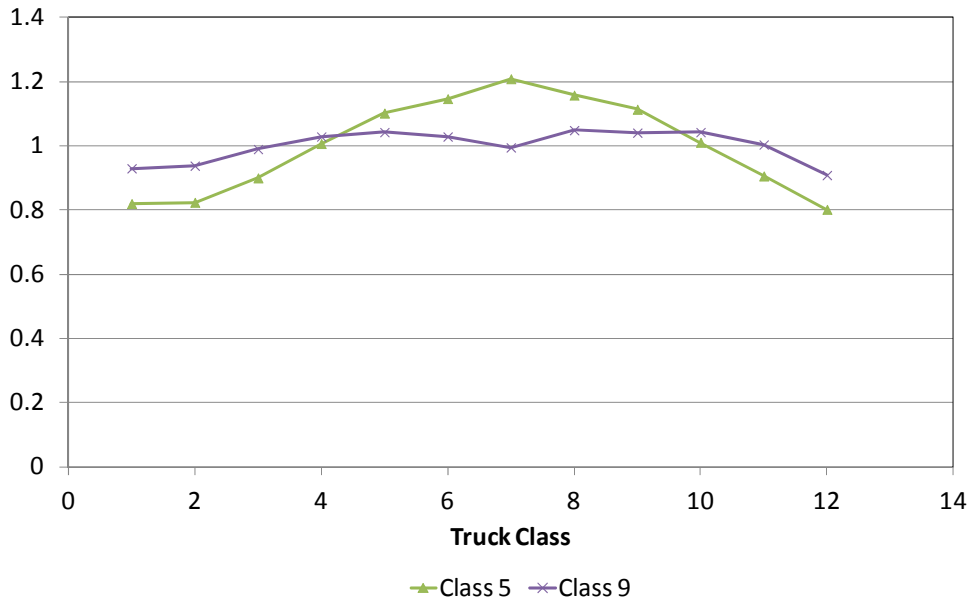

Figure 36. Statewide averages and default MAFs for class 5 and 9 trucks.

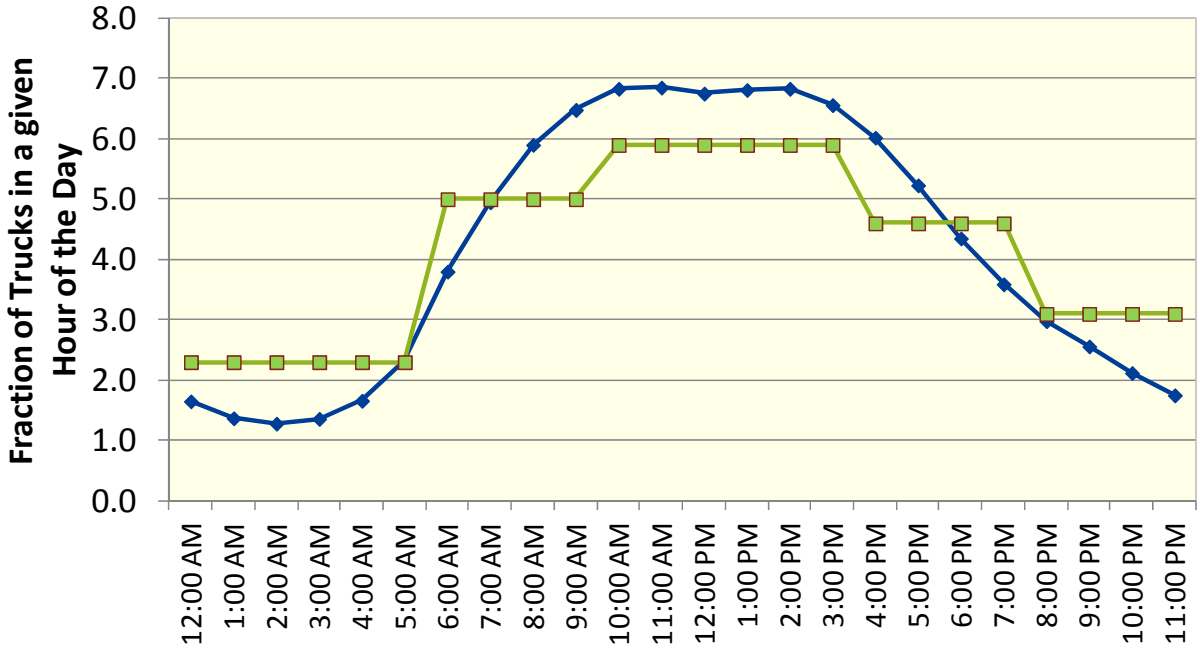

Figure 37. CDOT statewide averages and MEPDG default hourly truck volume distribution.

Estimating Missing Climate Data

Assessing Climate Data Availability

The MEPDG contained 20 Colorado weather stations for use in developing virtual pavement location/site specific climate data for design and analysis. Another 8 to 10 weather stations in neighboring states (Utah, Wyoming, Nebraska, Kansas, Oklahoma, New Mexico, Arizona) could be used in creating virtual weather stations in Colorado's border regions. Table 23 contains a summary list of the weather stations included in the MEPDG for Colorado, and Figure 38 shows their locations across the state.

A review of the MEPDG default Colorado weather stations indicated the following:

- On average, the weather stations contained 10 years of data.
- There was considerable distance between the weather stations. Increasing the distance between weather stations does negatively impact the accuracy of virtual weather stations created for pavement design.
- Thirteen of the 20 weather stations were located in elevations < 6000 ft. Only one weather station was located in a region with elevation greater than 8500 ft. The remaining weather stations were located in regions with elevation between 6000 and 8500 ft. This implied that higher elevations (very cold and cold climate zones) were under-represented.
- Some of the weather stations reported gaps in available data.

Table 23. Summary list of weather stations included in the MEPDG for Colorado.

City	Airport	Longitude, deg	Latitude, deg	Elevation, ft
Akron	Colorado Plains Regional Airport	40.1	-103.14	4664
Alamosa	San Luis Valley Regional Airport	37.26	-105.52	7536
Aspen	Aspen-Pitkin County Airport	39.13	-106.52	7725
Burlington	Kit Carson County Airport	39.14	-102.17	4198
Colorado Springs	City of Colorado Springs Municipal Airport	38.49	-104.43	6183
Cortez	Cortez Municipal Airport	37.18	-108.38	5899
Craig	Craig-Moffat Airport	40.3	-107.31	6192
Denver	Denver International Airport	39.5	-104.4	5382
Denver	Centennial Airport	39.34	-104.51	5827
Durango	Dura-La Plata County Airport	37.08	-107.46	6677
Grand Junction	Walker Field Airport	39.08	-108.32	4826
La Junta	La Junta Municipal Airport	38.03	-103.32	4193
Lamar	Lamar Municipal Airport	38.04	-102.41	3675
Leadville	Leadville/Lake County Airport	39.14	-106.19	9938
Limon	Limon Municipal Airport	39.11	-103.43	5350
Meeker	Meeker Airport	40.03	-107.53	6333
Montrose	Montrose Regional Airport	38.31	-107.54	5753
Pueblo	Pueblo Memorial Airport	38.17	-104.3	4655
Rifle	Garfield County Regional Airport	39.32	-107.44	5506
Trinidad	Perry Stokes Airport	37.16	-104.2	5749

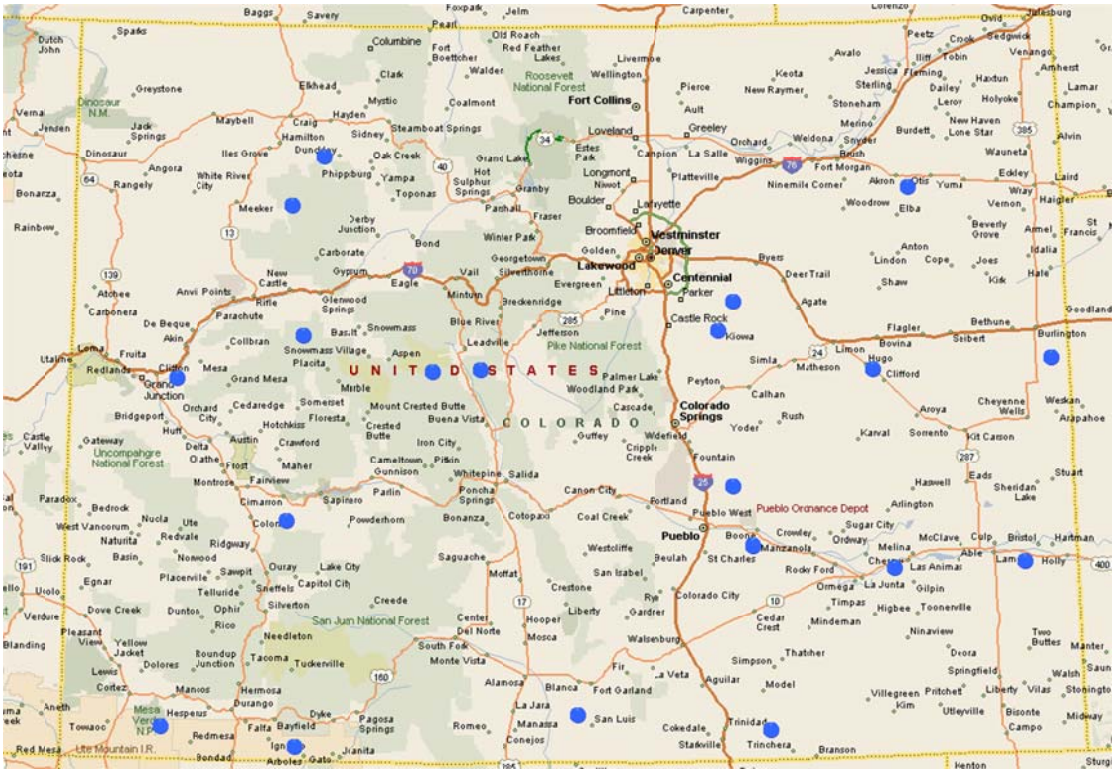

Figure 38. Locations of Colorado weather stations included in the MEPDG.

Therefore, it was necessary to update and augment the Colorado weather stations to include, as a minimum:

- Additional data as available (i.e., missing years).
- Quality assurance/quality control (QA/QC) on available data to assure reasonableness of data/trends and to fill identified gaps in data.
- Additional weather stations to better characterize and represent Colorado climate conditions.

Identification of Additional Weather Stations

Updating and augmenting Colorado MEPDG climate data began by identifying weather stations in the state with the data types required for the MEPDG. This was done through CDOT, which identified all significant weather stations in the state, including cooperative weather stations. Figure 39 shows the locations of selected cooperative stations in Colorado. These weather stations are mostly operated by local observers and report maximum/minimum temperatures and precipitation. The National Weather Service (NWS) includes other pertinent information in cooperative stations data sets and subjects the data to extensive automated and manual QC checks.

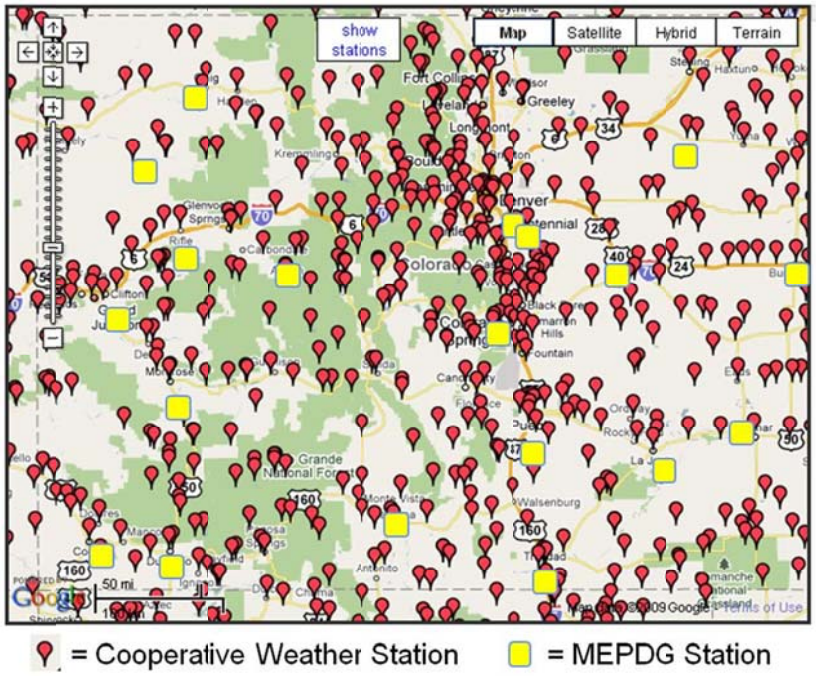

Figure 39. Locations of Colorado weather stations included in the MEPDG and NWS cooperative stations.

Criteria for selecting additional weather stations to augment the MEPDG defaults were as follows:

- Must contain all climate data elements required by the MEPDG (temperature, humidity, percent cloud cover, precipitation, wind speed).
- Must contain a minimum of 5 years of data.
- Must be located in an unrepresented region/area.
- Must contain good quality data (in terms of both data element magnitude and trends).

An efficient and consistent methodology was designed to update the Colorado weather station climate data files. The methodology began with obtaining selected Colorado NWS cooperative stations climate data from CDOT. The locations of the NWS cooperative stations were reviewed, leading to the selection of projects located in regions/areas of interest. Next was a preliminary review of data contained in the climate data sets to determine the availability and reasonableness of data. All weather stations with reasonable data available were flagged for possible inclusion into the MEPDG. Based on the criteria presented above, an additional 22 weather stations were identified for use in developing virtual weather stations in Colorado.

Development of MEPDG Climate Files for Additional Colorado Weather Stations

The final step in updating and augmenting the CDOT MEPDG climate data was to conduct a detailed review of all selected weather stations' climate data and transform the data into the form required by the MEPDG (i.e., HCD file format). Transformation of data included cleaning up the raw data, filling gaps in the data, and transforming data into the units of measurement required

by the MEPDG. The procedure utilized for data transformation and creation of HCD files is as follows:

1. Import raw climate data into project climate databases in MS Access format. Note that climate data were reported hourly. The raw data included the following variables as a minimum, reported on an hourly basis:
    a. Time stamp (comprised of Year|Month|Day|Hr presented as a string).
    b. Ambient temperature in degrees F.
    c. Wind speed, in miles per hour.
    d. Percent sunshine or cloud cover (percentage).
    e. Precipitation in inches.
    f. Humidity as a percentage.
2. Conduct basic QC of raw climate data. The QC checks were to ensure that the raw climate data fell within the typical ranges provided in Table 24. Raw data that fell outside the typical range was either removed from the data set or had its value capped at the extreme value of the range.
3. Transform time stamp to Year|Month|Day|Hr into a unique date/hour.
4. Round reported time to the nearest hour (e.g., 9:57 AM becomes 10:00HRS and 9:57 PM becomes 22:00HRS) and then transform to MEPDG format for hours (e.g., 10:00 becomes 10 while 22:00 becomes 22).
5. Determine mean hourly climate values on an annual basis (i.e., for each combination of Month|Day|Hr, determine average temperature, wind speed, percent sunshine, precipitation, and humidity).
6. Determine earliest reporting date/time (e.g., 10:00 January 16, 1957).
7. Determine latest reporting date/time (e.g., 16:34 June 26, 2007).
8. Establish climate file start/end (e.g., 00:00 January 1, 1957, to 23:00 December 31, 2007).
9. Generate hourly time stamp for the period between the start and end dates established in step 8. Call this the baseline HCD file. See example below in Table 25.
10. Using the hourly time stamp for the period between the start and end dates established in step 9 as reference, determine all the hours within the start and end dates with and without climate data. For hours with data, assume the data values reported in the climate data sets have undergone QA/QC checks. For all hours with missing data, assume the mean values computed in step 5.
11. Recheck the hourly time stamp for the period between the start and end dates established in step 9 to determine if there are still hours with missing data (i.e., hours for which average values are not available). For this situation, apply statistical algorithms (interpolation/extrapolation based on assumed distribution of climate data variable [e.g., normal, beta, and log-normal]) to determine best estimate of missing data.
12. Use the climate data set developed in steps 9 through 11 to develop HCD files.
13. Update MEPDG station.dat file to enable MEPDG to read in new HCD files
14. Test HCD files using MEPDG interface to determine reasonableness of data entries (MEPDG will flag outliers and erroneous data inputs).
15. Revise HCD files as needed based on MEPDG outcomes
16. Prepare final files and include in MEPDG database for Colorado.

Table 24. Typical climate data ranges used in conducting QA/QC checks.

Climate Variable	Range	
	Minimum	Maximum
Temperature, °F	-100	150
Wind speed, mph	0	100
Percent sunshine	0	100
Precipitation	0	10
Relative humidity	0	100

Table 25. Baseline time stamp for MEPDG HCD file development.

Date/Hr	Temp, °F	Wind Speed, mph	Sunshine, percent	Precipitation, in	Humidity, percent
1957010100					
1957010101					
1957010102					
2007123122					
2007123123					

The date and hour have been merged to provide reference date/hr in column 1.

Figure 40 shows the locations of MEPDG and CDOT climate stations included in the MEPDG for Colorado. Figures 41 through 45 present plots of MEPDG climate data variables developed using the methodology presented above. The plots show clearly the original climate data available and estimates included to replace missing data. Table 26 presents a summary of weather stations included in the MEPDG for Colorado.

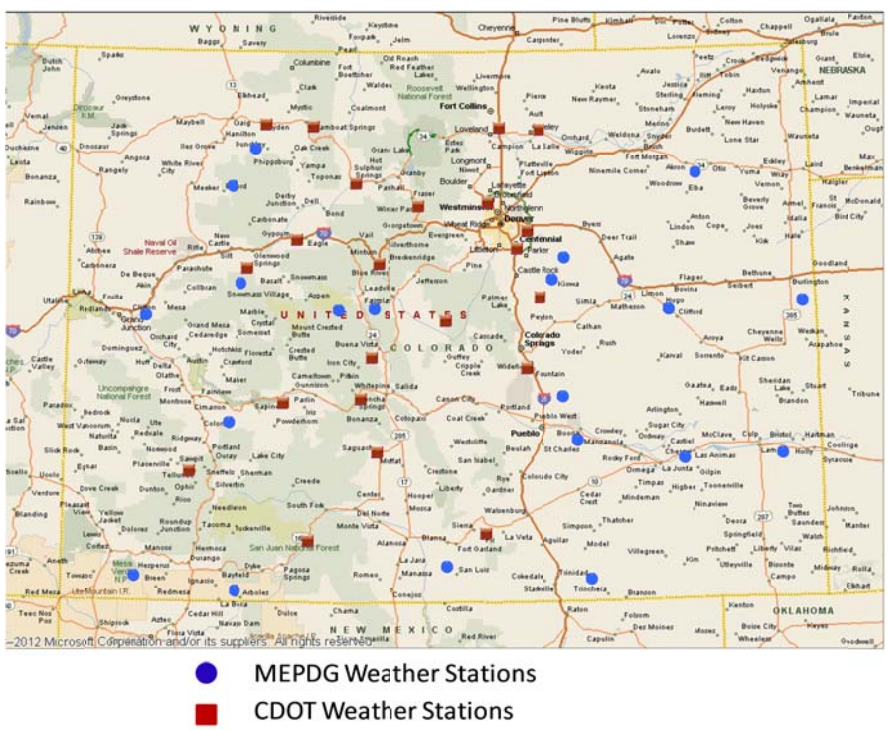

Figure 40. Map showing location of MEPDG and CDOT weather stations.

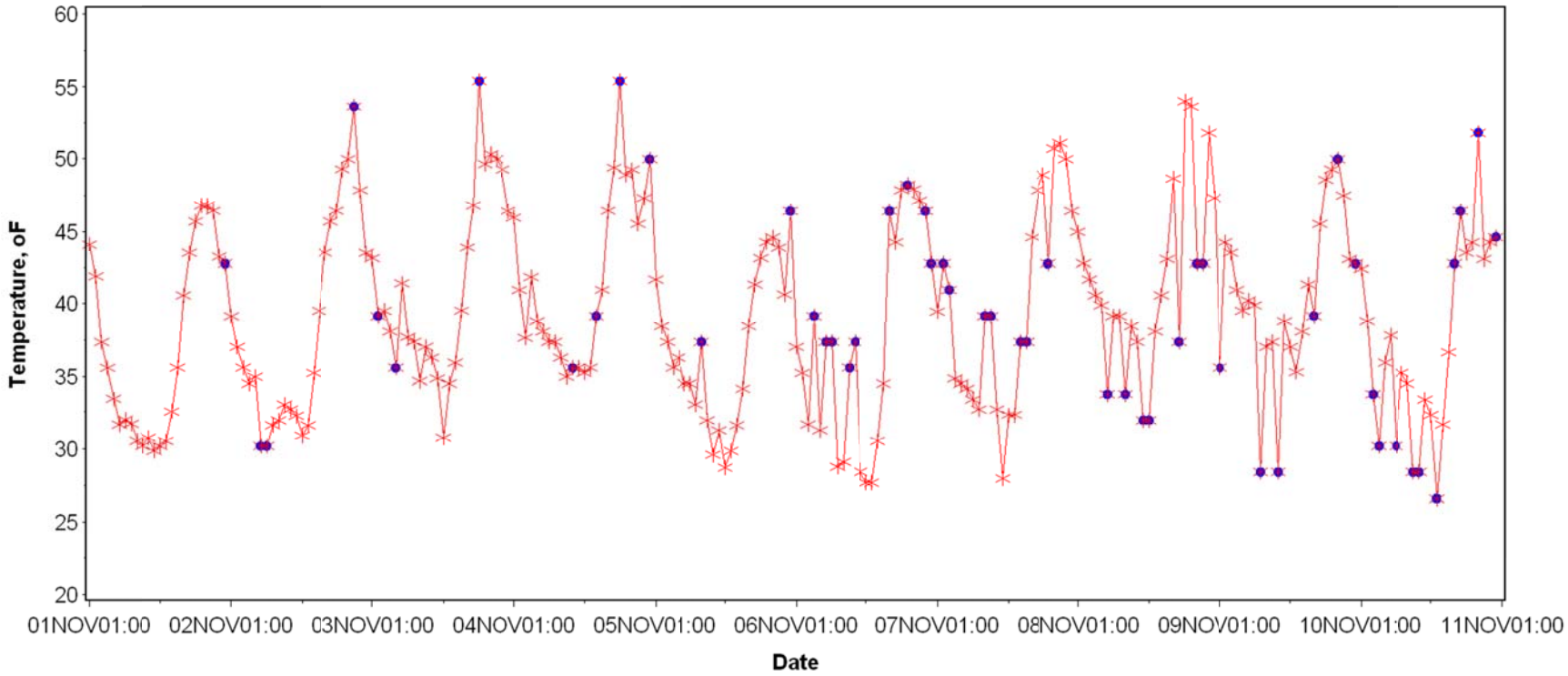

Figure 41. Plot showing reported (blue dot) and estimated (red star) temperature data for HCD file 31013 in Colorado.

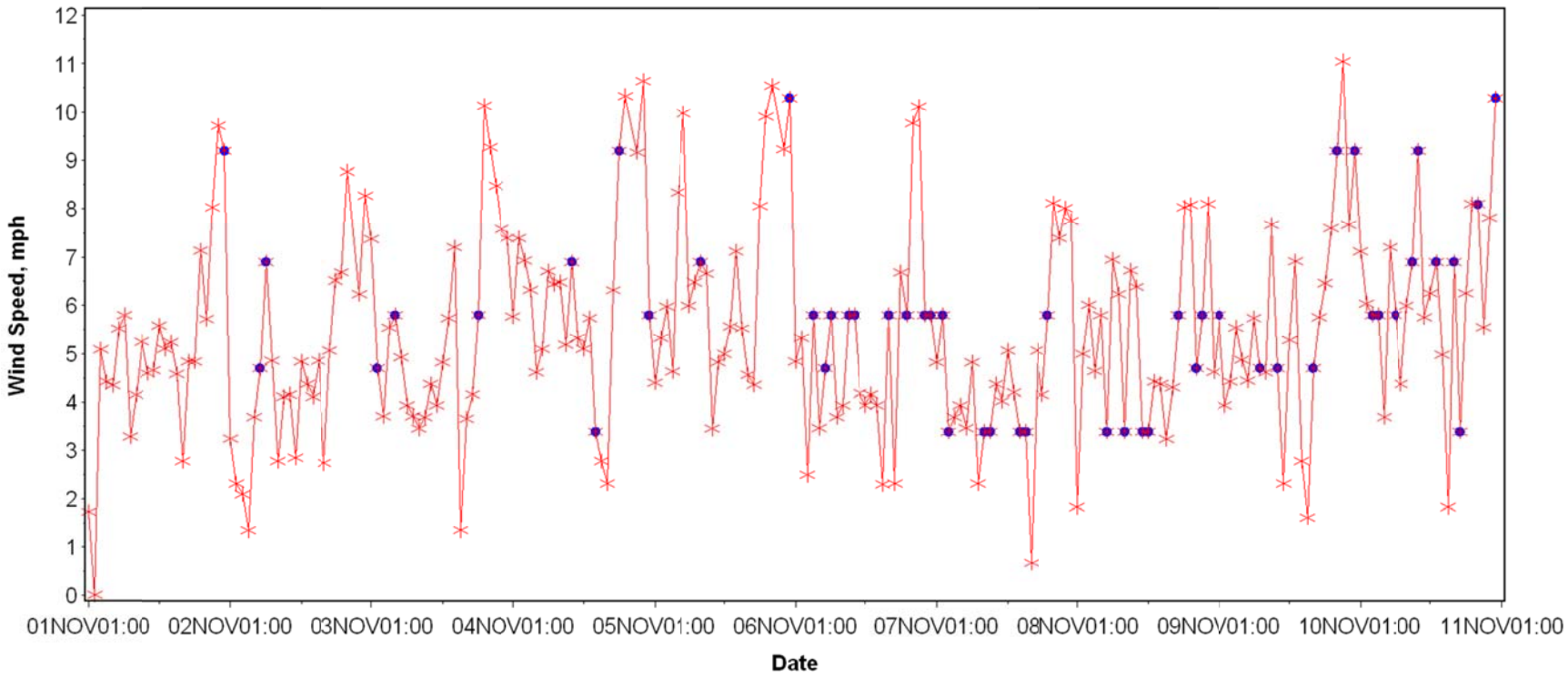

Figure 42. Plot showing reported (blue dot) and estimated (red star) wind speed data for HCD file 31013 in Colorado.

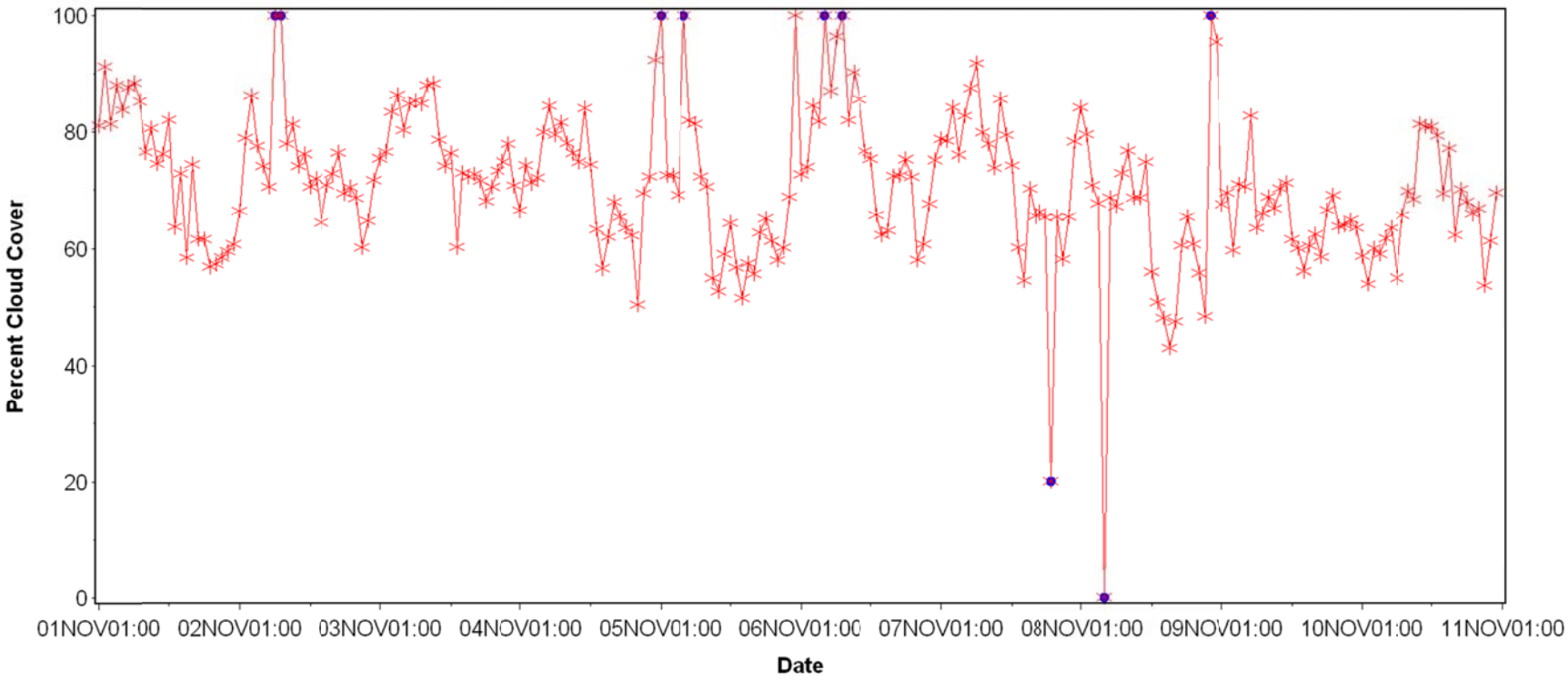

Figure 43. Plot showing reported (blue dot) and estimated (red star) percent cloud cover data for HCD file 31013 in Colorado.

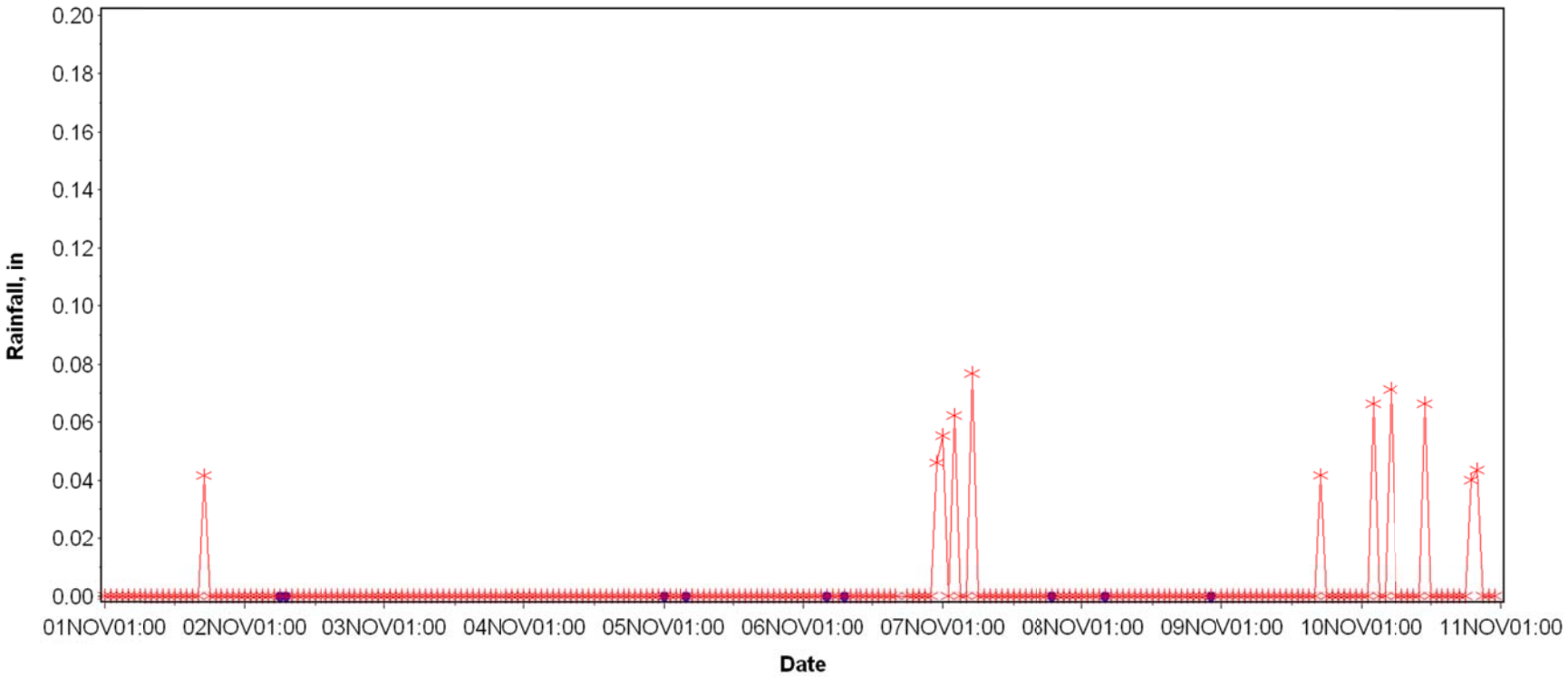

Figure 44. Plot showing reported (blue dot) and estimated (red star) rainfall data for HCD file 31013 in Colorado.

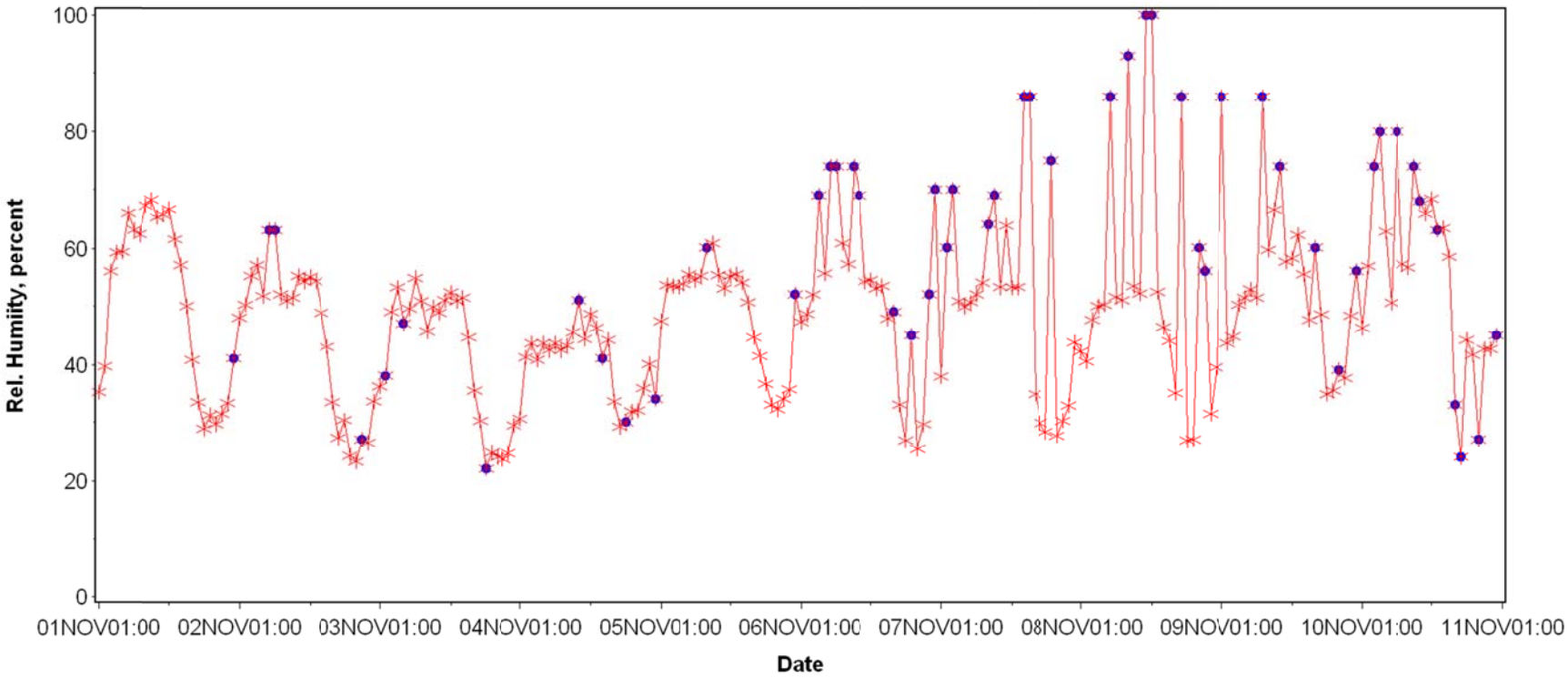

Figure 45. Plot showing reported (blue dot) and estimated (red star) relative humidity data for HCD file 31013 in Colorado.

Table 26. CDOT and MEPDG weather stations included in the MEPDG for Colorado.

MEPDG Station Name	Airport	Longitude, deg	Latitude, deg	Elevation, ft
Akron| Co	Akron/Washington Co	40.172	-103.232	4621
Alamosa| Co	Alamosa Muni(Awos)	37.436	-105.866	7540.9
Aspen| Co	Aspen Pitkin Co Sar	39.223	-106.868	7742
Aurora| Co	Buckley Afb	39.702	-104.752	5662
Broomfield| Co	Broomfield/Jeffco	39.909	-105.117	5669.9
Burlington| Co	Burlington	39.245	-102.284	4216.8
Centennial| Co	Centennial Airport	39.57	-104.849	5828
Colorado Springs| Co	Colorado Springs Muni	38.812	-104.711	6169.9
Copper Mountain| Co	Copper Mountain Resort	39.467	-106.15	12074
Cortez| Co	Cortez/Montezuma Co	37.303	-108.628	5914
Cottonwood Pass| Co	Cottonwood Pass	38.783	-106.217	9826
Craig| Co	Craig-Moffat	40.495	-107.521	6192.8
Denver| Co	Denver Intl Ap	39.833	-104.658	5431
Denver| Co	Denver Nexrad	39.783	-104.55	5606.9
Durango La Plata| Co	Durango/La Plata Ap	37.143	-107.76	6685
Eagle Co| Co	Eagle Co Airport	39.643	-106.918	6535
Elbert Co| Co	Elbert Co Airport	39.217	-104.633	7060
Fort Carson| Co	Fort Carson/Butts	38.7	-104.767	5869.4
Fort Collins| Co	Fort Collins Airport	40.452	-105.001	5016
Glenwood Springs| Co	Sunlight Mtn Glenwood Spg	39.433	-107.383	10603.5
Grand Junction| Co	Grand Junction Ap	39.134	-108.538	4838.8
Greeley| Co	Greeley/Weld Cnty Ap	40.436	-104.618	4648.9
Gunnison Co| Co	Gunnison Cnty Ap	38.452	-107.034	7673.8
Hayden| Co	Hayden/Yampa (Awos)	40.481	-107.217	6602
Kremmling| Co	Kremmling Airport	40.054	-106.368	7411
La Junta| Co	La Junta Muni Ap	38.051	-103.527	4214.8
La Veta Pass| Co	La Veta Pass	37.5	-105.167	10216.7
Lamar| Co	Lamar Muni Airport	38.07	-102.688	3070
Leadville| Co	Leadville/Lake Cnty Ap	39.228	-106.316	9926.7
Limon| Co	Limon Muni Ap	39.189	-103.716	5365.1
Meeker| Co	Meeker	40.049	-107.885	6390
Montrose| Co	Montrose Rgnl Ap	38.505	-107.898	5758.8
Pagosa Springs| Co	Pagosa Springs Wol	37.45	-106.8	11790.9
Pueblo| Co	Pueblo Airport	38.29	-104.498	4720.1
Rifle| Co	Rifle/Garfield Ap	39.526	-107.726	5543.9
Saguache| Co	Saguache Muni Ap	38.097	-106.169	7826
Salida| Co	Salida/Monarch Pass	38.483	-106.317	12030.7
Steamboat Sprimgs| Co	Mount Werner/Steamboat	40.467	-106.767	10633.1
Telluride| Co	Telluride Rgnl Ap	37.954	-107.901	9078
Trinidad| Co	Trinidad/Animas Cnty Ap	37.259	-104.341	5743
Wilkerson Pass| Co	Wilkerson Pass	39.05	-105.517	11279.4
Winter Park| Co	Winter Park Resort	39.883	-105.767	9091.1

CHAPTER 5. DEVELOPMENT OF MATERIALS DATABASE FOR MEPDG MODEL VALIDATION/CALIBRATION

This chapter describes work done to develop a materials database for use in MEPDG model calibration/validation.

Developing the CDOT MEPDG materials input database began with a detailed description of all required MEPDG materials data inputs, along with a summary of data availability (see Table 27). Table 27 shows a significant lack of HMA, PCC, and unbound aggregate materials input data for most CDOT pavement management system projects and some LTPP projects. This was as expected, as projects in pavement management system databases typically do not contain such detailed information.

Table 27. Summary of data availability for MEPDG models validation/calibration.

Input Group		Input Parameter	Recommended Input Level	Data Availability	
				LTPP	CDOT
Material Properties	Unbound aggregate & Subgrade	Resilient modulus – subgrade	Level 2 (FWD deflection measurements & backcalculation)	Available	Not available
		Unbound base/subgrade soil classification	Level 1 (lab test data)	Available	Not available
		Moisture-density relationships & other volumetric properties	Level 2 (Computed from gradation and Atterberg limits data)	Available	Not available
		Saturated hydraulic conductivity	Level 2 (Computed from gradation and Atterberg limits data)	Available	Not available
	HMA	HMA dynamic modulus	Level 1 (Testing for a range of temperatures and load frequencies)	Not available	Not available
		HMA creep compliance & indirect tensile strength	Level 1 (Testing for a range of temperatures and load frequencies)	Not available	Not available
		Volumetric properties	Level 3 (CDOT defaults)	Not available	Not available
		HMA coefficient of thermal contraction	Level 1 (lab testing)	Not available	Not available
	PCC	PCC elastic modulus	Level 1 (lab test data) Level 2 (computed from PCC compressive strength)	Available	Not available
		PCC flexural strength	Level 1 (lab test data) Level 2 (computed from PCC compressive strength)	Available	Not available
		PCC CTE	Level 1 (lab test data) Level 2 (based on coarse aggregate)	Available	Not available

Next, the project team reviewed CDOT pavement design and construction records to determine material data available in CDOT QA/QC databases for use in developing default material inputs. Note that default material inputs are not project-specific material property values but rather Level 3 statewide defaults estimated from tests conducted on similar materials with similar property values.

The outcome of the data availability checks and records review was used as the basis for developing a comprehensive field/laboratory forensic evaluation, laboratory testing, and

construction records and QA/QC data review program. The program consisted of the following steps:

1. Construction records and CDOT pavement project QA/QC data review.
    - Identification of typical CDOT paving materials.
        - HMA and asphalt treated material.
        - PCC.
        - Chemically treated materials.
        - Unbound granular (base/subbase) materials.
        - Subgrade soils.
    - Identification of pertinent materials data available in QA/QC databases.
        - Gradation.
        - Strength.
        - Modulus.
        - Asphalt binder type, content, and volumetrics.
        - PCC CTE.
2. Refinement of data needs (revise information in Table 27 to reflect data available in CDOT materials QA/QC databases) and development of list of missing project specific or statewide (Level 3) data.
3. Development of field/laboratory test program to acquire missing data.
    - Identification of material sources (laboratory or field destructive/nondestructive testing locations).
    - Identification of test protocols and equipment needs.
    - Development of testing schedule.
4. Performance of field/laboratory testing and development of test database.
5. Evaluation of test data for accuracy and reasonableness.
6. Development of default MEPDG inputs.

The research team implemented this plan with assistance from CDOT. The following sections present a detailed description of the plan implementation and outcomes.

Construction Records and CDOT Pavement Projects QA/QC Data Review

For the identified missing data, only as-placed HMA air voids and binder content data were available in the CDOT QA/QC databases. These data were extracted and assembled for inclusion in the project materials database.

Laboratory/Field Testing

With the review of CDOT materials databases completed, the only feasible means of obtaining the remaining missing data was through laboratory/field testing. Details are presented in the following sections.

Extraction, Examination, and Laboratory Testing of Cores

Forty pavement projects were identified for field testing. Specifically, field testing was performed on the 16 new HMA pavement project sites, 21 HMA overlay over existing HMA pavement project sites, and 3 HMA overlay over existing JPCP project sites. The locations of the projects selected for field testing are presented in Figure 46. Figure 47 presents a schematic of the field testing layout for each selected project.

Figure 46. Map of the locations of the 40 projects selected for field testing.

MATERIALS SAMPLING & FIELD TESTING PLAN FOR
FLEXIBLE PAVEMENTS PROJECTS – NON-LTPP SECTIONS

Sampling and Field Testing Plan Layout

Number of Cores = 6 (8 if wheelpath longitudinal cracking or alligator cracking exists)

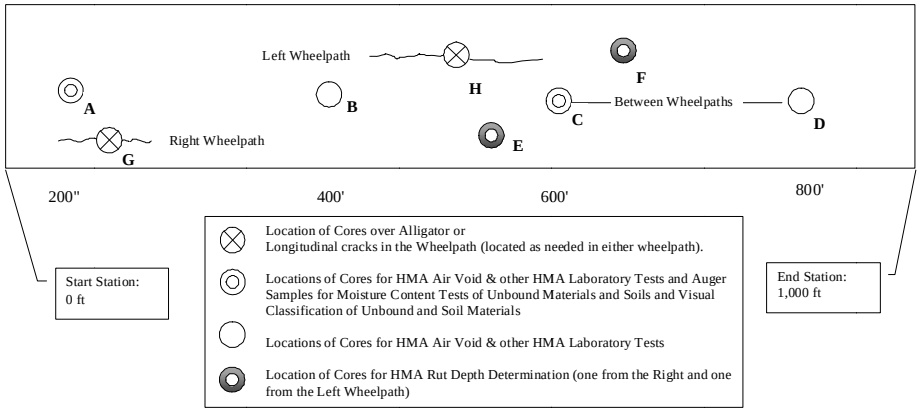

Figure 47. Schematic showing the outline of the field testing plan for each selected project, along with coring patterns.

Field testing essentially consisted of HMA coring and extraction of HMA/PCC cores and unbound aggregate base and subgrade soil samples. The extracted cores were examined and tested for basic volumetric, strength, thickness, and durability properties. Other laboratory/field testing performed included layer thickness measurements, trenching, distress surveys, and rut depth measurements.

A photographic journal of the extracted cores was created and used throughout the project as a visual identification of the pavement and material condition. Photos were also taken to document the condition of the pavement in the area of sampling, and the location of the sampling with reference to the lane and wheel path. Photos of the coring process and core extraction was kept for use in interpreting laboratory results.

The key elements of the field/laboratory test program were as follows:

- Identification and marking of the 1000-ft sampling area within each project site.
- Identification and marking coring of locations and extraction of cores.
    - Between wheel paths (lane center). Four 6-in-diameter HMA cores were extracted. Hand augers were used at the four core locations to extract base/subgrade materials. The sampled material was sealed in plastic bags and labeled.
    - Within 12-in left/right wheel path. Four 6-in-diameter HMA cores were extracted.
    - The extracted cores were labeled, photographed, and logged in the field. Core holes were patched with either cold patch mix or rapid set mortar to match pavement type.
- Examination and laboratory testing of extracted cores.
    - All cores were checked for debonding from the original pavement and signs of stripping, moisture damage, etc.
    - The 6-in HMA cores extracted from the lane center were tested to determine HMA layer thickness and to determine as-placed HMA air voids, volumetric binder content, gradation, bulk specific gravity, and maximum theoretical specific gravity (“Rice” density).
    - Atterberg limits, sieve analysis (gradation), and in situ moisture content tests were determined for the extracted unbound aggregate and subgrade soil materials. Results were used to determine base/subgrade materials type (i.e., AASHTO soil class) and in situ moisture content.
    - The four HMA cores extracted from within the wheel path were examined to determine the amount of rutting within HMA layers and to determine whether longitudinal wheel path cracks were top-down fatigue (longitudinal) or bottom-up fatigue (alligator) cracking.

Figures 48 through 50 present photos/schematics of various aspects of the field testing program. Table 28 presents a summary of information derived from the coring effort (HMA air voids and volumetric binder content), and Figures 51 and 52 show the distribution of HMA air voids and volumetric binder content, respectively.

Figure 48. Sampling section layout, core locations, and sample of extracted HMA core.

Figure 49. Pavement coring rig used for materials extraction.

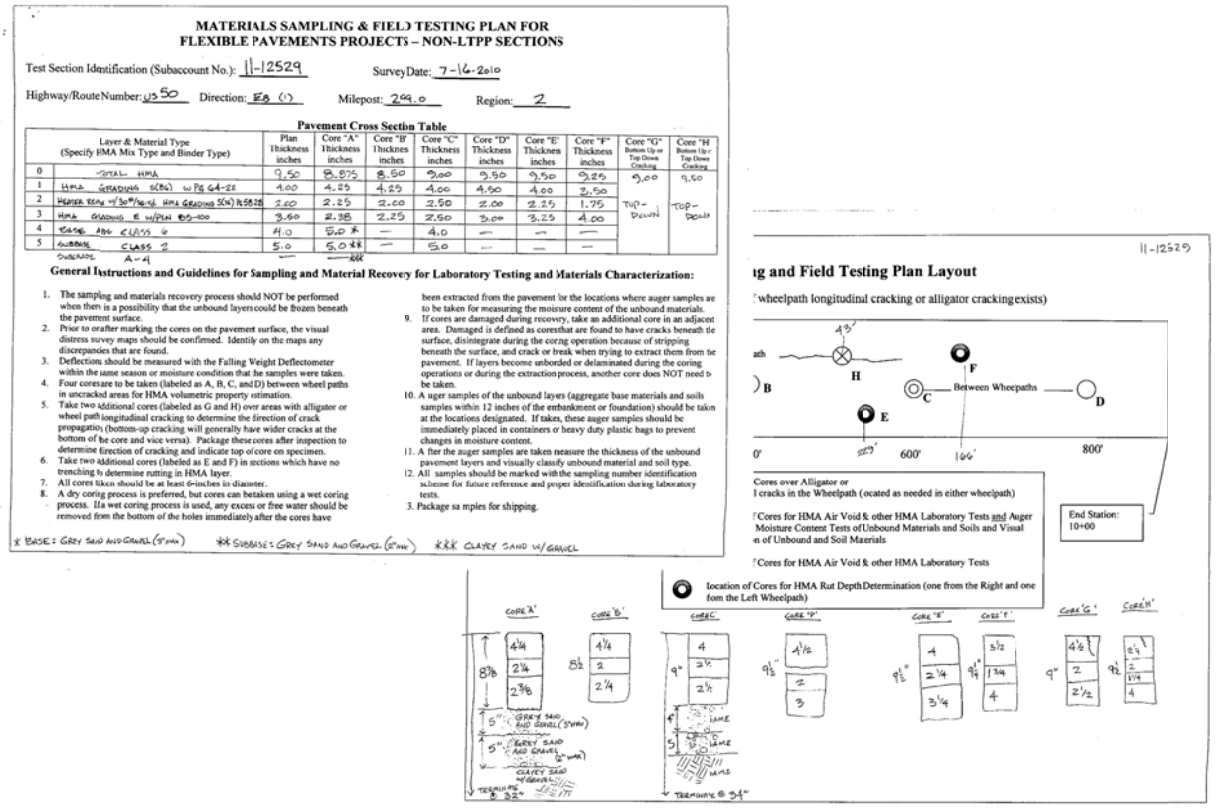

MATERIALS SAMPLING & FIELD TESTING PLAN FOR
FLEXIBLE PAVEMENTS PROJECTS – NON-LTPP SECTIONS

Test Section Identification (Subaccount No.): 11-12529 Survey Date: 7-16-2010

Highway/Route Number: US 50 Direction: EB (1) Milepost: 299.0 Region: 2

Pavement Cross Section Table

	Layer & Material Type (Specify HMA Mix Type and Binder Type)	Plan Thickness inches	Core "A" Thickness inches	Core "B" Thickness inches	Core "C" Thickness inches	Core "D" Thickness inches	Core "E" Thickness inches	Core "F" Thickness inches	Core "G" Bottom Up or Top Down Cracking	Core "H" Bottom Up or Top Down Cracking
0	TOTAL HMA	9.50	8.875	8.50	9.00	9.50	9.50	9.25	9.00	9.50
1	HMA GRADING S(SG) W PG 64-28	4.00	4.25	4.25	4.00	4.50	4.00	2.50		
2	HEATER REM W/30#/SQ YD HMA GRADING S(SG) R5828	2.00	2.25	2.00	2.50	2.00	2.25	1.75	TOP-DOWN	TOP-DOWN
3	HMA GRADING E W/PEN 85-100	3.50	2.38	2.25	2.50	3.00	3.25	4.00		
4	BASE AGG CLASS 6	4.0	5.0 *	—	4.0	—	—	—		
5	SUBBASE CLASS 2	5.0	5.0 **	—	5.0	—	—	—		
	SUBGRADE A-4		—	***						

General Instructions and Guidelines for Sampling and Material Recovery for Laboratory Testing and Materials Characterization:

1. The sampling and materials recovery process should NOT be performed when then is a possibility that the unbound layers could be frozen beneath the pavement surface.
2. Prior to orafter marking the cores on the pavement surface, the visual distress survey maps should be confirmed. Identify on the maps any discrepancies that are found.
3. Deflection should be measured with the Falling Weight Deflectometer within the same season or moisture condition that he samples were taken.
4. Four coresare to be taken (labeled as A, B, C, and D) between wheel paths in uncracked areas for HMA volumetric property estimation.
5. Take two additional cores (labeled as G and H) over areas with alligator or wheel path longitudinal cracking to determine the direction of crack propagatio (bottom-up cracking will generally have wider cracks at the bottom of he core and vice versa). Package these cores after inspection to determine direction of cracking and indicate top of core on specimen.
6. Take two additional cores (labeled as E and F) in sections which have no trenching to determine rutting in HMA layer.
7. All coresTaken should be at least 6-inches in diameter.
8. A dry coring process is preferred, but cores can betaken using a wet coring process. If a wet coring process is used, any excess or free water should be removed from the bottom of the holes immediately after the cores have been extracted from the pavement for the locations where auger samples are to be taken for measuring the moisure content of the unbound materials.
9. If cores are damaged during recovery, take an additional core in an adjacent area. Damaged is defined as coresthat are found to have cracks beneath the surface, disintegrate during the coring operation because of stripping beneath the surface, and crack or break when trying to extract them from the pavement. If layers become unbonded or delaminated during the coring operations or during the extraction process, another core does NOT need to be taken.
10. A uger samples of the unbound layers (aggregate base materials and soils samples within 12 inches of the embankment or foundation) should be taken at the locations designated. If taken, these auger samples should be immediately placed in containers or heavy duty plastic bags to prevent changes in moisture content.
11. A fter the auger samples are taken measure the thickness of the unbound pavement layers and visually classify unbound material and soil type.
12. All samples should be marked with the sampling number identification scheme for future reference and proper identification during laboratory tests.
3. Package samples for shipping.

* BASE: GREY SAND AND GRAVEL (8"MAX) ** SUBBASE: GREY SAND AND GRAVEL (6"MAX) *** CLAYEY SAND W/ GRAVEL

11-12529

ıg and Field Testing Plan Layout

wheelpath longitudinal cracking or alligator cracking exists)

Between Wheepaths

Cores over Alligator or
l cracks in the Wheelpath (ocated as needed in either wheelpath)

Cores for HMA Air Void & other HMA Laboratory Tests and Auger
Moisture Content Tests of Unbound Materials and Soils and Visual
n of Unbound and Soil Mazerials

Cores for HMA Air Void & other HMA Laboratory Tests

location of Cores for HMA Rut Depth Determination (one from the Right and one
fom the Left Wheelpath)

End Station:
10+00

Figure 50. Example of field logging of extracted cores.

Table 28. Summary of extracted HMA cores air voids and binder content test results.

Section ID	Core ID	Binder	As-constructed Air Voids, percent	As-constructed Vol. Binder Content, percent
04-91044	F	PG 58-40	7.5	9.5
05-12441	D-top	AC-20	5.8	11.0
05-12441	D-bottom	Pen 85-100	8.6	16.1
07-13817	A-bottom	Pen 85-100	11.6	14.7
07-13817	A-top	PG 64-28	5.3	12.5
08-12685	E	PG 64-22	8.0	6.3
09-13969	B	PG 64-22	6.0	8.5
10-12393	F	PG 64-28	5.5	17.0
11-12529	F	PG 64-22	6.5	9.6
12-13390	B	PG 64-22	5.3	12.5
14-13131	C	PG 58-28	6.2	13.4
15-11959	C	PG 58-28	8.0	12.4
16-13440	A	PG 64-22	6.8	9.2
17-13932	F	PG 64-28	6.8	9.6
20-13353	C	PG 76-28	4.5	14.6
21-91094	A	PG 64-22	7.2	10.1

Table 28. Summary of extracted HMA cores air voids and binder content test results.

Section ID	Core ID	Binder	As-constructed Air Voids, percent	As-constructed Vol. Binder Content, percent
22-12297	A	PG 76-28	8.2	13.5
23-11918	D	PG 76-28	6.2	10.6
24-13356	E	PG 76-28	6.4	8.6
27-13959	E-middle	PG 58-28	3.7	11.4
27-13959	B-top	PG 58-34	7.5	7.0
28-11865	B	PG 58-28	3.9	9.2
30-11979	C	AC-20	5.5	9.0
31-13258	F	PG 58-28	5.8	11.2
32-12448	F	AC-20	4.4	12.2
33-13435	F	PG 58-28	6.8	10.3
34-13513	C	PG 58-28	3.2	13.8
35-13087	F	PG 58-28	6.5	11.9
36-13880	E	PG 58-34	4.5	16.4
37-92976	A	PG 58-40	4.5	16.6
38-13505	E	PG 58-28	4.8	11.7
39-11970	E	PG 58-28	8.2	11.4
41-13325	F	PG 76-28	7.4	11.1
42-12153	A	PG 76-28	6.6	8.9
43-13085	F	PG 58-28	4.1	11.5
44-11213	F	PG 58-28	5.9	9.6
45-13106	D	PG 64-28	6.2	7.9
47-12018	C	PG 58-34	6.5	7.0
48-13866	F	PG 64-28	7.8	5.9
49-13864	B	PG 64-28	7.9	9.2
50-11780	F	PG 58-28	9.8	8.6
51-12271	C	PG 58-28	6.6	10.1
52-12321	F	PG 64-22	6.9	7.5
MEAN			**6.4**	**10.9**

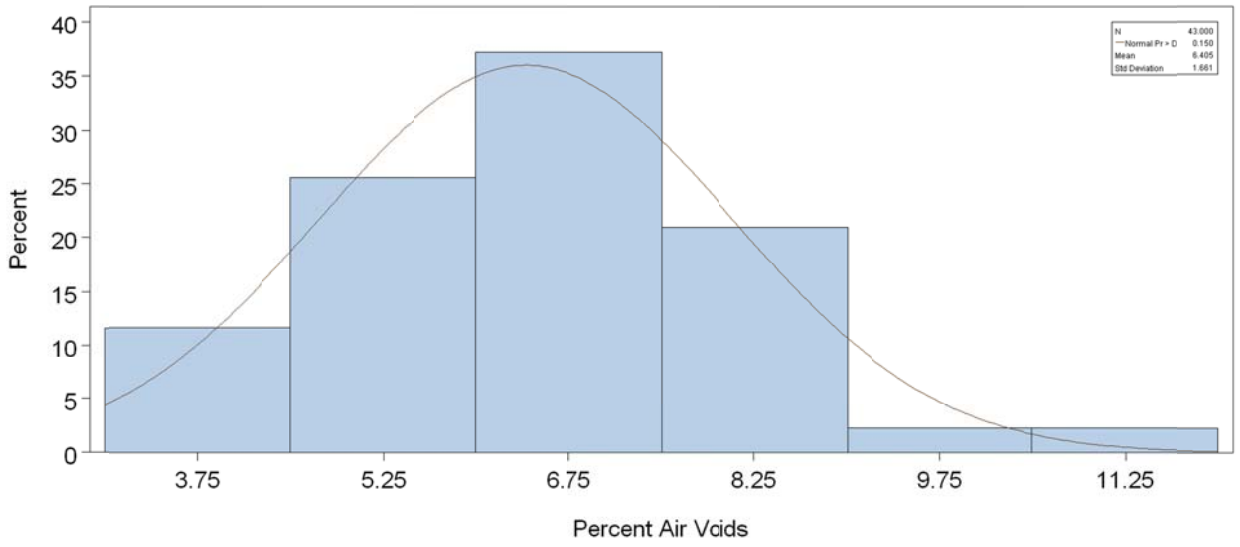

Figure 51. Distribution of as-placed HMA air voids estimated from field cores.

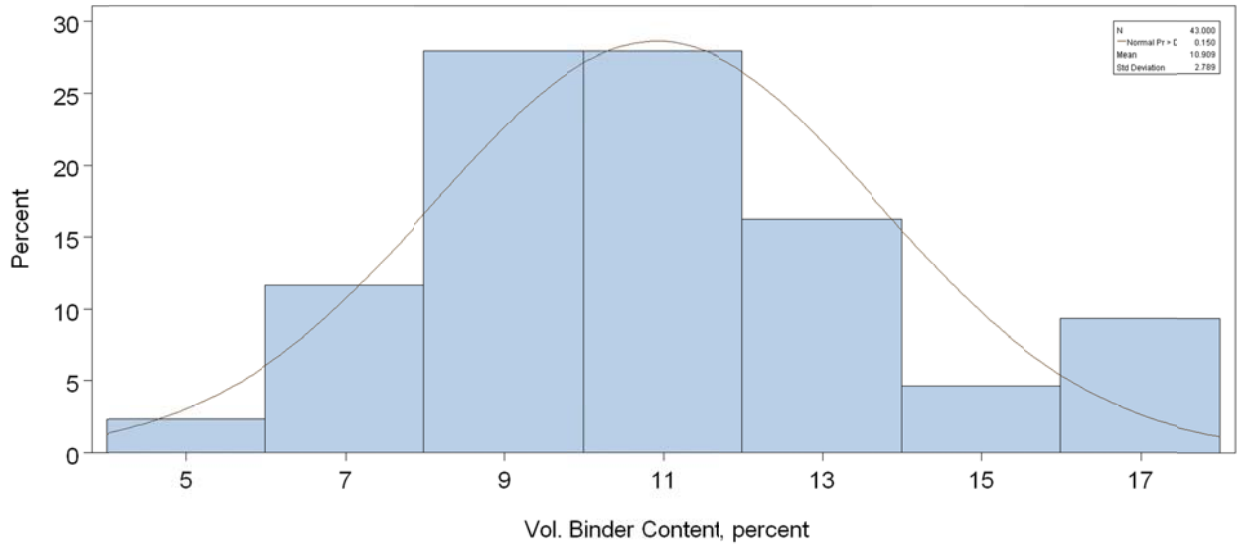

Figure 52. Distribution of as-placed volumetric binder content estimated from field cores.

Trenching

A key component of field testing was trenching of new HMA pavements to determine how measured total rutting at the pavement surface is distributed within the pavement structure (surface HMA, aggregate base, and subgrade). Trenching consisted of:

- Sawing a full-depth 4-ft by 6-ft rectangular cut in the wheel path (right or left wheel path, depending on the severity of rutting).

- Double cutting the trench along the transverse sides to protect the trench face from damage when excavated.
- Removal of the sawcut pavement.
- Partial excavation of the unbound base material.
- Complete base excavation by hand and cleaning the trench face.
- Placement of a straightedge atop the trench face and measurement of the distance from the straightedge to each pavement layer as follows:
    - Depth to each layer measured from a straightedge placed across top of trench.
    - Measurements recorded every 3 inches along trench face.
    - Measurements taken from both sides of the trench for comparison.
- Backfilling of trench and placement of HMA patch.

Trenching for this project was done at three locations: I-25 near Colorado Springs, SH 82 near Glenwood Springs, and on Colorado Boulevard in Denver. Figures 53 through 56 show various aspects of the trenching operations and outcome in terms of layer profiles and rut depth. The distribution of total rutting within the pavement structure for the three projects examined is presented in Table 29. This information will be used in rutting model calibration to apportion predicted total rutting within the pavement structure.

Figure 53. Sawing and lifting of surface HMA layer during the trenching operation.

Figure 54. Lifting of the surface HMA layer during the trenching operation.

Figure 55. Inside of the completed trench (not the HMA and aggregate base layers).

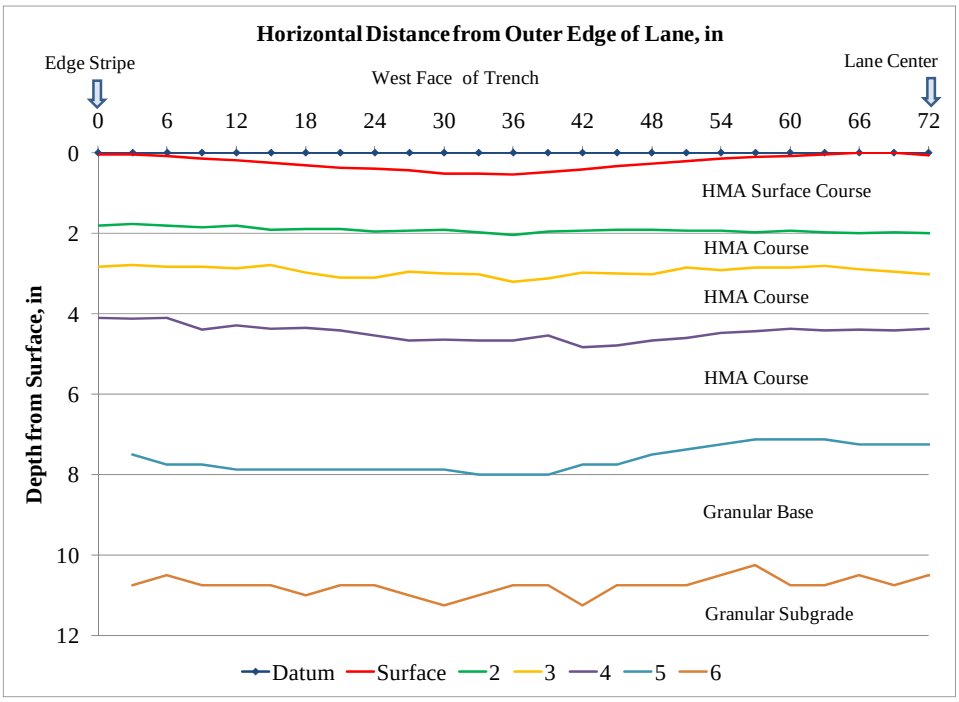

Figure 56. Plots of layer profile and rut depth across the 12-ft lane width.

Table 29. Distribution of total rutting (percentage within layer) within the pavement structure.

Layer Type/Material	Projects			Mean
	I-25 (near Colorado Springs)	Glenwood Springs (SH 82)	Colorado Blvd*	
HMA surface	70	63	55	63
Aggregate base/subbase	5	9	20	11
Subgrade (top 12 in)	25	28	25	26

*Includes subbase.

Nondestructive Deflection Testing

CDOT performed FWD testing in a separate effort to obtain deflection test data for use in backcalculating pavement layer moduli and modulus of subgrade reaction for PCC and composite pavements. For all the HMA pavement projects selected, FWD testing was performed in 25-ft intervals. For PCC pavements, FWD testing was performed at slab centers, at transverse joints (to determine load transfer efficiency), and at the slab corners to determine maximum joint deflections.

The deflection data were used to estimate the following through backcalculation using the EVERCALC software:

- HMA layer modulus (damage in situ modulus).
- Base layer elastic modulus (for unbound and treated base materials).
- Subgrade elastic modulus E_{SG} (at in situ moisture) for HMA pavements and modulus of subgrade reaction (k-value) at in situ moisture for PCC pavements.

As the MEPDG requires "lab tested" Mr at optimum moisture for subgrade soils under HMA pavements, the backcalculated E_{SG} (at in situ moisture) was transformed into an equivalent "lab" Mr at optimum moisture as follows:

1. Convert in situ moisture E_{SG} to lab Mr (at in situ moisture) using conversion factors (C value) presented in Table 30.
2. Adjust lab Mr (in situ moisture) to lab Mr (opt moisture) by applying a moisture correction factor using the iterative procedure described below:
    a. Run MEPDG using national default subgrade Mr at optimum moisture as input. Note that national default subgrade Mr at optimum moisture is available in the AASHTO Interim MEPDG Manual of Practice for each AASHTO soil class.
    b. Extract monthly MEPDG estimates of in situ Mr for the subgrade layer. Note that the MEPDG transforms the input lab Mr at optimum moisture to lab Mr at in situ moisture.
    c. Determine MEPDG in situ Mr for the month of FWD testing from the Mr data extracted in step b.
    d. Compare MEPDG in situ Mr for the month of FWD testing to lab Mr (in situ moisture) (see Step 1).
        i. If the difference in MEPDG in situ Mr and lab Mr (in situ moisture) is less than 10 percent then the national default subgrade Mr at optimum moisture is assumed to be the same as the projects default subgrade Mr at optimum moisture.
        ii. Otherwise, adjust default subgrade Mr at optimum moisture as needed and run MEPDG and follow steps b, c, and d(i) until a reasonable project default subgrade Mr at optimum moisture is obtained (i.e., difference < 10 percent).
    e. Determine subgrade Mr (at in situ moisture) to subgrade Mr (at optimum moisture) adjustment factor. Call this Mr/Mr(opt) Ratio.
    f. Apply the correction factor (Mr/Mr(opt) Ratio) to convert lab Mr (in situ moisture) obtained in step 1 to an equivalent lab Mr (at optimum moisture). See equation 3.

$$\text{Equivalent "Lab" Mr} = E_{SG} * C * \text{Mr/Mr(opt) Ratio} \quad (3)$$

Table 31 presents a summary of backcalculated subgrade elastic modulus (E_{SG}) and subgrade lab Mr at optimum moisture content estimated from the backcalculated E_{SG}, along with subgrade AASHTO soil classification.

Table 30. C1 values to convert calculated layer modulus values to an equivalent resilient modulus measured in the laboratory.

Layer Type	Location	C Value
Aggregate base/subbase	Between a stabilized & HMA layer	1.43
	Below a PCC layer	1.32
	Below an HMA layer	0.62
Subgrade/embankment	Below a stabilized subgrade/ embankment	0.75
	Below an HMA or PCC layer	0.52
	Below an unbound aggregate base	0.35

Table 31. Summary of HMA pavement backcalculated subgrade elastic modulus (E_{SG}) and subgrade lab Mr at optimum moisture content estimated from the backcalculated E_{SG}.

Section ID	Soil Class	Elastic Modulus, psi	C Value	Mr/Mr(opt) Ratio	Corrected Lab Mr_{OPT}, psi	Mean Mr (at Opt. Moisture Content), psi
16_13440	A-1-a	30,670	0.350	0.822	13,059	13,011
27_13959	A-1-a	30,670	0.350	0.674	15,927	
51_12271	A-1-a	30,670	0.350	0.868	12,367	
8_7780	A-1-a	30,670	0.350	1.004	10,692	
14_13131	A-1-b	10,335	0.520	1.001	5,369	9,561
17_13932	A-1-b	28,356	0.350	1.001	9,915	
28_11865	A-1-b	28,356	0.350	1.001	9,915	
31_13258	A-1-b	28,356	0.350	1.001	9,915	
32_12448	A-1-b	28,356	0.520	1.001	14,730	
33_13435	A-1-b	28,356	0.350	1.001	9,915	
34_13513	A-1-b	28,356	0.350	1.001	9,915	
43_13085	A-1-b	18,466	0.350	1.001	6,457	
50_11780	A-1-b	28,356	0.350	1.001	9,915	
9_13936	A-4	15,249	0.350	0.527	10,127	11,884
11_12529	A-4	34,831	0.350	0.612	19,920	
15_11959	A-4	16,468	0.350	0.594	9,703	
36_13380	A-4	15,249	0.350	0.561	9,514	
44_11213	A-4	27,554	0.350	0.546	17,663	
47_12018	A-4	15,249	0.350	0.686	7,780	
48_13866	A-4	15,249	0.350	0.508	10,506	
52_12321	A-4	15,249	0.520	0.591	13,417	
8_1029	A-4	15,249	0.350	0.641	8,326	
5_12441	A-7-6	27,156	0.350	0.656	14,489	11,185
12_13390	A-7-6	15,772	0.350	0.591	9,340	
23_11918	A-7-6	27,156	0.350	0.576	16,501	
39_11970	A-7-6	27,156	0.350	0.568	16,733	
8_2008	A-7-6	15,772	0.520	0.696	11,784	
8_B310	A-7-6	15,772	0.350	0.694	7,954	
8_B320	A-7-6	15,772	0.350	0.694	7,954	
8_B330	A-7-6	15,772	0.350	0.694	7,954	
8_B350	A-7-6	15,772	0.350	0.694	7,954	

Table 31. Summary of backcalculated subgrade elastic modulus (E_{SG}) and subgrade lab Mr at optimum moisture content estimated from the backcalculated E_{SG}, continued.

Section ID	Soil Class	Elastic Modulus, psi	C Value	Mr/Mr(opt) Ratio	Corrected Lab Mr_{OPT}, psi	Mean Mr (at Opt. Moisture Content), psi
35_13087	A-2	27,461	0.350	1.001	9,602	
4_91044	A-2-4	22,460	0.520	1.001	11,668	
7_13817	A-2-4	22,460	0.350	1.001	7,853	
42_12153	A-2-4	19,198	0.350	1.002	6,706	8,732
49_13864	A-2-4	22,460	0.350	1.001	7,853	
8_6013	A-2-4	24,443	0.350	1.001	8,547	
37_92976	A-2-5	25,439	0.350	1.001	8,895	
8_12685	A-6	16,020	0.350	0.582	9,634	
10_12393	A-6	21,921	0.350	0.642	11,951	
21_91094	A-6	26,858	0.520	0.646	21,619	
22_12297	A-6	22,128	0.350	0.561	13,805	
38_13505	A-6	16,020	0.350	0.589	9,520	
41_13325	A-6	16,020	0.350	0.734	7,639	
45_13106	A-6	16,020	0.350	0.628	8,928	
8_0501	A-6	23,014	0.520	0.628	19,056	
8_0502	A-6	29,762	0.520	0.627	24,683	
8_0503	A-6	32,029	0.520	0.627	26,563	
8_0504	A-6	27,983	0.520	0.627	23,208	
8_0505	A-6	22,614	0.520	0.628	18,725	
8_0506	A-6	23,249	0.520	0.628	19,251	
8_0507	A-6	23,083	0.520	0.627	19,144	
8_0508	A-6	25,123	0.520	0.627	20,836	15,932
8_0509	A-6	34,171	0.520	0.628	28,294	
8_0559	A-6	29,635	0.520	0.626	24,617	
8_0560	A-6	24,780	0.520	0.627	20,551	
8_1047	A-6	22,185	0.350	0.678	11,452	
8_1053	A-6	23,181	0.350	0.641	12,657	
8_1057	A-6	15,769	0.350	0.674	8,189	
8_6002	A-6	16,020	0.350	0.641	8,747	
8_7781	A-6	19,843	0.350	0.671	10,350	
8_7783	A-6	36,028	0.350	0.646	19,520	
8_A310	A-6	23,181	0.350	0.643	12,618	
8_A320	A-6	23,181	0.350	0.643	12,618	
8_A330	A-6	23,181	0.350	0.643	12,618	
8_A340	A-6	23,181	0.350	0.643	12,618	
8_A350	A-6	23,181	0.350	0.643	12,618	

For new JPCP projects, equivalent subgrade Mr (at optimum moisture) was estimated iteratively using the MEPDG as follows:

1. Obtain backcalculated modulus of subgrade reaction (k-value) at in situ moisture content through backcalculation.
2. Run MEPDG using default subgrade Mr for given soil class. Obtain monthly in situ (predicted) k-value for the subgrade layer and MEPDG estimated in situ moisture.
3. Compare MEPDG estimates of k-value and in situ moisture with backcalculated k-value and field-measured in situ moisture content values.

4. If there are significant differences between the two k-values (> 10 percent), adjust the default subgrade Mr for the given soil class and repeat steps 2 and 3 until the difference is less than 10 percent and obtain default subgrade Mr for the given project.

Table 32 presents a summary of backcalculated subgrade k-value and subgrade lab Mr at optimum moisture content estimated from the backcalculated subgrade k-value, along with subgrade soil AASHTO classification.

Table 32. Summary of rigid pavement backcalculated subgrade k-value and subgrade lab Mr at optimum moisture content estimated from the backcalculated subgrade k-value.

Section ID	AASHTO Soil Class	Backcalculated Dynamic k-Value, psi/in	Backcalculated Elastic Modulus, in	Mean Mr (at Opt. Moisture Content), psi
18-12187	A-1-a	376	18,000	14,900
54-11546	A-1-a	240	15,500	
55-93015	A-1-a	170	10,000	
8_3032	A-1-a	250	13,000	
13-10175	A-1-b	270	18,000	
19-92021	A-2-4	260	16,500	13,808
8_0213	A-2-4	190	12,000	
8_0215	A-2-4	286	22,000	
8_0216	A-2-4	190	12,500	
8_0218	A-2-4	154	8,000	
8_0219	A-2-4	170	9,000	
8_0220	A-2-4	195	10,500	
8_0222	A-2-4	198	13,000	
8_0223	A-2-4	165	10,000	
8_0259	A-2-4	228	16,500	
8_9019	A-2-4	271	16,500	
8_0214	A-2-6	218	16,000	
8_7776	A-2-6	240	17,000	
29-89168	A-3	180	8,000	8,000
26-93216	A-4	206	18,000	18,200
46-00000	A-4	216	15,000	
2-11327	A-4	400	24,000	
3-88452	A-4	334	20,000	
8_9020	A-4	260	14,000	
6-91022	A-6	124	6,300	12,860
8_0217	A-6	160	9,000	
8_0221	A-6	212	17,000	
8_0224	A-6	181	11,000	
1-11328	A-6	444	21,000	
25-10326	A-7-6	190	13,000	12,000
53-84076	A-7-6	165	11,000	

On average, multiplying E_{SG} by a factor of 0.39 for coarse-grained soils and 0.64 for fine-grained subgrade soils provides an approximate value for subgrade resilient modulus Mr at optimum moisture content. For PCC pavements, MEPDG input subgrade resilient modulus Mr at optimum moisture can be obtained by using the relationship below (also see Figure 57):

$$Mr(opt) = 60.754 * k\text{-value} \quad (4)$$

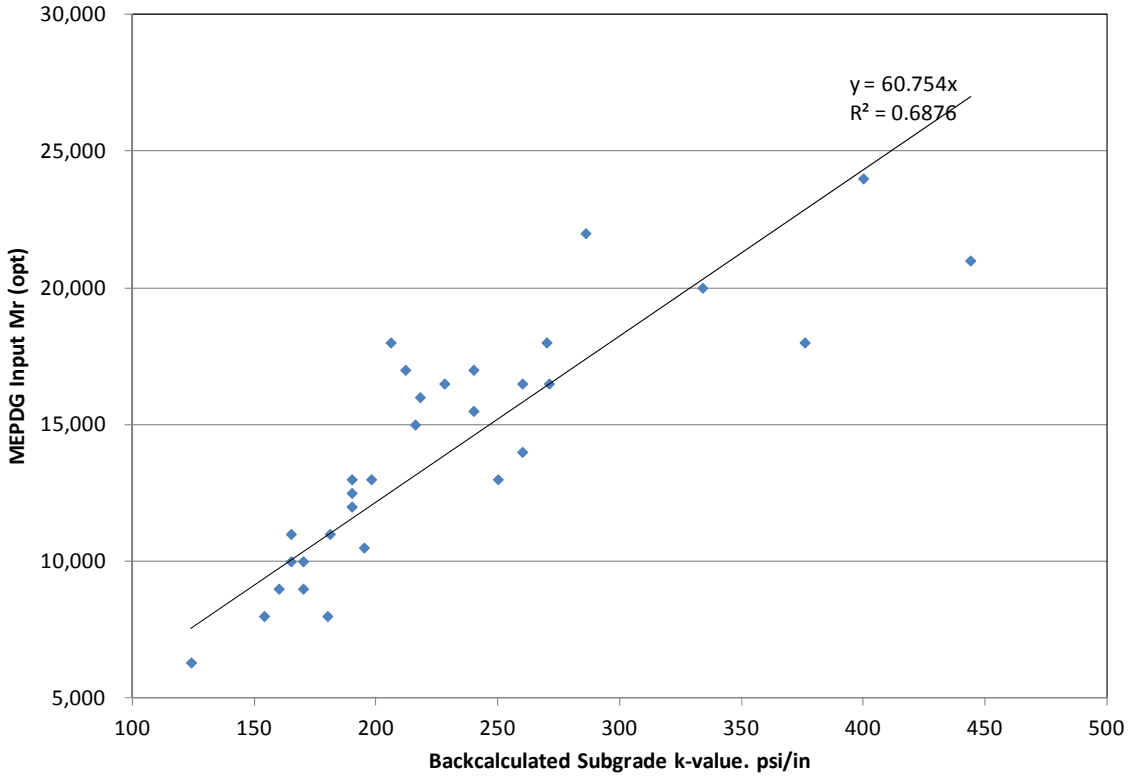

Figure 57. Plots showing relationship between backcalculated k-value and MEPDG input subgrade resilient modulus Mr at optimum moisture for month of FWD testing.

Laboratory Testing

Laboratory-prepared HMA and PCC specimens were tested and characterized using CDOT, AASHTO, and ASTM test protocols as well as nonstandardized test methods to obtain properties required for computing default CDOT MEPDG material inputs. In total, several replicates of nine typical CDOT HMA mixtures were develop along with standard CDOT PCC mixtures with different coarse aggregate types. The following laboratory tests were conducted:

- HMA.
  - Dynamic modulus test.
  - Indirect tensile strength and creep compliance test.
  - Repeated load deformation test.
  - Rut testing using the Hamburg Wheel Tracking (HWT) test.
- PCC.
  - Fresh concrete and mix properties (e.g., slump).
  - Compressive strength.
  - Flexural strength.
  - CTE.
  - Elastic modulus.

The following sections present a detailed description of the laboratory testing and outcomes (default MEPDG materials inputs).

HMA Mixtures Characterization

Description of HMA Mixtures

Laboratory testing was conducted on nine HMA samples and field cores—four conventional HMA, three HMA with PMA, and two SMA. The goal was to determine default HMA inputs such as dynamic modulus, creep compliance, indirect tensile strength, and in-place air voids and volumetric binder content. Tables 33 and 34 describe the nine CDOT mixes.

Table 33. CDOT mixes tested in the laboratory to develop MEPDG default inputs.

Mix ID	Sample No.	Mix Type	Binder Grade	Mix ID	Gradation
FS1918-9	United 58-28-2	Conv HMA	PG 58-28	FS1918-9	SX
FS1919-2	#181603	SMA	PG 76-28	FS1919-2	SMA
FS1920-3	#183476	Conv HMA	PG 58-28	FS1920-3	SX
FS1938-1	#16967C	Conv HMA	PG 64-22	FS1938-1	SX
FS1939-5	#194140	PMA	PG 76-28	FS1939-5	SX
FS1940-5	#17144B	Conv HMA	PG 58-28	FS1940-5	SX
FS1958-5	Wolf Creek Pass	PMA	PG 58-34	FS1958-5	SX
FS1959-8	I70 Gypsum to Eagle	PMA	PG 64-28	FS1959-8	SX
FS1960-2	I25 N of SH34	SMA	PG 76-28	FS1960-2	SMA

Table 34. Volumetric properties and gradation of the selected typical CDOT HMA mixes.

ID & Properties	Mix ID			
	FS1918-9	FS1920-3	FS1938-1	FS1940-5
Sample no.	United 58-28-2	#183476	#16967C	#17144B
Binder grade	PG 58-28	PG 58-28	PG 64-22	PG 58-28
Gradation	SX	SX	SX	SX
Passing ¾” sieve	100	100	100	100
Passing ⅜” sieve	83	88	89	82
Passing No 4 sieve	53	62	69	56
Passing No. 200 sieve	6.5	7.1	6.8	5.9
Mix AC binder	5	5.6	5.4	5.5
Voids in mineral aggregate (VMA) (%)	16.2	17	16.3	17.2
Voids filled with asphalt (VFA) (%)	65.9	64.1	68.5	68.2
Air voids (%)	5.5	6.1	5.1	5.5
Effective volumetric moisture content (Vbeff) (%)	10.7	10.9	11.2	11.7

Table 34. Volumetric properties and gradation of the 9 selected typical CDOT HMA mixes, continued.

ID & Properties	Mix ID				
	FS1958-5	**FS1959-8**	**FS1919-2**	**FS1939-5**	**FS1960-2**
Sample no.	Wolf Creek Pass	I70 Gypsum to Eagle	#181603	#194140	I25 N of SH34
Binder grade	PG 58-34	PG 64-28	PG 76-28	PG 76-28	PG 76-28
Gradation	SX	SX	SMA	SX	SMA
Passing ¾" sieve	100	95	95	100	100
Passing ⅜" sieve	81	87	46	87	69
Passing No 4 sieve	54	65	22	62	25
Passing No. 200 sieve	5	7.1	8	6.6	8.1
Mix AC binder	7	5.4	6.2	5.4	6.5
VMA (%)	19.6	16.4	16.9	16.3	17.1
VFA (%)	73.4	65.5	72	68.2	76.8
Air voids (%)	5.2	5.7	4.7	5.2	4.0
Vbeff (%)	14.4	10.7	12.2	11.1	13.1

HMA Dynamic Modulus Testing

The dynamic modulus values were measured in accordance with AASHTO TP 62, Standard Method of Test for Determining Dynamic Modulus of Hot Mix Asphalt (HMA), for a combination of five test temperatures and five test frequencies, as required for MEPDG Level 1. The results are presented in Table 35.

Table 35. Dynamic modulus values of typical CDOT HMA mixtures.

Mix ID	Temperature (°F)	Testing Frequency			
		25 Hz	**10 Hz**	**1 Hz**	**0.5 Hz**
FS1918 (PG 58-28, Gradation SX)	14	2,900,099	2,818,038	2,537,265	2,428,970
	40	2,257,965	2,075,896	1,549,873	1,381,660
	70	1,112,586	906,142	484,540	390,933
	100	323,971	239,391	111,912	90,140
	130	86,719	66,421	37,785	32,918
FS1919 (PG 76-28, Gradation SMA)	14	2,758,515	2,662,007	2,351,059	2,237,401
	40	2,045,581	1,865,812	1,378,519	1,230,679
	70	980,835	809,521	464,947	387,592
	100	323,623	252,537	137,906	116,443
	130	110,901	90,227	58,256	52,283
FS1920 (PG 58-28, Gradation SX)	14	2,788,941	2,698,644	2,397,288	2,283,742
	40	2,100,335	1,914,978	1,397,712	1,237,621
	70	978,820	791,037	418,926	338,214
	100	277,921	206,455	98,884	80,365
	130	76,798	59,571	34,858	30,574

Table 35. Dynamic modulus values of typical CDOT HMA mixtures.

Mix ID	Temperature (°F)	Testing Frequency			
		25 Hz	10 Hz	1 Hz	0.5 Hz
FS1938 (PG 64-22, Gradation SX)	14	2,950,163	2,887,740	2,680,448	2,601,704
	40	2,417,122	2,276,774	1,860,432	1,720,558
	70	1,391,643	1,198,776	753,641	639,073
	100	496,933	385,970	194,405	157,140
	130	135,576	102,799	53,830	45,192
FS1939 (PG 76-28, Gradation SX)	14	2,776,809	2,674,640	2,339,581	2,215,718
	40	2,037,766	1,843,321	1,317,308	1,159,645
	70	930,020	750,969	404,138	330,013
	100	281,928	214,540	111,276	92,946
	130	91,132	73,216	46,546	41,736
FS1940 (PG 58-28, Gradation SX)	14	2,849,460	2,764,473	2,473,915	2,362,175
	40	2,156,745	1,967,527	1,433,170	1,266,797
	70	971,195	779,370	407,026	328,213
	100	260,831	194,792	97,113	80,429
	130	75,318	60,298	38,496	34,650
FS1958 (PG 58-34, Gradation SX)	14	2,436,678	2,299,130	1,871,731	1,723,419
	40	1,567,260	1,358,215	854,152	721,055
	70	575,990	443,437	217,831	175,189
	100	157,715	119,392	63,837	54,320
	130	55,485	45,673	31,101	28,460
FS1959 (PG 64-28, Gradation SX)	14	2,645,996	2,535,875	2,190,535	2,067,626
	40	1,867,004	1,680,477	1,194,431	1,052,657
	70	822,141	666,566	366,356	301,596
	100	249,892	192,068	101,355	84,788
	130	80,788	64,960	40,838	36,386
FS1960 (PG 76-28, Gradation SMA)	14	2,773,716	2,674,443	2,352,150	2,233,847
	40	2,077,688	1,893,732	1,393,018	1,241,085
	70	1,031,593	852,589	491,260	410,107
	100	362,392	283,780	156,557	132,697
	130	132,036	107,672	70,033	63,020

The dynamic moduli of the laboratory-tested HMA mixes were evaluated to determine reasonableness and how they compared with MEPDG Level 3 "global" defaults. To check for reasonableness, the researchers evaluted trends in the measured HMA dynamic modulus with increasing test temperature and increasing loading frequency. As expected, HMA dynamic modulus increased with increasing loading frequency and decreased with increased test temperature. Next was to compare the test and Level 3 global dynamic modulus estimates. This was done by fitting the CDOT test data to the MEPDG dynamic modulus master curve (by developing master curve parameters for each mix type) and comparing trends in the CDOT laboratory-determined and MEPDG master curves for each mix type. The HMA dynamic modulus master curve equation is presented below:

$$\log(E^*) = \delta + \frac{\alpha}{1 + e^{\beta + \gamma\left\{\log(f) + \frac{\Delta E_a}{19.14714}\left[\left(\frac{1}{T}\right) - \left(\frac{1}{T_r}\right)\right]\right\}}} \quad (5)$$

where

δ	=	log (E_{min})
α	=	log (E_{max}) - log (E_{min})
f	=	frequency, Hz
T	=	temperature of interest, ˚K
T_r	=	reference temperature, ˚K
ΔE_a	=	activation parameter
β, γ	=	shape parameters

The fitted master curve parameters are presented in Table 36. Comparisons of HMA dynamic modulus E* for different binder grades, mix types (Superpave vs. SMA), and hierarchal level of estimation (Level 1 vs. Level 3) are presented in Figures 58 through 63.

Table 36. HMA dynamic modulus master curve parameters for typical CDOT HMA mixtures.

Mix ID	δ	α	β	γ	ΔEa
FS1918-9	4.110062	2.403987	-0.6423	-0.5568	205347.9
FS1919-2	4.366954	2.146171	-0.4303	-0.5050	209368.3
FS1920-3	4.087468	2.419617	-0.5505	-0.5393	206824.9
FS1938-1	3.952260	2.562730	-1.1046	-0.4794	223377.0
FS1939-5	4.297267	2.217203	-0.3660	-0.5384	202863.5
FS1940-5	4.250315	2.258170	-0.4136	-0.5653	211738.7
FS1958-5	4.211077	2.284814	0.0269	-0.5522	194062.3
FS1959-8	4.174802	2.337297	-0.3819	-0.4919	208726.3
FS1960-2	4.470080	2.044498	-0.3943	-0.5227	199965.8

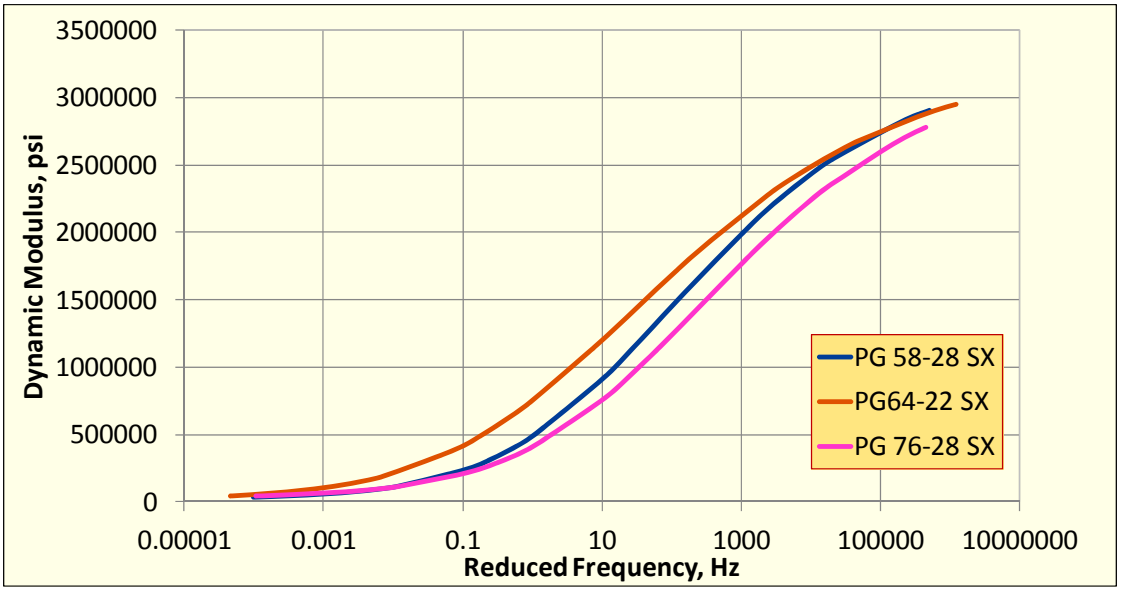

Figure 58. Comparison of HMA dynamic modulus E* for different binder grades.

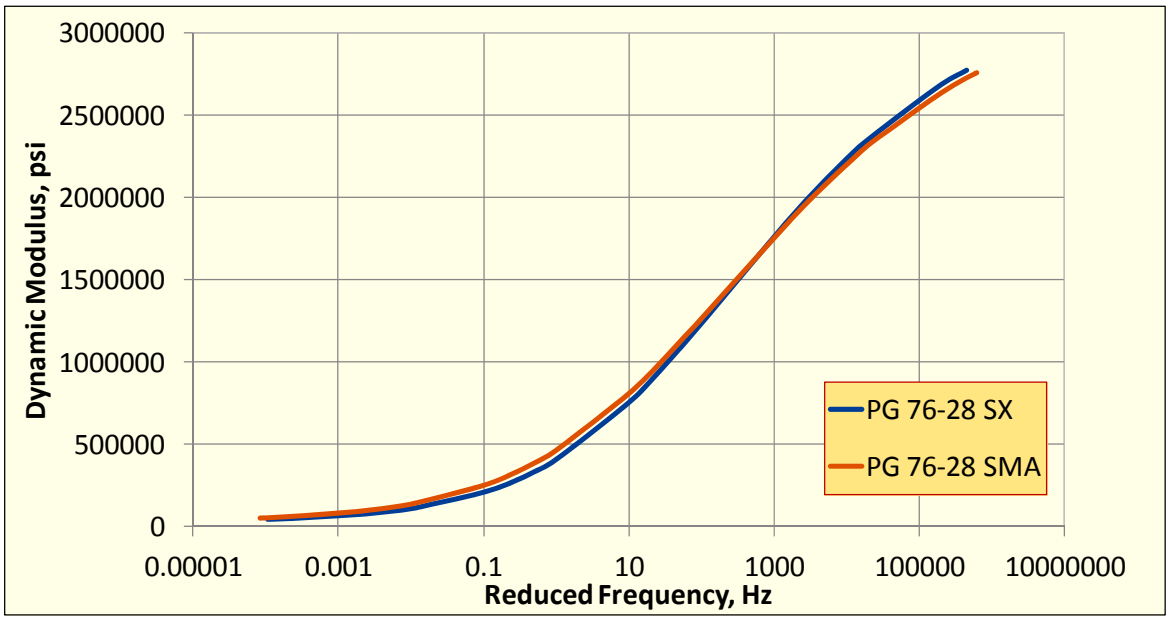

Figure 59. Comparison of HMA dynamic modulus E* for Superpave and SMA mixes.

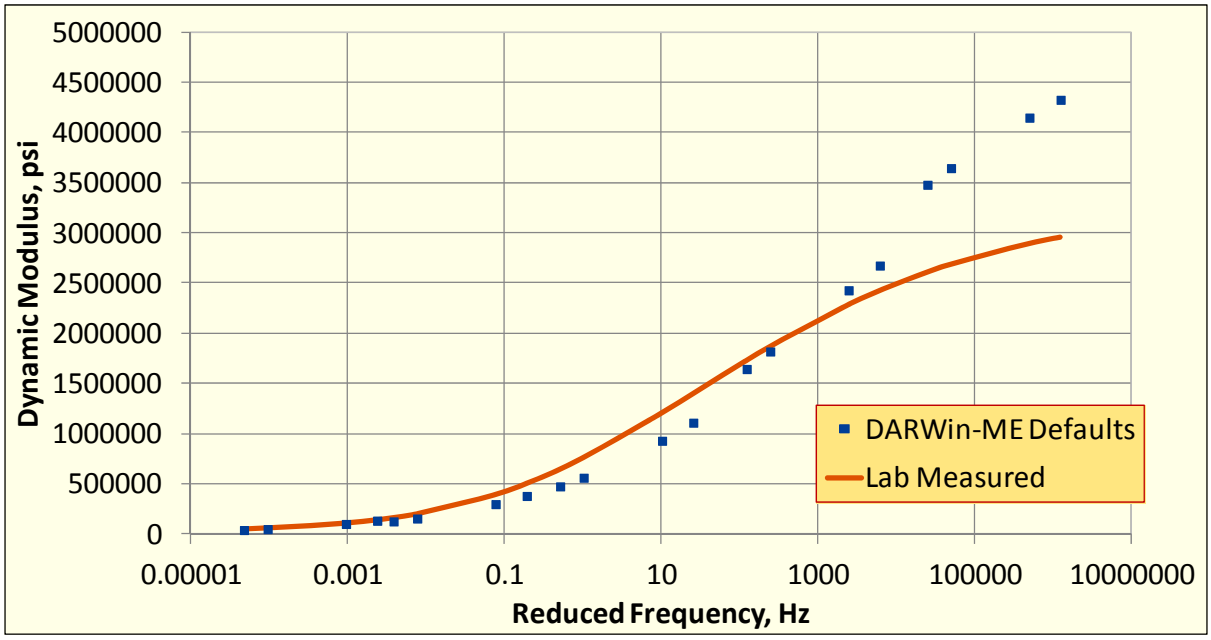

Figure 60. Comparison of HMA dynamic modulus E* for Level 1 and Level 3 estimates (Mix FS-1938 (PG 64-22 & SX)).

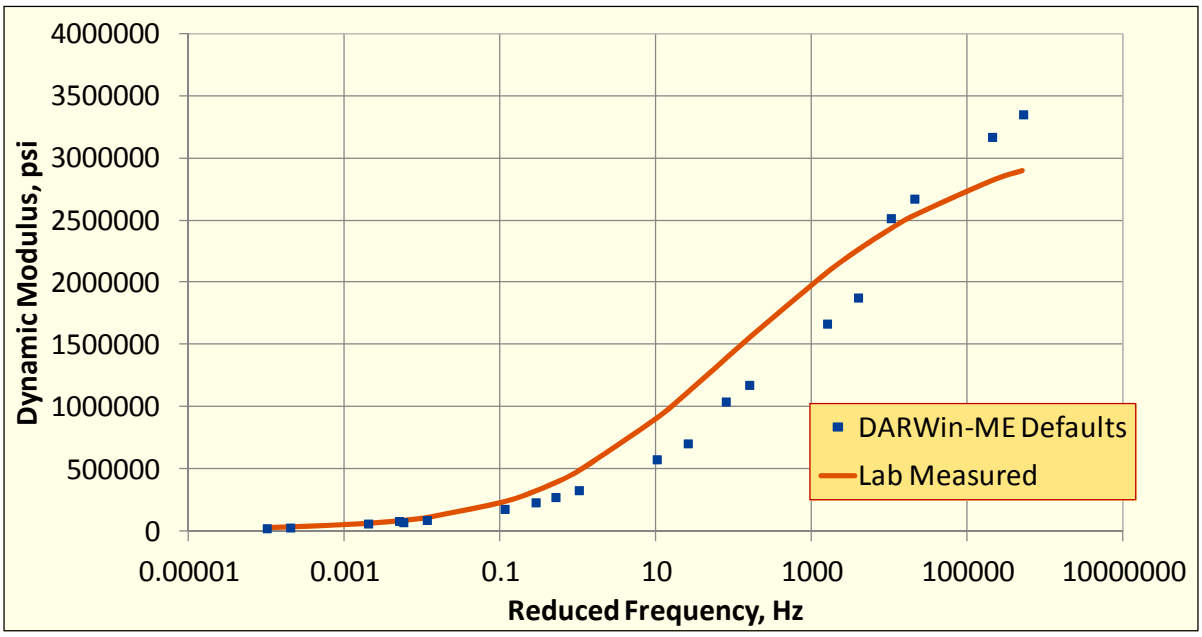

Figure 61. Comparison of HMA dynamic modulus E* for Level 1 and Level 3 estimates (Mix FS-1918 (PG 58-28 & SX)).

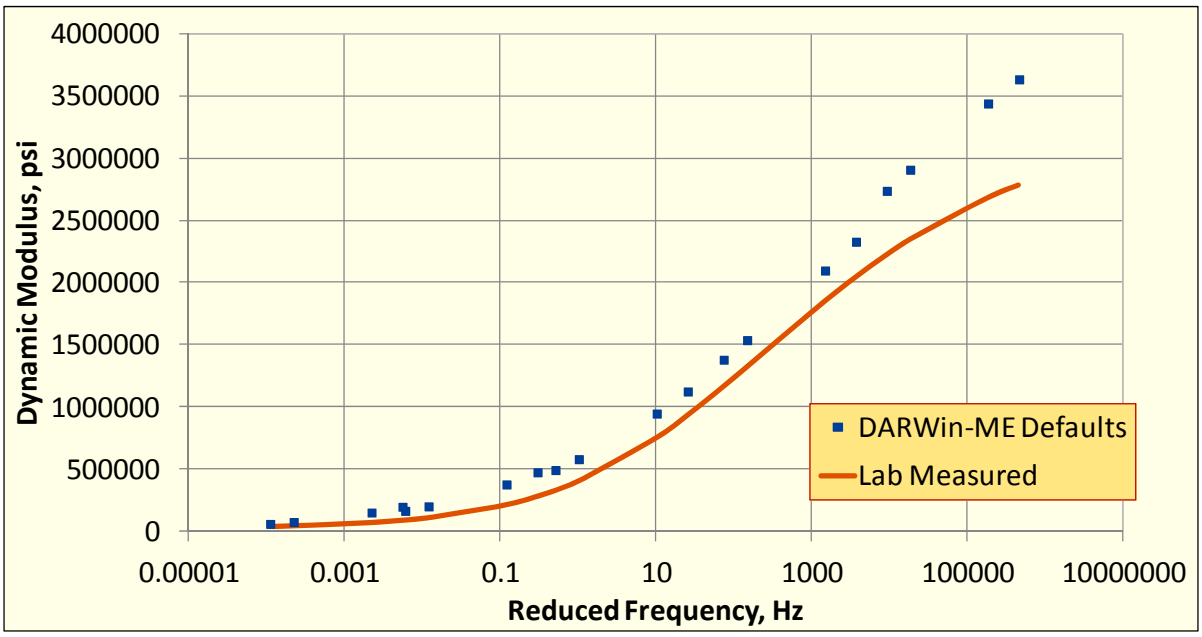

Figure 62. Comparison of HMA dynamic modulus E* for Level 1 and Level 3 estimates (Mix FS-1939 (PG 76-28 & SX)).

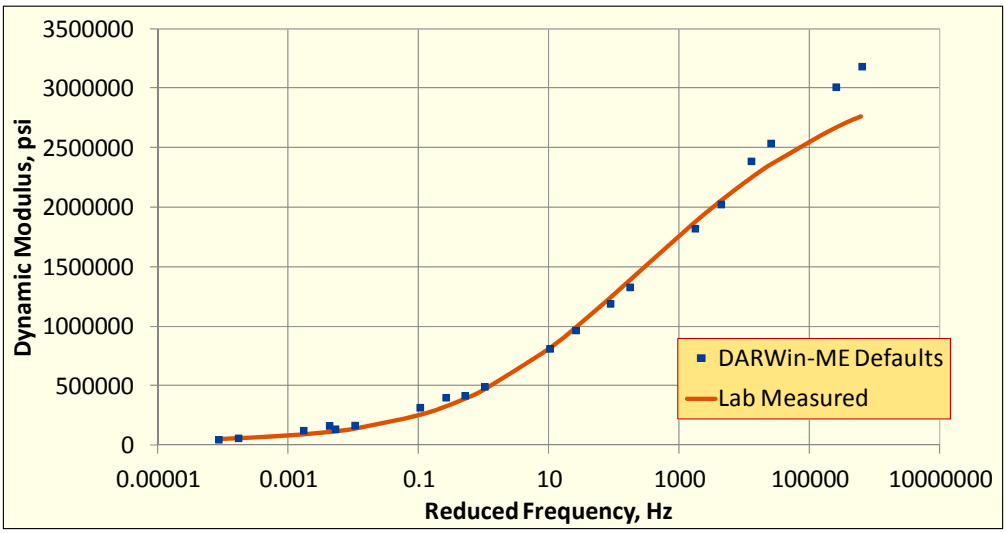

Figure 63. Comparison of HMA dynamic modulus E* for Level 1 and Level 3 estimates (Mix FS-1919 (PG 76-28 & SMA)).

The following were observed from the comparisons:

- Binder type had a significant impact on E* for loading frequencies ranging from 0.1 to 10,000 Hz.
- Superpave and SMA mixes produced similar estimates of E* for the frequency range tested.
- The MEPDG global E* model significantly overestimated E* for higher test frequencies (> 1000 Hz) for SMA and PMA mixes.

Thus, it was recommended that the CDOT HMA dynamic modulus values presented in Table 35 be adopted for use as default statewide (Level 2/3) inputs in lieu of actual project-specific dynamic test values (Level 1).

HMA Creep Compliance and Indirect Tensile Strength

HMA creep compliance—D(t)—is the ratio of time-dependent strain response to a constant stress input at controlled temperature/loading, and it is a required input for the MEPDG HMA transverse "thermal" cracking model (TCMODEL). Laboratory testing for D(t) was done using AASHTO TP 322, Standard Method of Test for Determining the Creep Compliance and Strength of Hot-Mix Asphalt (HMA) Using the Indirect Tensile Test Device. Testing was done for all nine selected CDOT mixes at three low test temperatures (-4 ^{o}F, 14 ^{o}F, and 32 ^{o}F) and 7 loading times (1 sec, 2 sec, 5 sec, 10 sec, 20 sec, 50 sec, and 100 sec). The test results are presented in Table 37.

HMA indirect tensile strength (IDT)—the strength of the HMA sample when subjected to indirect tension (by applying compressive load diametrically)—is also a key input required by the MEPDG TCMODEL. IDT testing was done according to AASHTO TP 322. The reference test temperature was 14 °F. The test results are presented in Table 38.

Table 37. Creep compliance values of typical CDOT HMA mixtures.

Mix ID	Loading Time, sec	Testing Temperature		
		-4°F	14°F	32°F
FS1918 (PG 58-28, Gradation SX)	1	2.78E-07	3.91E-07	2.65E-07
	2	3.11E-07	4.79E-07	3.91E-07
	5	3.48E-07	5.57E-07	6.33E-07
	10	3.74E-07	6.94E-07	9.55E-07
	20	4.22E-07	8.31E-07	1.28E-06
	50	4.63E-07	1.08E-06	1.99E-06
	100	5.28E-07	1.35E-06	2.72E-06
FS1919 (PG 76-28, Gradation SMA)	1	4.01E-07	4.45E-07	6.88E-07
	2	4.28E-07	5.41E-07	8.96E-07
	5	4.98E-07	6.37E-07	1.27E-06
	10	5.51E-07	7.85E-07	1.69E-06
	20	6.17E-07	9.33E-07	2.23E-06
	50	7.19E-07	1.18E-06	3.14E-06
	100	7.96E-07	1.39E-06	4.01E-06
FS1920 (PG 58-28, Gradation SX)	1	3.38E-07	4.31E-07	5.28E-07
	2	3.66E-07	5.02E-07	7.44E-07
	5	4.1E-07	6.27E-07	1.12E-06
	10	4.53E-07	7.61E-07	1.51E-06
	20	4.92E-07	8.55E-07	1.98E-06
	50	5.53E-07	1.11E-06	3.03E-06
	100	6.02E-07	1.31E-06	4.05E-06
FS1938 (PG 64-22, Gradation SX)	1	3.34E-07	4.19E-07	4.99E-07
	2	3.53E-07	4.64E-07	6.19E-07
	5	3.79E-07	5.15E-07	7.49E-07
	10	4.05E-07	5.7E-07	9.08E-07
	20	4.31E-07	6.26E-07	1.08E-06
	50	4.87E-07	7.27E-07	1.43E-06
	100	5.05E-07	8.41E-07	1.79E-06
FS1939 (PG 76-28, Gradation SX)	1	3.46E-07	4.12E-07	7.13E-07
	2	3.83E-07	4.76E-07	9.57E-07
	5	4.34E-07	5.97E-07	1.33E-06
	10	4.85E-07	7.25E-07	1.8E-06
	20	5.29E-07	8.45E-07	2.29E-06
	50	5.99E-07	1.05E-06	3.25E-06
	100	6.87E-07	1.32E-06	4.24E-06
FS1940 (PG 58-28, Gradation SX)	1	3.53E-07	3.82E-07	6.92E-07
	2	3.81E-07	4.62E-07	8.61E-07
	5	4.21E-07	5.92E-07	1.23E-06
	10	4.64E-07	7.07E-07	1.69E-06
	20	5.11E-07	8.15E-07	2.21E-06
	50	5.9E-07	1.1E-06	3.22E-06
	100	6.35E-07	1.27E-06	4.47E-06

Table 37. Creep compliance values of typical CDOT HMA mixtures, continued.

Mix ID	Loading Time, sec	Testing Temperature		
		-4°F	14°F	32°F
FS1958 (PG 58-34, Gradation SX)	1	4.82E-07	5.95E-07	9.61E-07
	2	5.30E-07	8.18E-07	1.48E-06
	5	6.05E-07	1.05E-06	2.18E-06
	10	6.85E-07	1.35E-06	3.14E-06
	20	7.71E-07	1.62E-06	4.19E-06
	50	8.72E-07	2.12E-06	6.23E-06
	100	1.00E-06	2.63E-06	8.74E-06
FS1959 (PG 64-28, Gradation SX)	1	3.61E-07	4.73E-07	7.12E-07
	2	4.04E-07	5.74E-07	9.97E-07
	5	4.51E-07	7.35E-07	1.52E-06
	10	5.11E-07	8.78E-07	1.99E-06
	20	5.67E-07	1.04E-06	2.59E-06
	50	6.57E-07	1.37E-06	3.75E-06
	100	7.68E-07	1.66E-06	4.66E-06
FS1960 (PG 76-28, Gradation SMA)	1	3.64E-07	4.64E-07	7.35E-07
	2	4.05E-07	5.70E-07	1.04E-06
	5	4.43E-07	7.15E-07	1.51E-06
	10	5.06E-07	8.79E-07	2.04E-06
	20	5.48E-07	1.03E-06	2.61E-06
	50	6.40E-07	1.31E-06	3.61E-06
	100	7.44E-07	1.70E-06	4.69E-06

Table 38. Indirect tensile strength values of typical CDOT HMA mixtures.

Mix ID	Indirect Tensile Strength at 14˚F
FS1918 (PG 58-28, Gradation SX)	555.9
FS1919 (PG 76-28, Gradation SMA)	515.0
FS1920 (PG 58-28, Gradation SX)	519.0
FS1938 (PG 64-22, Gradation SX)	451.0
FS1939 (PG 76-28, Gradation SX)	595.0
FS1940 (PG 58-28, Gradation SX)	451.0
FS1958 (PG 58-34, Gradation SX)	446.0
FS1959 (PG 64-28, Gradation SX)	519.0
FS1960 (PG 76-28, Gradation SMA)	566.0

Plots of creep compliance versus loading time were generated and evaluated to assess the reasonableness of the laboratory test values (see Figure 64). The observed trends (increasing creep compliance with increase time) were deemed reasonable.

The Level 1 laboratory-measured and Level 3 MEPDG “global” model estimates of creep compliance and indirect tensile strength were compared statistically to determine whether the two sets of estimates were significantly different. A summary of the results is presented in Tables 39 and 40.

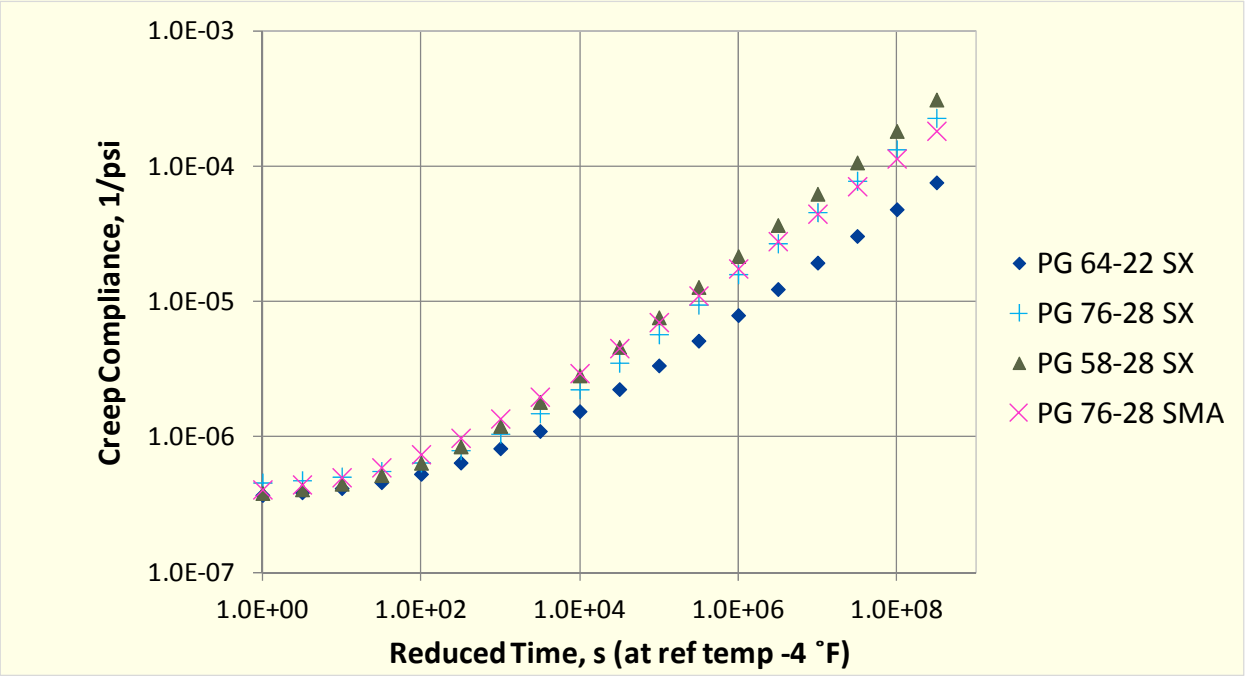

Figure 64. Laboratory-measured creep compliance versus loading time.

Table 39. Statistical comparison of Level 1 laboratory-tested and Level 3 MEPDG computed creep compliance for the selected CDOT HMA mixtures.

Mix ID	Mix Type	Binder Grade	Student t-test	t-critical at 95% CI	Result
FS1918-9	Conv HMA	PG 58-28	3.166	2.086	Significant
FS1919-2	SMA	PG 76-28	0.140	2.086	Not Significant
FS1920-3	Conv HMA	PG 58-28	6.006	2.086	Significant
FS1938-1	Conv HMA	PG 64-22	0.730	2.086	Not Significant
FS1939-5	PMA	PG 76-28	14.08	2.086	Significant
FS1940-5	Conv HMA	PG 58-28	0.183	2.086	Not Significant
FS1958-5	PMA	PG 58-34	0.941	2.086	Not Significant
FS1959-8	PMA	PG 64-28	2.719	2.086	Significant
FS1960-2	SMA	PG 76-28	1.281	2.086	Not Significant

Table 40. Statistical comparison of Level 1 laboratory-tested and Level 3 MEPDG computed indirect tensile strength for the selected CDOT HMA mixtures.

Mix ID	Mix Type	Binder Grade	Indirect Tensile Strength		Result
			Level 1 Measured	Level 3 Predicted	
FS1918-9	Conv HMA	PG 58-28	555.9	420.3	Significant
FS1919-2	SMA	PG 76-28	515.0	453.2	Significant
FS1920-3	Conv HMA	PG 58-28	519.0	377.5	Significant
FS1938-1	Conv HMA	PG 64-22	451.0	376.3	Significant
FS1939-5	PMA	PG 76-28	595.0	431.3	Significant
FS1940-5	Conv HMA	PG 58-28	451.0	382.0	Significant
FS1958-5	PMA	PG 58-34	446.0	397.5	Significant
FS1959-8	PMA	PG 64-28	519.0	424.6	Significant
FS1960-2	SMA	PG 76-28	566.0	445.8	Significant

The statistical evaluation showed no consensus that Level 3 predictive equations provide statistically similar values to those of Level 1 measurements. Thus, the Level 1 creep compliance estimates were deemed more representative of CDOT HMA materials. For IDT, Level 3 predictive equations consistently underestimated IDT strength values. Thus, the Level 1 IDT estimates were deemed more representative of CDOT HMA materials.

HMA Repeated Load Permanent Deformation Test & Hamburg Wheel Tracking Test

The MEPDG rutting model uses three main parameters—k_1, k_2, and k_3—to characterize the nature and rate of progression of rutting in the HMA layer. The MEPDG models only the "primary" and "secondary" portions of rutting, shown in Figure 65, using equation 6:

$$\left(\frac{\varepsilon_p}{\varepsilon_r}\right) = k_z * \beta_{r_1} * 10^{k_1} * T^{k_2 * \beta_{r2}} * N^{k_3 * \beta_{r3}} \quad (6)$$

where

ε_p	=	plastic strain
ε_r	=	resilient strain
k_z	=	depth confinement factor
k1	=	intercept term
k2	=	exponent of T (i.e. temperature)
k3	=	exponent of N (i.e. load repetitions)
β_{r1}, β_{r2}, β_{r3}	=	local calibration factors
T	=	layer temperature (˚F)
N	=	number of load repetitions

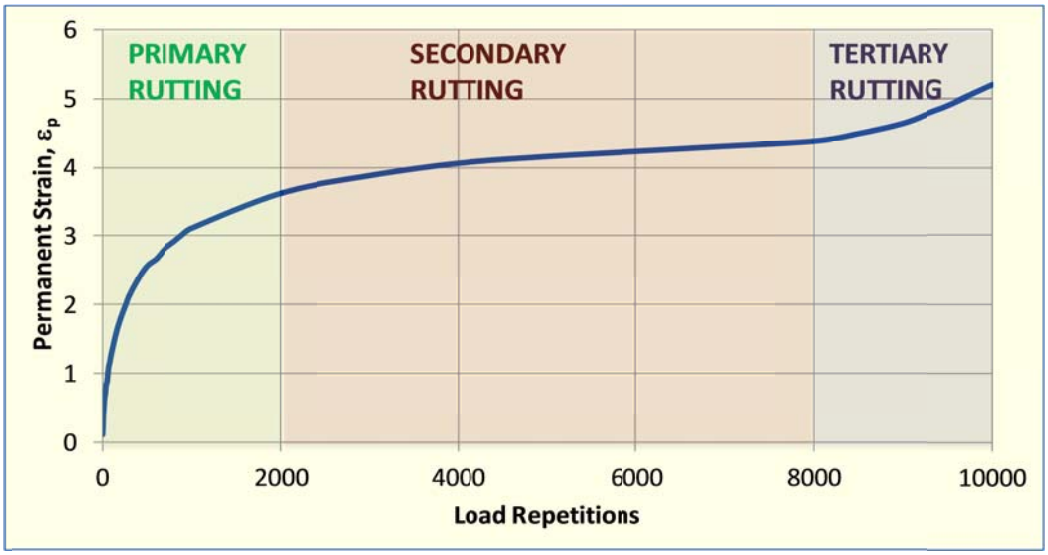

Figure 65. Progression of HMA rutting with repeated load application obtained from repeated load permanent deformation testing.

For this project, laboratory estimates of the HMA rutting model parameters k_1, k_2, and k_3 were determined using the following tests:

- Repeated load permanent deformation (RLPD) test (Von Quintus et al. 2012).
- HWT test.

For both tests, samples of HMA are repeatedly loaded in a controlled environment while permanent deformation is observed and measured along with the number of loading repetitions. A plot of permanent deformation versus number of loading repetitions is then developed and the relationship between the two evaluated. As shown in Figure 66, rutting development and progression in the HMA layer begins with an initial, almost instantaneous compaction of the HMA mix "primary rutting," followed by a slow rate of creeping of the HMA mix "secondary rutting," and then the stripping/disintegration of the HMA "tertiary rutting."

From both the RLPD and HWT tests, information was obtained to estimate MEPDG HMA rutting model k1, k2, and k3 as follows:

- Perform repeated load permanent deformation test/HWT test for a range of test temperatures.
- Plot permanent strain versus load repetitions and define primary, secondary, and tertiary rutting for the given HMA mix.
- Determine the slope (m) and intercept (Is) for the secondary rutting portion of the permanent strain versus load repetitions curve (see Figure 67).
- Plot intercept computed Is versus test temperature.
- Fit the non-linear equation $Is = d*(T)^n$ to the computed Is and test temperature data and obtain non-linear model parameters d and n (see Figure 68).
- Determine mix-specific k_1, k_2, and k_3 rutting model parameters:

- k_1 = log(d).
- k_2 = n (exponent of Is = d*(T)^n model).
- k_3 = m (average m for the range of test temperatures).

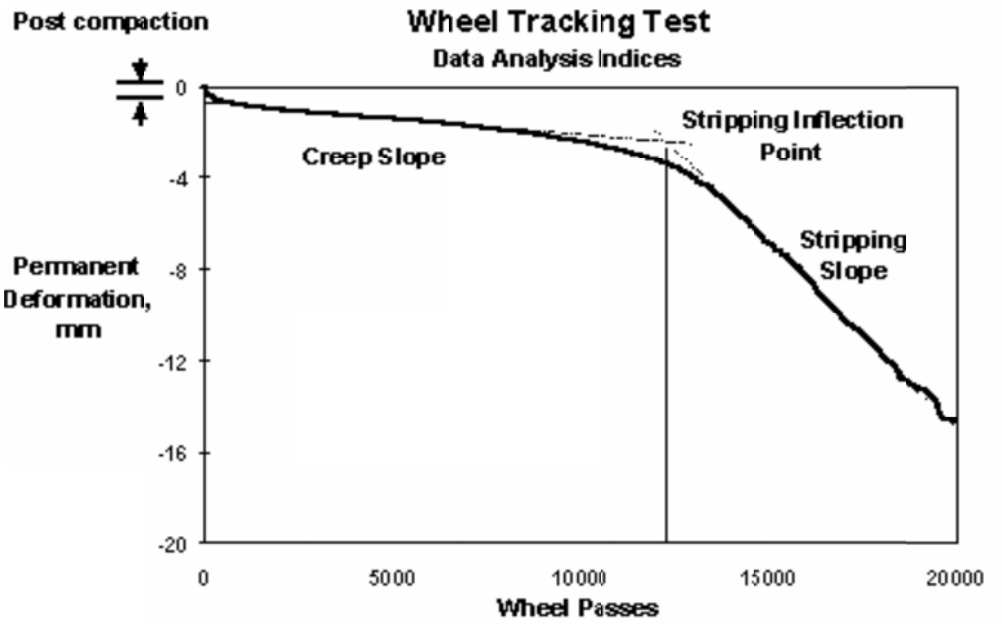

Figure 66. Example plot of permanent deformation vs. number of loading repetitions obtained from HWT testing.

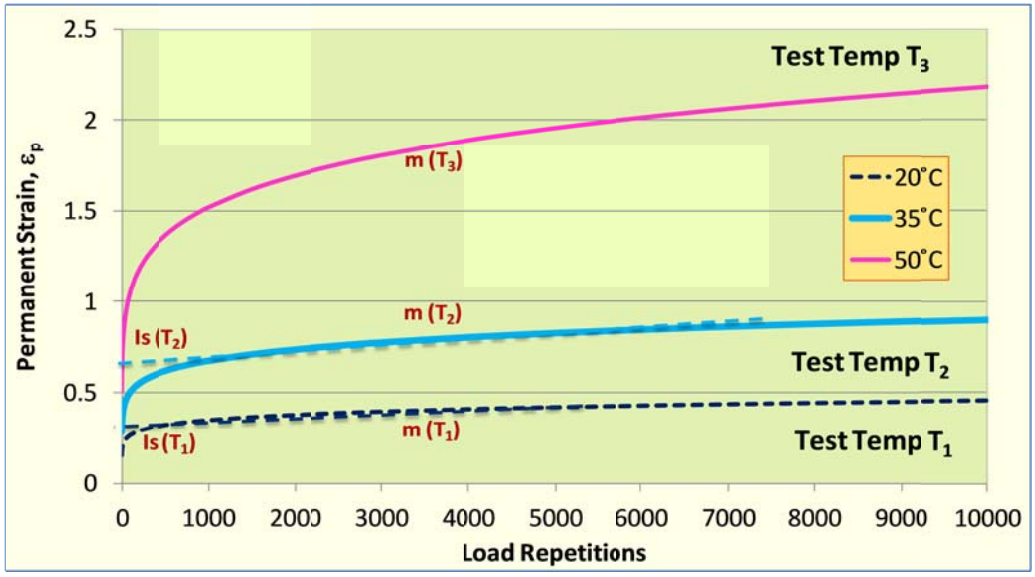

Figure 67. Plot showing slope (m) and intercept (Is) computed from the secondary rutting portion of plot of permanent strain vs. load repetitions.

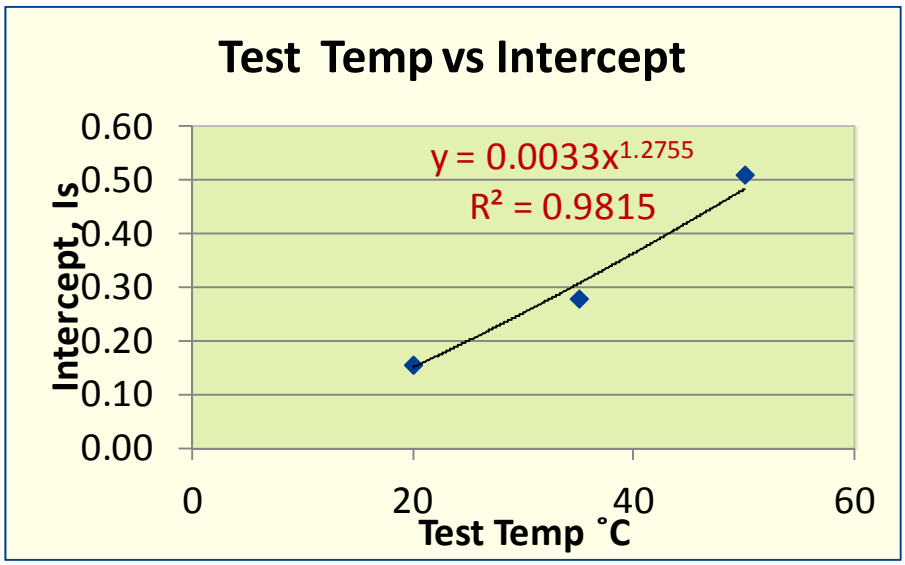

Figure 68. Plot of intercept (Is) vs. repeated load permanent deformation test temperature.

For this project, RLPD tests were conducted on the selected CDOT HMA mixes for up to 10,000 repeated load cycles, 3 test temperatures (20, 35, and 50 ˚C), HMA confinement pressure of 10 psi, and applied deviator stress of 70 psi. Three replicates of each of the HMA mixtures were tested. The HWT test was conducted on the selected CDOT HMA mixes at a test temperature of 55 ˚C for up to 10,000 loading cycles. Results from the two tests are presented in Tables 41 and 42.

A comparison of k1, k2, and k3 parameters from the RLPD and HWT tests showed no direct relationship.

Table 41. Estimates of HMA rutting model k_1, k_2, and k_3 parameters for the selected CDOT HMA mixtures using the repeated load permanent deformation test procedure (Von Quintus et al. 2012).

Mix ID	Binder Grade	Gradation	m-slope, k_3	n-slope, k_2	log(d), k_1
FS1918-9	PG 58-28	SX	0.137	2.068	-2.58
FS1919-2	PG 76-28	SMA	0.179	2.395	-3.159
FS1920-3	PG 58-28	SX	0.164	0.525	-1.169
FS1938-1	PG 64-22	SX	0.17	2.758	-3.506
FS1939-5	PG 76-28	SX	0.136	2.79	-3.357
FS1940-5	PG 58-28	SX	0.178	1.25	-1.892
FS1958-5	PG 58-34	SX	0.15	1.132	-1.582
FS1959-8	PG 64-28	SX	0.132	1.647	-2.214
FS1960-2	PG 76-28	SMA	0.185	0.952	-1.818
		Mean	**0.16**	**1.72**	**-2.36**

Table 42. Estimates of HMA rutting model k_1, k_2, and k_3 parameters for the selected CDOT HMA mixtures using the HWT test procedure.

Mix ID	Binder Grade	Gradation	Max Rut Depth mm	Intercept	Slope
FS1918-9	PG 58-28	SX	2.02	0.1197	0.294
FS1919-2	PG 76-28	SMA	N.A.	N.A.	N.A.
FS1920-3	PG 58-28	SX	2.06	0.1533	0.284
FS1938-1	PG 64-22	SX	1.98	0.1111	0.314
FS1939-5	PG 76-28	SX	2.65	0.1641	0.291
FS1940-5	PG 58-28	SX	3.36	0.1437	0.334
FS1958-5	PG 58-34	SX	3.85	0.0374	0.512
FS1959-8	PG 64-28	SX	N.A.	N.A.	N.A.
FS1960-2	PG 76-28	SMA	2.46	N.A.	N.A.

PCC Mixtures Characterization

Description of PCC Mixtures

Four PCC mix types were prepared in the laboratory and tested. The PCC mixtures were prepared following CDOT guidance for PCC mixtures to be used as paving materials. Table 43 presents mix proportions and fresh concrete properties of the selected typical CDOT PCC mixtures (including slump, air content, and unit weight). The following test protocols were used in ensuring that the PCC mixes (constituent proportions and fresh concrete properties) were in accordance with CDOT guidelines:

- PCC slump: ASTM C143, Standard Test Method for Slump of Portland Cement Concrete.
- PCC air content: ASTM C231, Standard Test Method for Air Content of Freshly Mixed Concrete by the Pressure Method.
- PCC unit weight: ASTM C138, Standard Test Method for Unit Weight, Yield, and Air Content (Gravimetric) of Concrete.

The sources of aggregate and cement materials used in developing the PCC mixtures in the laboratory are presented in Table 44. The sources were selected to be as representative of Colorado aggregates used for pavement construction as much as possible, as aggregate type and source significantly impact PCC thermal properties. Laboratory specimens (standard 4-in-diameter by 8-in-high cylinders) of the typical mixtures were prepared and tested as described in the following sections.

Table 43. Properties of typical CDOT PCC mixtures.

Mix ID	Region	Cement Type	Cement Content (lbs/yd)	Flyash Content (lbs/yd)	Water/ Cement Ratio	Slump (in)	Air Content (%)	Unit Weight (pcf)
2008160	2	I/II	575	102	0.44	3.75	6.3	139.8
2009092	3	I/II	515	145	0.42	4.00	6.8	138.6
2009105	4, 1, 6	I/II	450	113	0.36	1.50	6.8	140.6
2008196	5	I/II	480	120	0.44	1.25	6.0	140.8

Table 44. Materials and sources used in typical CDOT PCC mixtures.

Mix ID	2008160	2009092	2009105	2008196
Region	2	3	4, 1, 6	5
Cement	GCC-Pueblo	Mountain	Cemex-Lyons	Holsim
Flyash	Boral-Denver Terminal	SRMG – Four Corners	Headwaters-Jim Bridger	SRMG – Four Corners
Aggregates	RMMA Clevenger Pit	Soaring Eagle Pit	Aggregate Industries	SUSG Weaselskin Pit (Fine agg.) C&J Gravel Home Pit (Coarse agg.)
Water Reducer	BASF Pozzolith 200N BASF PolyHeed 1020 (mid-range)	BASF PolyHeed 997	BASF Masterpave	BASF PolyHeed 997
Air Entrainment	BASF MB AE 90	BASF Micro Air	BASF Pave-Air 90	BASF MB AE 90

PCC Compressive Strength

PCC compressive strength, $f_c^{'}$, was determined in accordance with ASTM C39, Standard Test Method for Compressive Strength of Cylindrical Concrete Specimens. Test results are as presented in Table 45. The results indicate that 28-day PCC compressive strength typically ranged from 5,000 to 5,400 psi, which is in agreement with CDOT guidelines.

A plot of strength gain versus pavement age was developed using the laboratory compressive strength data (Figure 69). Strength gain for the CDOT PCC mixes was compared to the MEPDG global default strength gain model, and the comparison showed the CDOT mixes gaining strength at a faster rate that the MEPDG model projected. It must be noted that, for PCC placed in the field, strength gain is typically less than that observed in laboratory testing. The PCC compressive strength data presented in Table 45 are recommended as Level 2/3 inputs.

Table 45. Compressive strength of typical CDOT PCC mixtures.

Mix Design ID	Region	Compressive Strength, psi				
		7-day	14-day	28-day	90-day	365-day
2008160	2	4290	4720	5300	6590	6820
2009092	3	3740	4250	5020	5960	7140
2009105	4, 1, 6	3780	4330	5370	5560	6390
2008196	5	4110	4440	5340	5730	5990

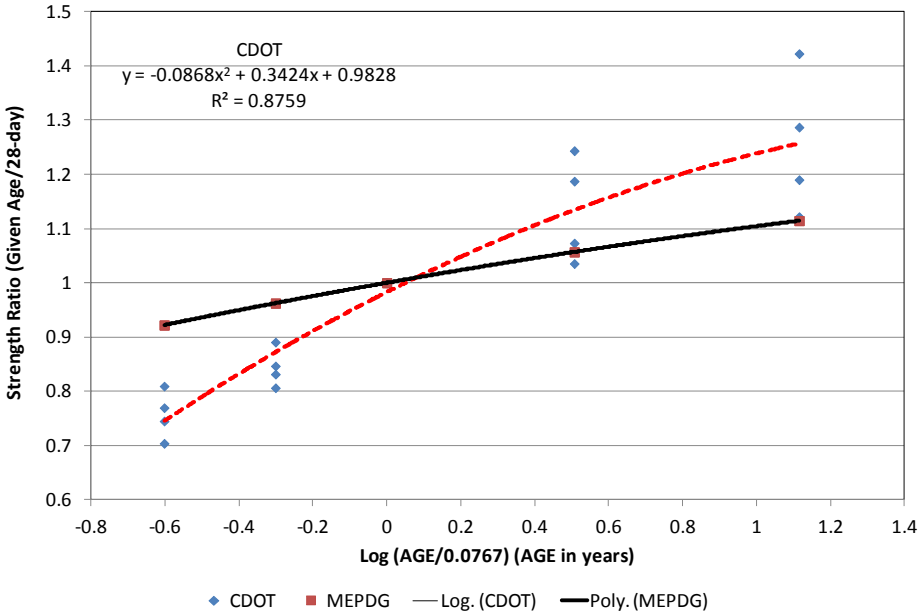

Figure 69. Plot of compressive strength gain versus pavement age for CDOT PCC mixes.

PCC Flexural Strength

PCC flexural strength MR was determined in accordance with ASTM C79, Standard Test Method for Flexural Strength of Concrete. The flexural strength test results are as presented in Table 46. The results indicate that 28-day PCC MR typically ranged from 700 to 900 psi, which is in agreement with CDOT guidelines. A plot of strength gain versus pavement age was developed using the laboratory-measured MR data (Figure 70). Strength gain for the CDOT PCC mixes was compared to the MEPDG global default strength gain model, and it showed the CDOT mixes initially gaining strength at a faster rate that the MEPDG predicted. At about 1 year, however, the rate of strength gain is similar. The PCC MR data presented in Table 46 are recommended as Level 2/3 inputs.

Table 46. Flexural strength of typical CDOT PCC mixtures.

Mix Design ID	Region	Flexural Strength, psi				
		7-day	14-day	28-day	90-day	365-day
2008160	2	660	760	900	935	940
2009092	3	570	645	730	810	850
2009105	4, 1, 6	560	620	710	730	735
2008196	5	640	705	905	965	970

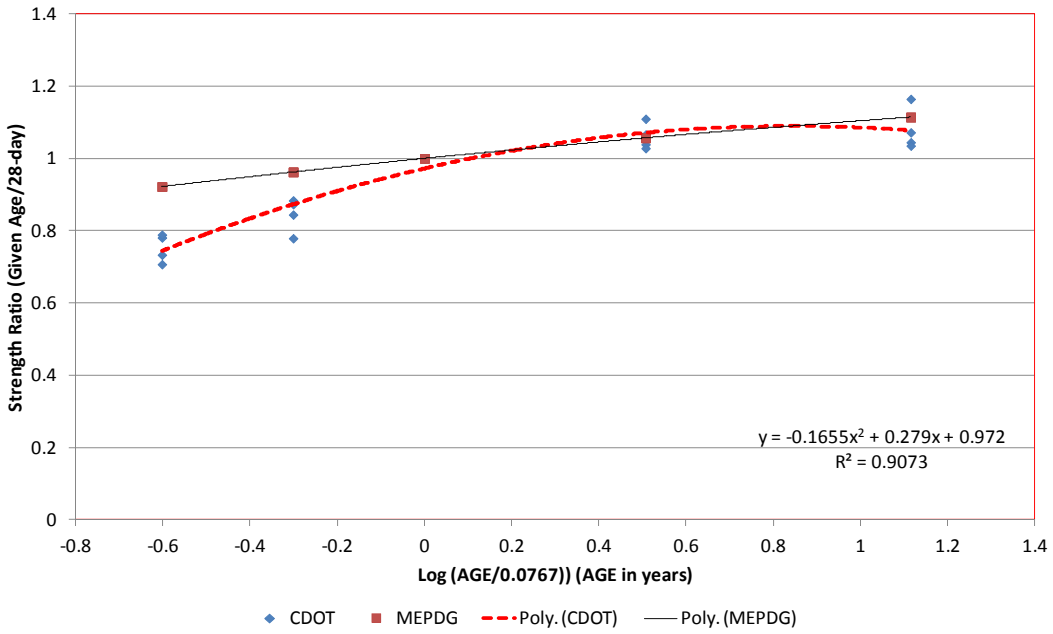

Figure 70. Plot of flexural strength gain versus pavement age for CDOT PCC mixes.

The laboratory-tested PCC compressive strength ($f_c^{'}$) and flexural strength (MR) data were used to evaluate the reasonableness of the MEPDG "global" compressive strength and flexural strength relationship (see equation 7) by performing a paired t-test between the measured and MEPDG global equation-predicted MR. The paired t-test produced a p-value of 0.0006, which implied that there was a significant difference in the laboratory-measured and MEPDG "global" equation predicted MR at the 95 percent significant level. A review of the plot of laboratory-measured vs. MEPDG global equation-predicted MR indicated a good correlation between the two estimated of MR (R^2 = 0.63) but with the MEPDG global equation underestimating MR for higher measured MR values.

$$MR = 9.5\left(f_c^{'}\right)^{0.5} \qquad (7)$$

Using the laboratory-measured $f_c^{'}$ and MR values, the project team performed further statistical analysis to revise the MEPDG global MR equation parameter to remove the observed bias. The new CDOT statewide MR equation is presented as equation 8.

$$MR = 0.53\left(f_c^{'}\right)^{0.85} \quad (8)$$

A paired t-test between the measured and CDOT statewide equation-predicted MR produced a p-value of 0.8613, which implied that there was no significant difference between the two at the 95 percent significant level. Figure 71 shows the laboratory-measured MR plotted against the CDOT statewide MR equation and the MEPDG global equation-predicted MR. The new CDOT statewide equation is recommended for estimating MR from measured compressive strength data. Note that this equation is valid for $f_c^{'}$ ranging from 3,000 to 5,000 psi.

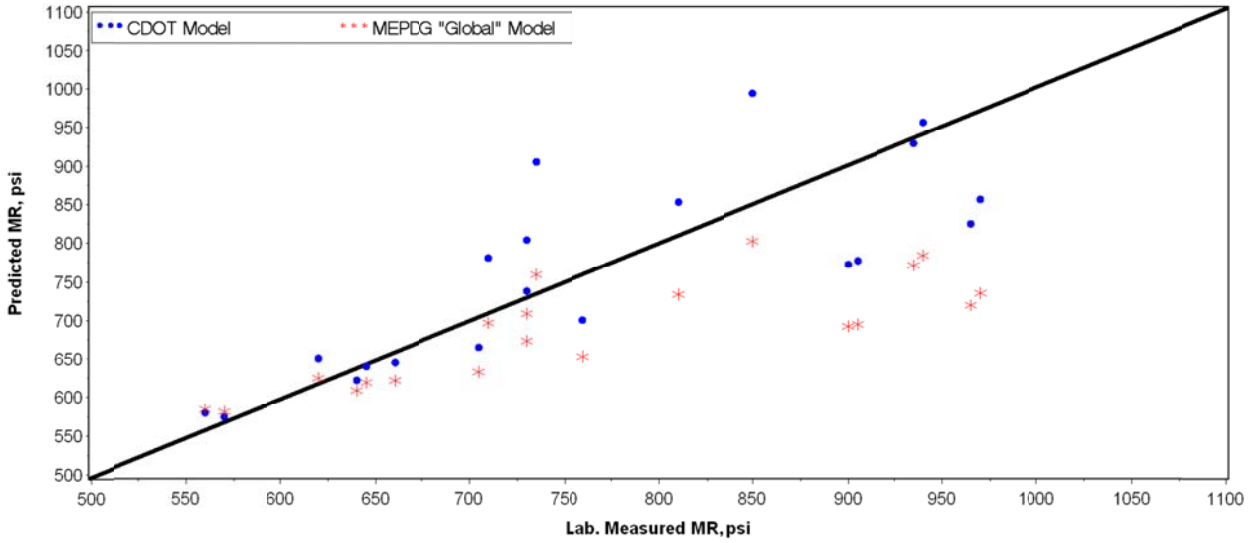

Figure 71. Plot of laboratory-measured MR vs. CDOT statewide MR equation and MEPDG global equation-predicted MR.

PCC Elastic Modulus and Poisson's Ratio

PCC elastic modulus (E_{PCC}) and Poisson's ratio (PR) were determined in accordance with ASTM C469, Standard Test Method for Static Modulus of Elasticity and Poisson's Ratio of Concrete in Compression. The E_{PCC} and PR test results are as presented in Table 47. The results indicate that 28-day E_{PCC} typically ranged from 3.5 to 4.3 million psi and PR averaged 0.2, which is in agreement with CDOT guidelines.

A plot of modulus gain versus pavement age was developed using the laboratory-measured E_{PCC} data (Figure 72). Modulus gain for the CDOT PCC mixes was compared to the MEPDG global default strength gain model, and it showed the CDOT mixes gaining strength at a faster rate that the MEPDG predicted (for the period of 7 to 365 days).

Table 47. Static elastic modulus and Poisson's ratio of typical CDOT PCC mixtures.

Mix Design ID	Region	Elastic Modulus, ksi					Poisson's Ratio
		7-day	14-day	28-day	90-day	365-day	
2008160	2	3140	3260	3550	3970	4240	0.21
2009092	3	3560	3860	4300	4550	4980	0.2
2009105	4, 1, 6	3230	3500	4030	4240	4970	0.2
2008196	5	3280	3510	3930	4170	4210	0.21

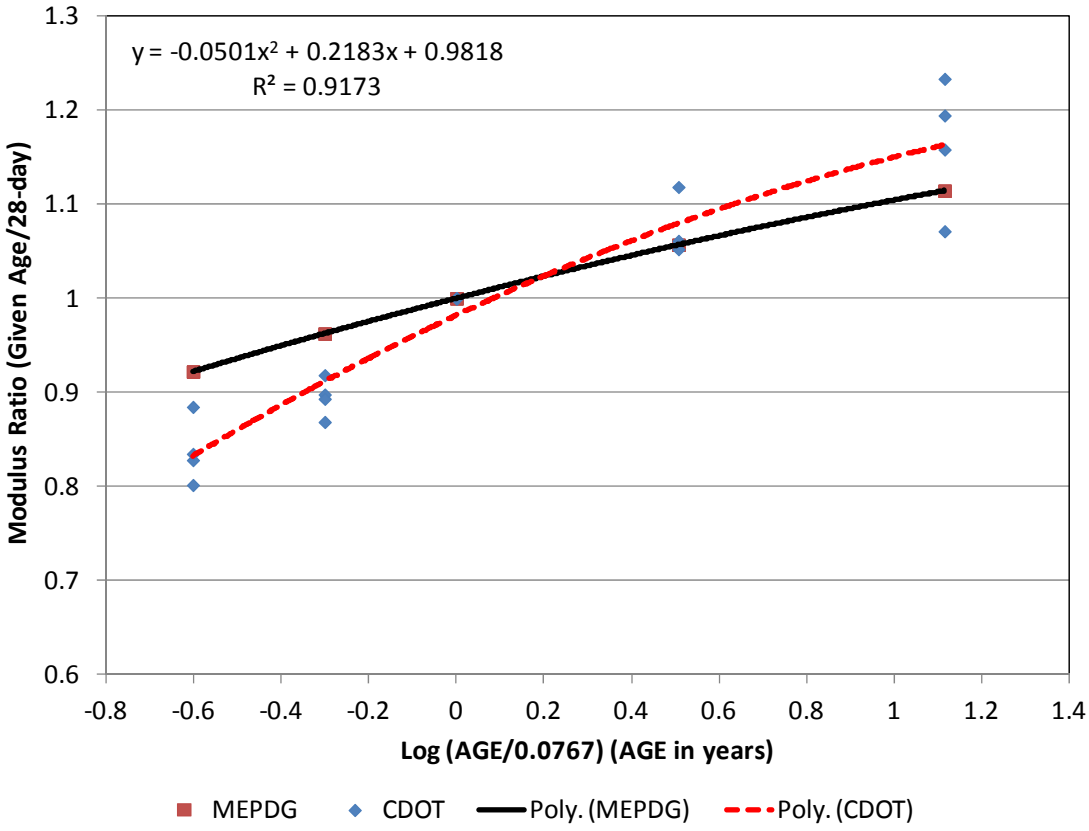

Figure 72. Plot of elastic modulus gain versus pavement age for CDOT PCC mixes.

The laboratory-tested PCC $f_c^{'}$ and E_{PCC} data were used to evaluate the reasonableness of the MEPDG global $f_c^{'}$ and flexural strength relationship (see equation 9) by performing a paired t-test between the measured and MEPDG global equation-predicted E_{PCC}.

$$E_{PCC} = 57000\left(f_c^{'}\right)^{0.5} \quad (9)$$

The paired t-test produced a p-value of 0.0178, which implied that there was a significant difference between the laboratory-measured E_{PCC} and MEPDG global equation-predicted E_{PCC} at the 95 percent significant level. A review of the plot of laboratory-measured E_{PCC} vs. MEPDG

global equation-predicted E_{PCC} indicated a good correlation between the two estimates (R2 = 0.67) but with the MEPDG global equation underestimating E_{PCC} for higher measured E_{PCC} values and overestimating E_{PCC} for lower measured E_{PCC} values. Using the laboratory-measured $f_c^{'}$ and E_{PCC} values, the project team performed further statistical analysis to revise the MEPDG global E_{PCC} equation parameter to remove the observed bias. The new CDOT statewide E_{PCC} equation is presented as equation 10.

$$E_{PCC} = 2688\left(f_c^{'}\right)^{0.85} \quad (10)$$

A paired t-test between the laboratory-measured E_{PCC} and CDOT statewide equation-predicted E_{PCC} produced a p-value of 0.7066, which implied that there was no significant difference between the two at the 95 percent significant level. A plot of laboratory-measured E_{PCC} vs. the CDOT statewide E_{PCC} equation and MEPDG global equation-predicted E_{PCC} is presented as Figure 73. The new CDOT statewide E_{PCC} equation is recommended for estimating E_{PCC} from measured compressive strength data. Note that the CDOT statewide E_{PCC} equation is valid for $f_c^{'}$ ranging from 3,000 to 5,000 psi.

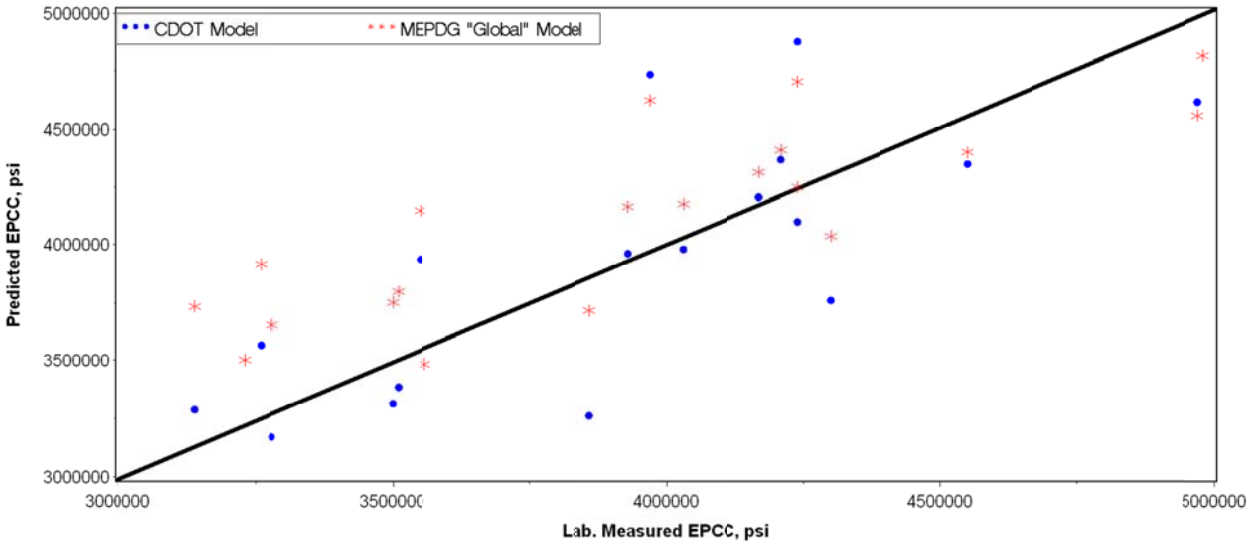

Figure 73. Plot of laboratory-measured EPCC vs. CDOT and MEPDG predicted EPCC.

PCC Coefficient of Thermal Expansion

PCC CTE was determined in accordance with AASHTO T336, Standard Method of Test for Coefficient of Thermal Expansion of Hydraulic Cement Concrete. The CTE test results are presented in Table 48. The results indicate that CTE typically ranged from 4.7 to 4.9 in/in/˚F for the different PCC mixes and coarse aggregate sources. The default inputs for CDOT are recommended in lieu of site-specific or mixture-specific data. However, site-specific or mixture-specific CTE data is recommended.

Table 48. CTE values of typical CDOT PCC mixtures.

Mix ID	Sample	CTE in/in./˚C	CTE in/in./˚F
2008160	1	8.5	4.72
	2	8.5	4.72
2009092	1	8.8	4.89
	2	8.6	4.78
2009105	1	8.8	4.89
	2	8.7	4.83
2008196	1	8.8	4.89
	2	8.6	4.78

Visual Distress Surveys

Visual distress surveys were performed in accordance with the LTPP Distress Identification Manual to identify, measure, and record visual distresses (Miller & Bellinger, 2003). Other pertinent information collected included pavement details such as lane and slab width, joint spacing, ambient temperature during survey and FWD testing, and so on. Total rutting for flexible and composite (HMA-surfaced) pavements was measured using the straightedge method, while JPCP faulting was measured using the Georgia Digital Faultmeter. Figure 74 presents a sample of the distress survey maps used in recording identified distress present at the pavement surface. Once the survey was completed, the information on the distress maps and other paper records was transferred into an MS Access database that contained all key information regarding project location and type, survey date, surveyor name, section ID, and so on.

Visual distress surveys were conducted only for the projects identified from the CDOT pavement management system, not the LTPP project sites. As possible, the cracking, rutting, faulting, and other data collected during the visual surveys were compared to the distress data available in the CDOT pavement management system database. This was only possible where the distress data were in a format compatible with LTPP and MEPDG. The comparisons were used to develop adjustment factors for correcting the CDOT pavement management system data to make them comparable to measured LTPP distress. This enabled the project team to include the CDOT pavement management system distress data in the project validation/calibration database, to the greatest extent possible.

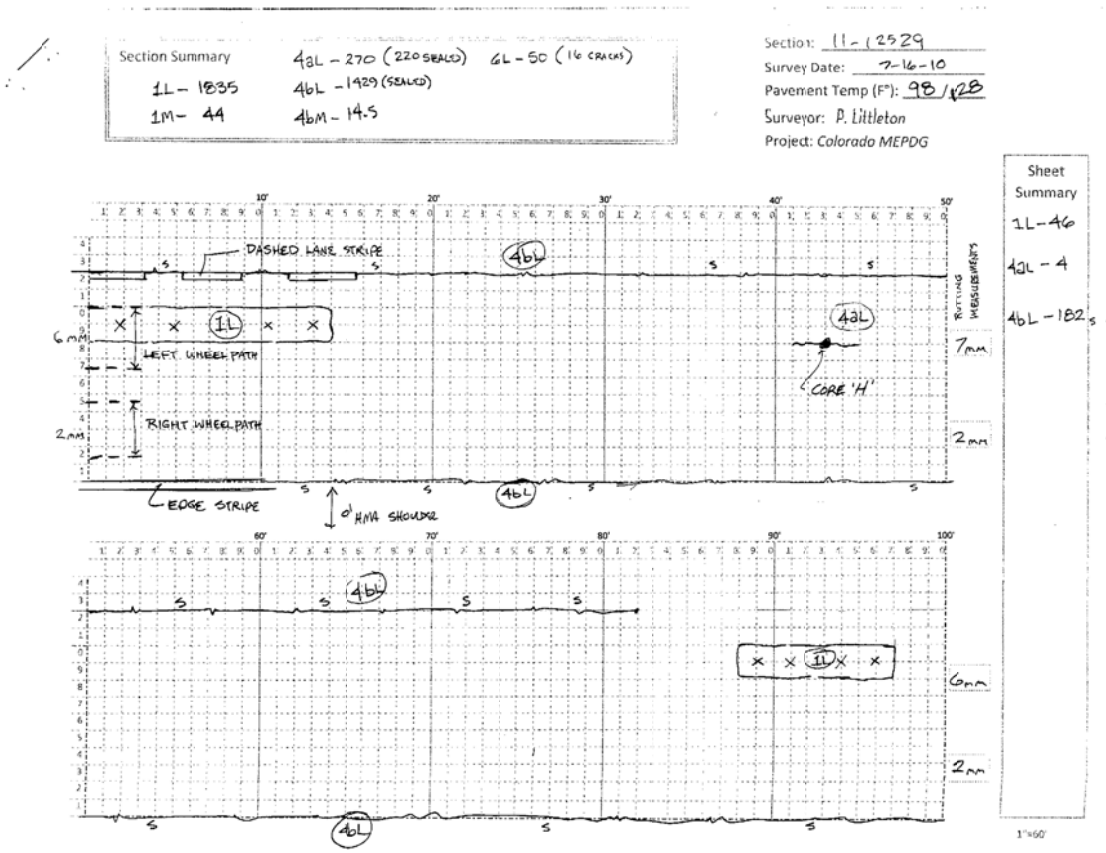

Figure 74. Example of distress map used for visual distress surveys.

CHAPTER 6. VERIFICATION AND CALIBRATION OF FLEXIBLE PAVEMENTS

This chapter describes work done to verify and calibrate (if needed) the MEPDG global flexible pavement distress and smoothness models for Colorado. For this project, "flexible pavement" refers to new HMA pavements and HMA-overlaid existing HMA pavements.

The criteria for performing local calibration were based on (1) whether the given global model exhibited a reasonable goodness of fit (between measured and predicted outputs) and (2) whether distresses/IRI were predicted without significant bias.

Reasonable goodness of fit was determine using the diagnostic statistics R^2 and SEE, while the presence or absence of bias was determined based on the hypothesis test described in chapter 2. The criteria used to determine the adequacy of the global models for Colorado conditions are presented in Table 49.

Table 49. Criteria for determining global models adequacy for Colorado conditions.

Criterion of Interest	Test Statistic	Range of R^2 & Model SEE	Rating
Goodness of fit	R^2, percent (all models)	81 to 100	Very good (strong relationship)
		64 to 81	Good
		49 to 64	Fair
		< 49	Poor (weak or no relationship)
	Global HMA alligator cracking model SEE	< 5 percent	Good
		5 to 10 percent	Fair
		> 10 percent	Poor
	Global HMA transverse cracking model SEE	—	N/A
	Global HMA total rutting model SEE	< 0.1 in	Good
		0.1 to 0.2 in	Fair
		> 0.2 in	Poor
	Global HMA IRI model SEE	< 19 in/mi	Good
		19 to 38 in/mi	Fair
		> 38 in/mi	Poor
Bias	Hypothesis testing of slope of the linear measured vs. predicted distress/IRI model (b1 = slope) H0: b1 = 0	p-value	Reject if p-value is < 0.05 (i.e., 5 percent significant level)
	Paired t-test between measured and predicted distress/IRI	p-value	Reject if p-value is < 0.05 (i.e., 5 percent significant level)

Chapter 2 provided a detailed description of the procedure used to verify and calibrate the global models. Table 50 presents a list of the flexible pavement models evaluated as part of the MEPDG implementation in Colorado. See appendix A for detailed descriptions of these models.

Table 50. MEPDG flexible pavement global models evaluated for Colorado local conditions.

Pavement Type	MEPDG Global Models Evaluated				
	HMA Alligator Cracking	HMA Transverse Cracking	Total Rutting	New HMA & HMA/HMA IRI	HMA/HMA Reflected Alligator Cracking
New HMA	✓	✓	✓	✓	
HMA-overlaid existing HMA	✓	✓	✓	✓	✓

Alligator Cracking

Global MEDPG Alligator Cracking Model Verification

Verification of the MEPDG global alligator cracking models for Colorado conditions consisted of the running the MEPDG with the global coefficients for all selected projects and evaluating goodness of fit and bias. Figure 75 shows a plot of cumulative fatigue damage versus alligator cracking for all Colorado HMA sections. Measured and MEPDG-predicted alligator cracking data were evaluated to determine model goodness of fit and bias in predicted alligator cracking. The results are presented in Table 51 and show the following:

- Goodness of fit was generally poor, with an $R^2 < 40$ percent, which implies a weak relationship between the MEPDG global model alligator cracking predictions and field-measured/observed cracking.
- Both the paired t-test and predicted versus measured cracking slope p-value indicated the presence of bias in predicted alligator cracking (p-value < 0.05).
- The plot presented in Figure 75 shows that the model consistently under-predicted alligator cracking with increasing levels of HMA fatigue damage, another indication of bias.

It was concluded that the MEPDG global alligator cracking model did not adequately predict alligator cracking for Colorado conditions. Local calibration of the MEPDG global alligator cracking model for Colorado was thus recommended.

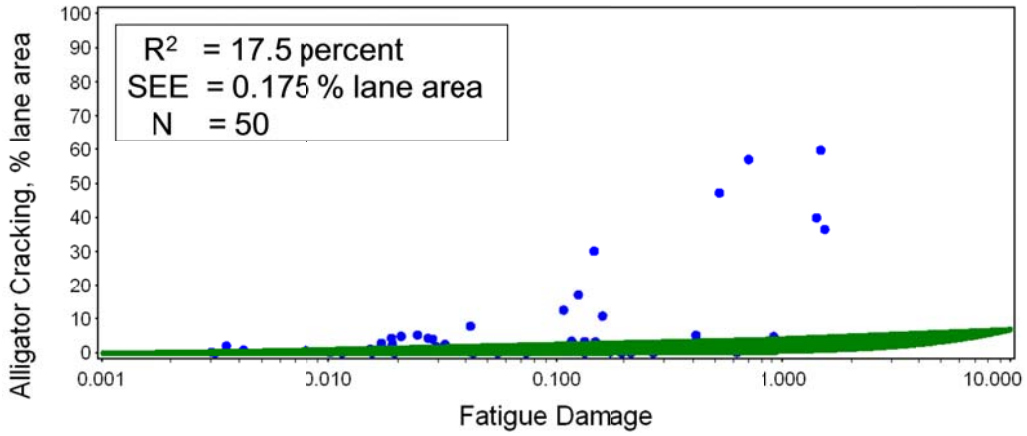

Figure 75. Verification of the HMA alligator cracking and fatigue damage models with MEPDG global coefficients, using Colorado new HMA pavement projects only.

Table 51. Results of statistical goodness of fit and bias evaluation of the MEPDG alligator cracking global model for Colorado conditions.

Statistical Analysis Type			
Goodness of Fit		**Bias**	
R^2, %	**SEE**	**p-value (paired t-test)**	**p-value (slope)**
17.5	0.175% lane area	0.0059	< 0.0001

Local Calibration of the MEDPG Alligator Cracking Model for Colorado

Description of Local Calibration Procedure

Local calibration of the MEPDG alligator cracking model was done simultaneously for both new HMA and HMA-overlaid existing HMA pavement and the MEPDG HMA fatigue, alligator cracking, and reflection cracking models. Calibration consisted of the following steps:

1. Determine the cause of poor goodness of fit and bias produced by the global models.
2. Adjust the MEPDG HMA fatigue and alligator cracking model calibration coefficients as needed based on information derived from step 1 to improve goodness of fit and reduce or eliminate bias. This step was done using data from only the new HMA pavement projects.
3. After determining the local calibration coefficients in step 2, perform a second round of calibration coefficient adjustments using all projects (new HMA and HMA-overlaid HMA projects) for only the reflection cracking model. In other words, the local calibration coefficients for the fatigue cracking and alligator cracking models were fixed while the local calibration coefficients of the reflection cracking model were adjusted as needed to improve overall goodness of fit and reduce bias.
4. Details of specific HMA fatigue cracking, alligator cracking, and reflection cracking models coefficients adjusted are presented below (see equations in Table 52).
    a. HMA fatigue model (allowable number of axle load applications, N equation):

i. Global calibration coefficients (kf1, kf2, kf3).
ii. Local calibration coefficients (βf1, βf2, βf3).

b. Alligator cracking model.
i. Local/Global calibration coefficients (C1, C2, C3).

c. Reflected alligator cracking model.
i. Global calibration coefficients (c, d).

5. Perform a final round of calibration coefficient adjustments, if needed, using all the local calibration estimates obtained in steps 2 through 4 as seed values. Adjustments to the calibration coefficients determined in steps 2 through 4 were constrained to ensure reasonableness of the final set of model coefficients.

A detailed description of the equations in Table 52 is presented in Appendix A.

Table 52. Description of HMA fatigue damage, HMA alligator cracking, and reflection "alligator" cracking models.

Model Type	Model Description*
HMA fatigue damage	$N_{f-HMA} = k_{f1}(C)(C_H)\beta_{f1}(\varepsilon_t)^{k_{f2}\beta_{f2}}(E_{HMA})^{k_{f3}\beta_{f3}}$
HMA alligator cracking	$FC_{Bottom} = \left(\frac{1}{60}\right)\left(\frac{C_4}{1+e^{(C_1C_1^*+C_2C_2^*Log(DI_{Bottom}))}}\right)$
HMA reflection "alligator" cracking	$RC = \frac{100}{1+e^{ac+bdt}}$

Summary of Alligator Cracking Model Local Calibration Results

The researchers investigated the possible causes of poor goodness of fit and bias, and no obvious reasons were found (such as erroneous inputs). Thus, local calibration proceeded as previously described. Calibration of the MEPDG global models using CDOT input data was done using nonlinear model optimization tools available in the SAS statistical software. Adjusted HMA fatigue damage and alligator cracking global model coefficients are presented in Table 53 and shows that four of the nine global coefficients were adjusted. The goodness of fit and bias statistics are presented in Table 54 and show an adequate goodness of fit with minimal bias for the locally calibrated alligator cracking and fatigue damage models developed using new HMA projects only.

Table 53. Summary of MEPDG global and CDOT local calibration coefficients for HMA alligator cracking and HMA fatigue damage models.

Model Type	Model Coefficients (See Table 52)	Global Model Values	CDOT Local Model Values
HMA fatigue damage	K1	0.007566	0.007566
	K2	3.9492	3.9492
	K3	1.281	1.281
	BF1	1	130.3674
	BF2	1	1
	BF3	1	1.217799
HMA alligator cracking	C1Bottom	1	0.07
	C2Bottom	1	2.35
	C3Bottom	6000	6000

Table 54. Results of statistical evaluation of MEPDG alligator cracking and fatigue damage local models for Colorado conditions.

Statistical Analysis Type					
Goodness of Fit			Bias		
R^2, %	SEE	N	p-value (paired t-test)	p-value (Slope)	N
62.7	9.4 % lane area	56	0.7566	0.3529	56

As described earlier, the next step was to calibrate to local conditions the reflection "alligator" cracking model. The results are presented in Table 55. The goodness of fit and bias statistics are presented in Table 56 and show that inclusion of the HMA reflection "alligator" cracking model did not introduce significant bias.

Table 55. Local calibration coefficients for HMA overlay reflection cracking model developed using new HMA and HMA overlaid HMA pavement projects.

Model Coefficients (See Table 52)	Global Model Values	Colorado Local Model Values
c	1	2.5489
d	1	1.2341

Table 56. Results of statistical bias evaluation of MEPDG reflection "alligator" cracking local model for Colorado conditions.

Statistical Analysis Type					
Goodness of Fit			Bias		
R^2, %	SEE	N	p-value (paired t-test)	p-value (Slope)	N
54.7	8.6 % lane area	87	0.7800	0.8799	87

The results in Tables 54 and 56 shows an adequate goodness of fit for all three HMA alligator cracking submodels with no significant bias.

Figure 76 presents a plot of HMA fatigue damage versus field-measured and CDOT local alligator cracking model predicted cracking. A plot showing the progression of reflection cracking with HMA overlay age for different HMA overlay thicknesses is presented in Figure 77. Figures 78 through 81 illustrate the CDOT local model prediction of alligator cracking for new HMA pavement and HMA-overlaid HMA pavement.

Local calibration of the HMA fatigue, alligator cracking, and reflection "alligator" cracking models produced CDOT-specific models that predict alligator cracking distress with adequate accuracy and minimal bias. Goodness of fit characterized using R^2 increased from 17.5 for the global models to 52.5 percent, while SEE increased from 5 to 17.1 percent lane area.

The new models will increase the accuracy of alligator cracking predictions while minimizing bias and will produce for CDOT more accurate and optimum (lower cost) new and overlaid HMA pavement designs at the desired design reliability.

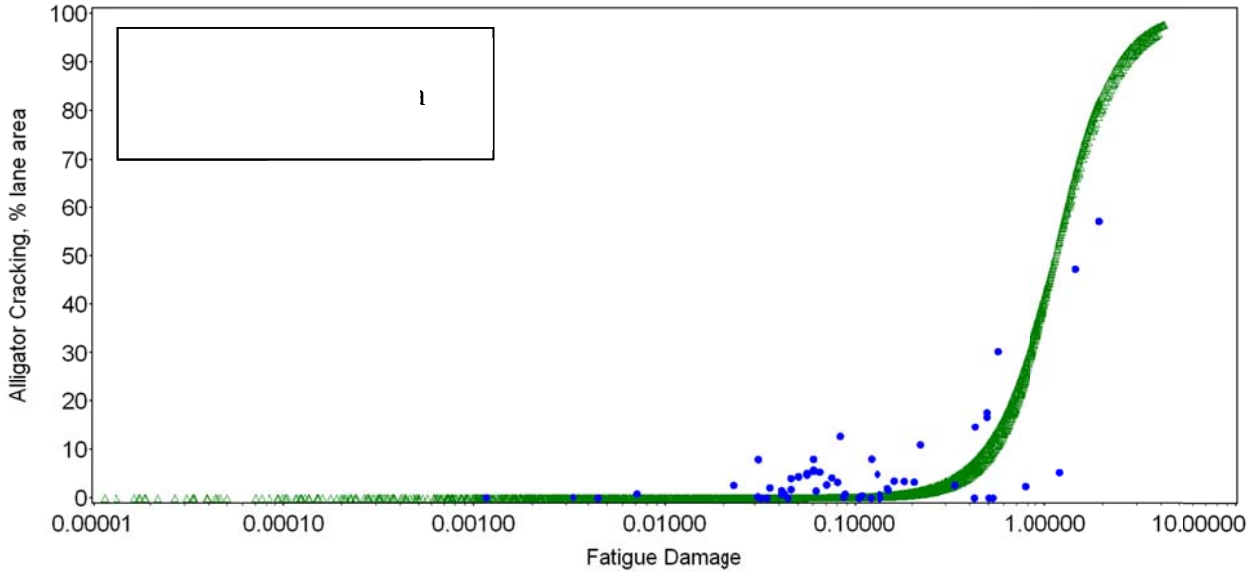

Figure 76. Plot showing predicted HMA alligator cracking versus computed fatigue damage developed using MEPDG models with CDOT local coefficients (for new HMA pavements only).

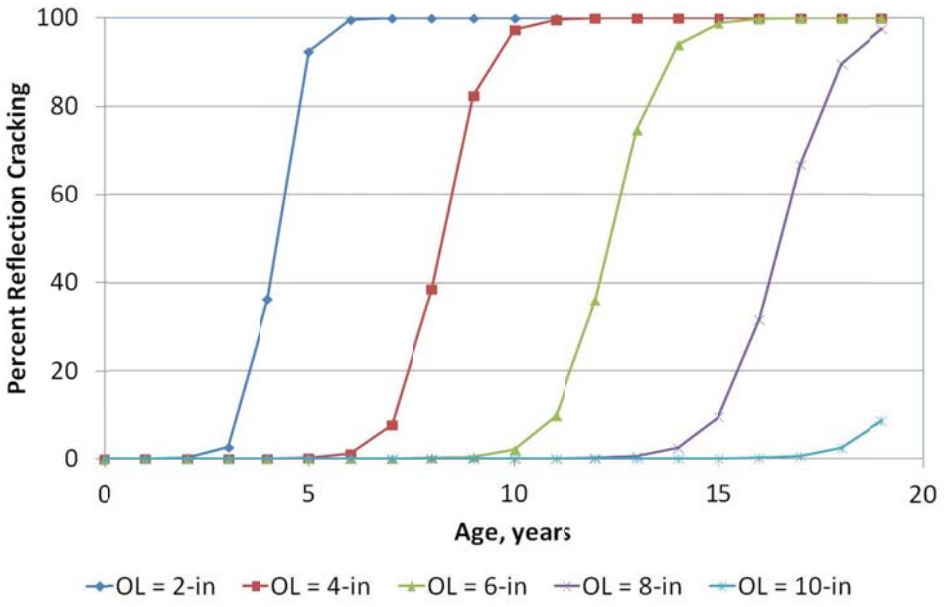

Figure 77. Plot showing progression of reflection cracking with HMA overlay age for different HMA overlay thicknesses.

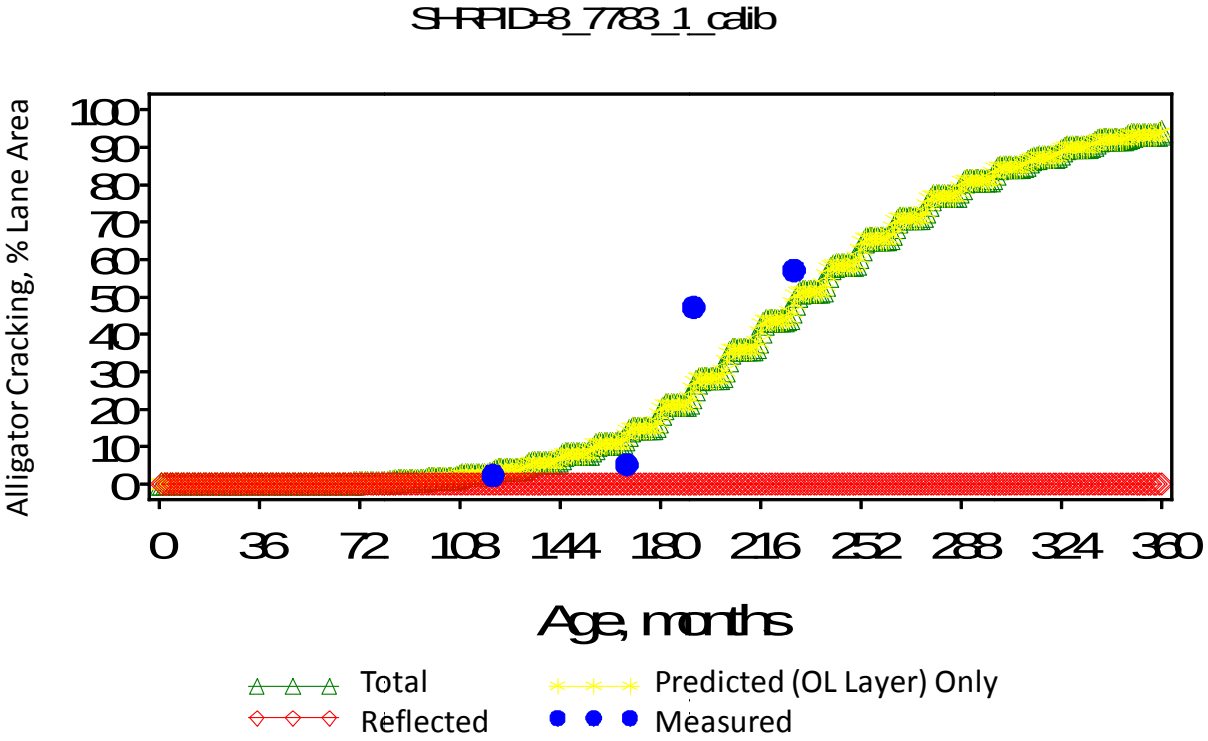

Figure 78. Plot of predicted alligator cracking versus age for LTPP project 7783 (new HMA pavement).

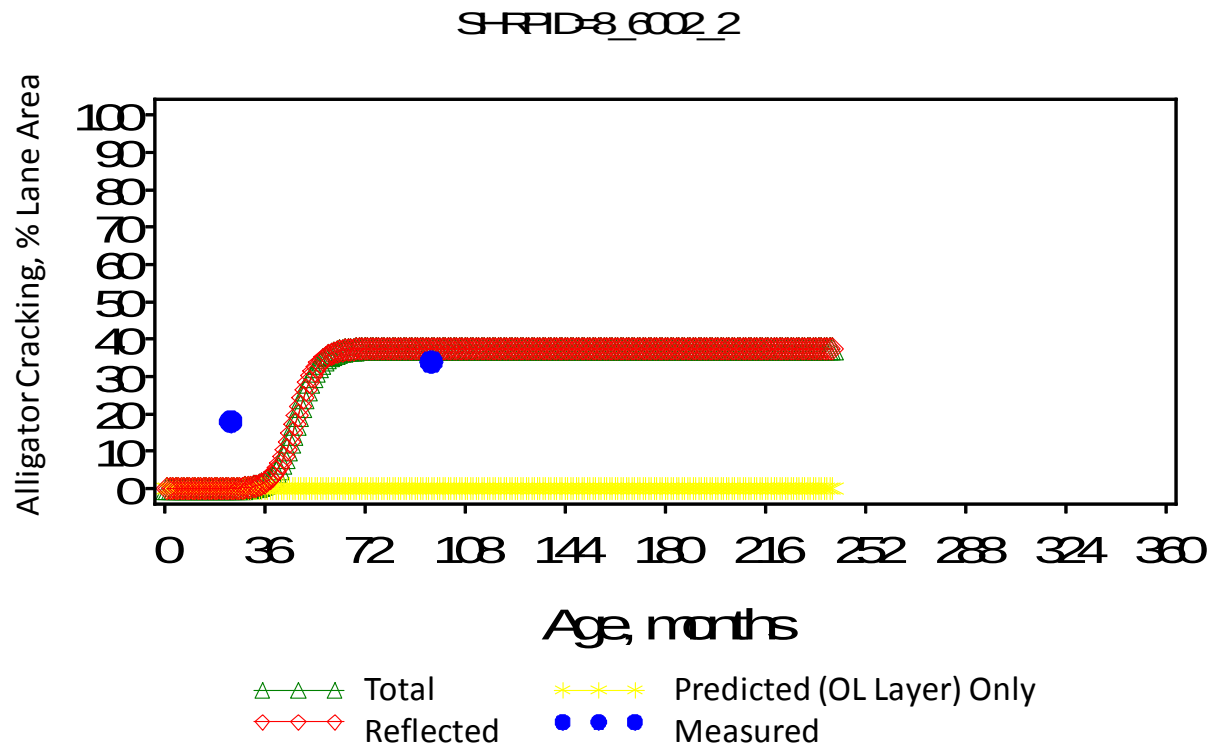

Figure 79. Plot of predicted alligator cracking versus age for LTPP project 6002 (HMA overlaid HMA pavement).

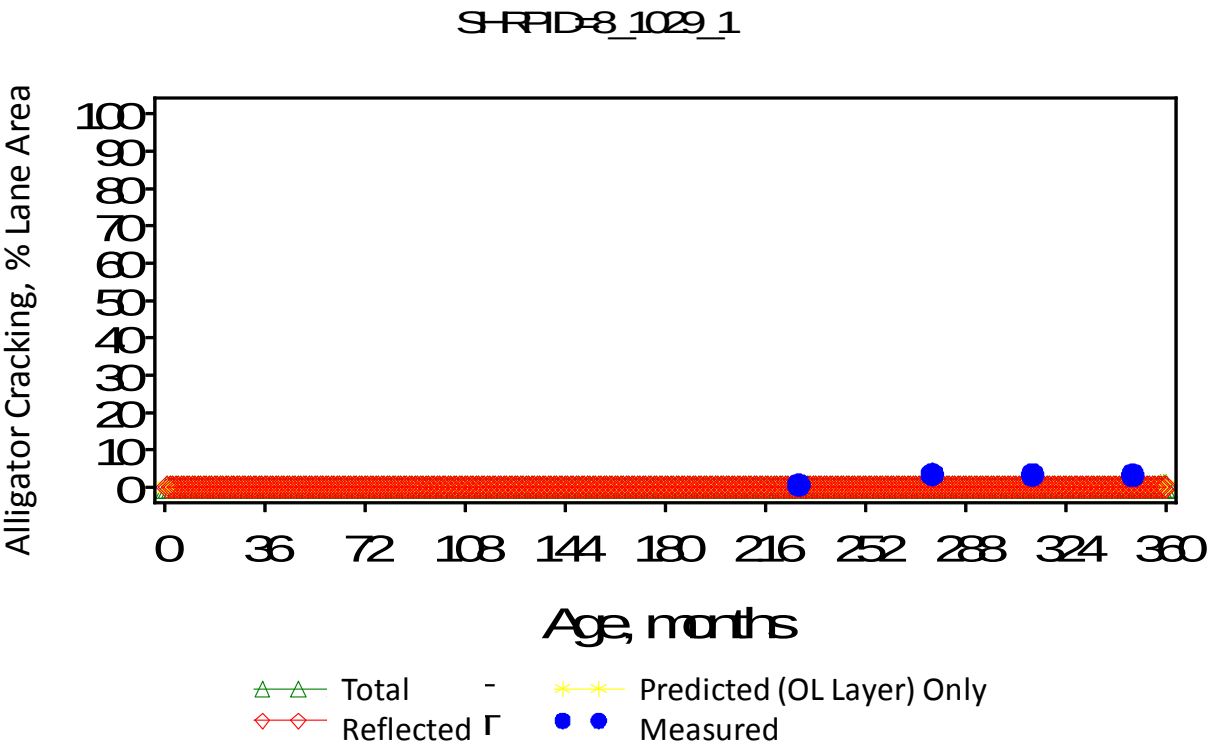

Figure 80. Plot of predicted alligator cracking versus age for LTPP project 1029 (new HMA pavement).

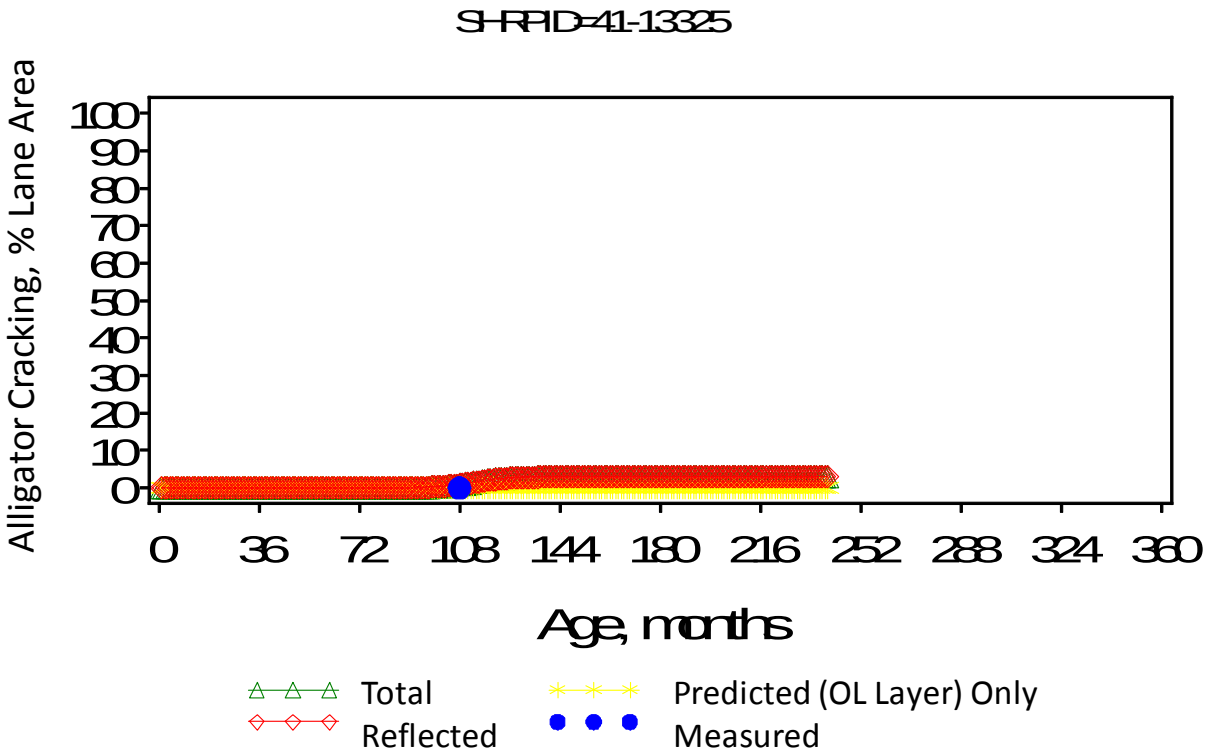

Figure 81. Plot of predicted alligator cracking versus age for CDOT pavement management system project 13325.

Total Rutting

Global MEDPG Total Rutting Model Verification

The MEPDG predicts HMA pavement total rutting using separate submodels for the surface HMA, unbound aggregate base, and subgrade soil. The same three submodels are utilized for HMA-overlaid HMA pavement, with modifications as needed to reflect the existing pavement material properties and permanent strain (existing rutting) present in all three layers.

Verification of the MEPDG global total rutting model consisted of the following steps:

1. Run the three MEPDG rutting submodels using global coefficients for all new HMA pavement and HMA-overlaid HMA pavement projects to obtain estimates of total rutting.
2. Perform statistical analysis to determine goodness of fit with field-measured total rutting and bias in estimated total rutting.
3. Evaluate goodness of fit and bias statistics and determine any need for local calibration to Colorado conditions.

Figure 82 shows a plot of the MEPDG global model predicted rutting versus field-measured rutting for all Colorado new HMA pavement and HMA-overlaid HMA pavement projects. Goodness of fit and bias statistics computed from the data are presented in Table 57.

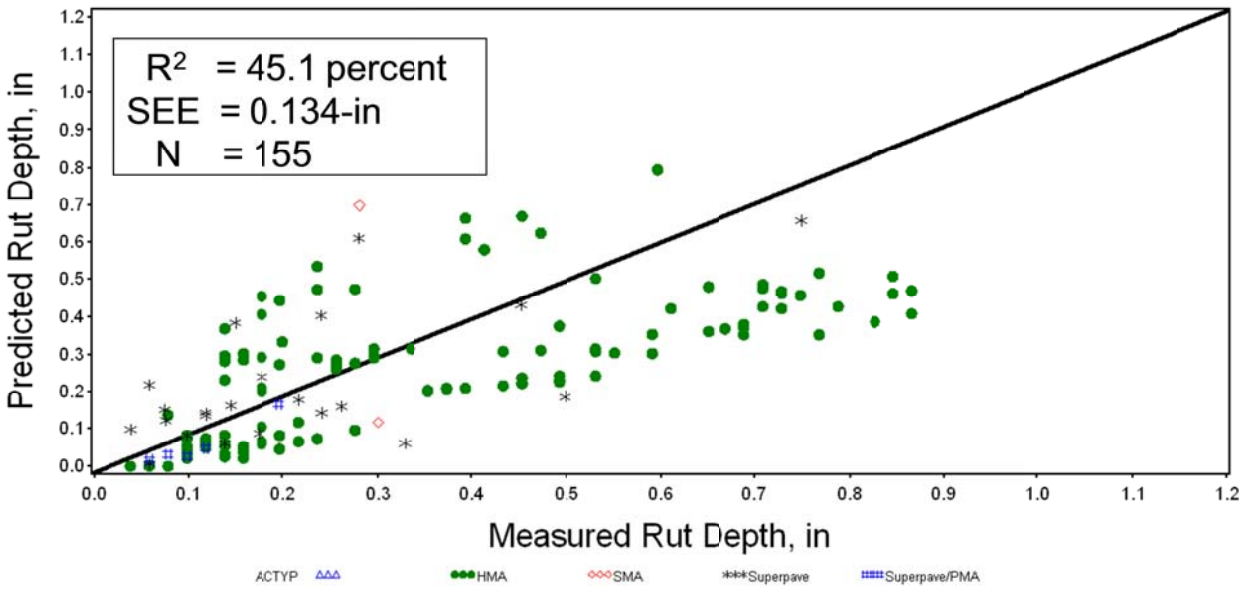

Figure 82. Plot showing MEPDG global model predicted rutting versus measured rutting (HMA, unbound aggregate base, and subgrade).

Table 57. Results of statistical evaluation of MEPDG total rutting global submodels for Colorado conditions.

Statistical Analysis Type					
Goodness of Fit			Bias		
R^2, %	SEE	N	p-value (paired t-test)	p-value (Slope)	N
45.1	0.134 in	155	< 0.0001	< 0.0001	155

The information presented in Table 57 shows a poor to fair goodness of fit when compared to the global model statistics and significant bias in predicted total rutting estimates. The MEPDG rutting global model coefficients were, therefore, deemed inadequate for Colorado conditions, and local calibration of this very important model was required.

Local Calibration of the MEDPG Total Rutting Model for Colorado

Description of Local Calibration Procedure

Local calibration of the three rutting submodels consisted of the following steps:

1. Determine the cause of poor to fair goodness of fit and bias produced by the global models.
2. Adjust submodel calibration coefficients as needed based on information derived from step 1 to improve goodness of fit and reduce or eliminate bias. Specifically, the following model coefficients can be adjusted:
    a. HMA rutting:
        i. Global calibration coefficients (k1r, k2r, k3r).

ii. Local calibration coefficients (β1r, β2r, β3r).

b. Granular base rutting model.
   i. Local/global calibration coefficients (ks1).

c. Subgrade rutting model.
   i. Local/global calibration coefficients (ks1).

In adjusting the three rutting submodels, the researchers considered information obtained through laboratory testing (repeated load permanent deformation and HWT tests) on the nature and rate of primary and secondary rutting development and from field trenching of new HMA pavements to determine the distribution of rutting within the pavement structure. This was done by (1) applying laboratory-derived HMA rutting submodel coefficients k1r, k2r, and k3r as seed values and constraining the new local models to be as close as possible to the seed values without compromising goodness of fit and bias and (2) ensuring that the contribution of each submodel to total rutting was close to the field trenching estimates without compromising goodness of fit and bias. A summary of laboratory-measured HMA rutting model coefficients k1r, k2r, and k3r and total rutting distribution is presented as follows:

- Laboratory-measured HMA rutting model coefficients:
  - $k_{1r} = -2.36$.
  - $k_{2r} = 1.72$.
  - $k_{3r} = 0.16$.
- Total rutting distribution:
  - HMA surface = 63 percent.
  - Aggregate base/subbase = 11 percent.
  - Subgrade (top 12 in) = 26 percent.

Local calibration was done simultaneously for new HMA pavements and HMA-overlaid HMA pavements. Summary descriptions of the three rutting submodels are presented in Table 58. A detailed description of MEPDG rutting submodels is presented in Appendix A.

Table 58. Description of total rutting prediction submodels.

Model Type	Model Description*
HMA	$\Delta_{p(HMA)} = \varepsilon_{p(HMA)} h_{HMA} = \beta_{1r} k_z \varepsilon_{r(HMA)} 10^{k_{1r}} n^{k_{2r}\beta_{2r}} T^{k_{3r}\beta_{3r}}$
Unbound aggregate base	$\Delta_{p(soil)} = \beta_{s1} k_{s1} \varepsilon_v h_{soil} \left(\frac{\varepsilon_o}{\varepsilon_r} \right) e^{-\left(\frac{\rho}{n}\right)^{\beta}}$
Subgrade soils	$\Delta_{p(soil)} = \beta_{s1} k_{s1} \varepsilon_v h_{soil} \left(\frac{\varepsilon_o}{\varepsilon_r} \right) e^{-\left(\frac{\rho}{n}\right)^{\beta}}$

Summary of Total Rutting Model Local Calibration Results

The researchers investigated the possible causes of poor goodness of fit and bias, and they found no obvious reasons (such as erroneous inputs). Thus, local calibration proceeded as previously described. Calibration of the MEPDG global models using CDOT input data was done using

nonlinear model optimization tools available in the SAS statistical software. Adjusted HMA rutting, unbound aggregate base rutting, and subgrade rutting global model coefficients obtained from step 2 are presented in Table 59 and show that three of the eight global coefficients were adjusted. The goodness of fit and bias statistics are presented in Table 60. A plot of field-measured versus CDOT-calibrated total rutting is presented in Figure 83. The goodness of fit and bias test results indicate an adequate goodness of fit with minimal bias not significant at the 5 percent significance level for the locally calibrated total rutting submodels.

The results presented Table 60 also show no appreciable change in the goodness of fit between the global models and the Colorado calibrated models (i.e., R^2 changed from 45.1 to 41.7 and SEE changed from 0.134 to 0.147 inches) with local calibration. Both the global and locally calibrated models goodness of fit was characterized as fair. The slight increase in SEE was attributed to high variability exhibited in field measurements of pavement rutting that contributes to lowering R^2 and increasing SEE. The results presented Table 60 also show that the significant bias produced by the global models in Colorado had been eliminated through local calibration. This improvement increases overall rutting prediction accuracy and reliability of pavement designs. Thus, new HMA pavement and HMA-overlaid HMA pavement designs in Colorado will be much more accurate and optimum (lower cost) at the selected level of design reliability with the application of the locally calibrated total rutting model.

Figures 84 through 88 present plots of measured and predicted rutting for several projects in Colorado. The plots show reasonable predictions of rutting using the locally calibrated models.

Table 59. Local calibration coefficients for HMA, unbound base, and subgrade soil rutting submodels.

Model	**Model Coefficients**	**Global Model Values**	**CDOT Local Model Values**
HMA rutting submodel	Kr1	-3.35412	-3.35412
	Kr2	1.5606	1.5606
	Kr3	0.4791	0.4791
	βr1	1	1.34
	βr2	1	1
	βr3	1	1
Granular base rutting submodel	ks1	1	0.4
Subbase rutting submodel	ks1	1	0.84

Table 60. Results of statistical evaluation of MEPDG alligator cracking and fatigue damage local models for Colorado conditions.

Statistical Analysis Type					
Goodness of Fit			Bias		
R^2, %	SEE	N	p-value (paired t-test)	p-value (Slope)	N
41.7	0.147 in	137	0.4306	0.0898	137

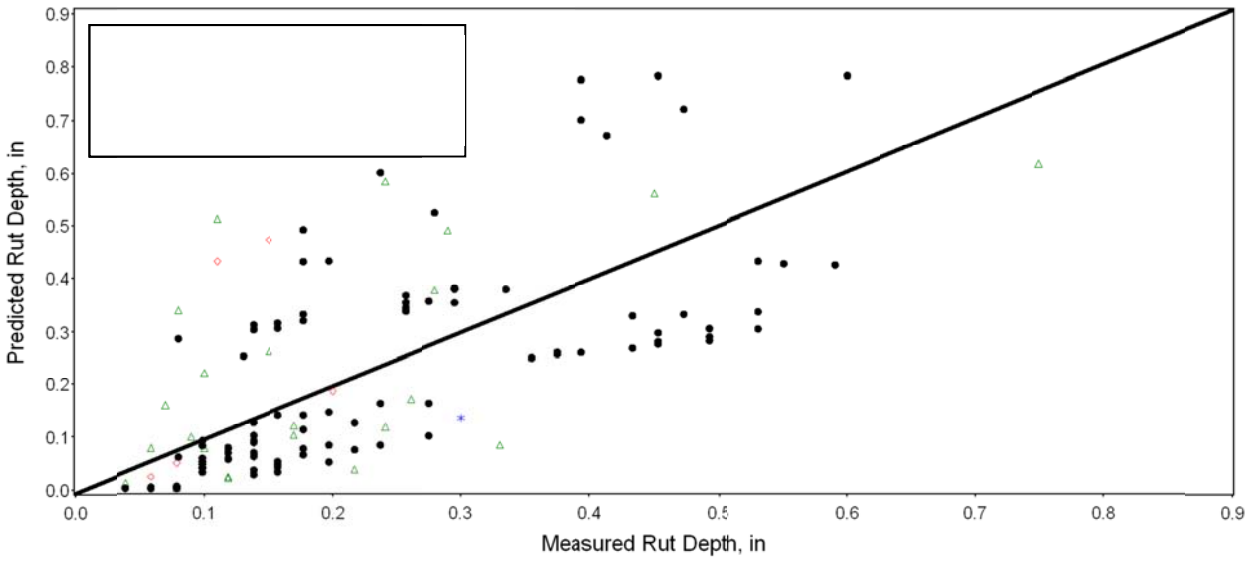

Figure 83. Plot showing predicted using MEPDG submodels with CDOT local coefficients (for all pavements) versus field-measured total rutting.

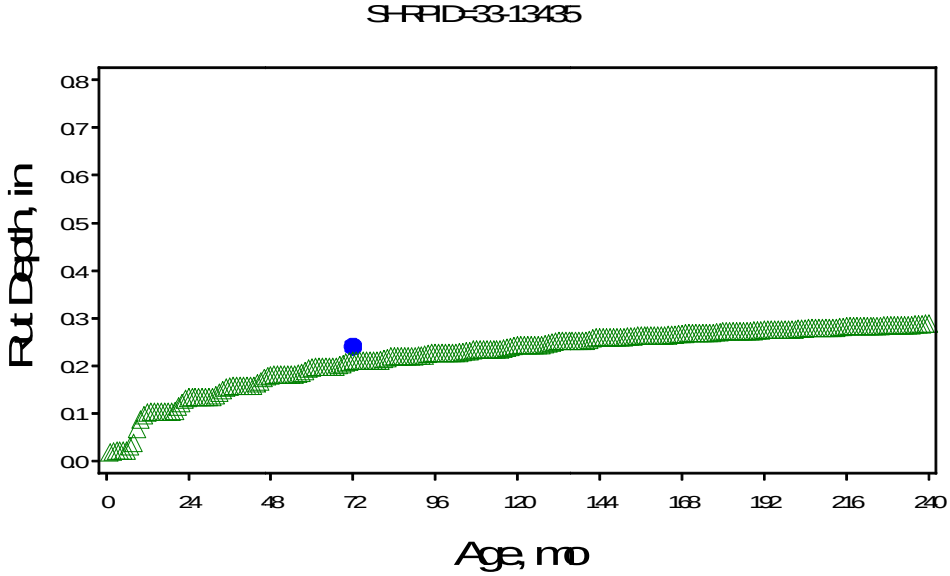

Figure 84. Plot showing high variation of measured rutting over time for CDOT pavement management system project 13435.

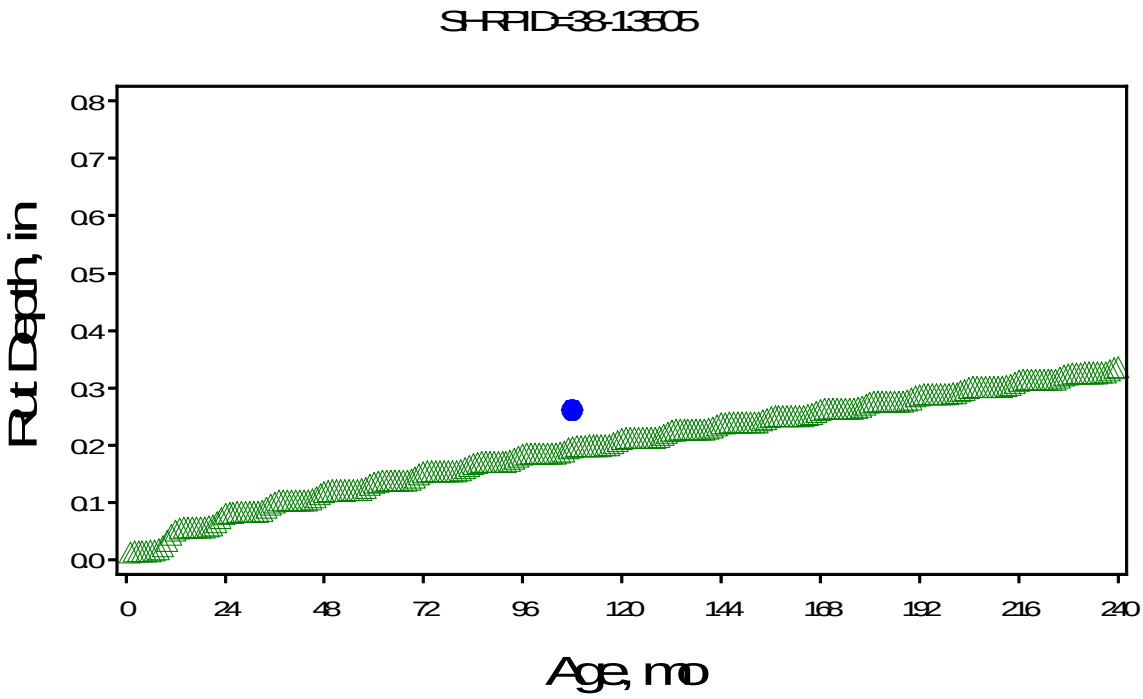

Figure 85. Plot showing high variation of measured rutting over time for CDOT pavement management system project 13505.

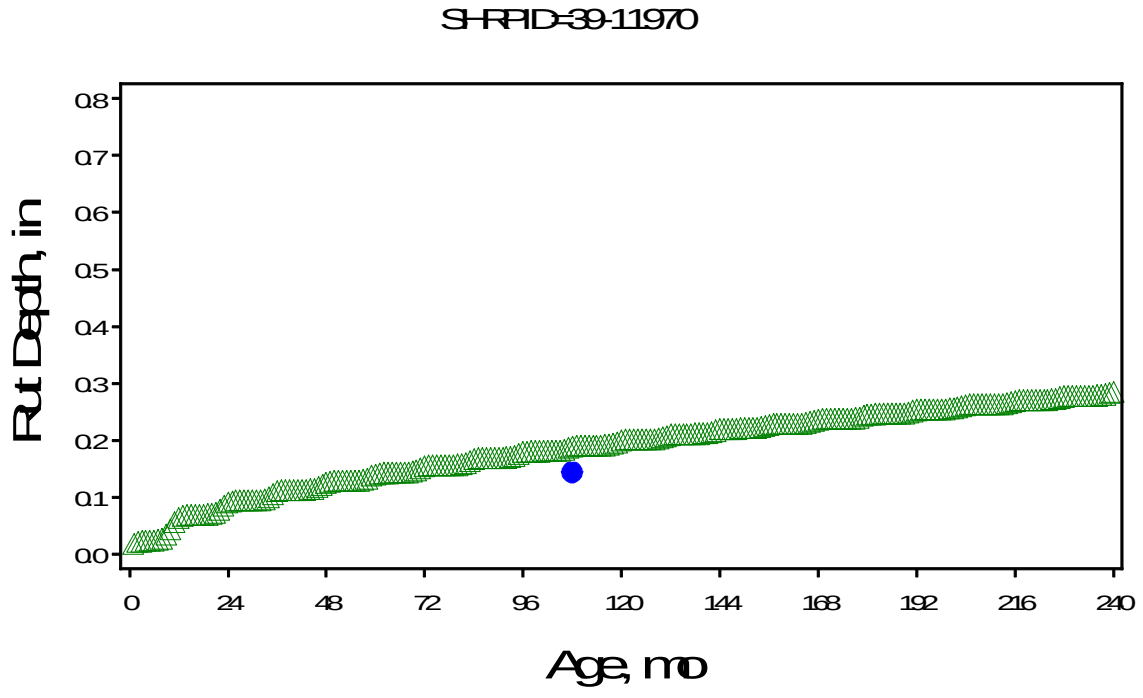

Figure 86. Plot showing high variation of measured rutting over time for CDOT pavement management system project 11970.

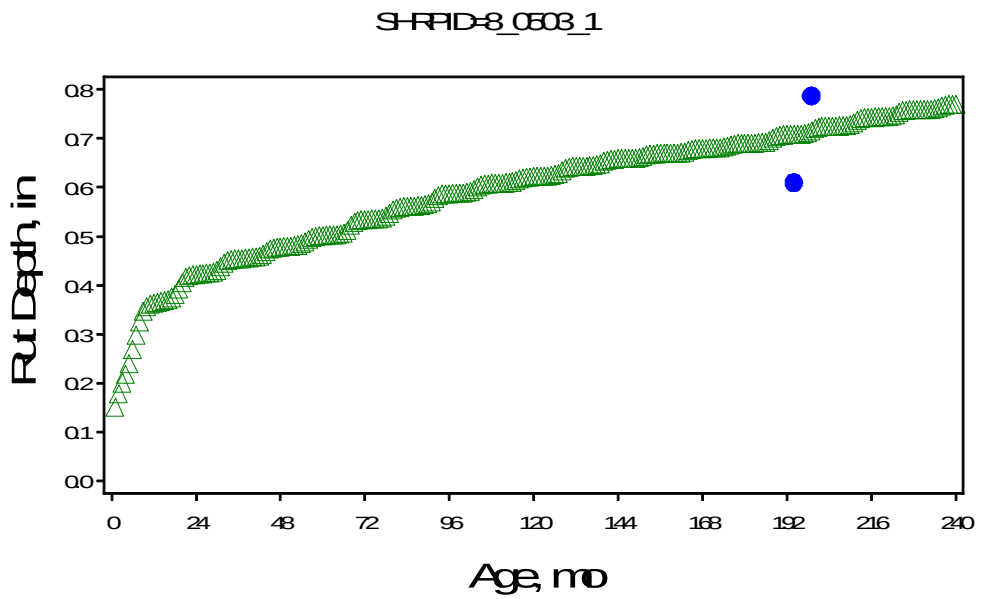

Figure 87. Plot showing high variation of measured rutting over time for LTPP project 0503 (original construction).

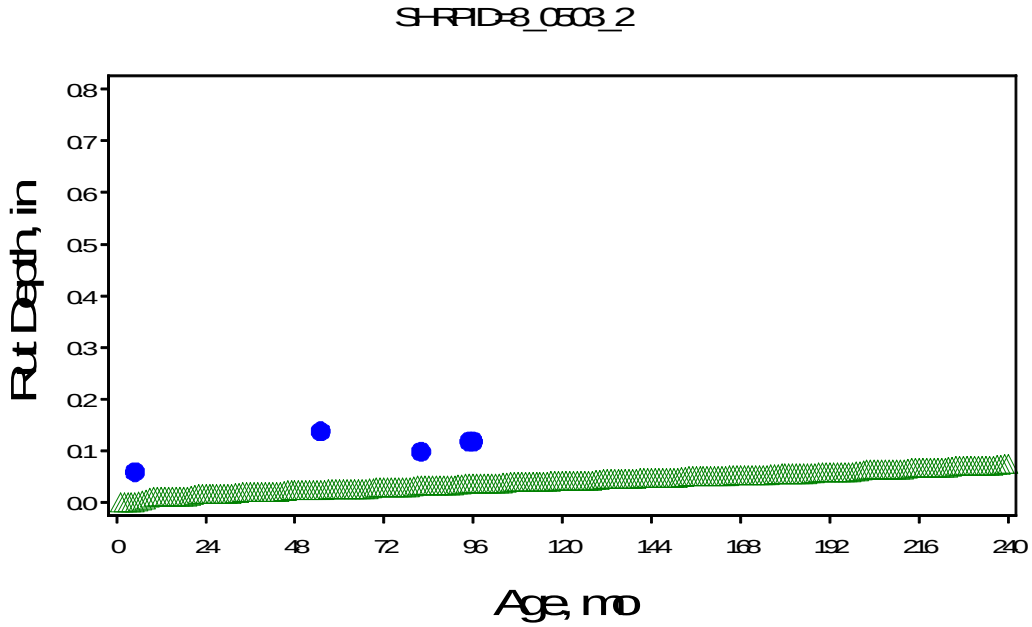

Figure 88. Plot showing high variation of measured rutting over time for LTPP project 0503 (with HMA overlay).

Transverse "Thermal" Cracking

Global MEDPG Transverse "Thermal" Cracking Model Verification

The HMA pavement transverse cracking models in the MEPDG are based on low temperature contraction of asphalt binders that lead to tensile stresses and the formation of transverse cracks.

In general, transverse cracking is expected to be more severe in very cool climate zones than in warmer areas. Colorado's climate is segmented into four zones (see Table 61) ranging from the very cool high elevations (> 8500 ft) to the moderate to hot lower elevations (< 6000 ft).

Table 61. Colorado environmental zones.

CDOT Environmental Zone	Highest 7-Day Average Maximum Air Temperature, °F
Hot (Southeast and West)	> 97
Moderate (Denver, Plains, and West)	90 to 97
Cool (Mountains)	81 to 88
Very cool (High Mountains)	< 81

The MEPDG HMA transverse cracking models is presented below:

$$TC = K\ N\left[\frac{1}{\sigma_d} Log\left(\frac{C_d}{H_{HMA}}\right)\right] \quad (11)$$

Key inputs required by the MEPDG HMA transverse cracking model include HMA creep compliance and indirect tensile strength. The key inputs can be measured at Level 1 or estimated based on HMA mixture volumetrics and aggregate properties (Level 3). Because of the sensitivity of the MEPDG HMA transverse cracking model to these inputs, it is recommended that only Level 1 HMA creep compliance and indirect tensile strength inputs be used for local calibration. Thus, the following MEPDG HMA transverse cracking model verification was done using only projects with Level 1 data:

1. Identify HMA projects with Level 1 HMA creep compliance and indirect tensile strength data. Twelve projects were used for verification, and they exhibited a wide range of transverse cracking after approximately 10 years in service.
2. Run the MEPDG with the global coefficients for all 12 projects.
3. Perform statistical analysis to characterize goodness of fit and bias.
4. Evaluate goodness of fit and bias, summarize the outcome, and develop recommendations for local calibration.

The outcome of the MEPDG runs for all of the HMA sections using the global calibration coefficients for Level 1 (e.g., K = 1.5) is presented in Table 62. Figure 89 shows a plot of the MEPDG global transverse cracking model-predicted transverse cracking versus field-measured transverse cracking. This information shows that using the MEPDG global transverse cracking model in Colorado produces biased estimates (under-prediction) and a poor goodness of fit. Thus, there was the need for local calibration of the MEPDG global transverse cracking model.

Table 62. Results of statistical evaluation of MEPDG transverse cracking global model for Colorado conditions.

Statistical Analysis Type					
Goodness of Fit			Bias		
R^2, %	SEE	N	p-value (paired t-test)	p-value (Slope)	N
39.1	0.00232 ft/mi		0.0123	< 0.0001	

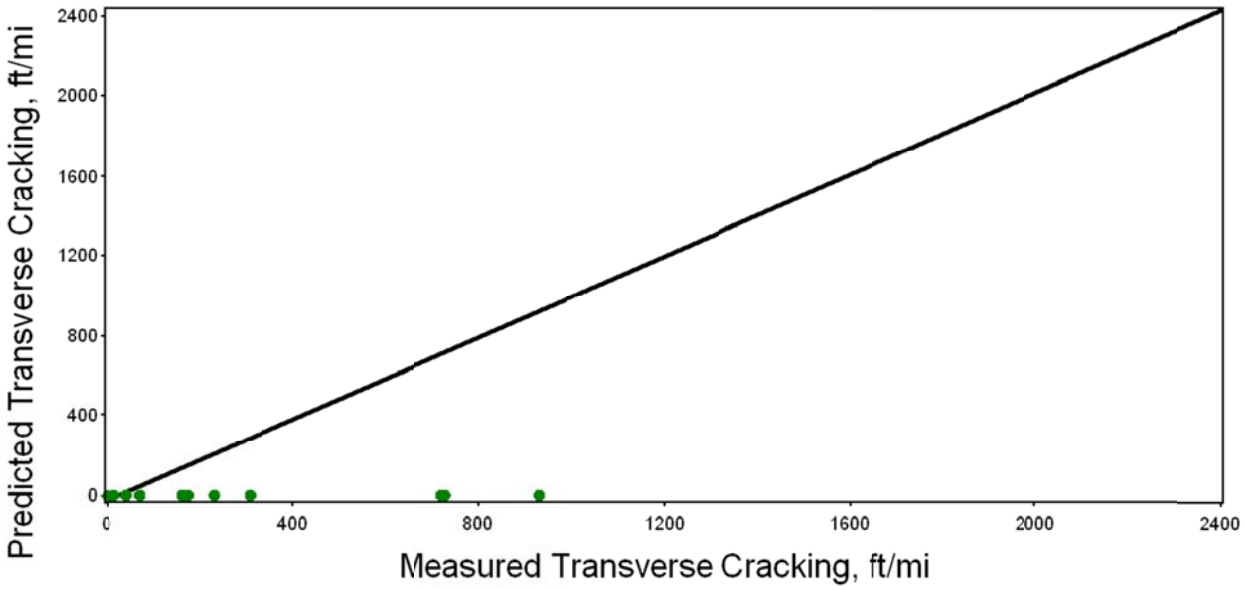

Figure 89. Predicted versus measured transverse cracking using global coefficients and Colorado pavement sections with Level 1 inputs.

Local Calibration of the MEPDG HMA Transverse Cracking for Colorado

Description of Local Calibration Procedure

Local calibration of the MEPDG HMA transverse cracking for Colorado comprised of the following steps:

1. Determine the cause of poor to fair goodness of fit and bias produced by the global models.
2. Adjust the transverse cracking calibration coefficients as needed based on information derived from step 1 to improve goodness of fit and reduce or eliminate bias. Specifically, the coefficient K in equation 11 was adjusted.
3. Run the MEPDG for all 12 projects for values of K ranging from 1.0 to 10 in increments of 1.
4. Perform statistical analysis to characterize goodness of fit and bias for each value of K. Goodness of fit and bias statistics were computed using only CDOT PMS sections with (1) lab tested HMA creep compliance and indirect tensile strength data available and (2) field measured HMA transverse cracking distress.

5. Evaluate goodness of fit and bias and select the value of K value that produces the best goodness of fit and least bias.

Summary of HMA Transverse Cracking Model Local Calibration Results

Coefficient K = 7.5 produced the best goodness of fit and minimal bias (i.e., predicted transverse cracking generally matched field-measured values). The global and locally calibrated transverse cracking K coefficients are presented in Table 63. A plot of predicted versus measured transverse cracking for all 12 CDOT PMS sections used in local calibration is presented in Figure 90. The CDOT locally calibrated model goodness of fit and bias statistics are presented in Table 64. The goodness of fit and bias test results indicates an adequate goodness of fit with insignificant bias at the 5 percent significance level for the locally calibrated transverse cracking model. The results presented Table 64 also indicates considerable improvement in the goodness of fit between the global model when applied in Colorado and the locally calibrated model (i.e., 39.1 to 43.1 percent). Even though SEE increased for 0.002 ft/mi to 194 ft/mi with local calibration, SEE for both the global and locally calibrated models were characterized as adequate.

Table 63. Local calibration coefficients for transverse cracking.

Model	Model Coefficients	Global Model Value	CDOT Local Model Value
HMA transverse cracking	K	1.5	7.5

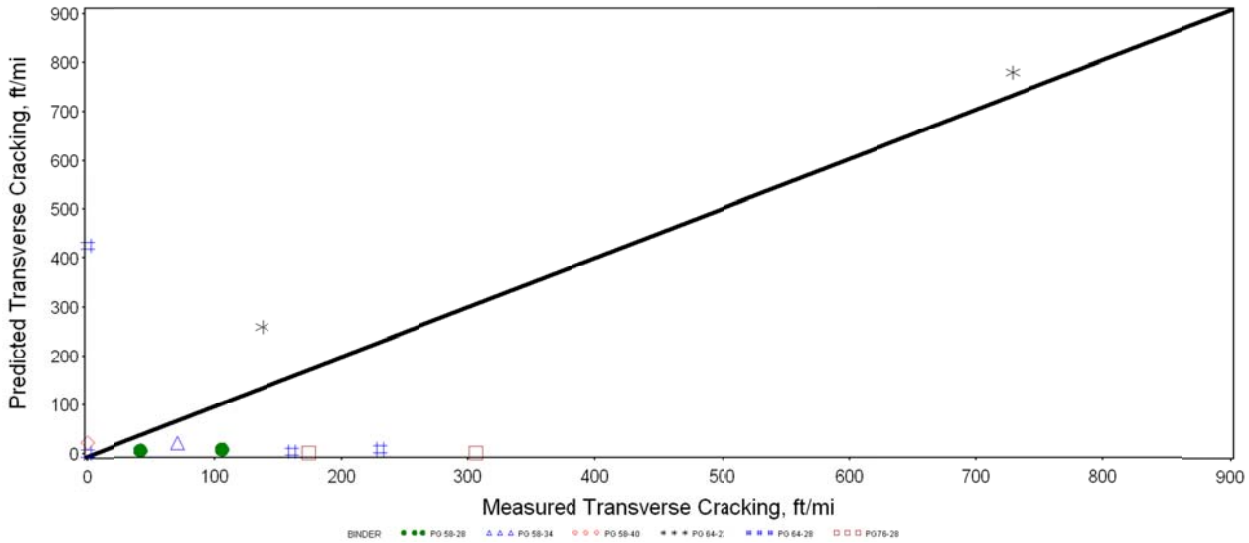

Figure 90. Plot showing predicted versus measured transverse cracking developed using the MEPDG model with CDOT local coefficients and HMA transverse cracking distress from project field testing.

Table 64. Results of statistical evaluation of MEPDG transverse cracking local model for Colorado conditions.

Statistical Analysis Type					
Goodness of Fit			Bias		
R^2, %	SEE	N	p-value (paired t-test)	p-value (Slope)	N
43.1	194 ft/mi	12	0.5290	0.3390	12

The CDOT locally calibrated HMA transverse cracking model was further validated using measured HMA transverse cracking data available in the CDOT PMS database. A plot of predicted versus measured transverse cracking for all 12 sections used in local calibration is presented in Figure 91, and goodness of fit and bias statistics are presented in Table 65. The results presented were deemed reasonable.

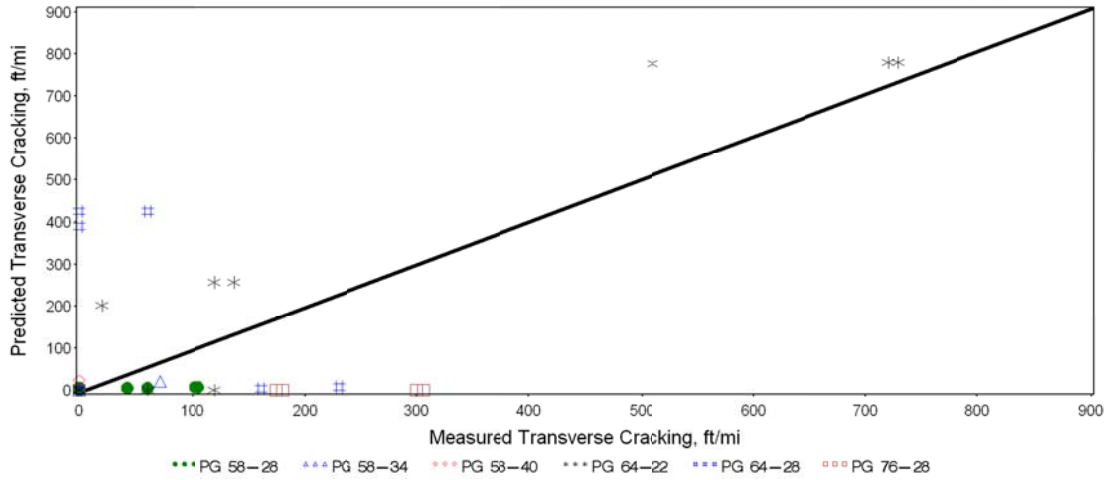

Figure 91. Plot showing predicted versus measured transverse cracking developed using MEPDG model with CDOT local coefficients and measured HMA transverse cracking distress.

Table 65. Results of statistical evaluation of MEPDG transverse cracking local model for Colorado conditions using measured HMA transverse cracking data.

Statistical Analysis Type					
Goodness of Fit			Bias		
R^2, %	SEE	N	p-value (paired t-test)	p-value (Slope)	N
44.4	178 ft/mi	37	0.6982	0.2660	37

The results presented in Table 64 and 65 show that the significant bias produced by the global models had been eliminated through local calibration. This improvement increases overall transverse cracking prediction accuracy and reliability of HMA pavement designs in Colorado. Figures 92 through 97 present plots of measured and predicted transverse cracking for several projects in Colorado. The plots show reasonable predictions of transverse cracking using the locally calibrated models.

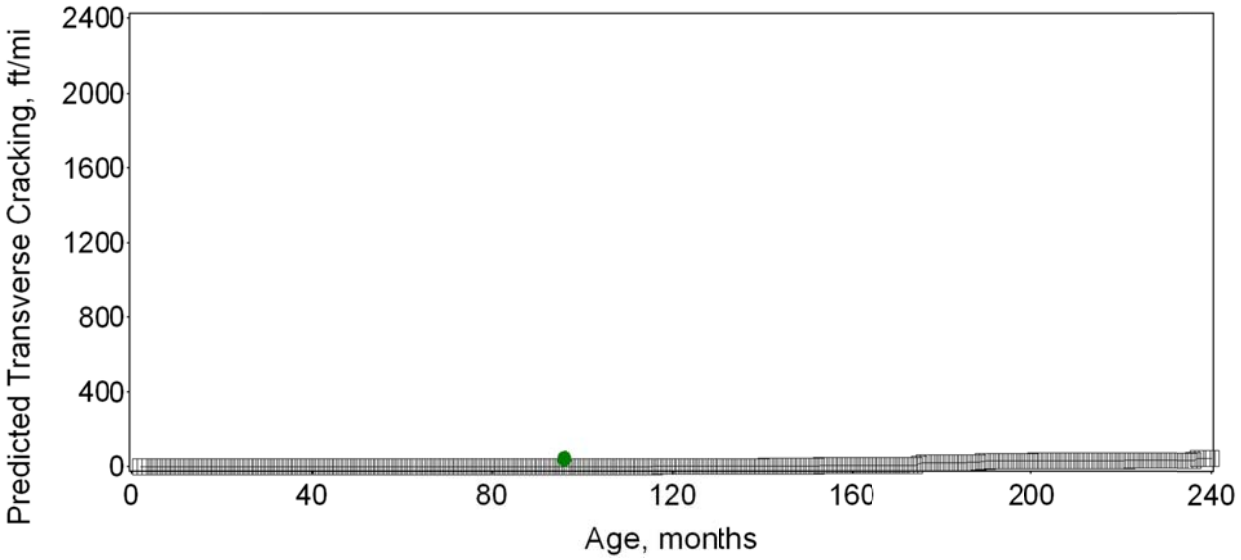

Figure 92. Plot showing predicted and measured transverse cracking versus pavement age for CDOT pavement management system project 13131.

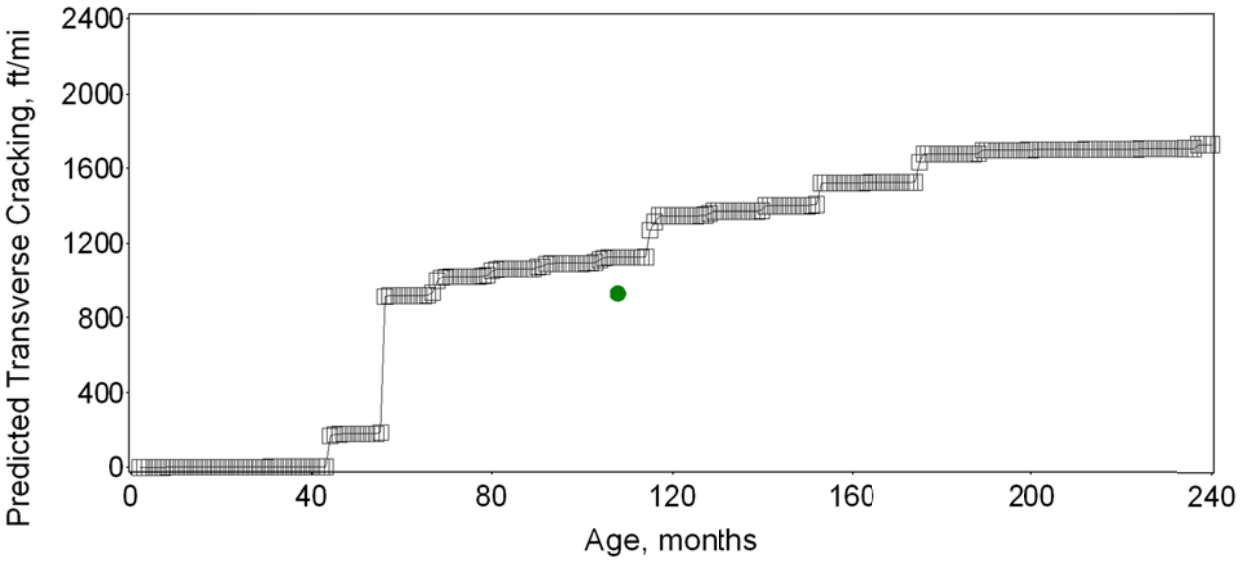

Figure 93. Plot showing predicted and measured transverse cracking versus pavement age for CDOT pavement management system project 13440.

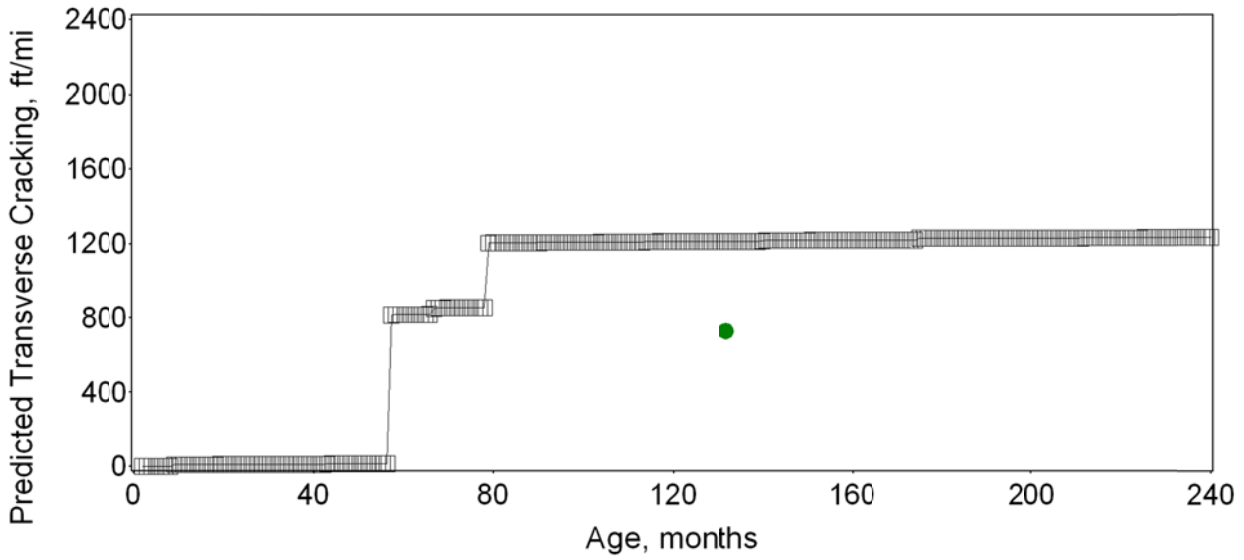

Figure 94. Plot showing predicted and measured transverse cracking versus pavement age for CDOT pavement management system project 91094.

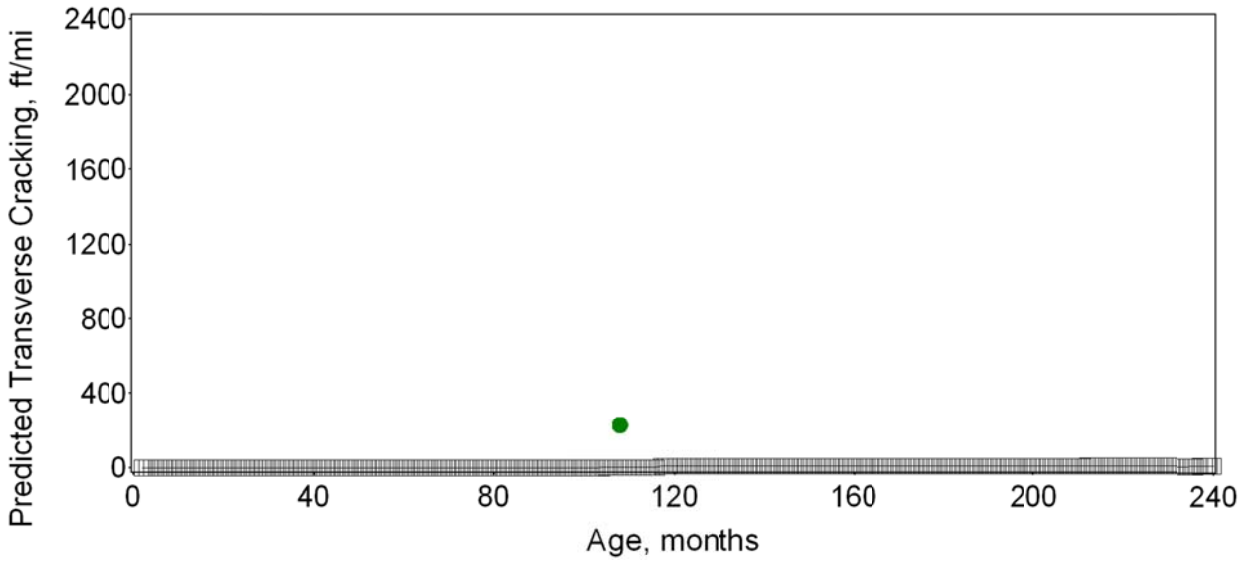

Figure 95. Plot showing predicted and measured transverse cracking versus pavement age for CDOT pavement management system project 11865.

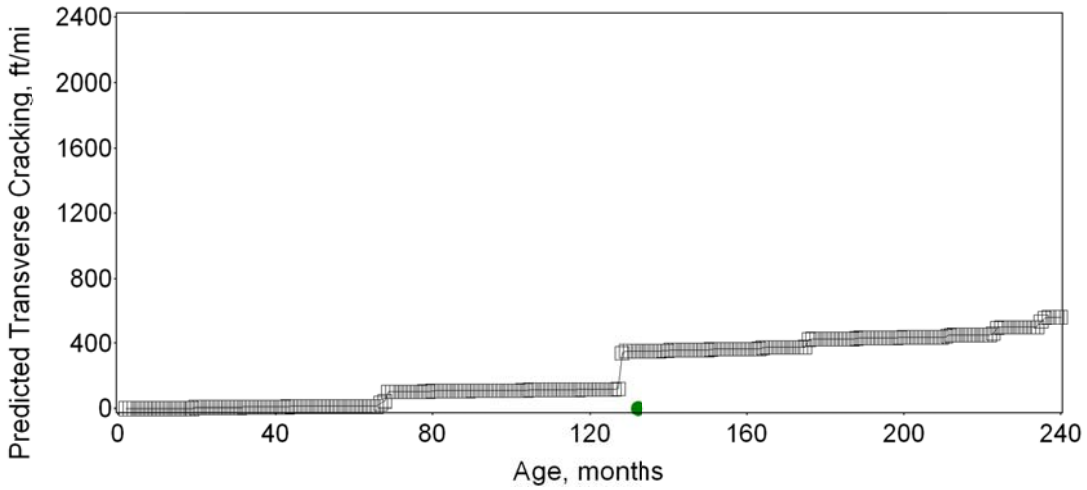

Figure 96. Plot showing predicted and measured transverse cracking versus pavement age for CDOT pavement management system project 92976.

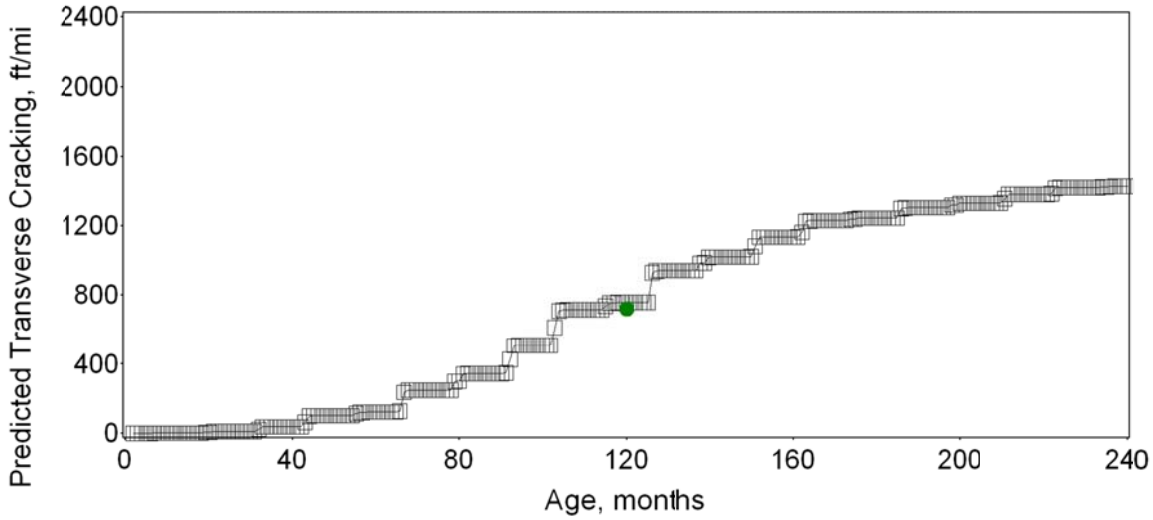

Figure 97. Plot showing predicted and measured transverse cracking versus pavement age for CDOT pavement management system project 12441.

Smoothness

Global MEDPG HMA Smoothness Model Verification

Verification of the MEPDG global new HMA pavement and HMA-overlaid HMA pavement IRI model for Colorado conditions consisted of running the MEPDG with the global coefficients for all projects and evaluating goodness of fit and bias. Figure 98 shows a plot of predicted versus measured IRI for all relevant pavement projects. Goodness of fit statistics and bias statistics are shown in Table 66.

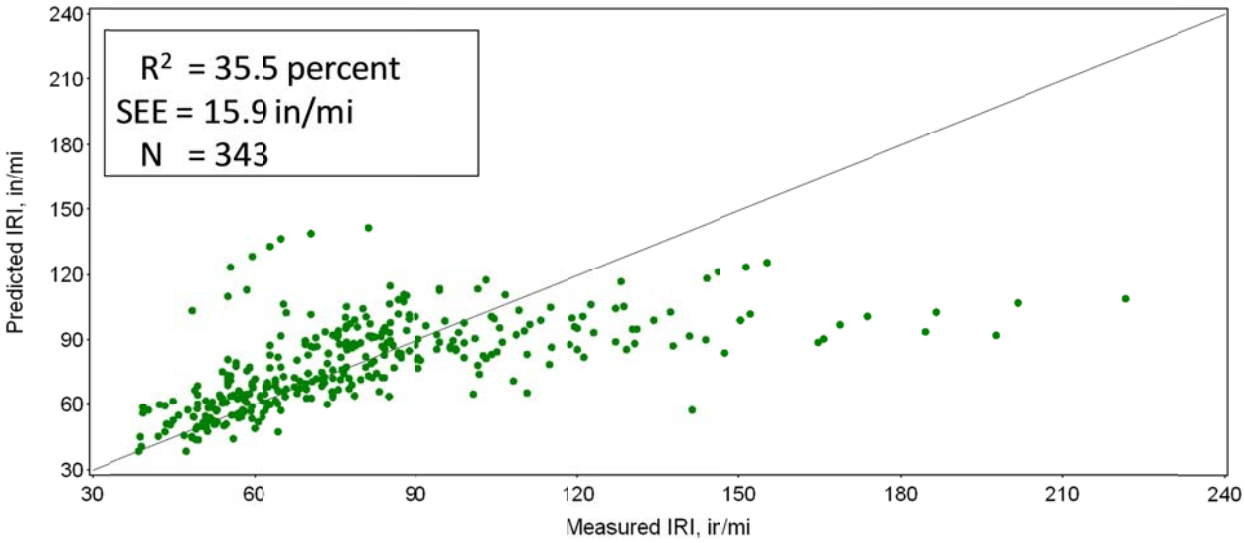

Figure 98. Predicted versus measured IRI using global MEPDG HMA IRI model and Colorado HMA pavement performance data.

Table 66. Results of statistical evaluation of MEPDG HMA IRI global model for Colorado conditions.

Statistical Analysis Type					
Goodness of Fit			Bias		
R^2, %	SEE, in/mi	N	p-value (paired t-test)	p-value (Slope)	N
35.5	15.9 in/mi	343	0.5530	< 0.0001	343

The goodness of fit statistics are poor, and the hypothesis test results indicate the global model predictions are biased (the model overpredicts IRI for higher measured IRI values). Thus, local calibration of this very important model was required.

Local Calibration of the MEPDG HMA Smoothness Model for Colorado

Description of Local Calibration Procedure

Local calibration of the MEPDG HMA IRI model for Colorado consisted of the following steps:

1. Determine the cause of poor to fair goodness of fit and bias produced by the global models.
2. Adjust the global model calibration coefficients as needed based on information derived from step 1 to improve goodness of fit and reduce or eliminate bias. This involved adjusting the MEPDG HMA IRI model global calibration coefficients (C1 through C4 in equation 12) using nonlinear optimization algorithms in SAS to produce a new set of local calibration coefficients that maximizes goodness of fit and significantly reduces or eliminates bias.

3. Perform statistical analysis (using SAS) to characterize goodness of fit and bias for the new local coefficients.
4. Evaluate goodness of fit and bias and summarize outcome.
5. Repeat steps 2 to 4 as needed until goodness of fit and bias are acceptable.

$$IRI = IRI_o + C1(SF) + C2(FC_{Total}) + C3(TC) + C4(RD) \qquad (12)$$

Where all inputs are as already defined.

Summary of HMA Smoothness Model Local Calibration Results

The new local calibration coefficients for the HMA smoothness model for Colorado are presented in Table 67. Goodness of fit and bias statistics for the locally calibrated HMA smoothness model are presented in Table 68. A plot of measured and predicted IRI for new HMA pavements and HMA-overlaid existing HMA pavements is presented in Figure 99.

The information presented in Table 68 indicates a large improvement in the goodness of fit between the global HMA smoothness model and the Colorado locally calibrated HMA smoothness model (i.e., R^2 after calibration was 64.4 percent, compared to a pre-calibration value of 35.5 percent). SEE increased marginally from 15.9 to 17.2 in/mile, which was considered fair. Hypothesis testing to determine the presence or absence of significant bias indicated that the locally calibrated model predictions were not significantly biased (at the 5 percent significance level). Thus, the significant bias present in the global model IRI predictions for Colorado has been eliminated.

Table 67. Local calibration coefficients for HMA smoothness (IRI) model.

Model Coefficients	CDOT Local Model Values	Global Model Values
C1 (for rutting)	35	Yes
C2 (for alligator cracking)	0.3	Yes
C3 (for transverse cracking)	0.02	Yes
C4 (for site factor)	0.019	Yes

Table 68. Results of statistical evaluation of MEPDG HMA IRI local model for Colorado conditions.

Statistical Analysis Type					
Goodness of Fit			Bias		
R^2, %	SEE, in/mi	N	p-value (paired t-test)	p-value (Slope)	N
64.4	17.2	343	0.1076	0.3571	343

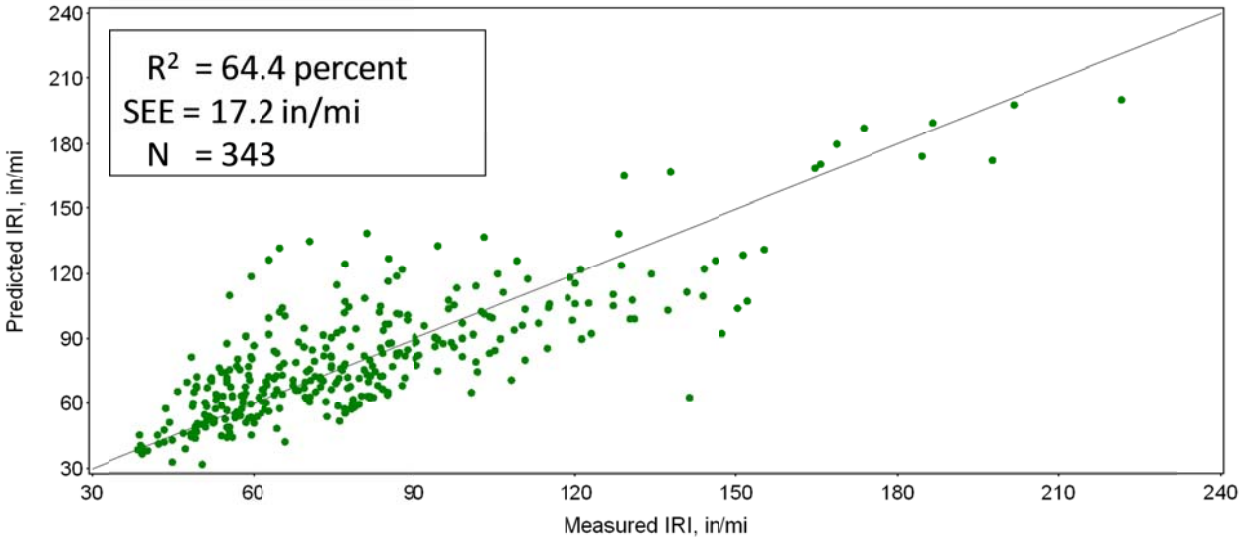

Figure 99. Plot of measured and predicted IRI for new HMA and HMA-overlaid HMA pavements developed using the locally calibrated CDOT HMA IRI model.

Figure 100 through 102 illustrate the model IRI prediction for typical HMA pavements. The impact of local calibration is most significant in removing the large under-prediction bias. HMA pavement designs based in part on HMA pavement IRI in Colorado will thus be much more accurate and optimum (lower cost) at the selected level of design reliability.

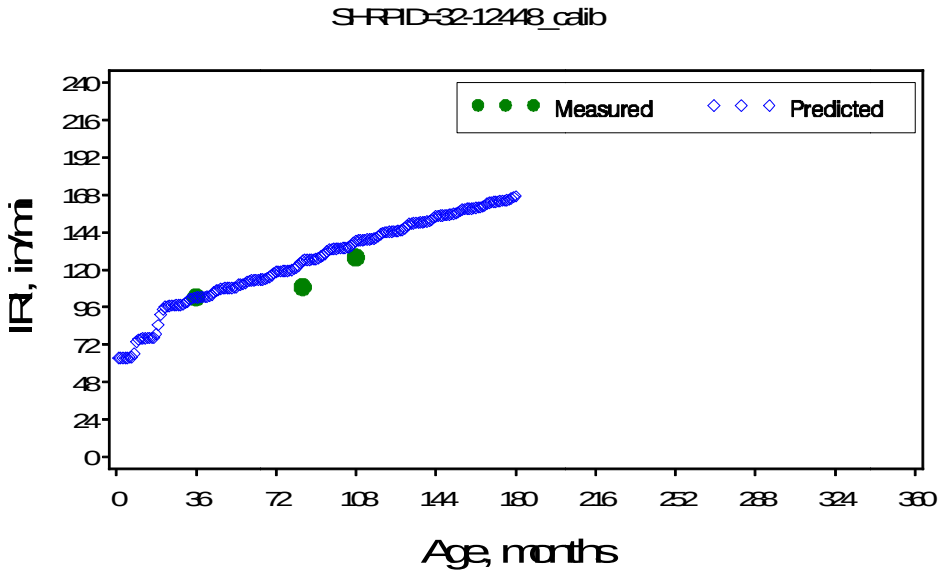

Figure 100. Plot showing measured and predicted IRI versus time for CDOT project 12448.

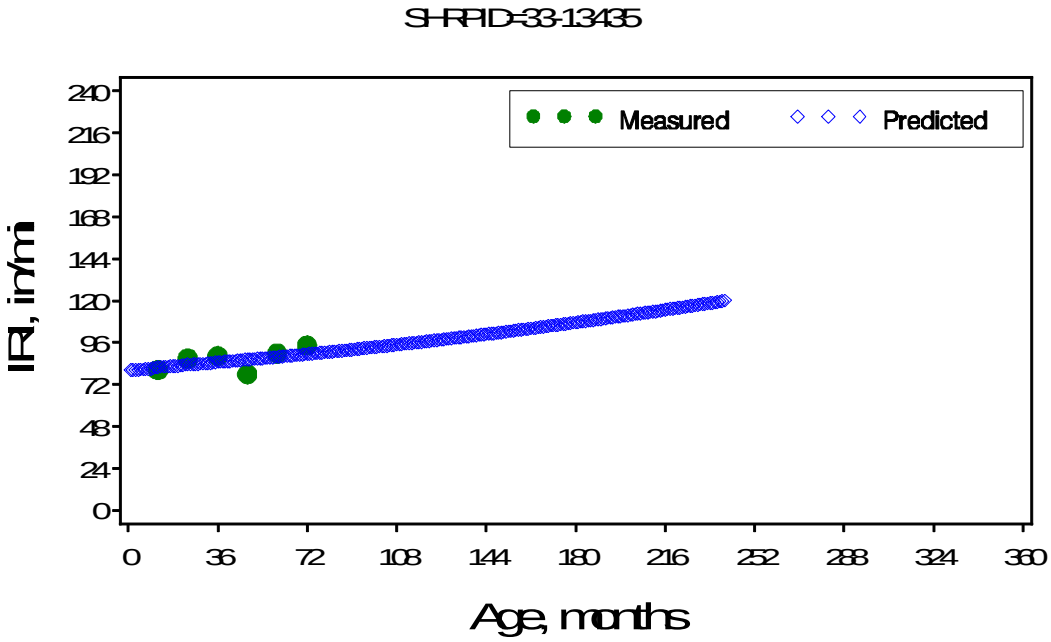

Figure 101. Plot showing measured and predicted IRI versus time for CDOT project 13435.

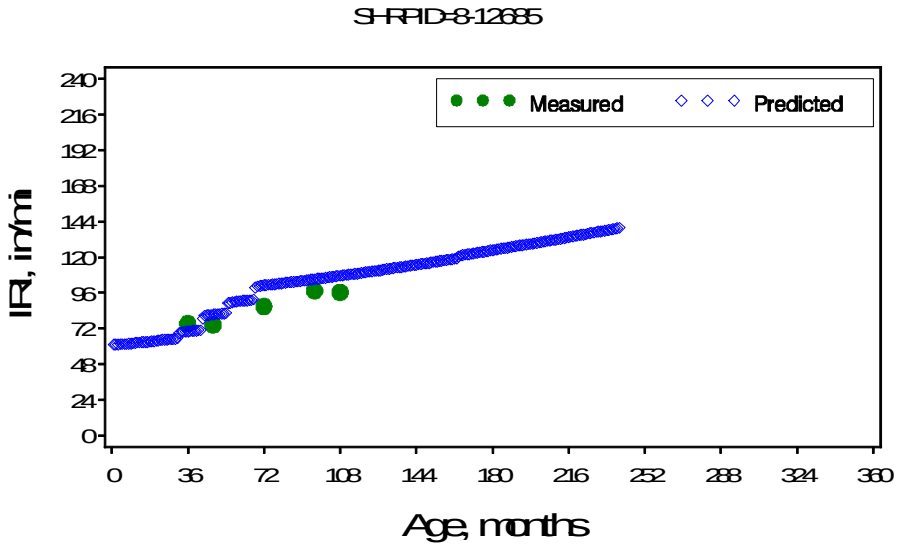

Figure 102. Plot showing measured and predicted IRI versus time for CDOT project 12685.

Estimating Design Reliability for New HMA and HMA Overlay Pavement Distress Models

The MEPDG estimates pavement design reliability using estimates of distress and IRI standard deviation for any given level of predicted distress or IRI. Thus, for each of the 3 HMA pavement distress models, there was a need to develop a relationship between predicted distress and the predictions standard error. Predicted distress standard error prediction equations were developed as follows:

1. Divided predicted distress into 3 or more intervals.

2. For each interval, determine mean predicted distress and standard error (i.e., standard variation of predicted – measured distress for all the predicted distress that falls within the given interval).
3. Develop a non linear model to fit mean predicted distress and standard error for each interval.

The resulting standard error of the estimated distress models developed using the locally calibrated CDOT HMA distress models are presented below:

$$SEE(GATOR) = 1 + \frac{15}{1 + e^{(-1.6673 - 2.4656 * \log 10(DAM))}} \quad (12)$$

$$SEE(ACRUT) = 0.2052 * ACRUT^{0.4} + 0.001 \quad (13)$$

$$SEE(BASERUT) = 0.2472 * BASERUT^{0.67} + 0.001 \quad (14)$$

$$SEE(SUBRUT) = 0.1822 * SUBRUT^{0.5} + 0.001 \quad (15)$$

$$SEE(TRANS) = 0.1468 * TRANS + 65.027 \quad (16)$$

where

SEE(GATOR)	=	alligator cracking standard deviation, percent lane area
SEE(TRANS)	=	transverse cracking standard deviation, ft/mi
SEE(ACRUT)	=	HMA layer rutting standard deviation, in
SEE(BASERUT)	=	base layer rutting standard deviation, in
SEE(SUBRUT)	=	subgrade layer rutting standard deviation, in
DAM	=	alligator cracking fatigue “bottom-up” damage
TRANS	=	predicted HMA transverse cracking, ft/mi
ACRUT	=	predicted HMA layer rutting, in
BASERUT	=	predicted base layer rutting, in
SUBRUT	=	predicted subgrade layer rutting, in

Note that smoothness (IRI) standard error is estimated internally by the MEPDG.

CHAPTER 7. VERIFICATION AND CALIBRATION OF RIGID PAVEMENTS

This chapter describes work done to verify and calibrate, if needed, the MEPDG global rigid pavement distress and smoothness models for Colorado. For this project, rigid pavements include new JPCP and unbonded JPCP overlay over existing JPCP.

The criteria for performing local calibration were based on whether the given global model exhibited a reasonable goodness of fit (between measured and predicted outputs) and whether distresses/IRI were predicted without significant bias.

Reasonable goodness of fit was determine using R^2 and SEE, while the presence or absence of bias was determined based on the hypothesis test described in chapter 3. The general criteria used to determine global model adequacy for Colorado conditions are presented in Table 69.

Table 70 lists the rigid pavement models evaluated as part of the MEPDG implementation in Colorado. Detailed descriptions of these models are presented in Appendix A.

Table 69. Criteria for determining global models adequacy for Colorado conditions.

Criterion of Interest	Test Statistic	Range of R^2, percent & SEE of Models	Rating
Goodness of fit	Coefficient of determination (R^2), percent (all models)	81 to 100	Very good (strong relationship)
		64 to 81	Good
		49 to 64	Fair
		< 49	Poor (weak or no relationship)
	Global JPCP transverse cracking model SEE	< 4.5 percent	Good
		4.5 to 9 percent	Fair
		> 9 percent	Poor
	Global JPCP transverse joint faulting model SEE	< 0.033 in	Good
		0.033 to 0.066 in	Fair
		> 0.066 in	Poor
	Global JPCP IRI model SEE	< 17 in/mi	Good
		17 to 34 in/mi	Fair
		> 34 in/mi	Poor
Bias	Hypothesis testing of slope of the linear measured vs. predicted distress/IRI model (b1 = slope) H0: b1 = 0	p-value	Reject if p-value is < 0.05 (i.e., 5 percent significant level)
	Paired t-test between measured and predicted distress/IRI	p-value	Reject if p-value is < 0.05 (i.e., 5 percent significant level)

Table 70. MEPDG rigid pavement global models evaluated for Colorado local conditions.

Pavement Type	MEPDG "Global" Models Evaluated		
	JPCP Transverse Cracking	JPCP Transverse Joint Faulting	New JPCP IRI
New JPCP	✓	✓	✓
Unbonded overlay over existing JPCP	✓	✓	✓

New JPCP and Unbonded JPCP Overlays Transverse Cracking Model

Global MEDPG JPCP Transverse "Mid-Panel Slab" Cracking Model Verification

Figure 103 presents a histogram of all measured (including time series) transverse "mid-panel slab" cracking for the CDOT pavement management system and LTPP projects included in the analysis. The figure shows a limited distribution of transverse cracking data, with most of the measured cracking being zero. Thus, commonly applied statistical procedures could not be used to characterize the model's goodness of fit and bias under Colorado conditions. The project team, therefore, applied a mostly non-statistical analysis procedure to verify the suitability of the MEPDG global transverse cracking model for Colorado conditions. The non-statistical goodness of fit and bias characterization procedure consisted of the following:

- Comparison of grouping of measured and predicted transverse cracking (grouped using engineering judgment into as many groupings as needed) to determine how often measured and predicted transverse cracking remained in the same group. Measured and predicted transverse cracking remaining in the same group implied reasonable goodness of fit and insignificant bias, while measured and predicted transverse cracking residing in different groups suggested otherwise.
- Comparison of distribution of residual (predicted – measured transverse cracking) to determine reasonableness of predictions. Basically, predicted transverse cracking that falls with 2 standard deviations of measured transverse cracking is deemed reasonable (i.e., predicted transverse cracking must fall within measured transverse cracking $\pm$ 2*SEE). A significant majority of data falling within the range of measured transverse cracking $\pm$ 1*SEE indicates very little bias.
- Apply the non-parametric Chi-square (χ^2) test to characterize and evaluate goodness of fit and bias between observed and predicted transverse cracking data.

Verification of the MEPDG global JPCP transverse cracking model for Colorado conditions began by running the MEPDG analysis for all JPCP projects. For this analysis, the NCHRP Project 20-07(288) JPCP MEPDG global model coefficients were applied, since these coefficients are compatible with CDOT and LTPP revised PCC CTE data used in transverse cracking predictions. The outcomes of the analyses are presented in the following sections.

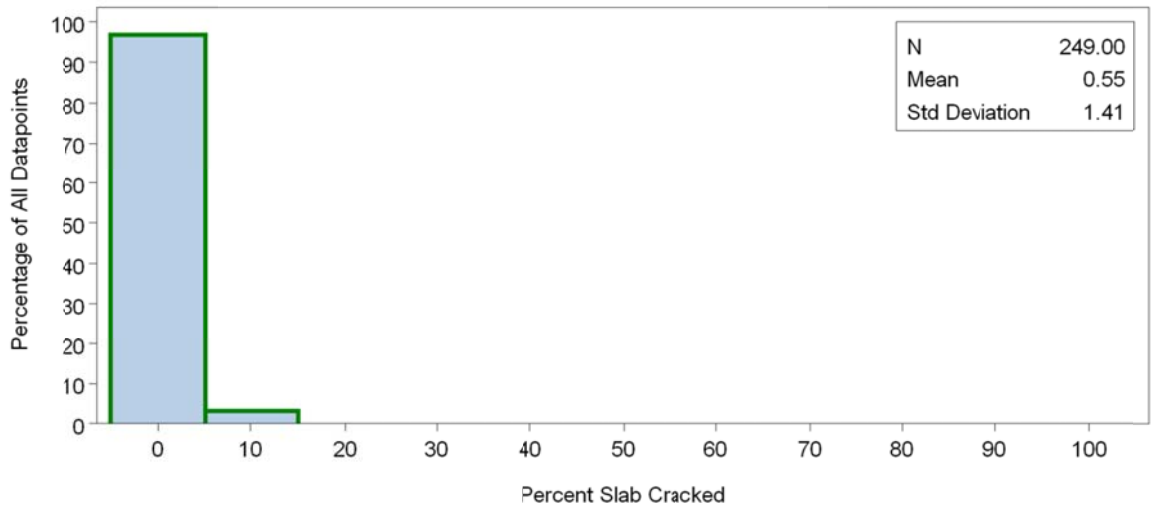

Figure 103. Histogram showing distribution of measured JPCP transverse "slab" cracking for CDOT and LTPP projects included in the analysis.

Summary of JPCP Transverse Cracking Verification Results

Comparison of Measured and Predicted Transverse Cracking Groupings

For this comparison, transverse "slab" cracking was categorized into four groups, as shown in Table 71. The goal was to determine how often measured and predicted transverse cracking fell in the same grouping. The range of each group was determined based on the distribution of the data available and using engineering judgment. A review of the information presented in Table 71 showed the following:

- Approximately 87 percent of all data points (218 of 249) fell within the same measured and predicted alligator cracking grouping (0 to 2 percent cracking).
- Three percent of the data points (23 of 249) fell within an adjacent grouping (i.e., measured grouping 2 to 5 against predicted grouping 0 to 2).
- For the remaining two data points, for measured groupings 5 to 10, the MEPDG predictions fell into predicted groupings 0 to 2.

Figure 104 shows a plot of measured and predicted transverse "slab" cracking versus pavement age for JPCP projects using MEPDG global transverse cracking model coefficients. The plot is in agreement with the trends reported in Table 71.

Table 71. Comparison of measured and predicted transverse cracking (percentage of all measurements).

Measured Transverse Slab Cracking, percent	MEPDG Predicted Transverse Slab Cracking, percent			
	0-2	2-5	5-10	>10
0-2	218	0	0	0
2-5	23	0	0	0
5-10	8	0	0	0
> 10	0	0	0	0

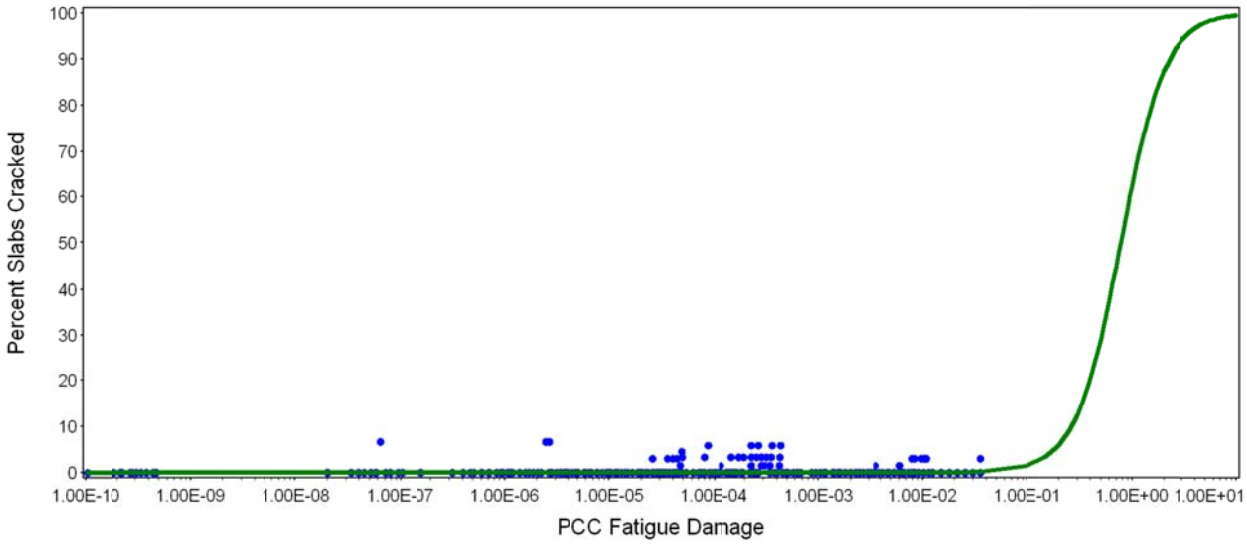

Figure 104. Plot showing measured and predicted transverse "slab" cracking versus pavement age for JPCP projects using MEPDG global transverse cracking model coefficients.

Evaluation of Distribution of Residuals

Figure 105 shows a distribution of residuals (predicted – measured percent slab with transverse cracking) for all 246 data points included in the analysis. The plot shows that over 90 percent of all the residuals fell within 1 SEE of the measured transverse cracking value. The remaining data points were all within 2 SEE of the measured transverse cracking value. Thus, deviations of all the predictions from actual measured transverse cracking were deemed good or fair.

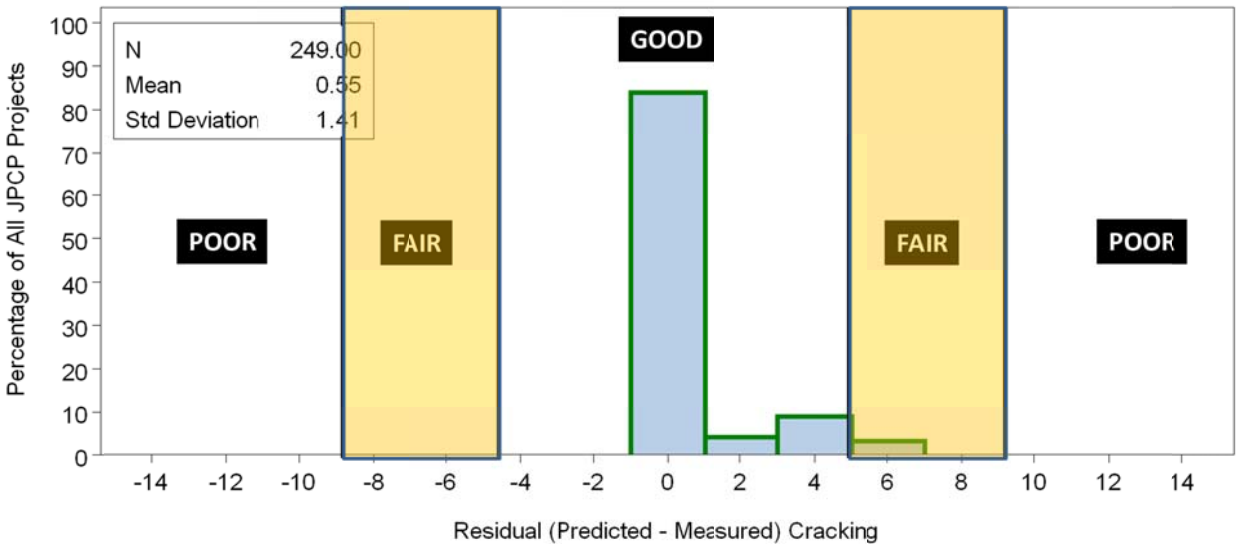

Figure 105. Plot showing distribution of residuals (predicted – measured percent slab with transverse cracking) for all 246 observations included in the analysis.

Statistical Chi-square Testing to Characterize Goodness of Fit and Bias

Statistical χ^2 testing was performed to test the hypothesis that the distribution of the random sample of measured transverse slab cracking (246 data points) and the distribution of MEPDG predicted transverse slab cracking were similar. This was done by dividing measured transverse cracking into several bins (e.g., three bins with transverse cracking values 0 to 2, 2 to 4, and > 4 percent).

A hypothesis was formulated and tested that states that if X percent of measured transverse cracking fall in the 0 to 2 percent bin, then a similar percentage of predicted transverse cracking will fall in the same bin. The χ^2 statistical analysis procedure consisted of the following steps:

1. Determine measured transverse cracking frequency distribution.
2. Formulate hypothesis.
3. Perform analysis.
    a. Calculate the χ^2 test statistic.
    b. Determine test degrees of freedom.
    c. Compare the χ^2 test statistic to the critical χ^2 value to estimate p-value.
4. Evaluate statistical test results and determine whether to reject the null hypothesis. The null hypothesis is rejected only when p-value is less than pre-determined level, usually 0.05, representing a 95 percent significance level.

The results of the χ^2 test are presented as follows:

- <u>Determine the frequency distribution of measured transverse cracking data.</u> The frequency distribution of the measured transverse cracking data was determined by dividing the range of transverse cracking values into bins and corresponding number of occurrences in the given bins. Because of the skewed distribution of the measured

transverse cracking data, the data could practically only be divided into two bins (zero and non-zero transverse cracking measurements). The distribution of measured transverse cracking into the two bins is presented in Table 72.

- Formulate hypothesis. The hypothesis assumed for statistical testing is presented below:
  - H_0: The percentages of predicted transverse cracking for the bins described in Table 72 is similar to that observed for measured transverse cracking (Bin A: 84%, Bin B: 16%).
  - H_A: The percentages of predicted transverse cracking for the bins described in Table 72 is NOT similar to that observed for measured transverse cracking (Bin A: 84%, Bin B: 16%).
- Perform analysis. The results of the χ^2 testing are presented below:
  - $\chi^2 = 0.0211$, degrees of freedom = 1, and sample size = 249.
  - p-value ($Pr > \chi^2$) = 0.8845.
- Evaluate statistical test results and determine whether to reject the null hypothesis. At the 95 percent significant level, the statistical χ^2 results indicate no significant difference in measured and predicted transverse cracking data. Thus, the null hypothesis was accepted. This implies that the global MEPDG transverse "slab" cracking model performed reasonably well for Colorado conditions and local calibration was not warranted at this stage. However, because this evaluation was done using projects in relatively good condition with little or no cracking, it will be necessary to observe this model in the future to determine how well it predicts cracking once the JPCP projects used in the analysis start deteriorating. This can be done through continuous monitoring of the selected projects.

Table 72. Frequency distributions of measured transverse cracking data.

Bins	Frequency	Percent	Cumulative Frequency	Cumulative Percent
A (0 to 0.2 percent)	209	84	209	84
B (> 0.2 percent)	40	16	249	100

Figures 106 through 108 illustrate the transverse fatigue cracking model for selected projects.

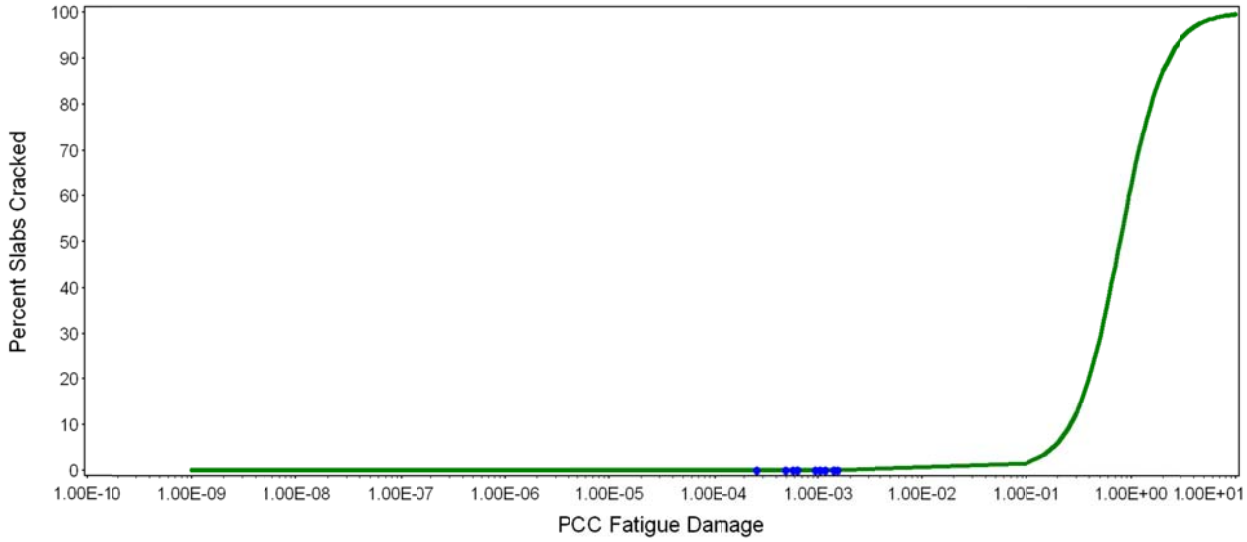

Figure 106. Plot of predicted and measured transverse cracking versus fatigue damage for LTPP 4_0213 (using global calibration factors and recommended loss of slab/aggregate base friction age).

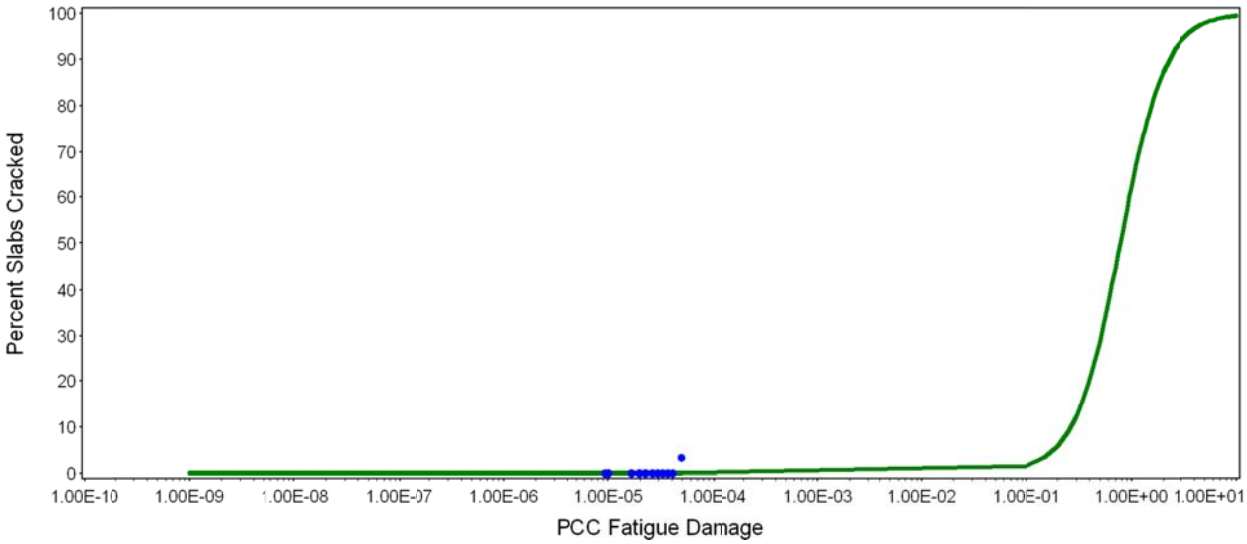

Figure 107. Plot of predicted and measured transverse cracking versus fatigue damage for LTPP 4_0217 (using global calibration factors and recommended loss of slab/lean concrete base friction age).

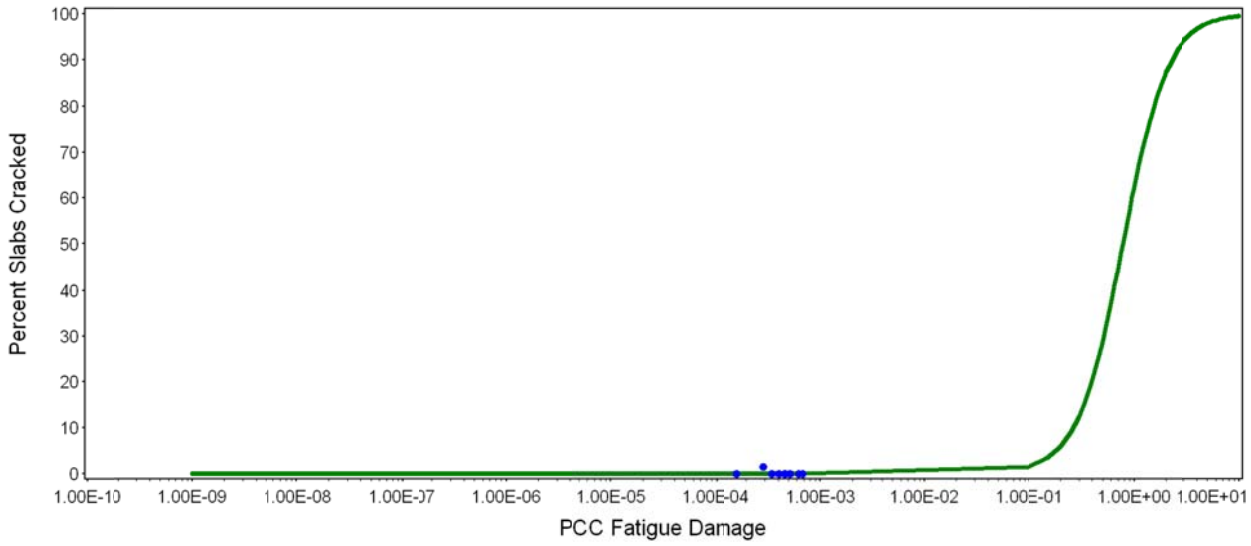

Figure 108. Plot of predicted and measured transverse cracking versus fatigue damage for Colorado JPCP 54-11546 (using global calibration factors and recommended loss of slab/aggregate base friction age).

New JPCP and Unbonded JPCP Overlays Transverse Joint Faulting Model

Global MEDPG JPCP Transverse Joint Faulting Model Verification

Figure 109 presents a histogram of all measured (including time series) transverse joint faulting for the CDOT pavement management system and LTPP projects included in the analysis. The information provided in the figure shows a limited distribution of measured transverse joint faulting data, with most of the measured faulting being zero. Because the measured transverse joint faulting was mostly zero, commonly applied statistical procedures could not be used to evaluate goodness of fit and bias. The project team thus applied the same non-statistical methods as described for JPCP transverse cracking to verify the suitability of the MEPDG global transverse joint faulting model for local Colorado conditions. The procedures are as follows:

Verification of the MEPDG global JPCP transverse joint faulting model for Colorado conditions consisted of the running the MEPDG analysis with the global transverse joint faulting model for all selected projects. For this analysis, the NCHRP Project 20-07(288) JPCP MEPDG global model coefficients were applied, since these coefficients are compatible with CDOT and LTPP revised PCC CTE data used in transverse joint faulting predictions. The outcomes of the analyses are presented in the following sections.

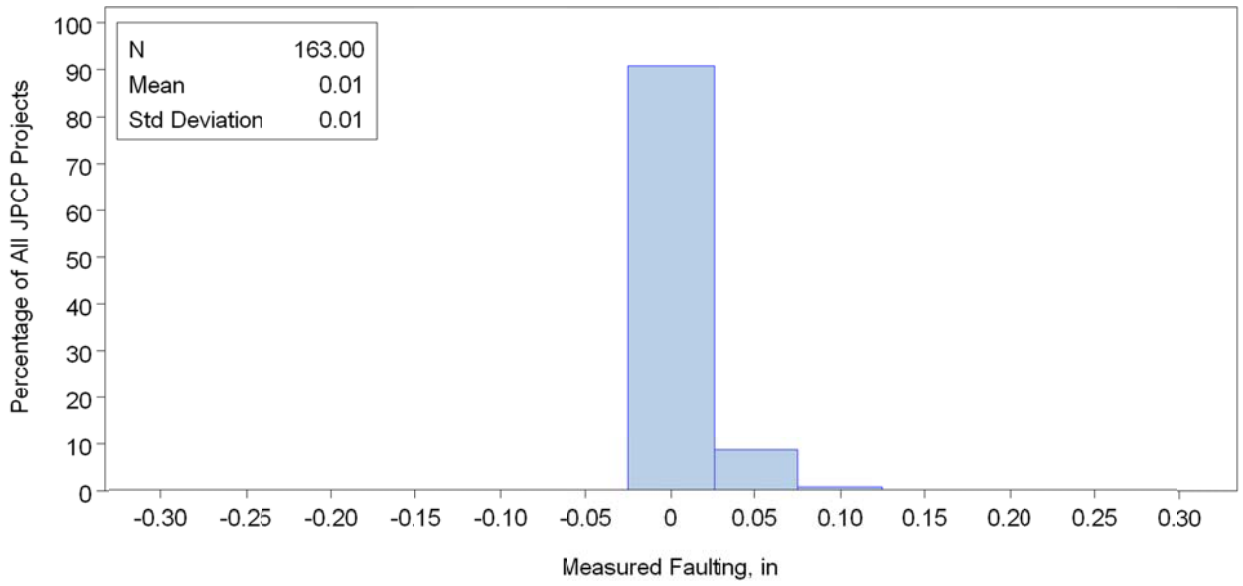

Figure 109. Histogram showing distribution of measured JPCP transverse joint faulting for CDOT pavement management system and LTPP projects included in the analysis.

Summary of JPCP Transverse Faulting Verification Results

Comparison of Measured and Predicted Transverse Faulting Groupings

For this comparison, transverse faulting was categorized into four groups, as shown in Table 73. The goal was to determine how often measured and predicted transverse faulting fell in the same grouping. The range of each group was determined based on the distribution of the data available and using engineering judgment.

Table 73. Comparison of measured and predicted transverse joint faulting (percentage of all measurements).

Measured Transverse Joint Faulting, in	MEPDG Predicted Transverse Joint Faulting, in		
	0 to 0.03	0.33 to 0.06	> 0.06
0 to 0.03	151	0	0
0.03 to 0.06	9	0	0
> 0.06	3	0	0

A review of the information presented in Table 73 showed the following:

- Approximately 92 percent of all data points (151 of 163) fell within the same measured and predicted transverse joint faulting grouping (0 to 0.03 in faulting).
- Six percent of the data points (9 of 163) fell within an adjacent grouping (i.e., measured grouping 0.03 to 0.06 against predicted grouping 0 to 2).
- For the remaining 2 percent of data points belonging to measured grouping > 0.06, MEPDG predictions fell in predicted grouping 0 to 0.03.

The results show that a significant majority of predicted transverse joint faulting fell within the same grouping (over 90 percent), indicating that the global model predicted transverse joint faulting accurately with little bias.

Evaluation of Distribution of Residuals

Figure 110 shows a distribution of residuals (predicted – measured percent slab with transverse joint faulting) for all 163 data points included in the analysis. The plot shows that over 90 percent of all the residuals fell within 1 SEE of the measured transverse faulting value. The remaining data points were mostly within 2 SEE, with only 2 percent of data points falling outside of this range.

The results here also show that a significant majority of predicted transverse joint faulting fell within 1 SEE of the measured transverse faulting value (over 90 percent). This indicates that the global model predicted transverse joint faulting accurately with little bias.

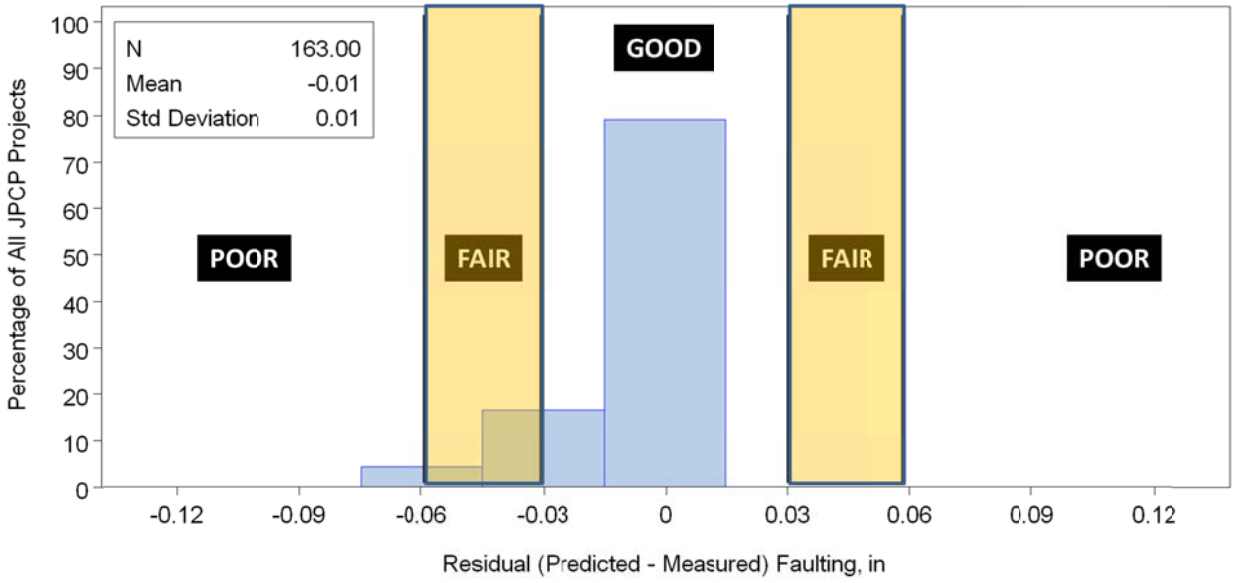

Figure 110. Plot showing distribution of residuals (predicted – measured faulting) for all 163 data points included in the analysis.

Statistical Chi-Square Testing to Characterize Goodness of Fit and Bias

The measured and predicted faulting data were mostly zero; thus, a reasonable representative distribution of faulting data could not be developed. Therefore, statistical χ^2 testing was not performed to test the hypothesis that the distribution of the random sample of measured transverse joint faulting and the distribution of MEPDG predicted transverse joint faulting were similar.

The non-statistical procedures applied to determine goodness of fit and bias indicated that the MEPDG global transverse joint faulting model predicted transverse joint faulting reasonably well, with no significant bias in Colorado. Therefore, there was no need for local calibration of the global transverse joint faulting model at this stage. However, the model should be evaluated in the future to determine how well it predicts significant levels of faulting (non-zero values). This can be done through continuous monitoring of the selected JPCP projects used in this analysis.

Figures 111 through 114 illustrate the transverse joint faulting predictions using the global MEPDG model for selected projects.

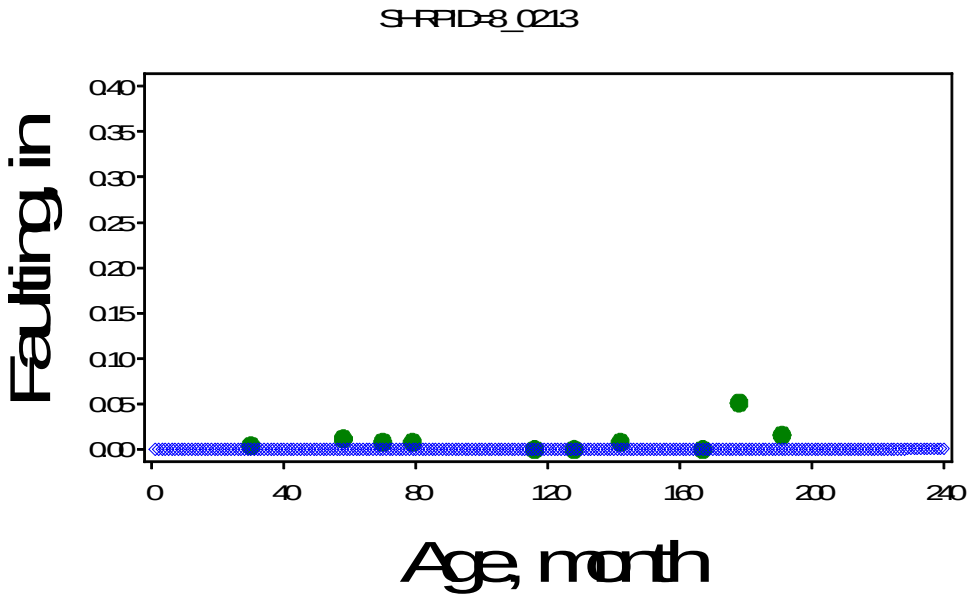

Figure 111. Predicted (using global calibration factors) and measured transverse joint faulting for Colorado JPCP 4_0213 (SPS-2) with dense graded aggregate base, dowel diameter = 1.5 in.

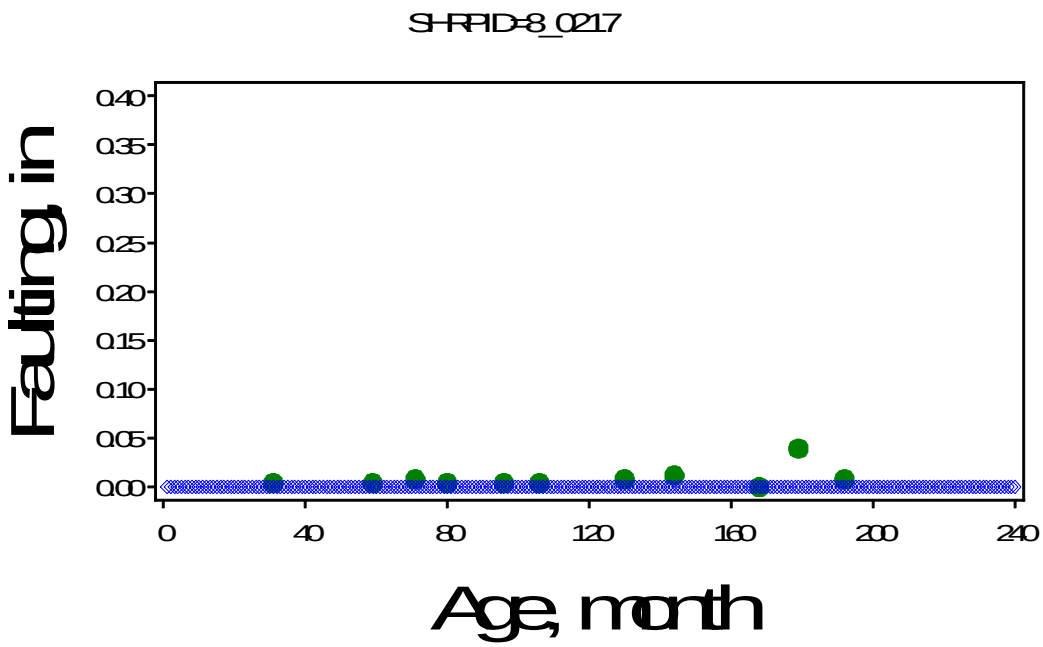

Figure 112. Predicted (using global calibration factors) and measured transverse joint faulting for Colorado JPCP 4_0217 (SPS-2) with lean concrete base dowel diameter = 1.5 in.

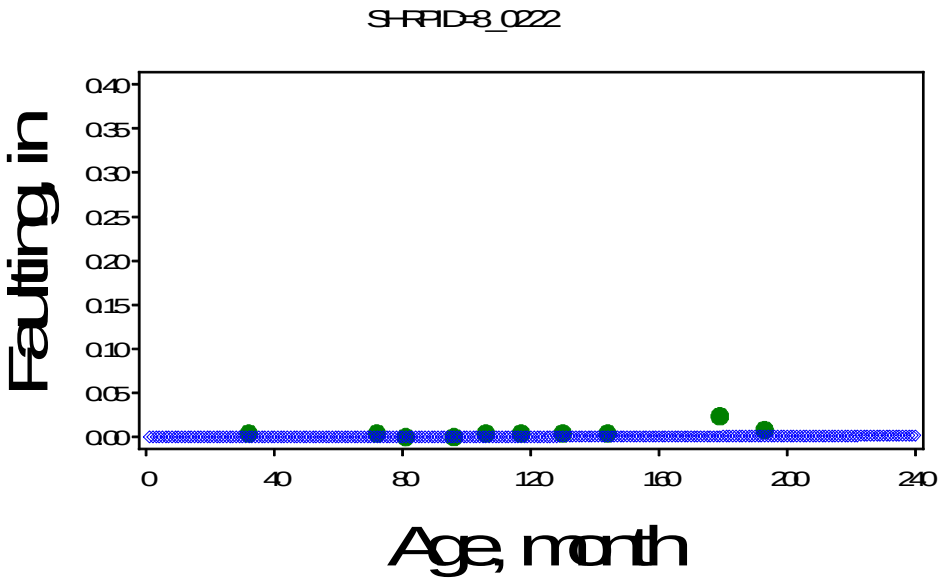

Figure 113. Predicted (using global calibration factors) and measured transverse joint faulting for Colorado JPCP 4_0222 (SPS-2) with permeable asphalt treated base dowel diameter = 1.5 in.

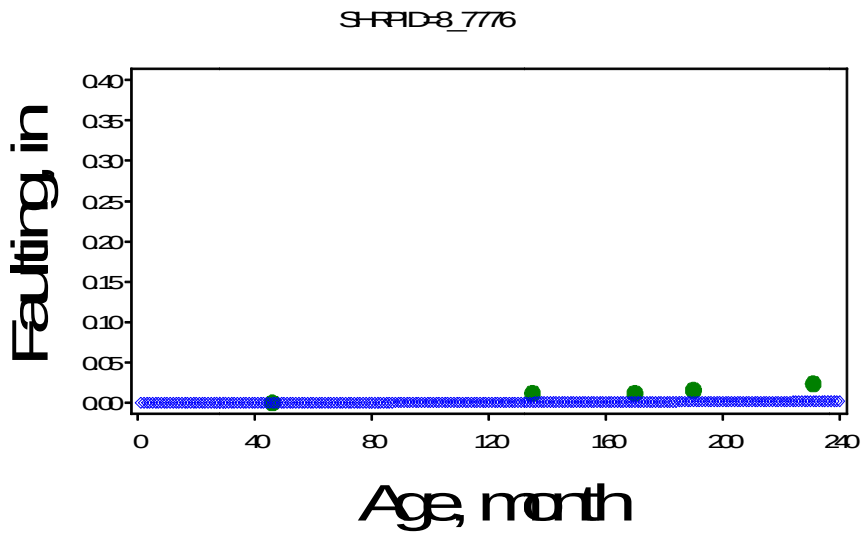

Figure 114. Predicted (using global calibration factors) and measured transverse joint faulting for Colorado JPCP 4_7776 (GPS-3) with dense graded aggregate base dowel diameter = 1.5 in.

New JPCP and Unbonded JPCP Smoothness

Global MEDPG JPCP Smoothness Model Verification

Verification of the MEPDG global JPCP IRI model for Colorado conditions consisted of running the MEPDG analysis for all selected projects and evaluating goodness of fit and bias. A plot of predicted versus measured IRI using the selected Colorado projects is shown in Figure 115, and full details of the outcome of statistical analysis to characterized goodness of fit and bias are presented in Table 74.

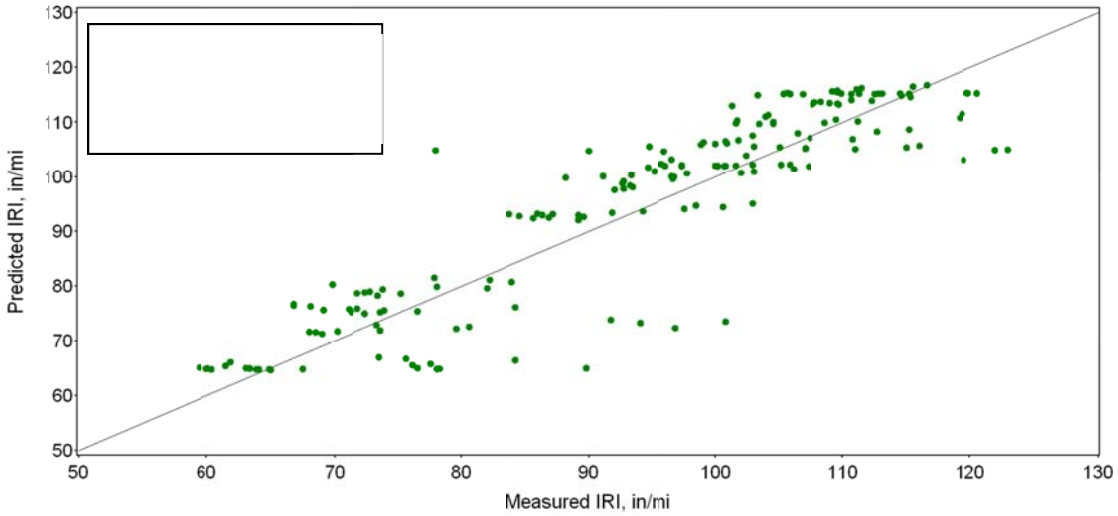

Figure 115. Predicted JPCP IRI versus measured Colorado JPCP with global calibration coefficients.

Table 74. Goodness of fit and bias test statistics for final Colorado calibrated JPCP IRI model (based on 100 percent of all selected projects).

Analysis Type	Diagnostic Statistics	Results
Goodness of Fit	R^2	80.9 percent
	SEE	9.85 in/mi
	N	279
Bias	H_0: Slope = 1.0	p-value = 0.6458
	H_0: Predicted - measured IRI = 0 (paired t-test)	p-value = 0.2760

These results indicate that goodness of fit was very good, and predicted IRI exhibited no significant bias. Based on the outcome of the global model verification analysis, there was no need for local calibration. Figures 116 through 118 illustrate the global JPCP IRI model prediction for various Colorado JPCP projects over time. The predictions show a good fit of predicted and measured IRI. JPCP designs based in part on IRI in Colorado will be more accurate and optimum (lower cost) at the selected level of design reliability when done with this model.

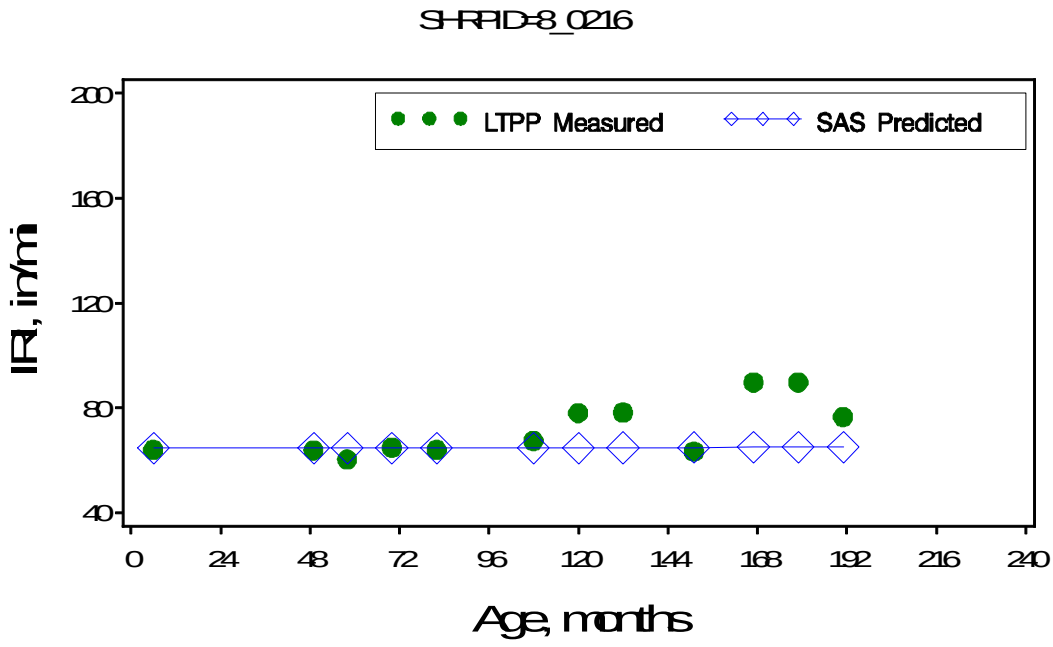

Figure 116. Predicted and measured JPCP IRI for Colorado LTPP section 0216 over time.

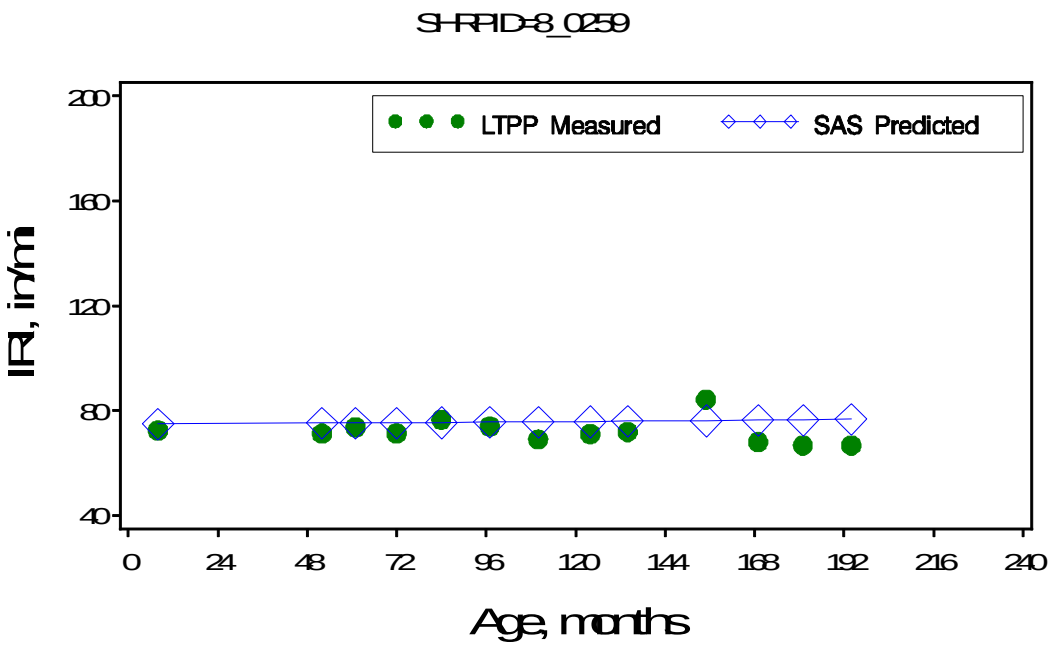

Figure 117. Predicted and measured JPCP IRI for Colorado LTPP section 0259 over time.

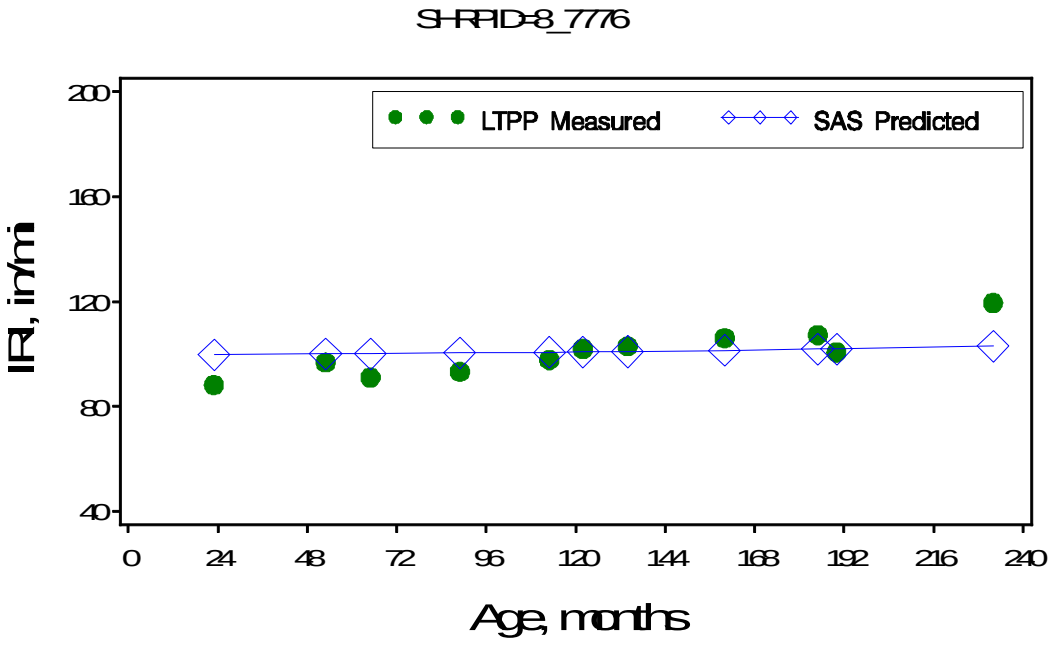

Figure 118. Predicted and measured JPCP IRI for Colorado LTPP section 7776 over time.

Estimating Design Reliability for New JPCP and Unbonded JPCP Overlay Distress Models

JPCP standard error of the estimated distress models was adopted from NCHRP 20-07(288) and are presented as follows (Mallela et al., 2011):

$$Stdev(CRK) = 1.5+(57.08*PCRK)^{0.33} \quad (17)$$

$$Stdev(FLT) = 0.0831*(PFLT^{0.3426})+0.00521 \quad (18)$$

where

Stdev(CRK)	=	transverse fatigue crack standard deviation, percent slabs
PCRK	=	predicted transverse fatigue cracking, percent slabs
Stdev(FLT)	=	faulting standard deviation, in
PFLT	=	predicted joint faulting

Smoothness IRI standard error is estimated internally by the MEPDG.

CHAPTER 8. INTERPRETATION OF RESULTS—DECIDING ADEQUACY OF CALIBRATION PARAMETERS

Verification of Colorado MEPDG Models (Sensitivity Analysis)

The researchers performed a comprehensive sensitivity study as the first step in validating the local CDOT MEPDG calibrated models. This was accomplished as follows:

- Selection of an analysis period of 20 years.
- Development of baseline new pavement designs (HMA and JPCP) with inputs that represent typical CDOT site conditions (climate, traffic, and subgrade), design and construction practices, and pavement materials:
    - For HMA pavement, inputs included AADTT, HMA thickness, asphalt binder type, AC air voids content, AC volumetric binder content, climate, granular base thickness, and granular subbase thickness.
    - For new JPCP, inputs included AADTT, base type and thickness, base erodibility index, loss of bond age at the PCC/base interface, joint spacing, PCC thickness, PCC 28-day flexural strength, shoulder type, transverse joint load transfer mechanism, PCC slab width, climate, and PCC CTE.
- Key inputs were varied one at a time (except where two inputs have known correlations, such as PCC modulus of rupture and elastic modulus) across the range of typical values.
- Predicted outcomes (distresses and IRI) were then plotted input by input to illustrate their impact on distress and IRI.
- The impact on key performance outputs was assessed.

The baseline designs are detailed in Tables 75 and 76. The range of the key inputs used for sensitivity analysis is also presented in the tables.

Figures 119 through 125 present sensitivity plots for HMA pavements and JPCP distresses and smoothness (IRI). The plots shows for each key pavement input of interest the levels of distress/IRI exhibited after 20 years in service. Cumulative traffic applied over the 20-year period was 9.3 million and 9.8 million for new HMA pavements and new JPCP, respectively.

Table 75. Mean (baseline) and range of key inputs used for sensitivity analysis of new HMA pavements.

Input Parameter	Values		
	Lower End	Mean (Baseline)	Upper End
Conventional HMA thickness, in	5 in	7 in	11
Granular base thickness, in	0 in	6 in	12 in
Granular subbase thickness, in	0 in	18 in	36 in
Air voids, percent	3%	7%	9%
Volumetric binder content, percent	7%	11%	13%
Binder type (Superpave)	PG 58-28	PG 64-22	PG 76-28
Initial AADTT	500	2000	5000
Cumulative trucks (after 20 years in service)			
Climate (weather stations)*	Very cool	Cool	Moderate

*See Table 10.

Table 76. Mean (baseline) and range of key inputs used for sensitivity analysis of new JPCP.

Input Parameter	Values		
	Lower End	Mean (Baseline)	Upper End
PCC Thickness, in	8-in	9-in	10-in
CTE, in/in/oF	4.5 in/in/deg. F	5 in/in/deg. F	5.5 in/in/deg. F
Base type/thickness	No base	4-in DGAB	ATB/CTB
Dowel diameter, in (used PCC thickness/8 rule)	No dowel (0-in)	1.25-in	1.5-in
Joint spacing	12-ft	15-ft	18-ft
Flexural strength, psi	600 psi	650 psi	750 psi
Shoulder type	AC shoulder	Tied PCC shoulder with 40% LTE	Tied PCC shoulder with 70% LTE
Climate (weather stations)*	Lamar (Moderate) Approximate 7-day highest temperature = 90.6 ^{o}F, elevation = 3,070 ft	Denver (Moderate) Approximate 7-day highest temperature = 94.2 ^{o}F, elevation = 5,607 ft	Elbert (Very cool) Approximate 7-day highest temperature = 79.7 ^{o}F, elevation = 7,060 ft

*See Table 10.

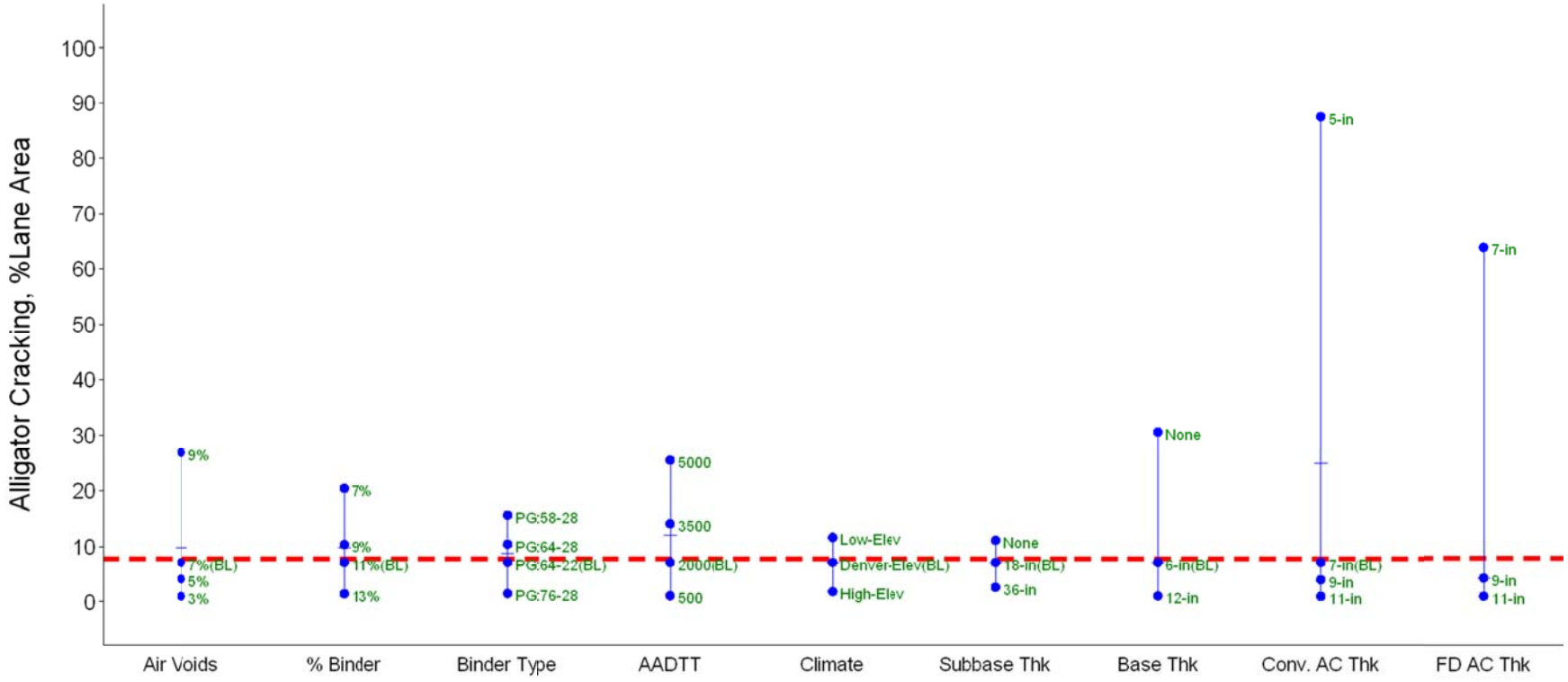

Figure 119. Sensitivity summary for HMA pavement alligator cracking. Note the red line represents predicted alligator cracking for the baseline project in Table 75.

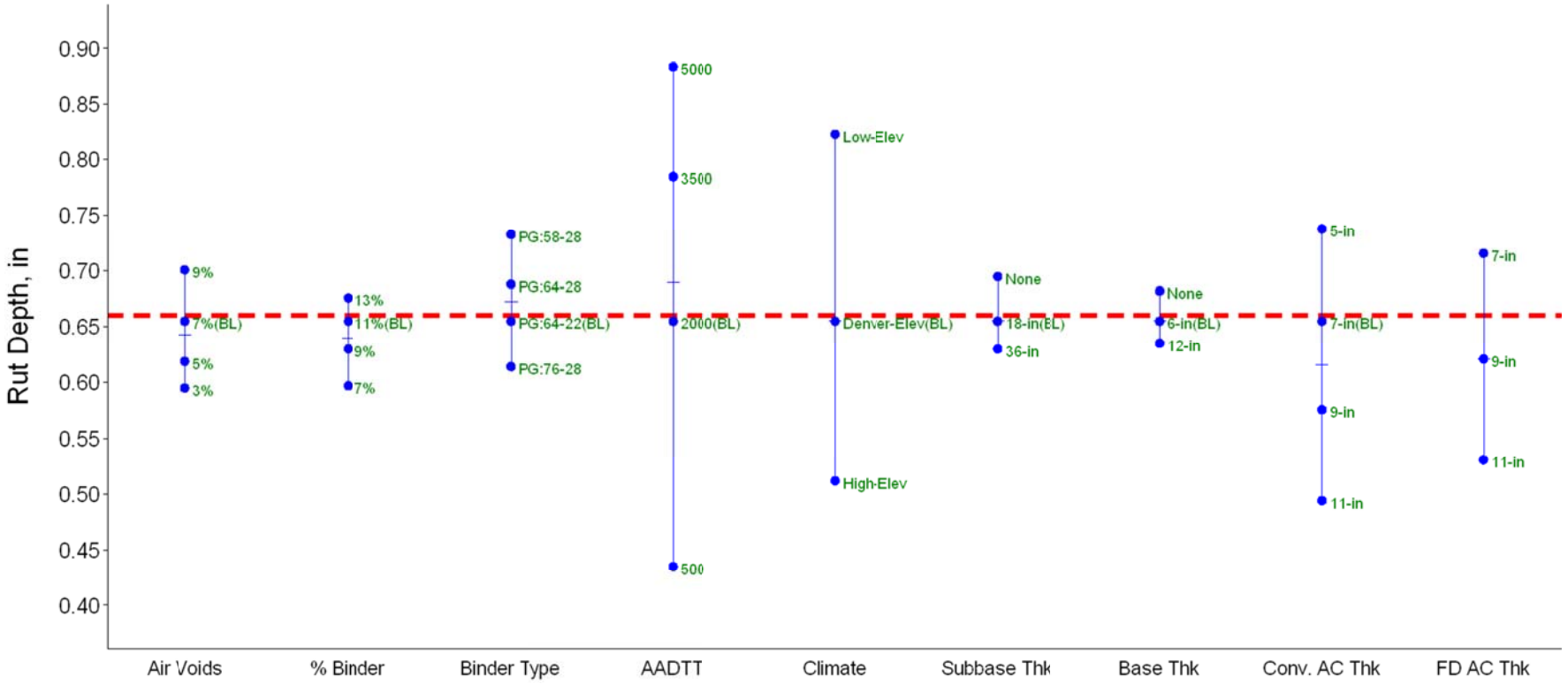

Figure 120. Sensitivity summary for HMA pavement total (HMA, granular base, and subgrade) rutting. Note the red line represents predicted rut depth for the baseline project in Table 75.

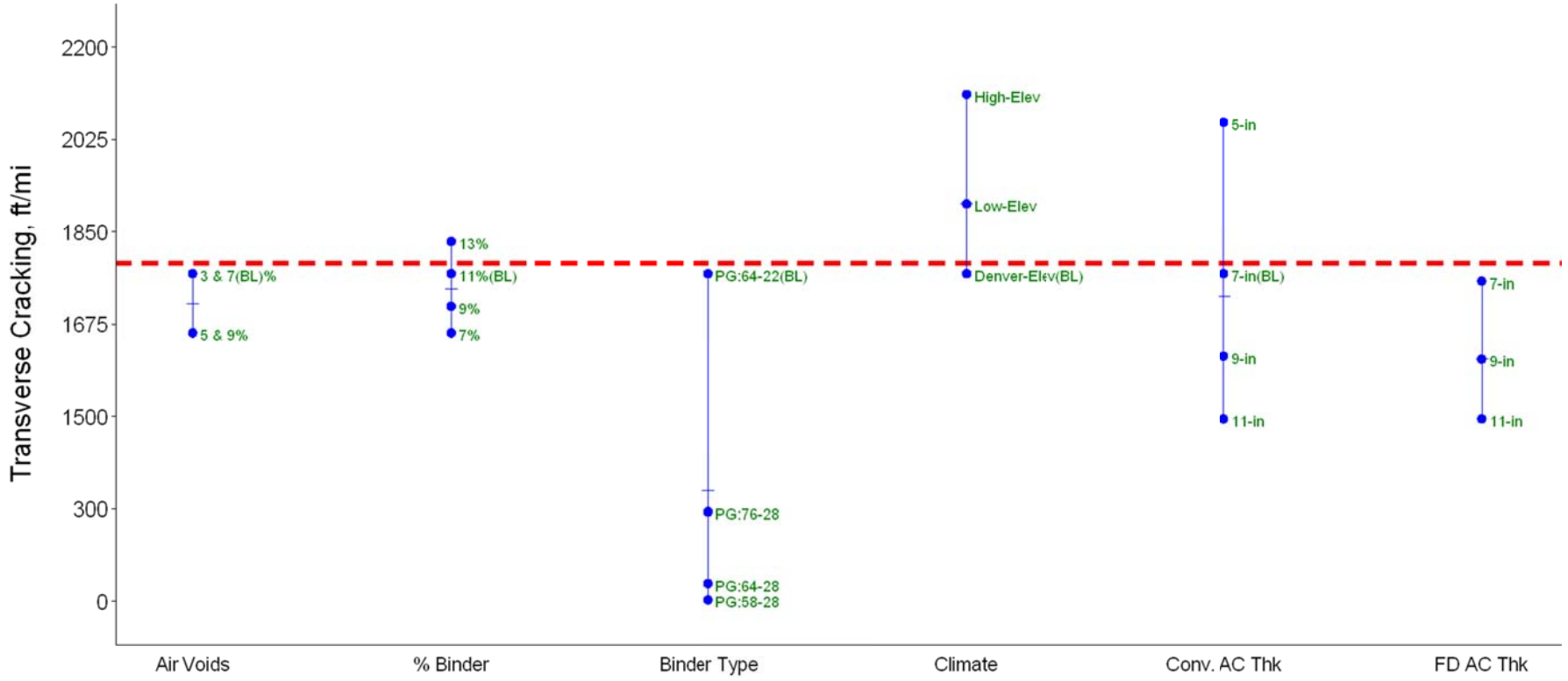

Figure 121. Sensitivity summary for HMA pavement transverse "thermal" cracking. Note the red line represents predicted transverse cracking for the baseline project in Table 75.

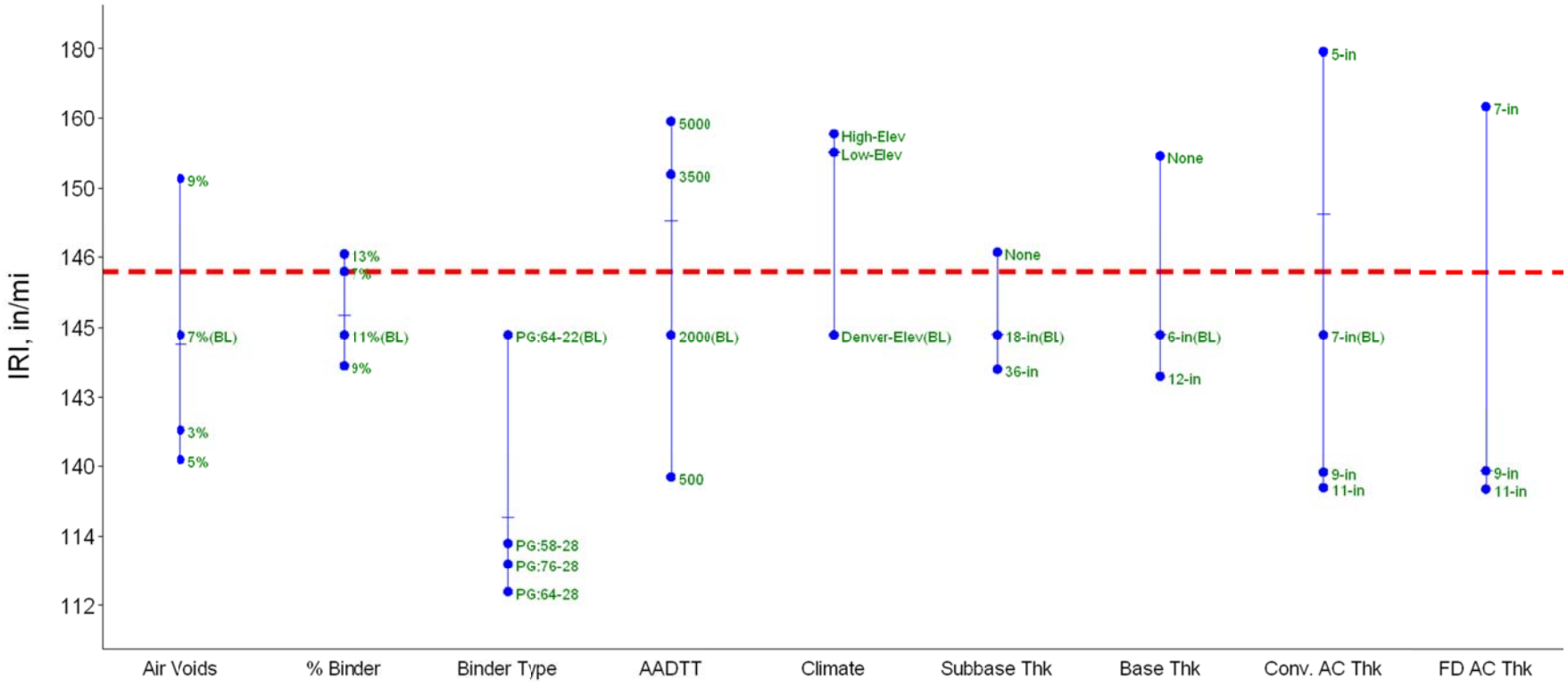

Figure 122. Sensitivity summary for HMA pavement IRI. Note the red line represents predicted IRI for the baseline project in Table 75.

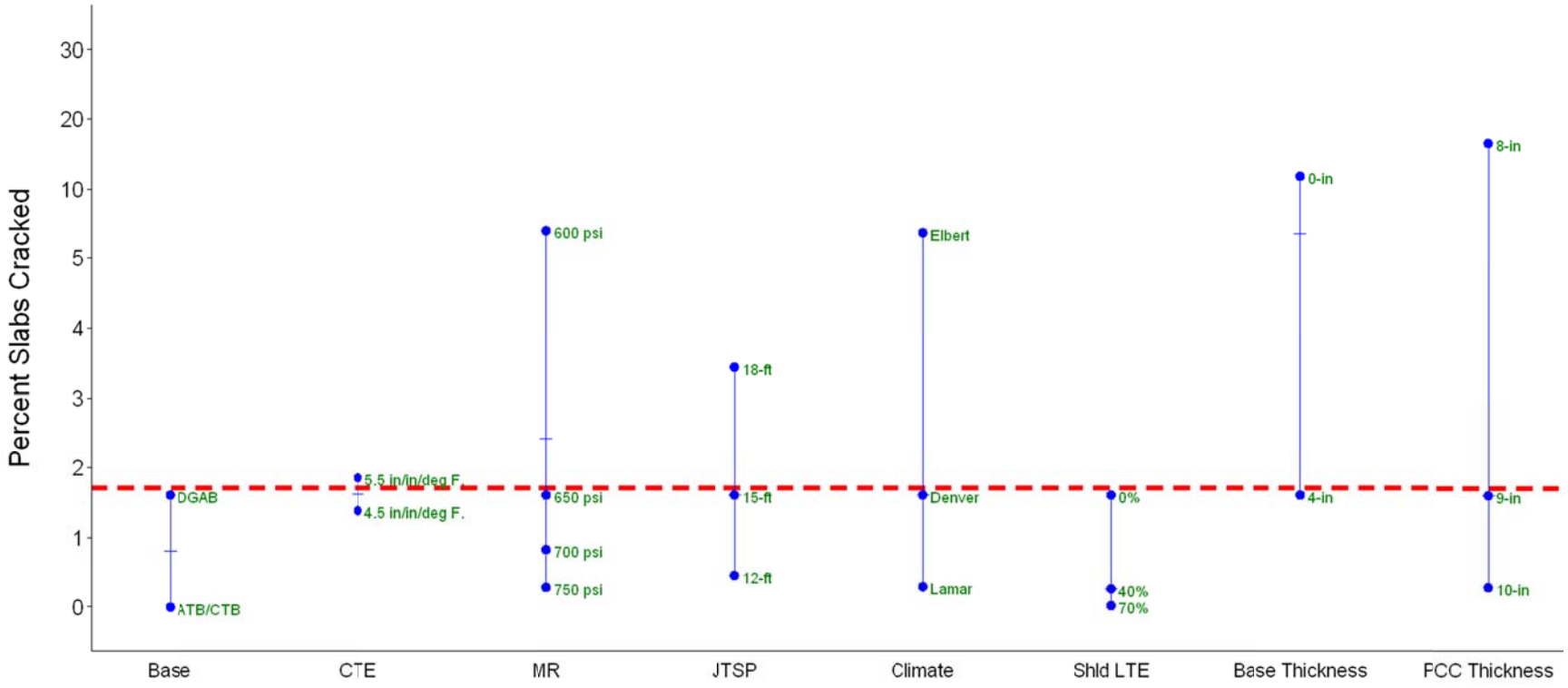

Figure 123. Sensitivity summary for JPCP transverse "slab" cracking. Note the red line represents predicted percent slabs cracked for the baseline project in Table 76.

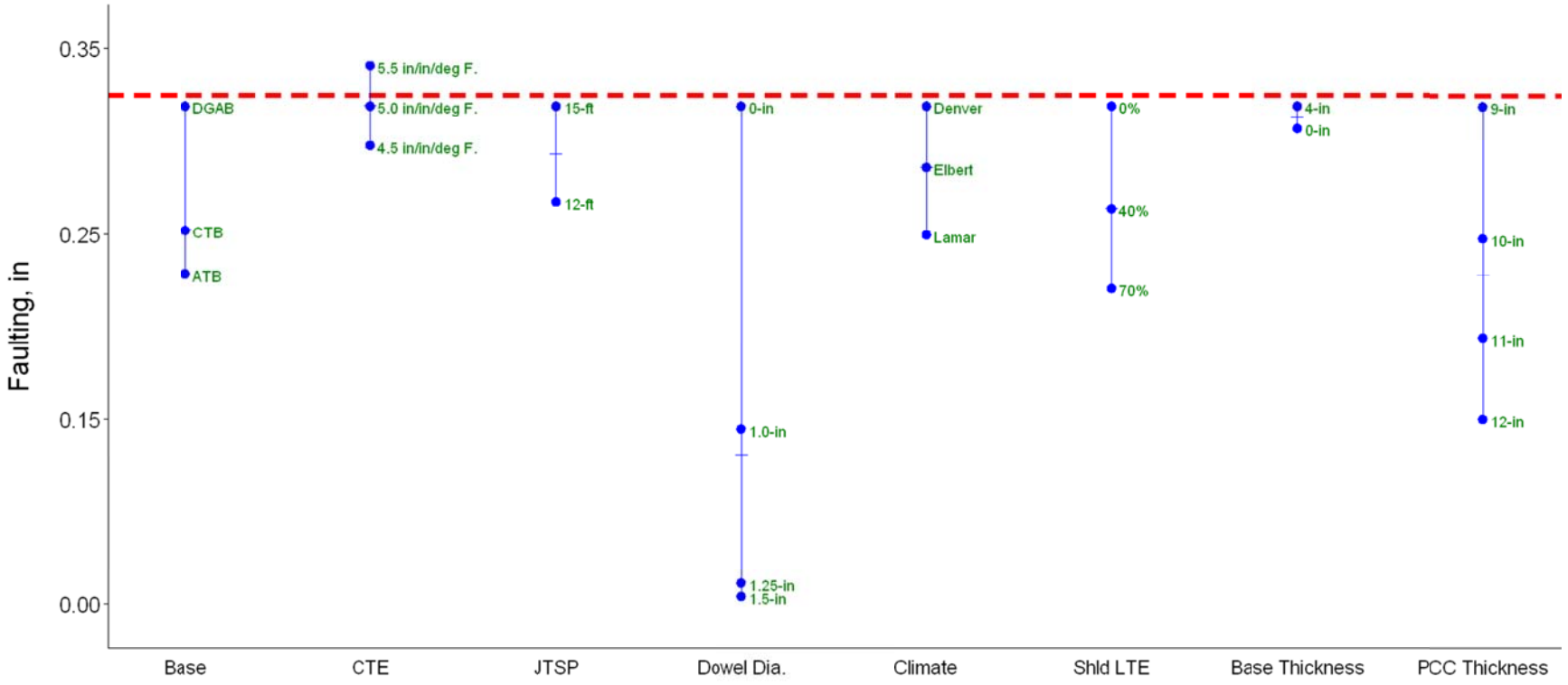

Figure 124. Sensitivity summary for JPCP transverse joint faulting. Note the red line represents predicted mean transverse joint faulting for the baseline project in Table 76.

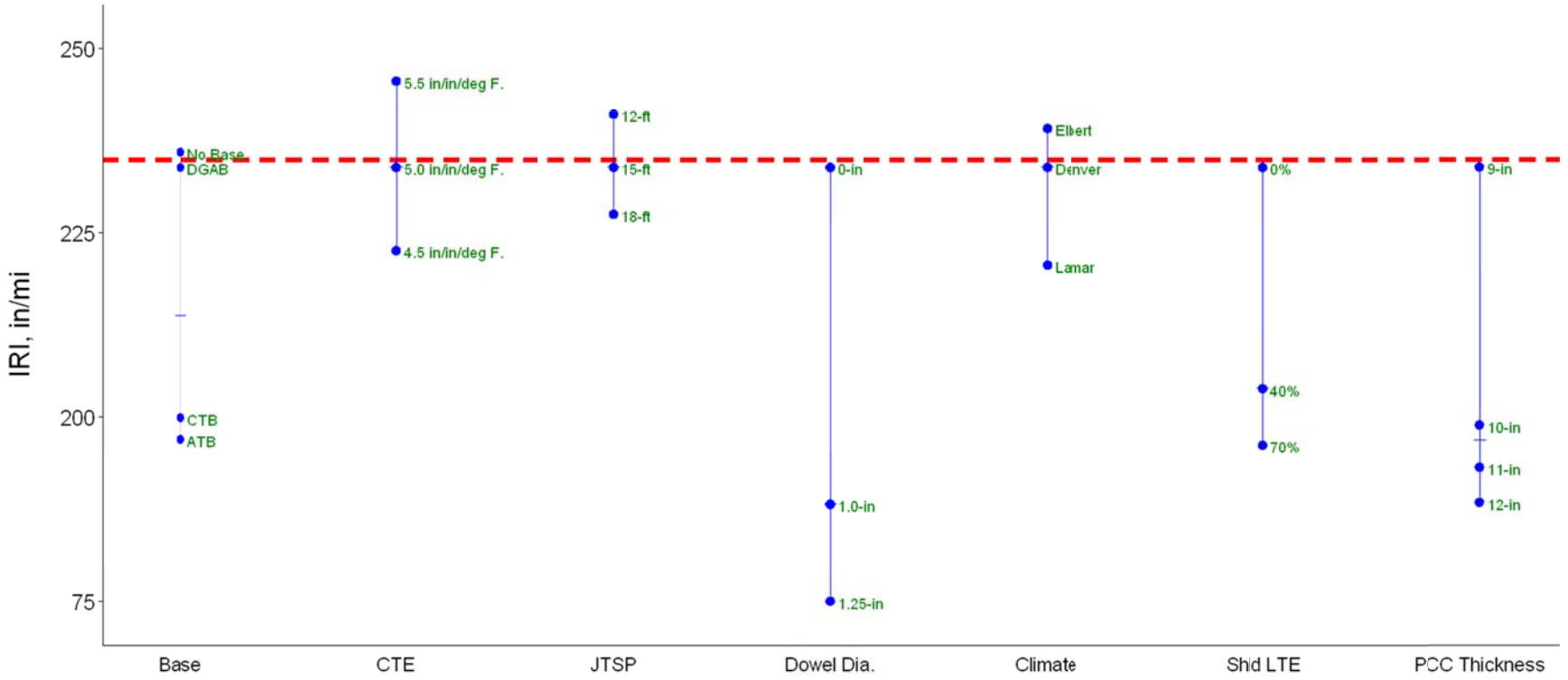

Figure 125. Sensitivity summary for JPCP IRI. Note the red line represents predicted IRI for the baseline project in Table 76.

HMA Pavements

Alligator Cracking

The sensitivity results for HMA alligator cracking show HMA thickness was the most sensitive of the input variables analyzed. A change in HMA thickness from 5 to 11 inches resulted in a significant reduction in alligator cracking from approximately 90 to 0 percent lane area after 20 years in service and cumulative application of 9.3 million trucks. A similar trend was observed for full-depth HMA pavements.

Base thickness, AC air void content, volumetric binder content, and the number of cumulative truck applications were the next most significant input variables, with an approximately 20 to 30 percent lane area change in alligator cracking with changes in these inputs from the lower to upper end values.

Asphalt binder type, subbase thickness, and climate were the least sensitive of the inputs evaluated, showing approximately 10 percent lane area change in alligator cracking with changes in these inputs from the lower to upper end values.

The sensitivity analysis trends for alligator cracking were reasonable. The magnitude of change in alligator cracking and direction of change as the input values changed were also assessed to be reasonable. The information assembled will be valuable in helping pavement design engineers optimize designs by modifying inputs as needed.

Total Rutting

The sensitivity results for total rutting (HMA, granular base, and subgrade) shows AADTT, HMA thickness, climate, and asphalt binder type as the most sensitive of the input variables analyzed. This implies that pavements with significant cumulative truck traffic applications over their design life (i.e., highly trafficked interstates) will experience significant levels of rutting if remedies such as thicker HMA layers and appropriate asphalt binder type are not considered in the design.

The rutting sensitivity analysis results also show that HMA pavements located in hotter climate zones exhibit significantly higher levels of rutting than comparable designs in cooler climates.

The HMA mix properties (percent air voids, binder content, and binder type) also had a considerable impact on rutting, although they are not the most significant. Thus, choosing and applying the right HMA mix for a given climate would help mitigate the development and progression of total rutting.

HMA Transverse "Thermal" Cracking

The three inputs with the most impact on HMA transverse "thermal" cracking were binder type, climate, and HMA thickness. Basically, the sensitivity analysis results showed that HMA pavement located in cooler climate zones are more likely to experience significant levels of transverse cracking. Pavements with thinner HMA layers also exhibited considerably highly cracking levels than thicker HMA sections. Finally, as expected, asphalt binders with lower pavement temperature rating (-22 versus -28 °C) were more resistant to low temperature cracking. Other key HMA mix properties (binder content and air voids) had minimal impact on transverse cracking development and progression.

New HMA IRI

The sensitivity analysis results show that, in general, the pavement design and material properties that had a significant impact on distress development and progression (alligator cracking, rutting, transverse cracking) also affect smoothness (IRI). This is as expected, as smoothness deterioration is mostly due to distress development and future deterioration rates (severity). Key inputs that had the most significant impact on IRI included HMA air voids, binder type, AADTT, climate zone, and HMA thickness.

JPCP

Transverse "Slab" Cracking

The sensitivity analysis results show that PCC flexural strength, PCC slab length (i.e., joint spacing), climate, PCC thickness, edge support (shoulder type and lane to shoulder load transfer efficiency), and base type had the most impact on transverse "slab" cracking development and progression. Designers can modify these inputs as needed to optimize JPCP designs. The sensitivity analysis results also show that the two site factors with the greatest impact on transverse cracking are truck traffic applications and climate (climate zone in which the pavement is located). JPCP subjected to high truck traffic applications or located in very cold climates (higher elevations) exhibited significantly higher levels of cracking.

Transverse Joint Faulting

Sensitivity analysis results show that the transverse joint load transfer mechanism (aggregate interlock versus dowels) and dowel diameter had the greatest impact on transverse joint faulting. Next were climate and PCC thickness. CTE, joint spacing, and edge support followed as the third group of sensitive inputs. Trends observed for all of these inputs were found to be reasonable. Designers can modify these inputs as needed to optimize JPCP designs.

JPCP IRI

The sensitivity analysis results show that, in general, the pavement design and material properties that had a significant impact on distress development and progression (transverse cracking and transverse joint faulting) also affected smoothness (IRI). This is as expected, as

smoothness deterioration is mostly due to distress development and future deterioration rates (severity). Key inputs that had the most significant impact on IRI included dowel diameter, climate, edge support, and PCC thickness.

Summary of Sensitivity Analysis Results

The sensitivity analysis results showed that the MEPDG design models calibrated/verified for Colorado conditions predict reasonable estimates of distress and IRI for HMA pavements and JPCP. The models also are sensitive to pavement design, materials, and site inputs, as expected. The levels of sensitivity observed were found to be reasonable, and it was determined that sensitivity was significant enough to enable pavement designers to modify inputs as needed to optimize pavement designs. A summary of the sensitivity analysis results is presented in Tables 77 and 78.

Table 77. Summary of sensitivity analysis of new HMA pavements results.

Input Parameter	Distress Types and Smoothness			
	Alligator Cracking	**Rutting**	**Transverse Cracking**	**IRI**
Conventional HMA thickness	H	H	H	M
Granular base thickness	M	M	L	L
Granular subbase thickness	L	L	L	L
Air voids	M	M	M	M
Volumetric binder content	M	M	M	M
Binder type (Superpave)	L	M	H	M
Initial AADTT	M	H	M	M
Climate (weather stations)	L	H	H	M

H = high, M = moderate, and L = None to low.

Table 78. Summary of sensitivity analysis of new JPCP results.

Input Parameter	Distress Types and Smoothness		
	Transverse Cracking	**Transverse Joint Faulting**	**IRI**
PCC thickness	H	M	M
CTE	M	M	M
Base type/thickness	L	M	L
Dowel diameter, in (used PCC thickness/8 rule)	L	H	M
Joint spacing	H	M	M
Flexural strength	H	L	L
Shoulder type	H	H	M
Climate (weather stations)	M	M	M

H = high, M = moderate, and L = None to low.

Validation of Colorado MEPDG Models (Design Comparisons)

The local CDOT MEPDG new pavement models (HMA and JPCP) were validated through direct comparison with new pavement designs obtained using the locally calibrated CDOT MEPDG and the 1993 AASHTO Pavement Design Guide/1998 Rigid Pavement Supplemental Guide.

Pavements were designed using seven test projects located throughout Colorado. Major efforts were made to apply comparable inputs for each project, regardless of the design methodology utilized. Table 79 lists the key inputs.

Table 79. Description of key inputs used for design comparisons.

Key Design Input	AASHTO 1993/1998	CDOT Locally Calibrated MEPDG
Traffic	Comparable cumulative ESALs computed using the MEPDG traffic inputs	Cumulative number of trucks, vehicle class distribution, number of axles per truck, & axle load distribution
Subgrade soil	Resilient modulus (Mr) that is typically wet of optimum (in situ moisture)*	Resilient modulus (Mr) at optimum moisture content
Climate	Appropriate drainage coefficient (Cd)	Hourly records of ambient temperature, precipitation, cloud cover, wind speed, and snowfall from the closest weather station with data available in DARWin-ME for CDOT's provided weather stations
Paving materials	Although the identical material types (e.g., HMA, granular base, etc.) were proposed for comparable designs, required inputs differed per design methodology. As much as possible, equivalent inputs were assumed (e.g., HMA dynamic modulus vs. appropriate structural coefficient OR dowel size vs. appropriate J-factor)	
Reliability		Same level of design reliability (90 percent) were used for each direct comparison**
Performance criteria	Pavement Serviceability Index (PSI)	IRI and several distress types. Efforts were made to select IRI values that were approximately equivalent to the CDOT PSI threshold

*Resilient modulus values presented in Table 4.5 of the CDOT Pavement Design Manual are at in situ moisture and density condition although they are labeled as optimum moisture and maximum dry density. Corrections will be made to these values, and resilient modulus at optimum moisture and maximum dry density will be presented in the Pavement Design Manual.

**Reliability is defined differently for each AASHTO 1993/1998 and MEPDG design methodologies.

New HMA Pavement Design Comparisons

Table 80 shows a summary of the results from the new HMA designs at seven project sites. Figure 126 shows a direct comparison of HMA thicknesses achieved for all project comparisons using the two design methodologies. Table 81 shows the results of tests performed to identify possible bias in design HMA thickness results. The results show very good 1-to-1 comparison between the AASHTO 1993 HMA design procedure and the AASHTO DARWin-ME design procedure for both reconstruction and overlays.

Table 80. Summary of the results from the new HMA design projects.

Project Site	Traffic (No. of Trucks)	HMA Design Thickness (in)	
		AASHTO 1993	DARWin-ME
US 285 Hampden Ave.	7.07 million	7.75	8.5
I-70 E of Mack	6.5 million	5.5	6.0
I-25 Denver (Reconstruction 20 years)	2.8 million	6.5	7.5
I-25 Denver (HMA Overlay 10 years)	1.26 million	4.0	4.0
US 50 East (HMA Overlay 10 years)	2.8 million	4.0	4.0
US 50 East (PCC Overlay 30 years)	9.0 million	No Design	No Design
US 85 Ault/Nunn	6.62 million	6.25	6.00

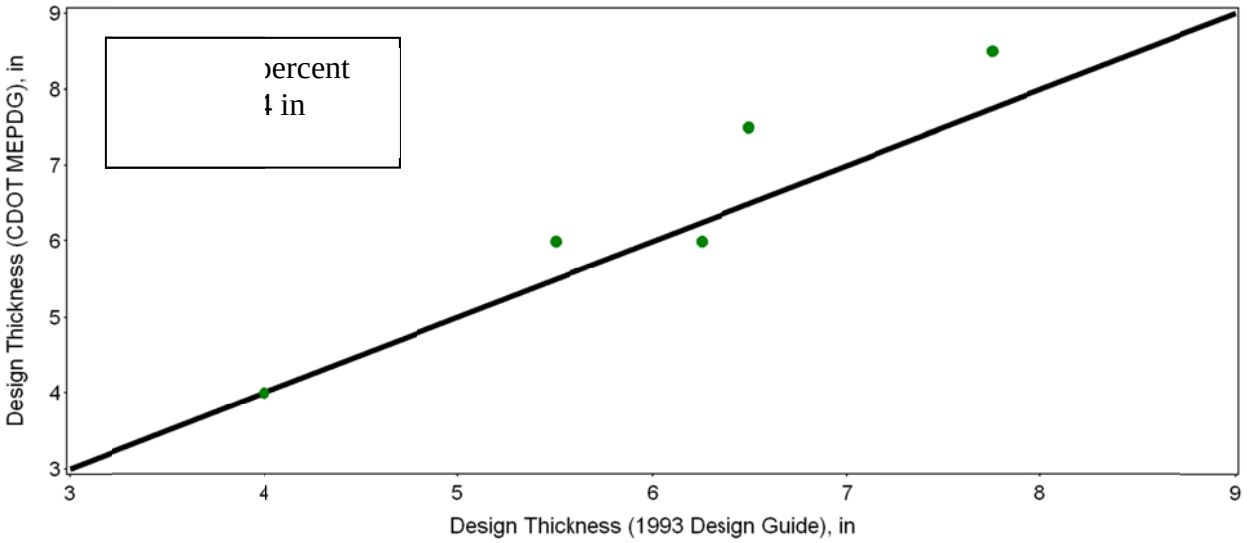

Figure 126. AASHTO 1993 HMA design thickness vs. AASHTO DARWin-ME HMA design thickness.

Table 81. New HMA pavement goodness of fit and bias test for final local CDOT MEPDG and 1993/1998 AASHTO Pavement Design Guide design thicknesses.

Analysis Type	Diagnostic Statistics	Results
Goodness of Fit	R^2	95.3 percent
	SEE	0.44 in
	N	5
Bias	H_0: Intercept = 0	p-value = 0.3684
	H_0: Slope = 1.0	p-value = 0.0856
	H_0: Predicted - measured thickness = 0 (paired t-test)	p-value = 0.1576

New JPCP Design Comparisons

Table 82 shows a summary of the results from the new JPCP designs at seven project sites. Figure 127 shows a direct comparison of PCC thicknesses achieved for all project comparisons. Table 83 shows the results of tests performed to identify possible bias in design PCC thickness results. The results show very good 1-to-1 comparison between the AASHTO 1998 PCC design procedure and the AASHTO DARWin-ME design procedure for both reconstruction and overlays.

A direct correlation of all the PCC thickness results was shown in Figure 127. The intercept and slope of the linear curve developed using thicknesses from the two design procedures shows an approximate intercept of 0.0 and slope of 1.0, as confirmed to the 95 significance level through statistical hypothesis testing. A paired t-test of the two sets of design HMA and PCC thicknesses also indicated no significant differences.

The outcomes indicate a good correlation between the CDOT MEPDG and the earlier AASHTO pavement design procedures for basic designs. Thus, the use of the CDOT MEPDG in general must yield basic designs comparable to current CDOT pavement designs. Using the superior analytical procedures of the MEPDG, however, CDOT engineers must be capable of optimizing the basic designs by selecting more appropriate materials and design inputs to produce more cost-effective pavement designs.

It is noted that all of these projects are at locations that experience relative lower truck traffic. For heavier truck traffic, there may be significant differences, with the MEPDG showing slightly lower thickness than the 1993/1998 AASHTO procedure.

Table 82. Summary of the results from the new JPCP design projects.

Project Site	Traffic (No. of Trucks)	PCC Design Thickness (in)	
		AASHTO 1998	DARWin-ME
US 285 Hampden Ave.	7.07 million	8.5	8.0
I-70 E of Mack	6.5 million	6.0	6.0
I-25 Denver (Reconstruction 20 years)	2.8 million	No Design	No Design
I-25 Denver (HMA Overlay 10 years)	1.26 million	No Design	No Design
US 50 East (HMA Overlay 10 years)	2.8 million	No Design	No Design
US 50 East (PCC Overlay 30 years)	9.0 million	8.5	8.5
US 85 Ault/Nunn	6.62 million	8.5	8.0

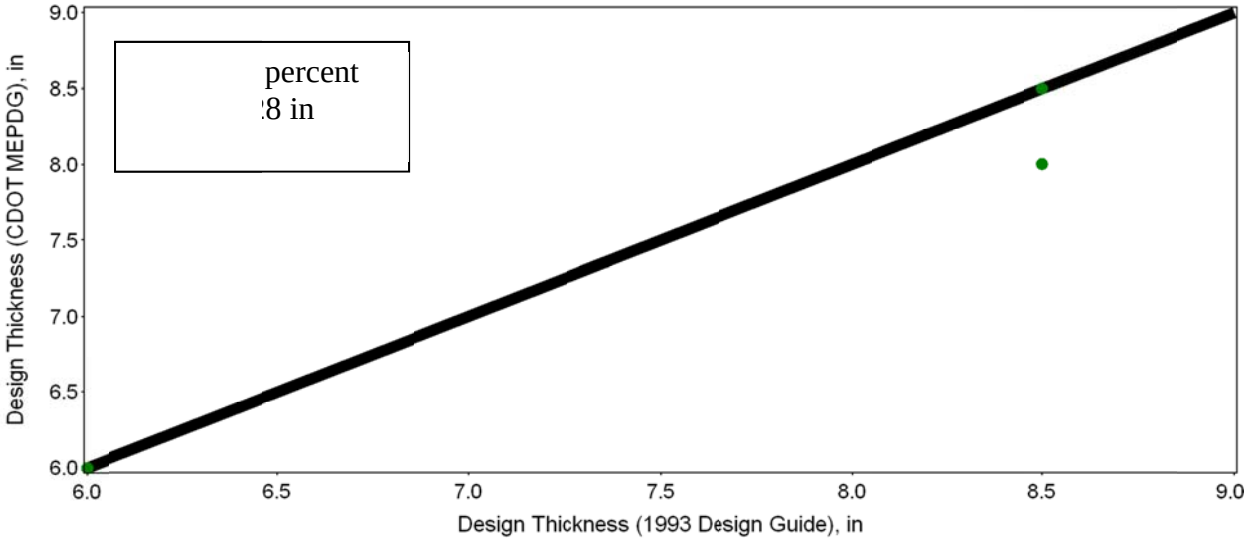

Figure 127. AASHTO 1993 PCC design thickness vs. AASHTO DARWin-ME PCC design thickness

Table 83. New JPCP goodness of fit and bias test for final local CDOT MEPDG and 1993/1998 AASHTO Pavement Design Guide design thicknesses.

Analysis Type	Diagnostic Statistics	Results
Goodness of Fit	R^2	95.5 percent
	SEE	0.28 in
	N	3
Bias	H_0: Intercept = 0	p-value = 0.5291
	H_0: Slope = 1.0	p-value = 0.1392
	H_0: Predicted - measured thickness = 0 (paired t-test)	p-value = 0.1817

CHAPTER 9. SUMMARY AND CONCLUSIONS

The MEPDG is based on mechanistic-empirical design concepts. This means that the design procedure calculates pavement responses such as stresses, strains, and deflections under axle loads and climatic conditions and then accumulates the damage over the design analysis period. The procedure then empirically relates calculated damage over time to pavement distresses and smoothness based on performance of actual projects.

Implementing the MEPDG in Colorado has involved several major efforts to provide assurance to CDOT that the MEPDG models will predict distresses and IRI that match Colorado experience:

- Development of Colorado procedures for proper inputs for using the MEPDG to design new, reconstructed, and rehabilitated pavement structures. This was accomplished through the development of a **Colorado MEPDG User's Guide** that provides guidance on obtaining proper design inputs.
- **Verification, validation, and calibration with Colorado performance data** of the MEPDG models (if necessary) to remove bias (consistent over- or under-prediction) and improve accuracy of prediction. This was accomplished through the verification, validation, and recalibration of Colorado calibration coefficients. In nearly all cases, this resulted in improved accuracy of the distress and IRI models and the removal of bias.
- **Design comparisons** and sensitivity studies that help to establish confidence in the pavement design results achieved when using the MEPDG.

The various MEPDG prediction models have been verified, validated, and if necessary, recalibrated using Colorado LTPP and pavement management system sections. One hundred twenty-six new HMA, new JPCP, HMA/JPCP, and unbonded JPCP over JPCP rehabilitated pavements were included in a valuable database that represents the performance of Colorado pavements over many years. The model verification and calibration effort was successful and provides CDOT with validated distress and IRI models.

This database was used in the verification, validation, and recalibration process to modify the prediction models to make them more accurate and unbiased (neither over- nor under-prediction). They were also used to establish Colorado design inputs and the appropriate standard deviation or error of each model for use in reliability design. This will make it possible to design a pavement in Colorado with the desired reliability at the optimum cost.

REFERENCES

AASHTO. (1961). *Interim Guide for Design of Pavement Structures*. American Association of State Highway and Transportation Officials, Washington, D.C.

AASHTO. (1972). *Interim Guide for Design of Pavement Structures*. American Association of State Highway and Transportation Officials, Washington, D.C.

AASHTO. (1986). *Guide for Design of Pavement Structures*. American Association of State Highway and Transportation Officials, Washington, D.C.

AASHTO. (1993). *Guide for Design of Pavement Structures*. American Association of State Highway and Transportation Officials, Washington, D.C.

AASHTO. (1998). *Supplement to the AASHTO Guide for Design of Pavement Structures, Part II-Rigid Pavement Design and Rigid Pavement Joint Design*. American Association of State Highway and Transportation Officials, Washington, D.C.

AASHTO. (2008). *Mechanistic-Empirical Pavement Design Guide, Interim Edition: A Manual of Practice*. American Association of State Highway and Transportation Officials, Washington, D.C.

AASHTO. (2010). *Guide for the Local Calibration of the Mechanistic-Empirical Pavement Design Guide*. American Association of State Highway and Transportation Officials, Washington, D.C.

AASHTO. (2013). AASHTOWare® Pavement ME Design™ software (formerly AASHTOWare® DARWin-ME™. American Association of State Highway and Transportation Officials, Washington, D.C.

ARA. (2004). "NCHRP Guide for Mechanistic-Empirical Design of New and Rehabilitated Pavement Structures." Final Report (Volumes 1, 2 & 3), NCHRP Project 1-37A. Applied Research Associates, Inc., Champaign, IL.

FHWA/NHI. (2006). "Geotechnical Aspects of Pavements." NHI Course No. 132040, National Highway Institute, Arlington, VA.

Highway Research Board. (1962). "AASHO Road Test Report 5—Pavement Research," *Special Report* 61E, Washington, D.C.

Mallela, J., Titus-Glover, L., Darter, M.I., Rao, C., and Bhattacharya, B., "*Recalibration of M-EPDG Rigid Pavement National Models Based on Corrected CTE Values*", Final Report #20-07/Task 288, National Cooperative Highway Research Program, Transportation Research Board of National Academics, Washington, D.C., October 2011.

Miller, J.S., and W.Y. Bellinger. (2003). *Distress Identification Manual for the Long-Term Pavement Performance Program*. Report No. FHWA-RD-03-031, Federal Highway Administration, McLean, VA.

Miner, M. A. (1945). "Cumulative Damage in Fatigue," *Journal of Applied Mechanics*, Vol. 12, Transactions of the American Society of Mechanical Engineers.

Von Quintus, H.L., J. Mallela, R. Bonaquist, C.W. Schwartz, and R.L. Carvalho. (2012). Calibration of Rutting Models for Structural and Mix Design. NCHRP Report 719, Transportation Research Board, Washington, D.C.

APPENDIX A. NEW HMA AND NEW JPCP PERFORMANCE PREDICTION MODELS

This appendix describes the MEPDG models used to predict performance. Additional information is available in several other publications (AASHTO 2008, ARA 2004).

New and Reconstructed HMA Pavements

Alligator Cracking

Alligator cracking initiates at the bottom of the HMA layers and propagates to the surface with repeated application of heavy truck axles. Alligator cracking prediction in the MEPDG begins with the computation incrementally of HMA bottom-up fatigue damage. This is done using a grid pattern throughout the HMA layers at critical depths to determine the location within the HMA layer subjected to the highest amount of horizontal tensile strain—the mechanistic parameters used to relate applied loading to fatigue damage. An incremental damage index, ΔDI, is calculated by dividing the actual number of axle loads by the allowable number of axle loads (note that computation of damage is based on Miner's hypothesis) within a specific time increment and axle load interval for each axle type (Miner 1945). The cumulative damage index for each critical location is determined by summing the incremental damage over time and traffic using equation A-1 (AASHTO 2008):

$$DI = \sum (\Delta DI)_{j,m,l,p,T} = \sum \left(\frac{n}{N_{f-HMA}} \right)_{j,m,l,p,T} \quad \text{(A-1)}$$

where

n = actual number of axle load applications within a specific time period
j = axle load interval
m = axle load type (single, tandem, tridem, quad, or special axle configuration)
l = truck type using the truck classification groups included in the MEPDG
p = month
T = median temperature for the five temperature intervals or quintiles used to subdivide each month, °F
$N_{f\text{-}HMA}$ = allowable number of axle load applications for a flexible pavement and HMA overlays to fatigue cracking

The allowable number of axle load applications needed for the incremental damage index computation is shown in equation A-2 (AASHTO 2008).

$$N_{f-HMA} = k_{f1}(C)(C_H)\beta_{f1}(\varepsilon_t)^{k_{f2}\beta_{f2}}(E_{HMA})^{k_{f3}\beta_{f3}} \quad \text{(A-2)}$$

where

$N_{f\text{-}HMA}$ = allowable number of axle load applications for a flexible pavement and HMA overlays to fatigue cracking
ε_t = tensile strain at critical locations and calculated by the structural response

model, in/in

E_{HMA} = dynamic modulus of the HMA measured in compression, psi

k_{f1}, k_{f2}, k_{f3} = global field calibration parameters (k_{f1} = 0.007566, k_{f2} = -3.9492, and k_{f3} = -1.281)

β_{f1}, β_{f2}, β_{f3} = local or mixture specific field calibration constants; for the global calibration effort, these constants were set to 1.0

$$C = 10^{M} \tag{A-3}$$

$$M = 4.84\left(\frac{V_{be}}{V_a + V_{be}} - 0.69\right) \tag{A-4}$$

V_{be} = effective asphalt content by volume, percent

V_a = percent air voids in the HMA mixture (in situ only, not mixture design)

C_H = thickness correction term as follows:

$$C_H = \frac{1}{0.000398 + \frac{0.003602}{1 + e^{(11.02 - 3.49 H_{HMA})}}} \tag{A-5}$$

H_{HMA} = total HMA thickness, in

Alligator cracking is calculated from the cumulative damage over time (equation 1) using the relationship presented as equation 6 (AASHTO 2008).

$$FC_{Bottom} = \left(\frac{1}{60}\right)\left(\frac{C_4}{1 + e^{(C_1 C_1^* + C_2 C_2^* Log(DI_{Bottom}))}}\right) \tag{A-6}$$

where

FC_{Bottom} = area of alligator cracking that initiates at the bottom of the HMA layers, percent of total lane area

DI_{Bottom} = cumulative damage index at the bottom of the HMA layers

$C_{1,2,4}$ = transfer function regression constants; C_4= 6,000; C_1=1.00; and C_2=1.00

$$C_1^* = -2C_2^* \tag{A-7}$$

$$C_2^* = -2.40874 - 39.748(1 + H_{HMA})^{-2.856} \tag{A-8}$$

where

H_{HMA} = total HMA thickness, in

Transverse Cracking (Low Temperature Induced)

For the MEPDG, the amount of crack propagation induced by a given thermal cooling cycle is predicted using the Paris law of crack propagation (AASHTO 2008).

$$\Delta C = A\left(\Delta K\right)^n \quad \text{(A-9)}$$

where

ΔC	=	change in the crack depth due to a cooling cycle
ΔK	=	change in the stress intensity factor due to a cooling cycle
A, n	=	fracture parameters for the HMA mixture

Experimental results indicate that reasonable estimates of A and n can be obtained from the indirect tensile creep compliance and strength of the HMA in accordance with equations A-10 and A-11 (AASHTO 2008):

$$A = 10^{k_t \beta_t \left(4.389 - 2.52\, Log\left(E_{HMA} \sigma_m n\right)\right)} \quad \text{(A-10)}$$

where

$$n = 0.8\left[1 + \frac{1}{m}\right] \quad \text{(A-11)}$$

k_t	=	coefficient determined through global calibration for each input level (Level 1 = 5.0; Level 2 = 1.5; and Level 3 = 3.0)
E_{HMA}	=	HMA indirect tensile modulus, psi
σ_m	=	mixture tensile strength, psi
m	=	m-value derived from the indirect tensile creep compliance curve measured in the laboratory
β_t	=	local or mixture calibration factor

Stress intensity factor, K, was incorporated in the MEPDG through the use of a simplified equation developed from theoretical finite element studies (equation A-12):

$$K = \sigma_{tip}\left(0.45 + 1.99\left(C_o\right)^{0.56}\right) \quad \text{(A-12)}$$

where

σ_{tip}	=	far-field stress from pavement response model at depth of crack tip, psi
C_o	=	current crack length, ft

The amount of transverse cracking is predicted by the MEPDG using an assumed relationship between the probability distribution of the log of the crack depth to HMA layer thickness ratio and the percent of cracking. Equation A-13 shows the expression used to determine the amount of thermal cracking (AASHTO 2008):

$$TC = \beta_{t1} N\left[\frac{1}{\sigma_d} Log\left(\frac{C_d}{H_{HMA}}\right)\right] \quad \text{(A-13)}$$

where

TC	=	thermal cracking, ft/mi
β_{t1}	=	regression coefficient determined through global calibration (400)
$N[z]$	=	standard normal distribution evaluated at [z]
σ_d	=	standard deviation of the log of the depth of cracks in the pavement (0.769), in
C_d	=	crack depth, in
H_{HMA}	=	thickness of HMA layers, in

Rutting

Rutting is caused by the plastic or permanent vertical deformation in the HMA, unbound base/subbase layers, and subgrade/foundation soil. For the MEPDG, rutting is predicted by calculating incrementally the plastic vertical strain accumulated in each pavement layer due to applied axle loading. In other words, rutting is the sum of all plastic vertical strain at the mid-depth of each pavement layer within the pavement structure, accumulated over a given analysis period. The rate of pavement layer plastic deformation could vary significantly over a given time increment since (1) the pavement layer properties (HMA and unbound aggregate material and subgrade) do change with temperature (summer versus winter months) and moisture (wet versus dry) and (2) applied traffic could also be very different.

The MEPDG model for calculating total rutting is based on the universal "strain hardening" relationship developed from data obtained from repeated load permanent deformation triaxial tests of both HMA mixtures and unbound aggregate materials and subgrade soils in the laboratory. The laboratory-derived relationship was then calibrated to match field measured rut depth.

For all HMA mixtures types, the MEPDG field calibrated form of the laboratory derived relationship from repeated load permanent deformation tests is shown in equation A-14:

$$\Delta_{p(HMA)} = \varepsilon_{p(HMA)} h_{HMA} = \beta_{1r} k_z \varepsilon_{r(HMA)} 10^{k_{1r}} n^{k_{2r}\beta_{2r}} T^{k_{3r}\beta_{3r}} \quad \text{(A-14)}$$

where

$\Delta_{p(HMA)}$	=	accumulated permanent or plastic vertical deformation in the HMA layer/sublayer, in
$\varepsilon_{p(HMA)}$	=	accumulated permanent or plastic axial strain in the HMA layer/sublayer, in/in
$\varepsilon_{r(HMA)}$	=	resilient or elastic strain calculated by the structural response model at the mid-depth of each HMA sublayer, in/in
$h_{(HMA)}$	=	thickness of the HMA layer/sublayer, in
n	=	number of axle load repetitions
T	=	mix or pavement temperature, °F
k_z	=	depth confinement factor

$k_{1r,2r,3r}$ = global field calibration parameters (from the NCHRP 1-40D recalibration; k_{1r} = -3.35412, k_{2r} = 0.4791, k_{3r} = 1.5606)

β_{1r}, β_{2r}, β_{3r}, = local or mixture field calibration constants; for the global calibration, these constants were all set to 1.0

$$k_z = (C_1 + C_2 D)0.328196^{D} \quad \text{(A-15)}$$

$$C_1 = -0.1039(H_{HMA})^2 + 2.4868 H_{HMA} - 17.342 \quad \text{(A-16)}$$

$$C_2 = 0.0172(H_{HMA})^2 - 1.7331 H_{HMA} + 27.428 \quad \text{(A-17)}$$

D = Depth below the surface, in

H_{HMA} = Total HMA thickness, in

Equation 18 shows the field-calibrated mathematical equation used to calculate plastic vertical deformation within all unbound pavement sublayers and the foundation or embankment soil.

$$\Delta_{p(soil)} = \beta_{s1} k_{s1} \varepsilon_v h_{soil} \left(\frac{\varepsilon_o}{\varepsilon_r} \right) e^{-\left(\frac{\rho}{n}\right)^{\beta}} \quad \text{(A-18)}$$

where

$\Delta_{p(Soil)}$ = permanent or plastic deformation for the layer/sublayer, in.

n = number of axle load applications

ε_o = intercept determined from laboratory repeated load permanent deformation tests, in/in

ε_r = resilient strain imposed in laboratory test to obtain material properties ε_o, β, and ρ, in/in

ε_v = average vertical resilient or elastic strain in the layer/sublayer and calculated by the structural response model, in/in

h_{Soil} = thickness of the unbound layer/sublayer, in

k_{s1} = global calibration coefficients; k_{s1}=1.673 for granular materials and 1.35 for fine-grained materials

β_{s1} = local calibration constant for the rutting in the unbound layers (base or subgrade); the local calibration constant was set to 1.0 for the global calibration effort. Note that β_{s1} represents the subgrade layer while β_{B1} represents the base layer

$$Log\beta = -0.61119 - 0.017638(W_c) \quad \text{(A-19)}$$

$$\rho = 10^9 \left(\frac{C_o}{\left(1 - (10^9)^{\beta}\right)} \right)^{\frac{1}{\beta}} \quad \text{(A-20)}$$

$$C_o = Ln\left(\frac{a_1 M_r^{b_1}}{a_9 M_r^{b_9}} \right) = 0.0075 \quad \text{(A-21)}$$

W_c = water content, percent

M_r	=	resilient modulus of the unbound layer or sublayer, psi
$a_{1,9}$	=	regression constants; a_1=0.15 and a_9=20.0
$b_{1,9}$	=	regression constants; b_1=0.0 and b_9=0.0

Smoothness (IRI)

The design premise included in the MEPDG for predicting smoothness degradation is that the development of surface distress will result in a reduction in smoothness (increasing IRI). Equations A-22 and A-23 were developed using data from the LTPP program and are embedded in the MEPDG to predict the IRI over time for new HMA pavements (AASHTO 2008).

$$IRI = IRI_o + 0.0150(SF) + 0.400(FC_{Total}) + 0.0080(TC) + 40.0(RD) \quad \text{(A-22)}$$

where

IRI_o	=	initial IRI after construction, in/mi
SF	=	site factor, refer to equation A-23
FC_{Total}	=	area of fatigue cracking (combined alligator, longitudinal, and reflection cracking in the wheel path), percent of total lane area. All load related cracks are combined on an area basis – length of cracks is multiplied by 1 foot to convert length into an area basis
TC	=	length of transverse cracking (including the reflection of transverse cracks in existing HMA pavements), ft/mi.
RD	=	average rut depth, in

The site factor is calculated in accordance with the following equation:

$$SF = FROSTH + SWELLP*AGE^{1.5} \quad \text{(A-23)}$$

where

FROSTH	=	LN([PRECIP+1]*FINES*[FI+1])
SWELLP	=	LN([PRECIP+1]*CLAY*[PI+1])
FINES	=	FSAND + SILT
AGE	=	pavement age, years
PI	=	subgrade soil plasticity index
PRECIP	=	mean annual precipitation, in.
FI	=	mean annual freezing index, deg. F Days
FSAND	=	amount of fine sand particles in subgrade (percent of particles between 0.074 and 0.42 mm)
SILT	=	amount of silt particles in subgrade (percent of particles between 0.074 and 0.002 mm)
CLAY	=	amount of clay size particles in subgrade (percent of particles less than 0.002 mm)

New JPCP

Transverse Slab Cracking

The MEPDG considers both JPCP bottom-up and top-down modes of transverse "slab" cracking. Under typical service conditions, the potential for either mode of cracking is present in all slabs. Any given slab may crack either from bottom-up or top-down, but not both. Therefore, the predicted bottom-up and top-down cracking are not particularly meaningful by themselves, and combined cracking is reported excluding the possibility of both modes of cracking occurring on the same slab. The percentage of slabs with transverse cracks (including all severities) in a given traffic lane is used as the measure of transverse cracking and is predicted using the following globally calibrated equation for both bottom-up and top-down cracking (AASHTO 2008):

$$CRK = \frac{1}{1 + 0.6 * \left(DI_F\right)^{-2.05}} \quad \text{(A-24)}$$

where

CRK	=	predicted amount of bottom-up or top-down cracking (fraction)
DI_F	=	fatigue damage calculated using the procedure described in this section

The general expression for fatigue damage accumulations considering all critical factors for JPCP transverse cracking is as follows (based on Miner's hypothesis) (Miner 1945):

$$DI_F = \sum \frac{n_{i,j,k,l,m,n,o}}{N_{i,j,k,l,m,n,o}} \quad \text{(A-25)}$$

where

DI_F	=	total fatigue damage (top-down or bottom-up)
$n_{i,j,k,\ldots}$	=	applied number of load applications at condition *i, j, k, l, m, n*
$N_{i,j,k,\ldots}$	=	allowable number of load applications at condition *i, j, k, l, m, n*
i	=	age (accounts for change in PCC modulus of rupture and elasticity, slab/base contact friction, traffic loads)
j	=	month (accounts for change in base elastic modulus and effective dynamic modulus of subgrade reaction)
k	=	axle type (single, tandem, and tridem for bottom-up cracking; short, medium, and long wheelbase for top-down cracking)
l	=	load level (incremental load for each axle type)
m	=	equivalent temperature difference between top and bottom PCC surfaces
n	=	traffic offset path
o	=	hourly truck traffic fraction

The applied number of load applications ($n_{i,j,k,l,m,n}$) is the actual number of axle type *k* of load level *l* that passed through traffic path *n* under each condition (age, season, and temperature difference). The allowable number of load applications is the number of load cycles at which fatigue failure is expected on average and is a function of the applied stress and PCC strength.

The allowable number of load applications is determined using the following globally calibrated PCC fatigue equation:

$$\log\left(N_{i,j,k,l,m,n}\right) = C_1 \cdot \left(\frac{MR_i}{\sigma_{i,j,k,l,m,n}}\right)^{C_2} \quad \text{(A-26)}$$

where:

$N_{i,j,k,...}$ = allowable number of load applications at condition *i, j, k, l, m, n.*
MR_i = PCC modulus of rupture at age *i*, psi.
$\sigma_{i,j,k,.}$ = applied stress at condition *i, j, k, l, m, n*
C_1 = calibration constant, 2.0
C_2 = calibration constant, 1.22

The fatigue damage calculation is a process of summing damage from each damage increment. Once top-down and bottom-up damage are estimated, the corresponding cracking is computed using equation A-24 and the total combined cracking determined using equation A-27.

$$TCRACK = \left(CRK_{Bottom-up} + CRK_{Top-down} - CRK_{Bottom-up} \cdot CRK_{Top-down}\right) \cdot 100 \quad \text{(A-27)}$$

where:

$TCRACK$ = total transverse cracking (percent, all severities)
$CRK_{Bottop-up}$ = predicted amount of bottom-up transverse cracking (fraction)
$CRK_{Top-down}$ = predicted amount of top-down transverse cracking (fraction)

Equation A-27 assumes that a slab may crack from either bottom-up or top-down, but not both.

Transverse Joint Faulting

The mean transverse joint faulting is predicted incrementally on a monthly basis. The magnitude of increment is based on current faulting level, the number of axle loads applied, pavement design features, material properties, and climatic conditions. Total faulting is determined as a sum of faulting increments from all previous months (i.e., since traffic opening) using the following equations (AASHTO 2008):

$$Fault_m = \sum_{i=1}^{m} \Delta Fault_i \quad \text{(A-28)}$$

$$\Delta Fault_i = C_{34} * (FAULTMAX_{i-1} - Fault_{i-1})^2 * DE_i \quad \text{(A-29)}$$

$$FAULTMAX_i = FAULTMAX_0 + C_7 * \sum_{j=1}^{m} DE_j * Log(1 + C_5 * 5.0^{EROD})^{C_6} \quad \text{(A-30)}$$

$$FAULTMAX_0 = C_{12} * \delta_{curling} * \left[Log(1 + C_5 * 5.0^{EROD}) * Log(\frac{P_{200} * WetDays}{P_s}) \right]^{C_6} \quad \text{(A-31)}$$

where

$Fault_m$ = mean joint faulting at the end of month *m*, in

$\Delta Fault_i$	=	incremental change (monthly) in mean transverse joint faulting during month *i*, in
$FAULTMAX_i$	=	maximum mean transverse joint faulting for month *i*, in
$FAULTMAX_0$	=	initial maximum mean transverse joint faulting, in
$EROD$	=	base/subbase erodibility factor
DE_i	=	differential density of energy of subgrade deformation accumulated during month *i*
$\delta_{curling}$	=	maximum mean monthly slab corner upward deflection PCC due to temperature curling and moisture warping
P_S	=	overburden on subgrade, lb
P_{200}	=	percent subgrade material passing No. 200 sieve
$WetDays$	=	average annual number of wet days (greater than 0.1 inch rainfall)
$C_{1,2,3,4,5,6,7,12,34}$	=	global calibration constants

Calibration Coefficients	New JPCP	JPCP subjected to CPR
C1	0.5104	0.5104
C2	0.00838	0.00838
C3	0.00147	0.00147
C4	0.008345	0.008345
C5	5999	5999
C6	0.8404	0.8404
C7	5.9293	5.9293
C8	400	400

C_{12} and C_{34} are defined by equations A-32 and A-33.

$$C_{12} = C_1 + C_2 * FR^{0.25} \quad \text{(A-32)}$$

$$C_{34} = C_3 + C_4 * FR^{0.25} \quad \text{(A-33)}$$

FR	=	base freezing index defined as percentage of time the top base temperature is below freezing (32 °F) temperature.

Since the maximum faulting development occurs during nighttime when the PCC slab is curled upward and joints are opened and the load transfer efficiencies are lower, only axle load repetitions applied from 8 PM to 8 AM are considered in the faulting analysis.

Smoothness (IRI)

In the MEPDG, JPCP smoothness is predicted as a function of the initial as-constructed smoothness and any change in pavement longitudinal profile over time and traffic due to distress development and progression and foundation movements. The IRI model was calibrated and validated using LTPP data that represented variety of design, materials, foundations, and climatic conditions. The following is the final globally calibrated model (AASHTO 2008):

$$IRI = IRI_I + C1*CRK + C2*SPALL + C3*TFAULT + C4*SF \quad \text{(A-34)}$$

where

IRI	=	predicted IRI, in/mi
IRI_I	=	initial smoothness measured as IRI, in/mi
CRK	=	percent slabs with transverse cracks (all severities)
$SPALL$	=	percentage of joints with spalling (medium and high severities)
$TFAULT$	=	total joint faulting cumulated per mi, in
$C1$	=	0.8203
$C2$	=	0.4417
$C3$	=	0.4929
$C4$	=	25.24
SF	=	site factor

$$SF = AGE\,(1+0.5556*FI)\,(1+P_{200})*10^{-6} \quad \text{(A-35)}$$

where

AGE	=	pavement age, yr
FI	=	freezing index, °F-days
P_{200}	=	percent subgrade material passing No. 200 sieve

The transverse cracking and faulting are obtained using the MEPDG models described earlier. The transverse joint spalling is determined in accordance with equation A-36, which was calibrated using LTPP and other data (AASHTO 2008):

$$\text{SPALL} = \left[\frac{\text{AGE}}{\text{AGE} + 0.01}\right]\left[\frac{100}{1 + 1.005^{(-12*\text{AGE} + \text{SCF})}}\right] \quad \text{(A-36)}$$

where

$SPALL$	=	percentage joints spalled (medium- and high-severities)
AGE	=	pavement age since construction, years
SCF	=	scaling factor based on site-, design-, and climate-related variables

$$SCF = -1400 + 350 \cdot AC_{PCC} \cdot (0.5 + PREFORM) + 3.4\, f'c \cdot 0.4 - 0.2\,(FT_{cycles} \cdot AGE) + 43\, H_{PCC} - 536\, WC_{PCC} \quad \text{(A-37)}$$

AC_{PCC}	=	PCC air content, percent
AGE	=	time since construction, years
$PREFORM$	=	1 if preformed sealant is present; 0 if not
$f'c$	=	PCC compressive strength, psi
FT_{cycles}	=	average annual number of freeze-thaw cycles
H_{PCC}	=	PCC slab thickness, in
WC_{PCC}	=	PCC water/cement ratio